ERDC/CHL TR-08-8

Coastal and Hydraulics Laboratory

US Army Corps of Engineers®
Engineer Research and Development Center

Houston-Galveston Navigation Channels, Texas Project

Navigation Channel Sedimentation Study, Phase 2

J. N. Tate, R. C. Berger, and C. G. Ross

July 2008

ERDC/CHL TR-08-8
July 2008

Houston-Galveston Navigation Channels, Texas Project

Navigation Channel Sedimentation Study, Phase 2

J. N. Tate, R. C. Berger, and C. G. Ross

Coastal and Hydraulics Laboratory
U.S. Army Engineer Research and Development Center
3909 Halls Ferry Road
Vicksburg, MS 39180

Final report

Prepared for U.S. Army Engineer District, Galveston
P.O. Box 1229 Galveston, TX 77553-1229

Abstract: The U.S. Army Engineer District, Galveston, recently enlarged the Houston Ship Channel in depth and width. Preliminary evaluations of the enlarged channel indicate a higher than anticipated rate of deposition in the channel reach near Atkinson Island. A Coastal and Hydraulics Laboratory investigation (Tate and Berger 2006) was charged with determining if this higher deposition rate is a permanent feature or only a temporary issue. A preliminary study focused on the change in currents, as determined by the model, from the pre-enlarged channel to the new configuration and a sediment tracer analysis. The results of this study determined that the dredging should have been only about 20-30 percent higher than for the pre-enlarged channel. This implies that a large increase would be due to other considerations, such as dredged material resuspended from disposal areas and redepositing in the channel, channel dimension equilibrating, or vessel impacts on the shoaling. This preliminary study used the sediment model in an unvalidated state for early results to aid planning. In addition to an unvalidated model, other limitations were that the sediment pathways and loadings were not modeled but assumed. A more general validated tool is needed to estimate the causes of the shoaling with the enlarged channel and suggest approaches to reduce the deposition rate. A full sediment model of the area is useful to direct decisions to reduce dredging and dredging costs. Knowing that there are many factors that contribute to sediment transport, the logical next step is to develop and validate the sediment model. With a validated sediment model, testing and decision making can be made while considering many factors simultaneously. This report presents the sediment model validation process and comparison of the model to field data. In the validation process it was determined that vessel traffic was important in the deposition and resuspension of sediment. Vessel effects, therefore, are included in this model. The end result is a model that is capable of reproducing tides, circulation, salinity, and sediment transport in Galveston Bay.

Contents

Figures and Tables

Figures

Tables

Preface

This report presents the validation of a full sediment model of the Houston-Galveston Ship Channels and surrounding areas. This work was generated after a previous investigation of the possible causes of increased shoaling in the Houston Ship Channel after its dimensions were increased from 40 × 400 ft (12.2 × 122 m) to 45 × 530 ft (13.7 × 162 m). This apparent increase in shoaling may subside in time if due to the dredging itself or the channel side slopes reestablishing equilibrium. It, however, may be due to the larger channel dimensions, in which case the increased shoaling would be a permanent condition. Additional disposal capability would then be required. The previous work did not show the estimated increase in shoaling as seen in the field, so a full sediment model was proposed.

This investigation was conducted from December 2005 through October 2007 at the U.S. Army Engineer Research and Development Center (ERDC) by Dr. R. C. Berger, A. R. Carrillo, T. O. McAlpin, C. G. Ross, and J. N. Tate of the Coastal and Hydraulics Laboratory (CHL). The data collection was conducted 5-7 December 2005. In addition to Berger and Tate, the data collection group included J. R. Bull and T. N. Waller. Funding was provided by the U.S. Army Engineer District, Galveston.

The work was performed under the general direction of Thomas W. Richardson, Director, CHL, Dr. William D. Martin, Deputy Director, CHL, B. A. Ebersole, Chief, Flood and Storm Protection Division, CHL, and Dr. R. T. McAdory, Chief, Estuarine Engineering Branch, CHL.

COL Richard B. Jenkins was Commander and Executive Director of ERDC. Dr. James R. Houston was Director.

Unit Conversion Factors

Multiply	By	To Obtain
cubic feet	0.02831685	cubic meters
cubic yards	0.7645549	cubic meters
feet	0.3048	meters
knots	0.5144444	meters per second
microns	1.0 E-06	meters
miles (nautical)	1,852	meters
miles (U.S. statute)	1,609.347	meters
miles per hour	0.44704	meters per second
pounds (force)	4.448222	newtons
pounds (mass)	0.45359237	kilograms
slugs	14.59390	kilograms
square feet	0.09290304	square meters
square miles	2.589998 E+06	square meters
square yards	0.8361274	square meters
yards	0.9144	meters

1 Introduction

Background

The U.S. Army Engineer District, Galveston, recently enlarged the Houston Ship Channel from a 40-ft (12.2-m) depth by 400-ft (122-m) width to a 45-ft (13.7-m) depth by 530-ft (162-m) width. Previously, a three-dimensional (3-D) numerical model study was implemented at the U.S. Army Engineer Research and Development Center's (ERDC's) Coastal and Hydraulics Laboratory (CHL) to evaluate the salinity and circulation impact of this enlargement. In Berger et al. (1995a) the model was shown to represent the salinity and circulation in the earlier channel configuration. Berger et al. (1995b) used the model to predict the impact of the enlarged channel. Carrillo et al. (2002) used the model to evaluate the addition of barge lanes along the ship channel flanks. The enlarged channel is now complete and preliminary evaluations indicate a higher than anticipated rate of deposition in the channel reach near Atkinson Island. A CHL investigation (Tate et al. 2006) was charged with determining if this higher deposition rate is a permanent feature or temporary. The study focused on the change in currents, as determined by the model, from the 40- × 400-ft (12.2- × 122-m) to the 45- × 530-ft (13.7- × 162-m) condition. The model hydrodynamics had been validated by comparison to the field data in previous studies. In order to get quick answers for District planners, the sediment component of the model was used without a validation with field data, although some parameters were set based upon the field sediment data. The results of this study determined that the dredging should have been only about 20-30 percent higher than for the 40- × 400-ft (12.2- × 122-m) channel. This implies that the large increase is due to other considerations, such as dredge disposal escape, channel dimension equilibrating, or vessel impacts on shoaling. However, this study made several assumptions about the sediment distribution, including the sediment transport preferred pathways and details of the bed material and its behavior. Knowing that there are many factors that contribute to sediment transport, the logical next step was to validate the sediment model. A validated sediment model can then be used to direct decisions to reduce dredging and dredging costs.

Approach

This phase of the study develops a validated sediment model of the Houston Ship Channel area from the Gulf of Mexico up to the area north of the Barbour's Cut Channel. Figure 1 shows the Houston Ship Channel and Trinity Bay area. The region in the model above Barbour's Cut is included to reproduce the complete tidal prism but it is not a region in which the sediment model is validated. The "existing" condition, 40- × 400-ft (12.2- × 122-m), model was used for validation given historical dredging records. Validation was judged by the rate of deposition for the period being simulated and the distribution of that deposited material along the channel, as well as by suspended sediment concentrations in the area.

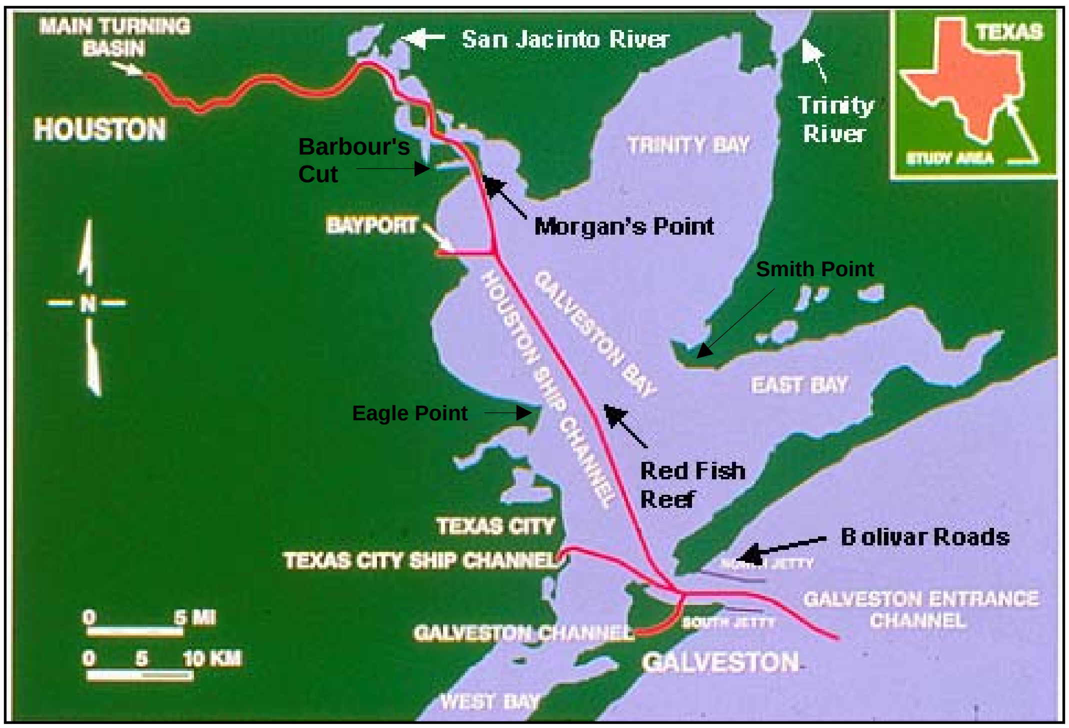

Figure 1. Houston Ship Channel area map.

Field Data

In order to validate the sediment model, field data collection was necessary to describe the nature of the bed and suspended material. Bed sediment samples were used to estimate parameters that determined the erodibility and composition of the bed. Although suspended sediment samples are available from existing sources, data taken in conjunction with the bed samples served as a check of the model's output as well as helped decipher the overall sediment character of the area. Chapter 2 describes the field data collection and analysis performed during this study.

Sediment Model

The sediment model was run in an uncoupled fashion. The hydrodynamics were created once and stored. This hydrodynamics file was then used to drive the sediment model. The assumption here is that the change in the bed produced by the sediment model is not large enough to significantly impact the hydrodynamics.

The model was run over an extended period, driven by hydrodynamics from the same time frame. The sediment loads entered the model system from the San Jacinto River and the Trinity River. The model included wind and currents in resuspending and transporting the bed sediment. Wind-induced wave stresses were also included in the resuspension and deposition processes. The model went through an initial validation and sensitivity to determine how the model behaves under various conditions.

The field data were used to estimate parameters associated with the erosion of the bed. Other parameters were adjusted during the validation process. The principal comparison was with suspended concentrations and the historical dredging records. Chapter 3 discusses the sediment model and the initial validation and sensitivity analysis.

Vessel Impacts

The vessel traffic in the channel is likely to have a significant impact on the sedimentation rates and locations of shoaling. Vessel movement simulations were performed to determine the shear stresses generated by a moving vessel. A vessel can cause stresses large enough to cause erosion of the bed or resuspension of sediment in the areas both inside and outside of the channel. A typical day of vessel traffic along the Houston Ship Channel was incorporated into the sediment model as an extension of the validation process. This typical day was repeated throughout the extended simulation period. The inclusion of the vessel effects is detailed in Chapter 4.

Model Validation

The model was validated with the inclusion of the vessel effects to match suspended sediment concentrations, as well as a comparison to the shoaling rate and distribution in the channel. Chapter 5 gives a full description of the validation process and its results.

2 Field Data Collection and Analysis

This chapter documents field data collection and analysis results for data collected in Trinity Bay, TX, during 5-7 December 2005. The field data were used to observe trends and determine bed characteristics within the model domain. Figure 1 shows the Houston Ship Channel area and locations of interest for this analysis. Field data were collected in Trinity Bay and the upper western portion of Galveston Bay north of Galveston, TX, over the three-day period. During this data collection, bed samples were taken by means of a push core at locations throughout the bay, east and west of the Houston Ship Channel. Suspended sediment samples were also taken at these locations. Figure 2 shows the locations of the samples taken.

Figure 2. Field data sample locations.

Generally the conditions during this three-day period were quite windy. Table 1 gives the sustained wind speed and direction at Morgan's Point and Eagle Point during these three days. These winds resulted in choppy wave conditions within the bay. This limited the speed at which data could be collected and some of the types of data that could be retrieved.

The analysis of the suspended sediment samples also included salinity. The bed sample analysis consisted of the determination of bulk density, moisture content, percent organics, and grain size distribution, as well as testing for erodibility parameters on some of the samples. All bed samples contained a thin layer of oxidized material that would easily suspend when the core tubes were handled. This layer ranged between 0.3 and 1.0 cm in thickness and was analyzed for all bed parameters as a single sample.

Table 1. Wind speed and direction during field data collection.

				Morgan's Point		Eagle Point	
Year	Month	Day	Hour	Wind Direction (CW degrees from North)	Wind Speed (m/s)	Wind Direction (CW degrees from North)	Wind Speed (m/s)
2005	12	5	0	350	8.2	340	5.7
2005	12	5	1	340	7.7	340	5.7
2005	12	5	2	350	7.2	330	6.2
2005	12	5	3	350	6.7	340	6.7
2005	12	5	4	350	5.1	340	6.2
2005	12	5	5	10	6.2	330	5.7
2005	12	5	6	360	7.2	350	6.7
2005	12	5	7	360	6.7	350	6.2
2005	12	5	8	360	7.7	350	7.2
2005	12	5	9	360	7.2	340	5.7
2005	12	5	10	***	***	340	7.2
2005	12	5	11	***	***	350	6.7
2005	12	5	12	***	***	360	8.2
2005	12	5	13	***	***	340	6.2
2005	12	5	14	***	***	360	6.7
2005	12	5	15	***	***	350	6.2
2005	12	5	16	10	8.2	340	6.7
2005	12	5	17	360	8.2	350	6.2
2005	12	5	18	350	6.7	350	6.2
2005	12	5	19	20	8.2	360	6.7
2005	12	5	20	10	10.3	350	7.7
2005	12	5	21	360	8.2	340	6.7
2005	12	5	22	10	6.2	350	5.1
2005	12	5	23	360	6.7	340	4.6

Year	Month	Day	Hour	Morgan's Point		Eagle Point	
				Wind Direction (CW degrees from North)	Wind Speed (m/s)	Wind Direction (CW degrees from North)	Wind Speed (m/s)
2005	12	6	0	360	5.1	340	4.6
2005	12	6	1	10	4.6	360	4.1
2005	12	6	2	10	3.6	10	5.1
2005	12	6	3	30	2.6	360	5.1
2005	12	6	4	30	2.6	10	5.1
2005	12	6	5	30	3.1	30	6.2
2005	12	6	6	20	2.6	30	6.7
2005	12	6	7	30	2.6	40	6.2
2005	12	6	8	30	2.1	50	6.2
2005	12	6	9	30	2.6	50	6.2
2005	12	6	10	30	3.1	60	5.7
2005	12	6	11	60	2.6	60	6.2
2005	12	6	12	60	2.6	60	6.7
2005	12	6	13	60	3.1	70	6.7
2005	12	6	14	80	4.1	70	6.7
2005	12	6	15	80	3.6	60	7.7
2005	12	6	16	90	5.1	60	7.7
2005	12	6	17	110	5.7	90	7.2
2005	12	6	18	130	4.6	80	7.2
2005	12	6	19	140	6.2	90	6.7
2005	12	6	20	120	4.6	90	6.2
2005	12	6	21	130	5.1	90	5.7
2005	12	6	22	140	5.1	110	5.7
2005	12	6	23	130	5.7	120	5.1
2005	12	7	0	110	4.1	110	6.2
2005	12	7	1	100	4.1	100	5.1
2005	12	7	2	80	4.1	100	6.2
2005	12	7	3	80	6.2	40	5.7
2005	12	7	4	80	5.1	60	6.2
2005	12	7	5	90	5.1	***	***
2005	12	7	6	80	6.2	***	***
2005	12	7	7	80	6.2	***	***
2005	12	7	8	80	6.2	***	***
2005	12	7	9	80	6.7	***	***
2005	12	7	10	70	6.2	***	***
2005	12	7	11	70	6.7	60	8.8
2005	12	7	12	70	6.2	50	8.2

Year	Month	Day	Hour	Morgan's Point		Eagle Point	
				Wind Direction (CW degrees from North)	Wind Speed (m/s)	Wind Direction (CW degrees from North)	Wind Speed (m/s)
2005	12	7	13	70	6.2	60	8.2
2005	12	7	14	60	5.7	60	10.3
2005	12	7	15	60	4.6	60	8.8
2005	12	7	16	70	5.7	60	9.8
2005	12	7	17	80	6.2	50	6.7
2005	12	7	18	80	4.6	60	7.2
2005	12	7	19	80	6.2	40	7.2
2005	12	7	20	70	5.7	50	4.1
2005	12	7	21	30	2.1	60	5.1
2005	12	7	22	30	3.1	20	3.6
2005	12	7	23	360	3.1	20	5.1
*** Indicates missing data.							

Suspended Samples

Salinity and suspended sediment concentration were determined for all water samples taken during the data retrieval. In deeper areas, two samples were taken – one at 3 ft (0.914 m) and another at 6 ft (1.83 m) in depth. The values given in Figures 3 and 4 are for the 3-ft (0.914-m) samples since that depth was taken at all sample locations.

The surface salinity is shown in Figure 3. The surface salinity is largest near the channel; and salinity tends to be higher on the western side of the channel than on the eastern side. This situation has been reported in prior studies. There is a large amount of fresh water entering the system from Trinity River and saline ocean water penetrates the bay along the Houston Ship Channel.

Figure 4 shows the surface suspended sediment concentration. Winds during data collection were generally from the north to the northeast. The suspended sediment concentrations tended to be higher toward the south and west as one would expect from wind wave suspension and boundary erosion. Although the winds ranged between 5 and 10 m/s (11-22 mph), the suspended sediment concentrations of the samples taken were not extremely high, indicating that winds of this magnitude are not high enough to generate much resuspension of the bed material.

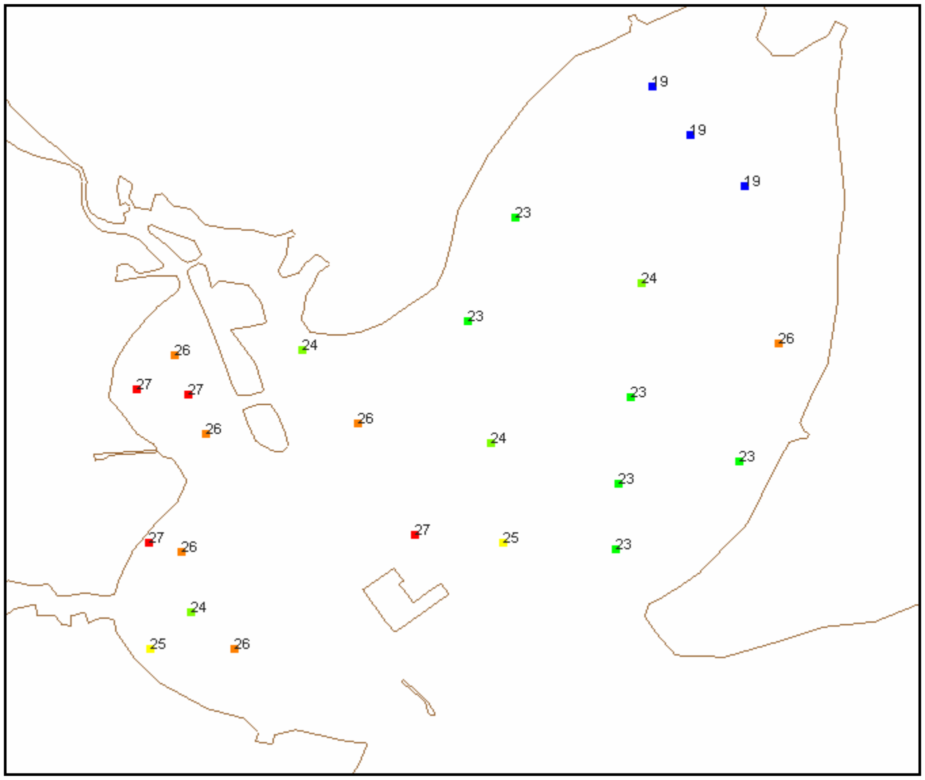

Figure 3. Salinity (ppt) at a depth of 3 ft.

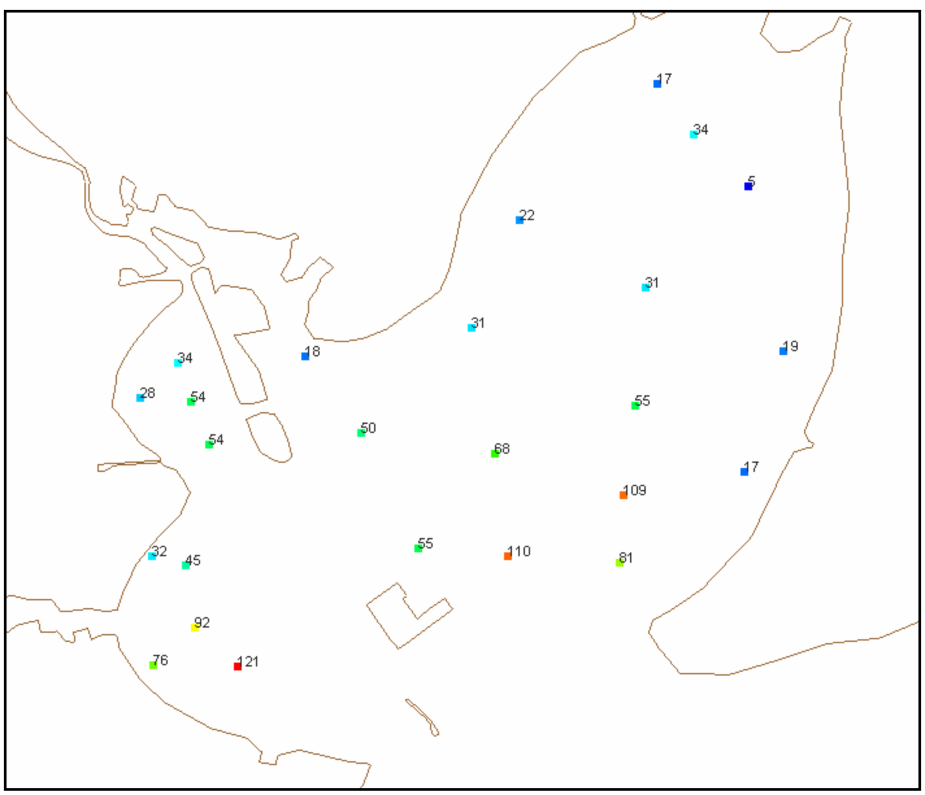

Figure 4. Suspended sediment concentration (mg/L) at a depth of 3 ft.

Bed Samples

The bed samples were taken using a 3-in.-diameter push core sampler at all field data locations. These samples were visually analyzed for layering, and then the layers were tested to determine bulk density, moisture content, and organic content. Selected samples were placed in the Vertical-Loop Sediment Water Tunnel (VOST) to determine erodibility parameters. All samples contained a 0.3- to 1-cm layer of oxidized material on the surface. This layer is distinguishable by its color (brown) and its low density. Figures 5 and 6 show this layer on the surface of the bed sample.

Figure 5. Bed sample in push core tube.

Figure 6. Bed sample after being extruded from the push core tube.

The oxidized layer material was combined from all samples and analyzed as a single sample. Its properties are given in Table 2 below.

Table 2. Properties of oxidized layer material.

Oxidized Layer	
Bulk density	1.234 g/cm^3
Moisture content	224.65% water mass/dry mass
Percent organics	6.823%
Mean grain size	8.944 μm

The bulk density for the top bed layer, below the oxidized layer, for the entire sample set is shown in Figure 7. The distribution of spatially averaged density by depth into the bed is given in Figure 8.

The bulk density is higher in the shallower regions along the edges of the bay, and is quite low in the center of Trinity Bay. This is consistent with wind wave resuspension. The waves would tend to erode and remove softer materials. Near the channel the density is higher, probably because of the vessel-generated waves and stresses as well as waves and stresses derived from the wind.

The bed samples were analyzed for moisture content and percent organics. The top layer, below the oxidized layer, values are shown in Figures 9 and 10 for all sample locations.

The moisture content is calculated as a percentage of sample water mass to the sample dry mass. The moisture content is inversely related to the bulk density. High moisture content implies a low bulk density. Along the bay edges the moisture content is typically low. However, in the center of Trinity Bay the moisture content is large.

The percent organics is shown to be inversely related with bulk density as well. The center of the bay is higher in organics than the area along the margins of the bay.

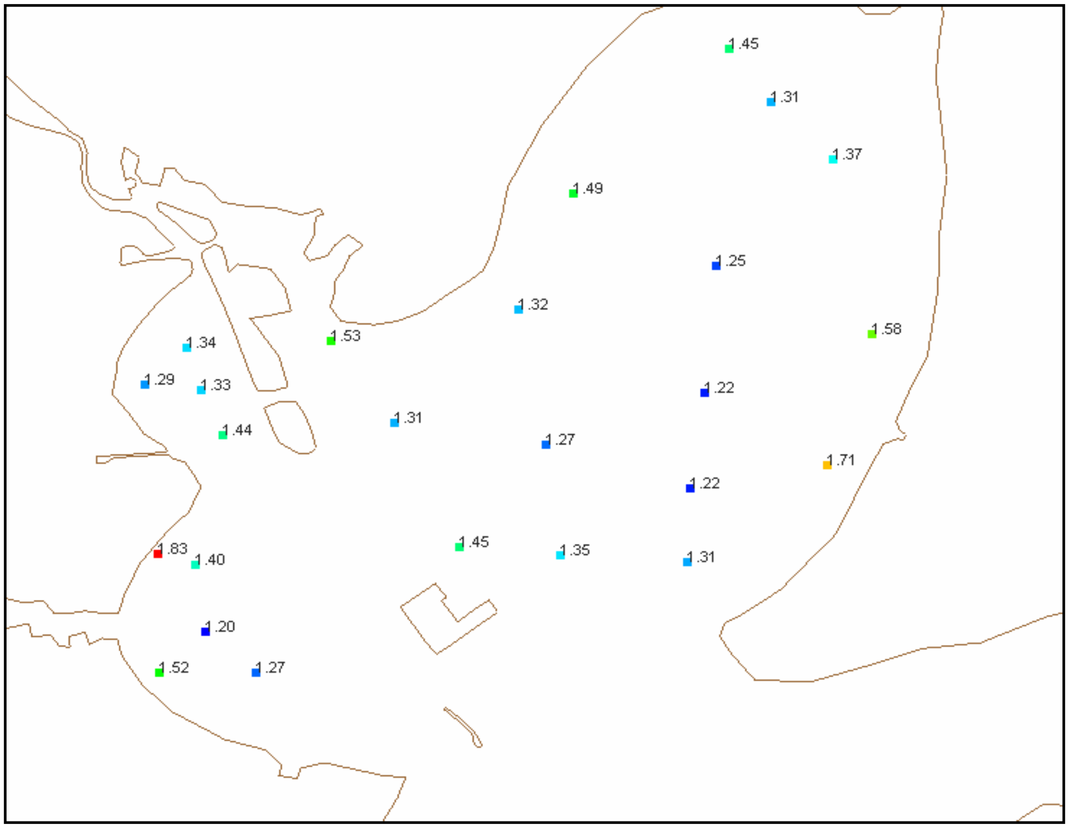

Figure 7. Bulk density (g/cm³) for the top layer (beneath the oxidized layer) of the bed samples.

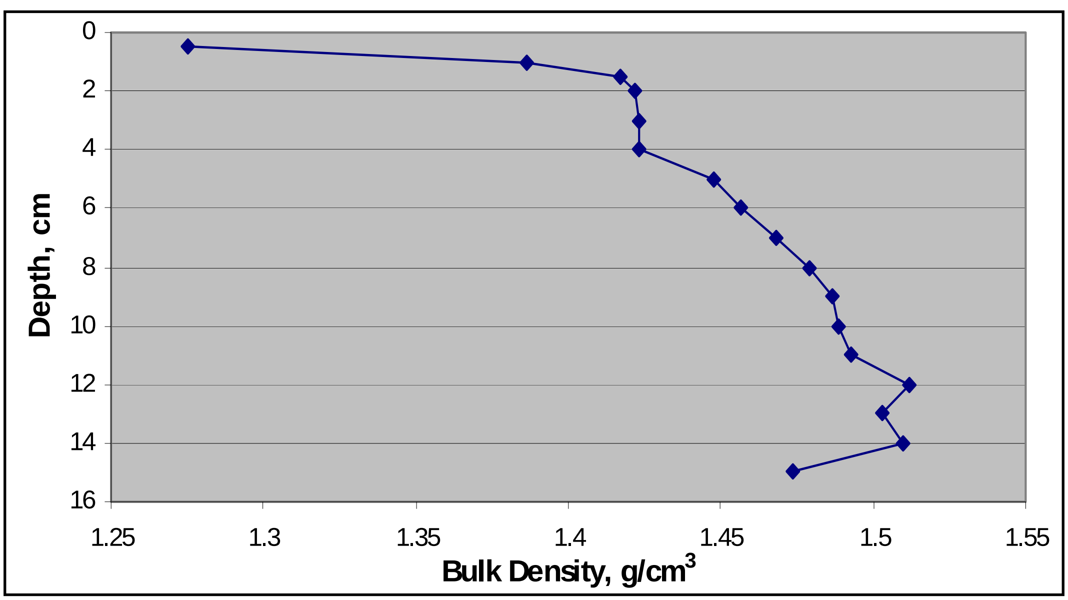

Figure 8. Spatially averaged bulk density in relation to bed depth (not including the oxidized layer).

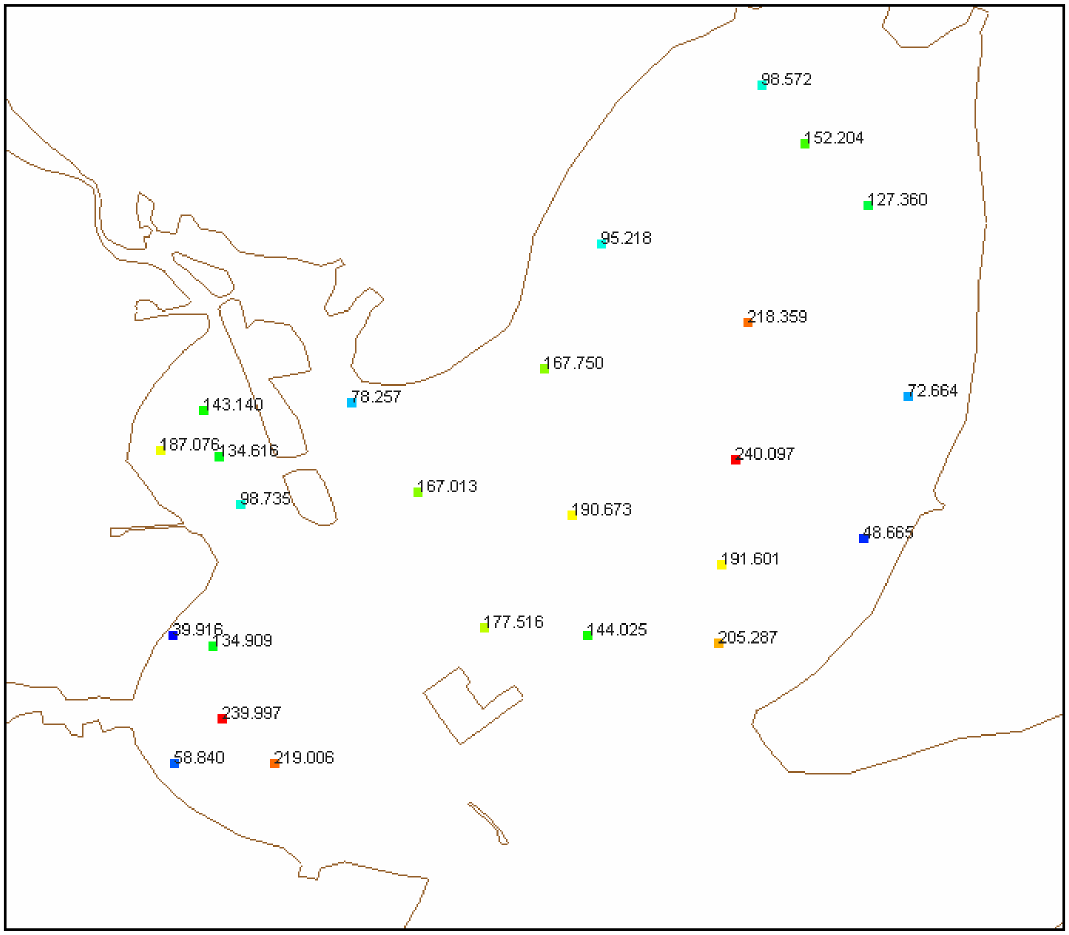

Figure 9. Moisture content for the top layer (beneath the oxidized layer) of the bed samples.

The particle sizes in the range of 0.4 to 100 µm were measured using a Coulter LS 100Q instrument, which uses laser near-forward scattering to estimate particle size. The grain size measured as the largest volumetric fraction of the sample for the top bed layer, below the oxidized layer, for the entire sample set is shown in Figure 11. This is the grain size that makes up the largest percentage (mode) of the sample. Figure 12 shows the 50 percent finer grain diameters with respect to the bed depth when averaged spatially over the entire domain. The mean grain size for all samples taken is 20.26 µm. The system is dominated by clay and fine silt fractions with only a few samples having high volumetric fractions of large silt and fine sand size classes and those higher fractions were found along the edges of the domain in shallow areas. Several of the samples were analyzed deeper into the bed (labeled as bottom samples, as in Figure 14). These results show large percentages of grain classes in the fine sand range – greater than 62 µm. Fine sands were also found in the oxidized layer.

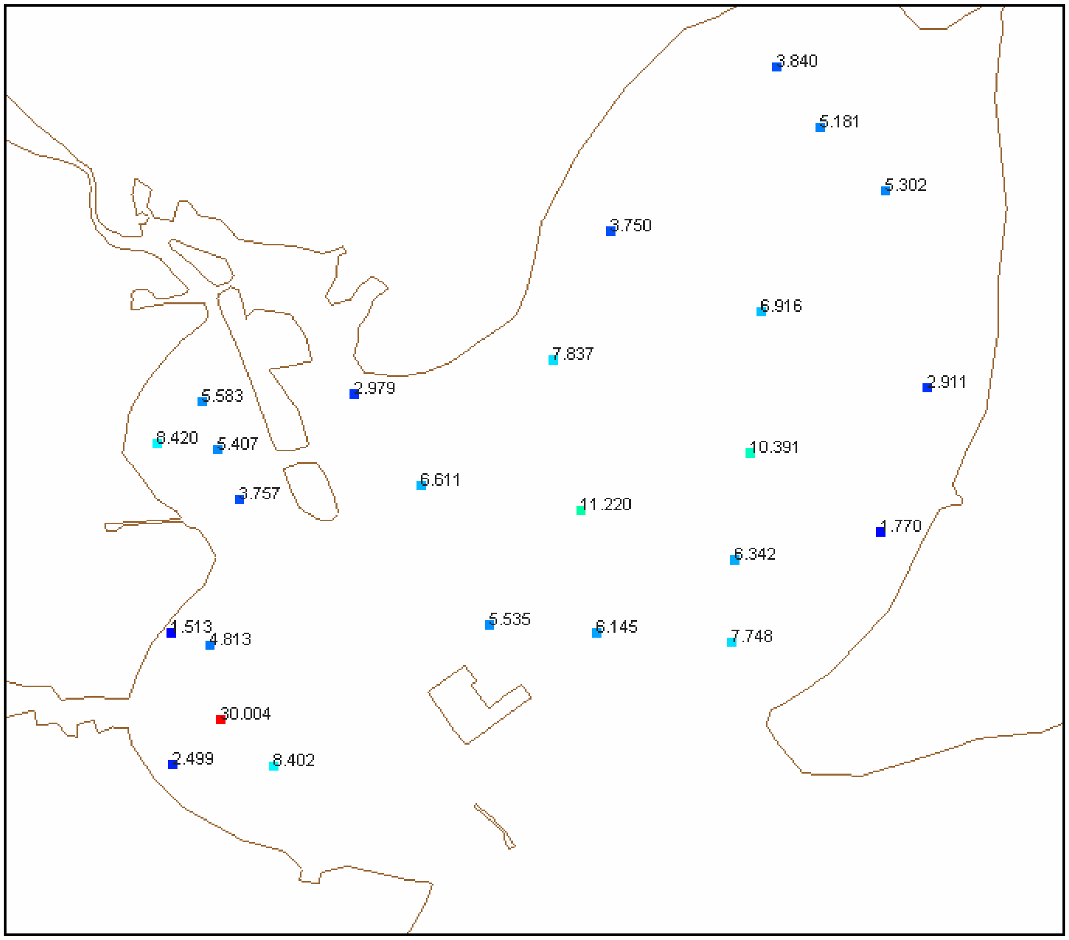

Figure 10. Percent organics (% LOI) for the top layer (beneath the oxidized layer) of the bed samples.

Figures 13 and 14 show the variation in grain size distribution with depth for one of the samples, the southernmost point in Eastern Trinity Bay labeled as B5 in Figure A1. Figure 15 shows the grain size distribution for the oxidized layer. The peaks of the curves indicate the size classes present in the greatest percentages.

Field data taken in August 2004 indicated that the bulk density of the bed on the western side of the Houston Ship Channel just south of Morgan's Point was 1.5 g/cm^3 (Tate et al. 2006). The samples taken in December 2005 indicate that the surface samples had a bulk density of 1.3 g/cm^3, whereas samples 7 cm below the surface had a value of 1.5 g/cm^3. The August 2004 samples contained some sands as well. In this data collection period this location also had a large percentage of fine sands in the lower layer and none in the top layer. At this time (2005) it is noted that there is a lower density layer above a firm layer throughout much of the bay. The weaker top layer (beneath the oxidized layer) is almost completely silts and clays (little to no sand). The deeper layer does contain significant amounts of fine sands. The deeper layer seems more in agreement with the surface samples from August 2004. It is possible that some major event has stirred up the bed and resulted in the finer material dominating the top layers. Perhaps this is a result of Hurricane Rita which produced nearly 40 knot (20.6 m/s, 46 mph) winds in Galveston Bay in late September 2005.

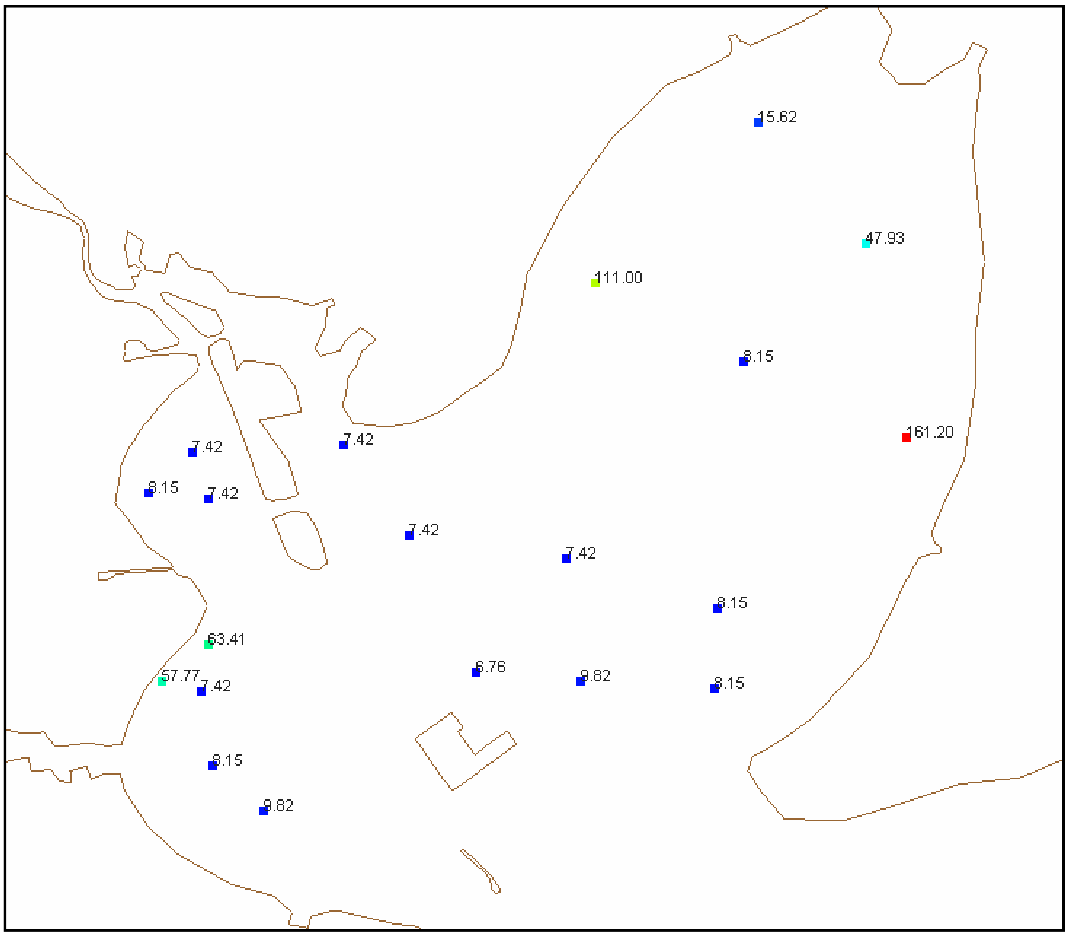

Figure 11. Grain size representing the mode of the top layer (beneath the oxidized layer) of the bed samples (0-4 μm is clay, 4-62 μm is silt, > 62 μm is fine sand).

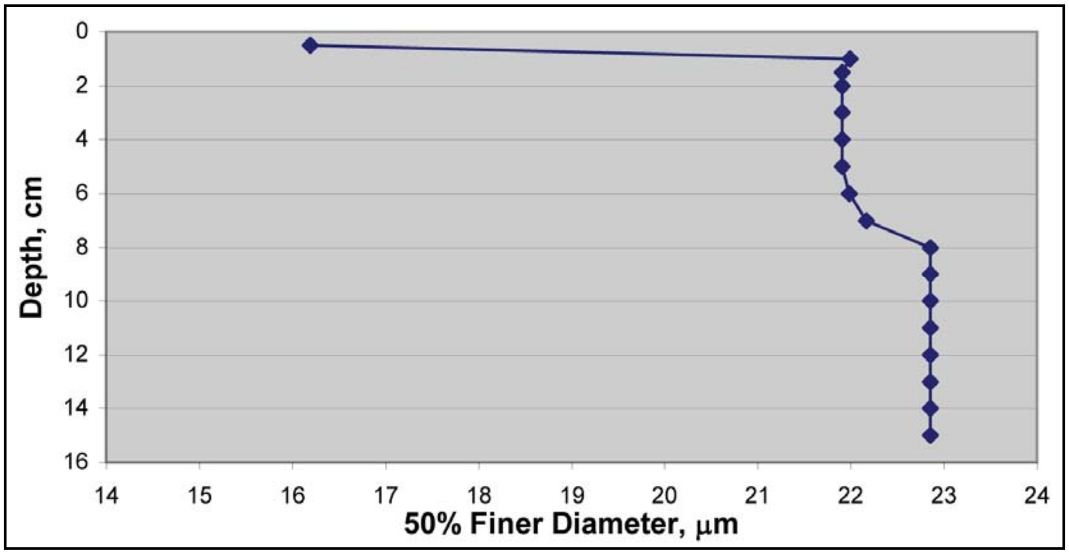

Figure 12. Spatially averaged D50 with respect to depth.

Erodibility parameters were determined by testing bed samples in the VOST. The VOST consists of two rectangular horizontal and two circular vertical sections arranged in a vertical plane. Flow in the VOST is driven by a propeller pump in one of the two 15.24-cm-diameter circular sections. The horizontal tunnel sections are 7.6 cm high by 24.1 cm wide. The test material is placed in a cylindrical sample holder that has an area of 42 cm^2. The flow cross-sectional area averages 183 cm^2 and the flow length around the VOST is 3.5 m. The volume of the system is 64 L. The propeller pump is 2.6 m upstream from the bed sediment sample tray. Flows in the VOST are up to 1.54 m/s, generating a maximum average shear stress of almost 3 Pa. Shear stresses in the VOST were increased hourly from 0.2 to 0.98 Pa, at which all samples began to fail by pitting of the sample surface. These aggregates remained on the surface of the flume, without complete suspension into the water column. Some samples were run beyond the initiation of pitting on the surface to shear stresses as large as 1.45 Pa. All tests, however, were stopped when the sample casing became exposed because surface exposure creates changes in the near bed flow and, therefore, inaccurate conclusions of erodibility. The critical shear stress for erosion is determined from the lowest shear that produced this pitting. However, since the failure mechanism did not result in suspension into the water column, it was not possible to accurately estimate the particle erosion constant. This will be estimated through other data and model runs.

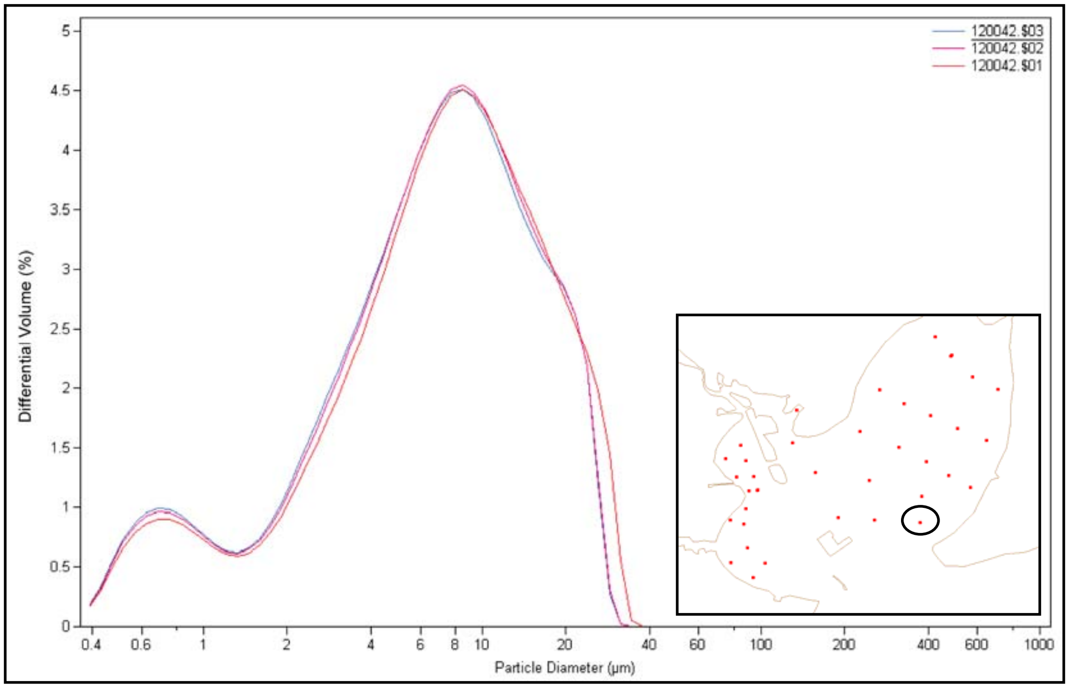

Figure 13. Grain size distribution for the top sample of the southernmost point in Eastern Trinity Bay. Shown are three tests performed on one sample.

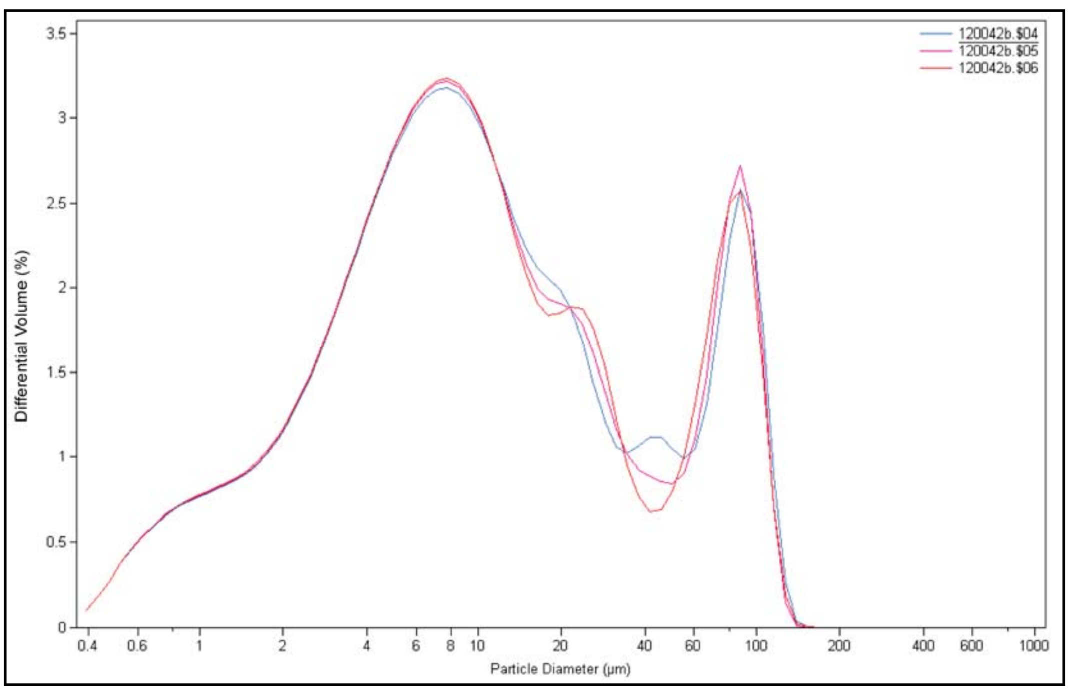

Figure 14. Grain size distribution for the bottom sample of the southernmost point in Eastern Trinity Bay. Shown are three tests performed on one sample.

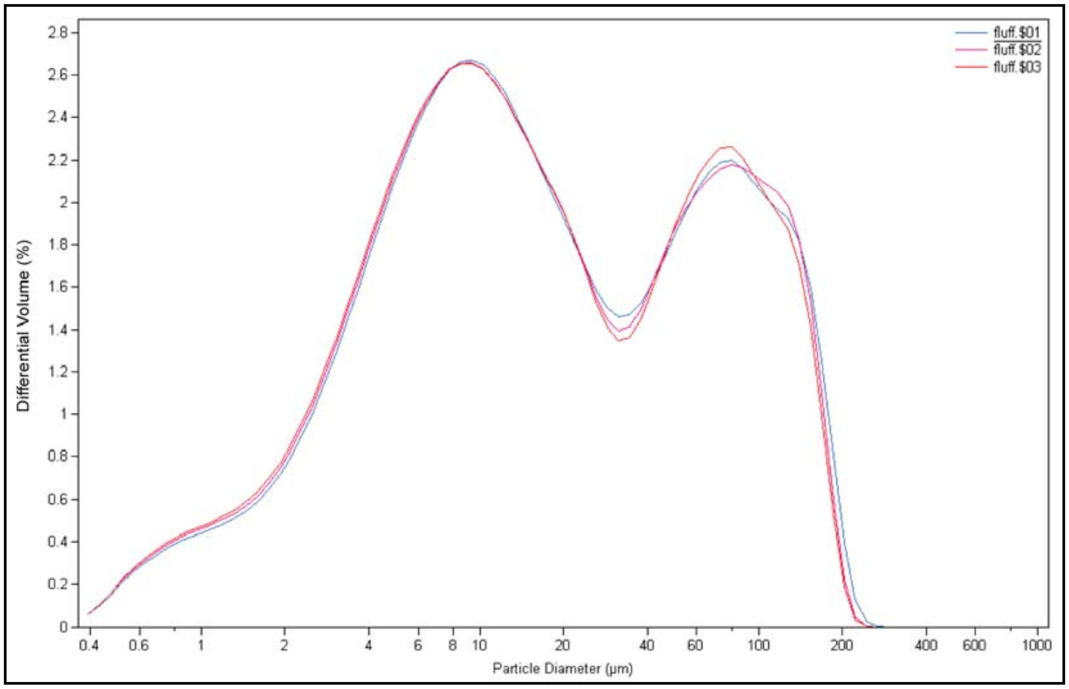

Figure 15. Grain size distribution for oxidized layer sample, combined from all locations. Shown are three tests performed on one sample.

3 Sediment Model

Sediment model validation is necessary to develop a tool that can be used to direct future engineering decisions. The validation process determines the bed and sediment properties necessary to match field data and accurately reproduce the physical properties occurring within the system. Initial properties are based on the analysis of field data. These properties are varied within their uncertainties in order to determine the values that best match the known field conditions during the validation period. The model simulation is run with TABS-MDS, a finite element numerical model for 3-D hydrodynamics and salinity as well as suspended sediment transport and bed changes. This model has been widely used by ERDC to model 3-D hydrodynamics and salinity at numerous locations, including Galveston Bay (Berger et al. 1995a,b). The hydrodynamic and salinity simulation is performed first to obtain the velocities, water depths, and salinity gradients used to drive the sediment runs. The sediment simulation is also run with TABS-MDS using bed characteristics taken from the field data analysis. The sediment inflow concentrations are based on rating curves generated from historic loads for the two major rivers entering the system, the Trinity River and the San Jacinto River. The results of these runs are analyzed for the magnitude and pattern of deposition along the channel and in the shallow areas, as well as for their agreement with suspended sediment samples.

Model Conditions

The model domain was maintained from the previous studies and validated hydrodynamic model (Berger et al. 1995a). The grid resolution within the bay portions of the model was increased in order to more accurately capture the sediment gradients in those areas. The model area begins at the Gulf of Mexico, and includes the Houston Ship Channel from Bolivar Roads, beyond the entrance of the San Jacinto River, as well as Trinity Bay, Galveston Bay, East Bay, and West Bay (see Figure 16).

Hydrodynamic Model Conditions

The simulation years are selected from the historical dredging records. The most recent dredge period before the channel enlargement was selected as the validation period and two water years were selected to be run: a high flow year – water year 1995 (October 1994 – September 1995), and a low flow year – water year 1996 (October 1995 – September 1996). Figure 17 shows the flows for the two major rivers entering the system, the San Jacinto River and the Trinity River, for both water years.

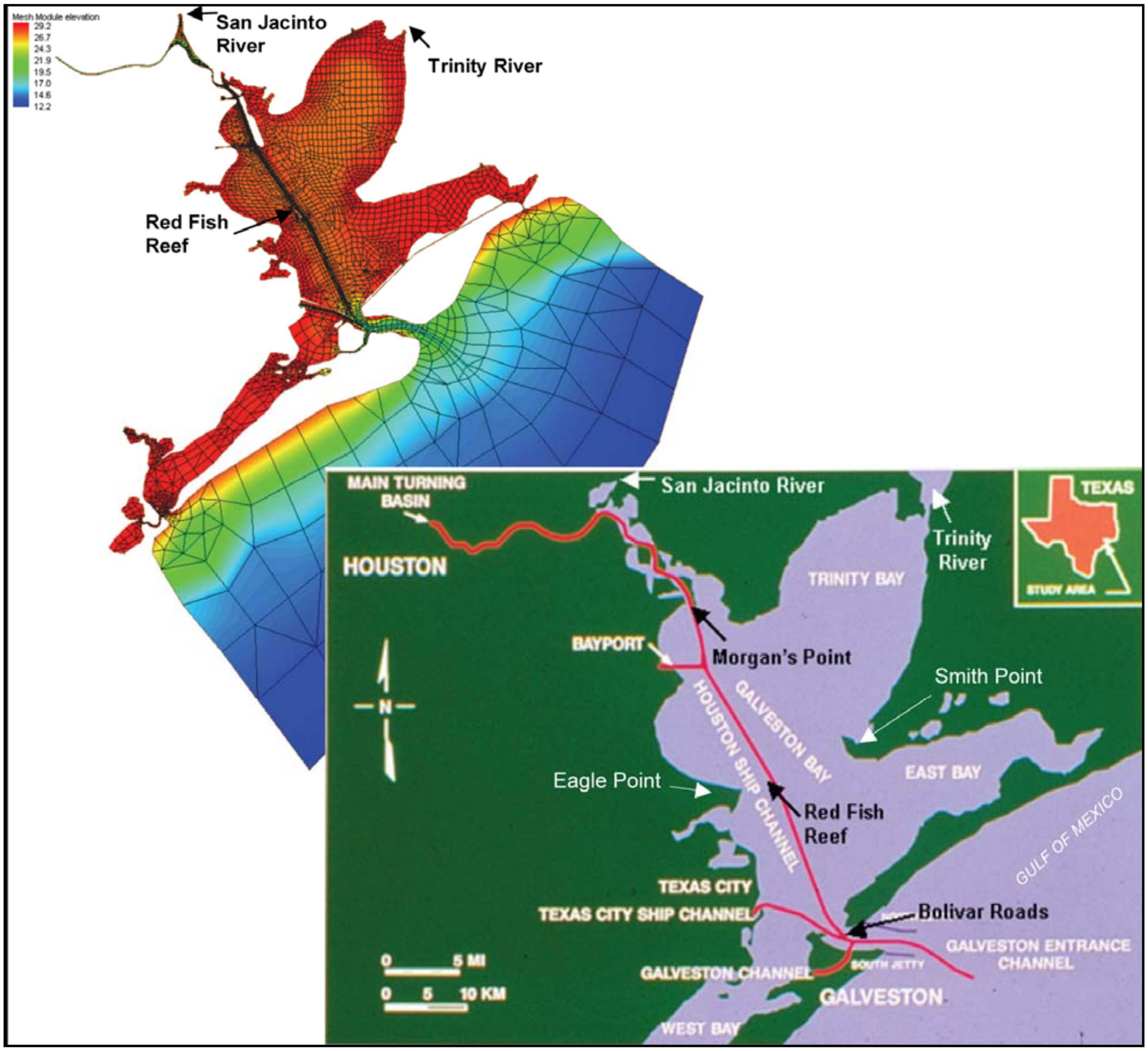

Figure 16. Houston Ship Channel model domain and area map.

The boundary conditions for these years are applied to the model in the same way as in the original validation study (Berger et al. 1995a). The wind data at Houston Intercontinental Airport are applied for the same time period and modified to be representative of winds over water as in the original model validation. Figures 18 and 19 show the wind speeds in miles per hour for both flow years. The tide data are taken at Pleasure Pier and shifted 1.31 hours as previously done. The inflows for the hydrodynamic model are taken from several gauge sites and incorporated into the primary tributaries entering the system in the same manner as in the validation study to ensure continued accuracy.

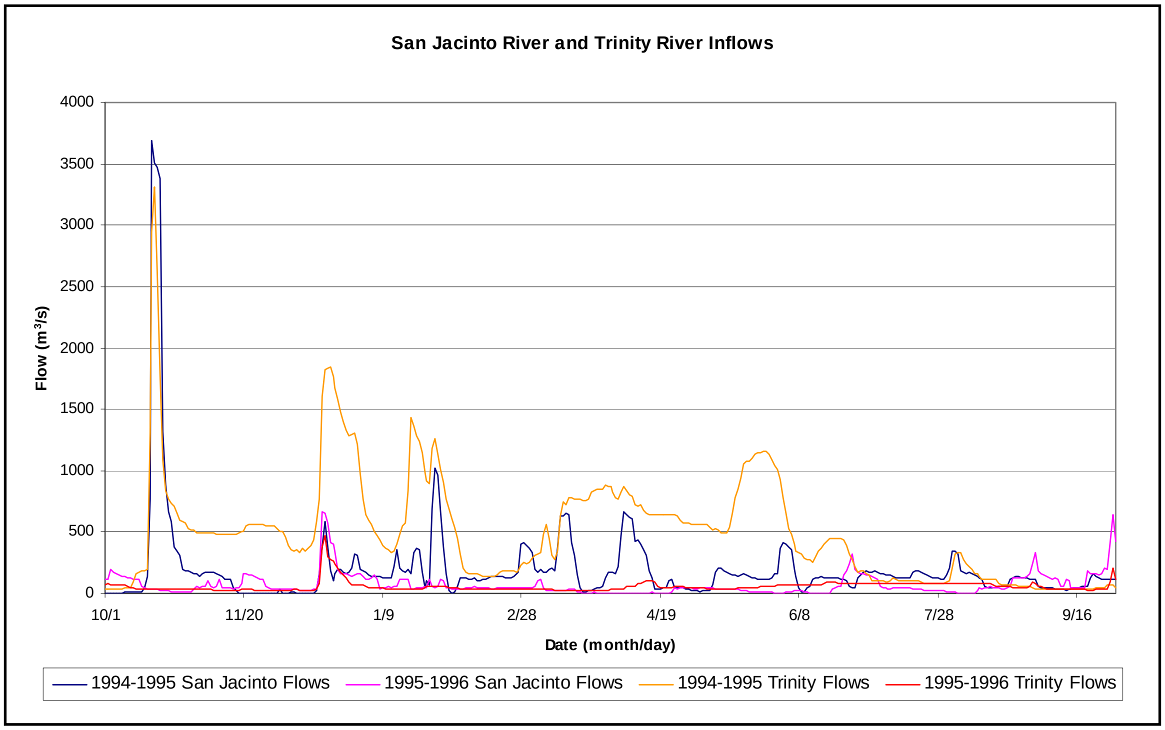

Figure 17. Flow data on the major rivers for both simulation years.

Sediment Model Conditions

The model is first run simulating only the hydrodynamics and salinity. Once these solutions are obtained, they are used to drive the sediment model. The sediment model is then run in an uncoupled fashion; that is, the change in bed and sediment concentrations are not allowed to affect the flow. This is reasonable because the concentrations and bed changes are relatively small. The sediment model includes the sediment loads for the two major rivers as well as the initial bed conditions. The bed character is based upon the field data analysis as well as the erodibility parameters.

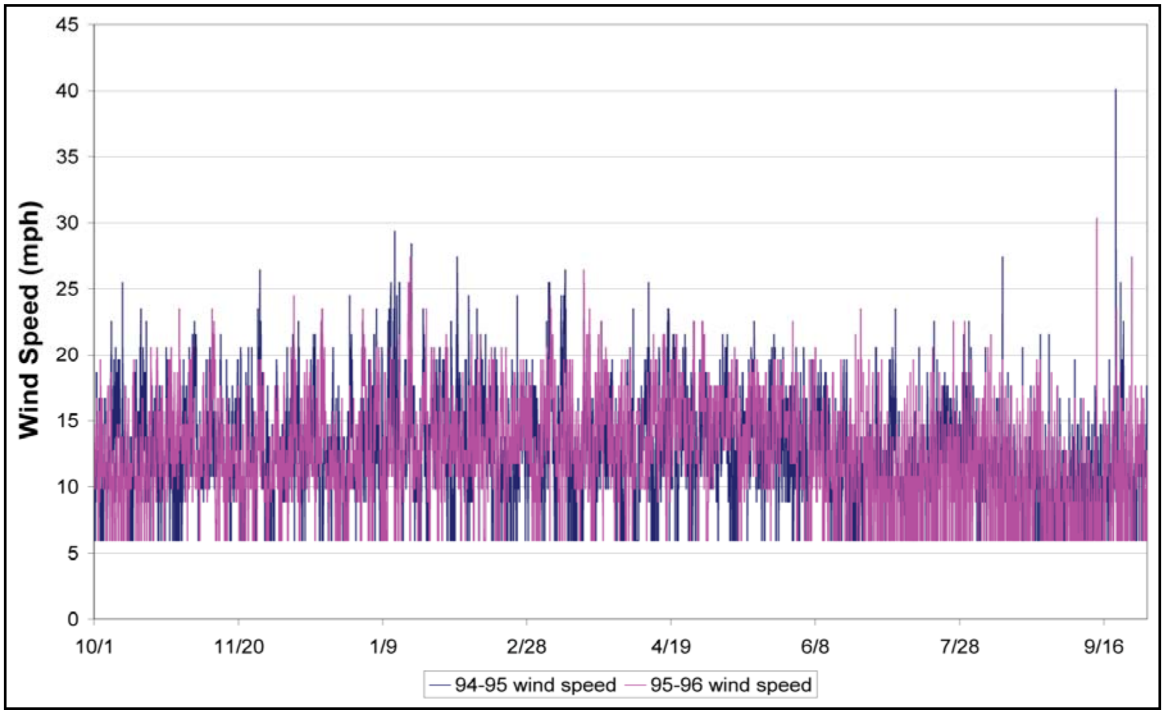

Figure 18. Wind data for both flow years.

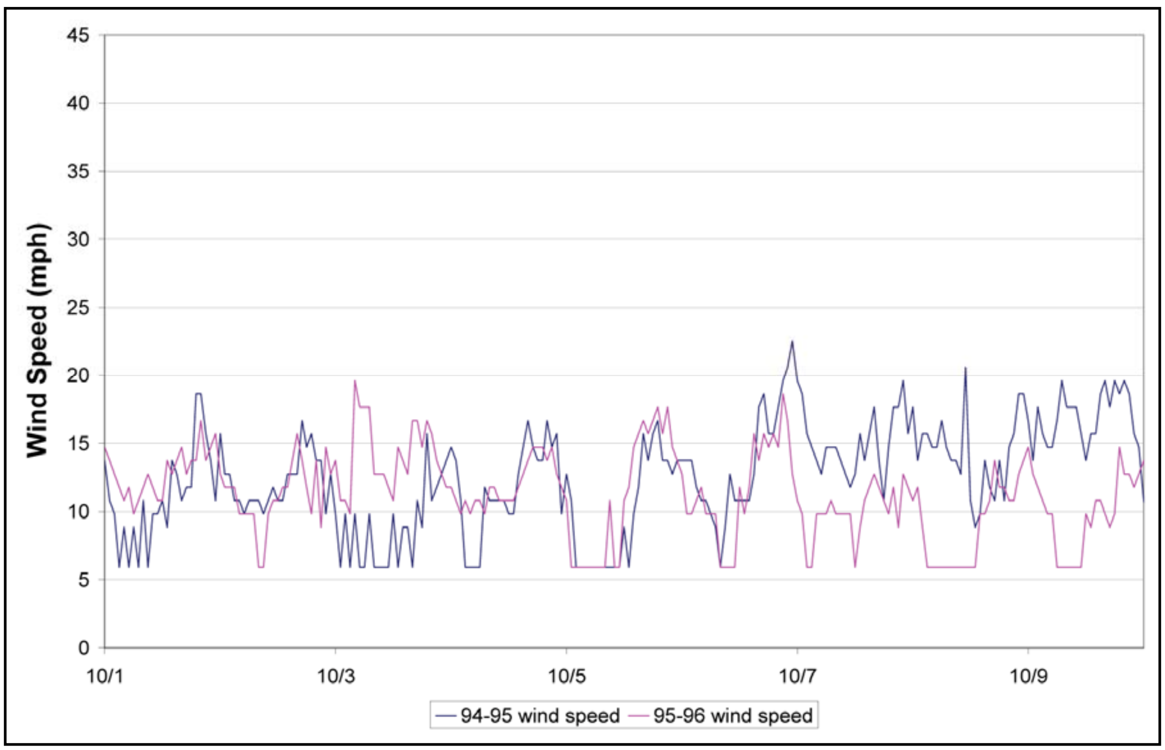

Figure 19. Wind data for both flow years (10 days).

The incoming sediment loads for the two rivers are obtained from historical data available from the U.S. Geological Survey (USGS). A sediment load rating curve is generated for each river from the available historical load data so that the appropriate load can be determined for flow rates entering the system. The Trinity River rating curve is generated from data taken in 1994 and 1995. The San Jacinto River rating curve includes data from 1965 to 1994 because there are not enough data during the most recent time frame. Figures 20 and 21 show the sediment loads applied at these river boundaries for the high flow water year and the low flow water year, respectively. The field data indicated that the sediment in the area is primarily clays and fine silts. Through model tests and adjusting parameters based on comparison to observed data, the inflow sediment is applied as 50 percent cohesive material (clay) and 50 percent silt material.

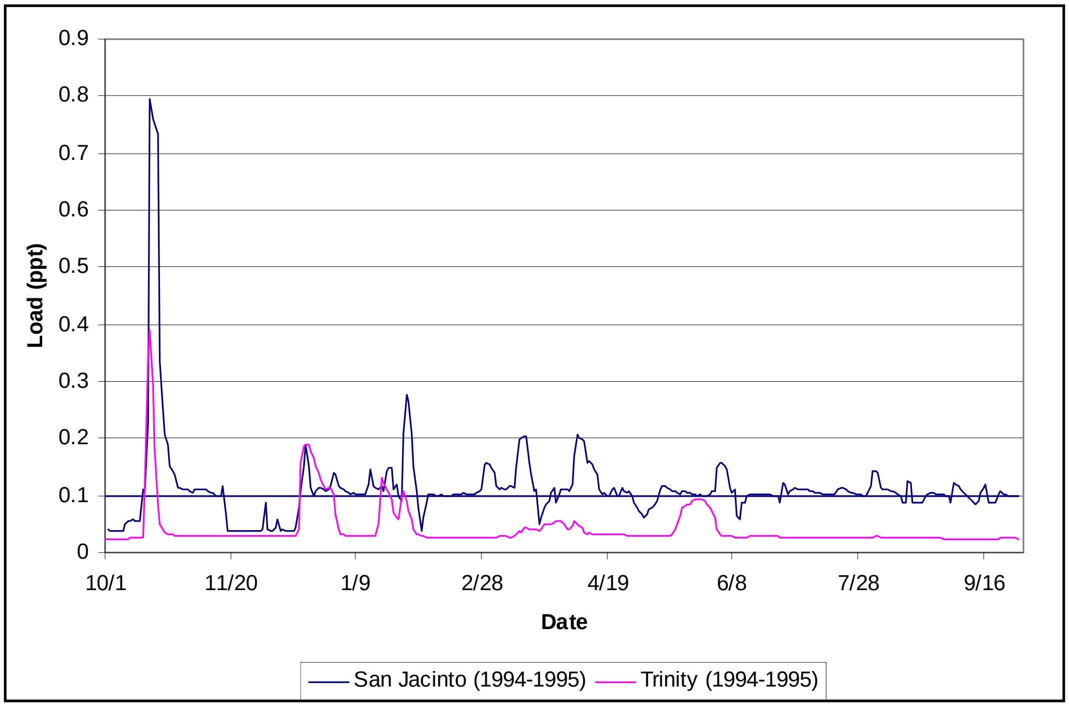

Figure 20. Sediment loads for the two major rivers for water year 1995.

The bed material is defined based on the field data sampling described in Chapter 2. The model bed is for the most part defined as four layers determined from the bulk density distribution by depth (see Figure 8) with the uppermost layer being largely the oxidized material of 0.5 cm with a density of 1,275 kg/m^3. The bed material is also divided into 50 percent silt material and 50 percent cohesive material. The characteristics of all four layers are given in Table 3.

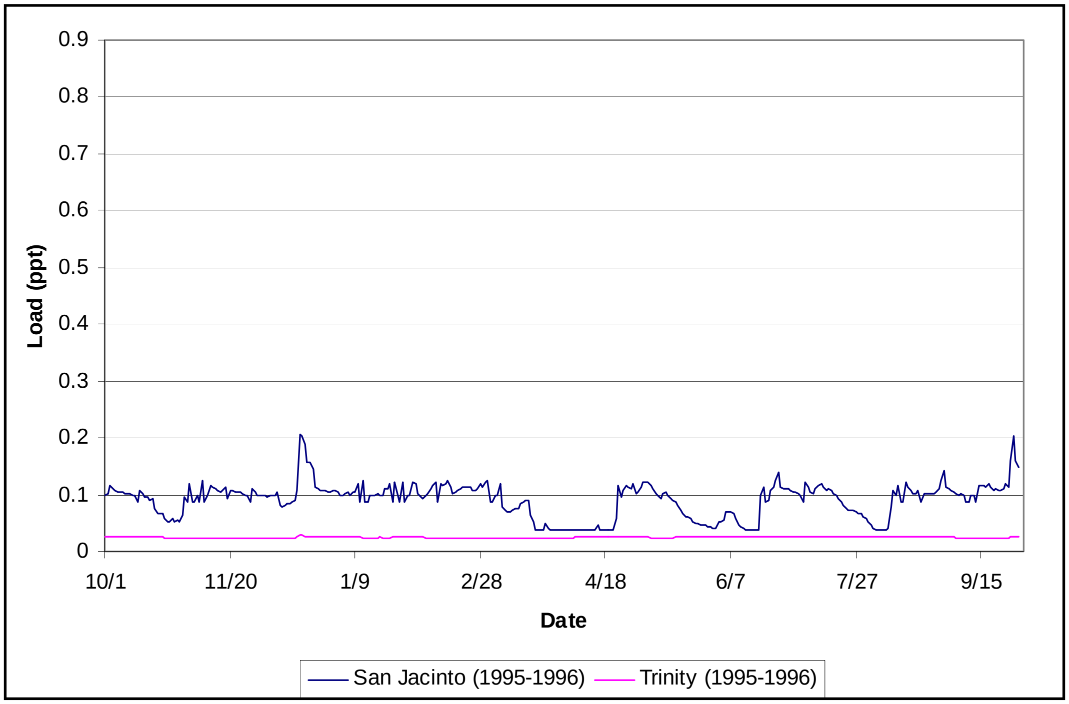

Figure 21. Sediment loads for the two major rivers for water year 1996.

Table 3. Bed layers and properties.

Layer (from bed surface)	Thickness (cm)	Density (kg/m^3)
1	0.5	1275
2	3.5	1414
3	7	1475
4	4	1500

The roughness for the various materials matches those developed for the hydrodynamic simulation except immediately adjacent to the model boundaries. The model boundaries are set such that they remain wet at all times. This is not the case in the field since the depth at the boundaries will vary with the changing tide and winds such that the erosion potential of these areas is actually greater. This forcing of erosion is done by increasing the bed roughness in these areas so that the critical shear stress for erosion will be exceeded along the model boundaries in order to match known field conditions. In the area of Bolivar Roads where the Gulf of Mexico meets Galveston Bay, the bed is sand in nature and therefore also in the model. The rest of the model domain is defined according to the field conditions, and the density of the bed material is such that no erosion will occur over much of the model domain.

The values of the sediment parameters determined during the sediment model validation are given in Table 4. These parameters were adjusted several times to determine model sensitivity as well as the combined impact of the various parameters. Comparison to suspended sediment data and the historical dredging records is used for this determination.

Each water year is simulated separately with the model having an initial suspended sediment concentration of 0 ppt and an initial bed displacement of 0 m.

Table 4. Sediment parameters and values used for validation.

Parameter	Value
Critical shear for deposition of cohesives	0.05 Pa
Critical shear for erosion of the cohesives	0.1 Pa
Settling velocity of the cohesives	0.05 mm/s
Particle erosion constant for the cohesives	3.84×10^{-5}
Critical shear for deposition of the silts	0.1 Pa
Critical shear for erosion of the silts	0.67 Pa
Settling velocity of the silts	0.22 mm/s

Sensitivity Analysis

In order to verify that the parameters chosen for the validation runs are the best suited to match the field data, a sensitivity of the model to several parameters is tested. The critical shear for deposition of the silts, a parameter that is not determined from the field data analysis, is varied 10-20% above and below the selected 0.1 Pa. The results of this sensitivity are that this term has a very slight effect on the distribution of shoaling along the channel as well as in the suspended sediment concentrations in Trinity Bay, but the model is overall insensitive to this parameter. The settling velocity for the silts is varied as well. This parameter affects the model results much more than the critical shear for deposition. The settling velocity greatly affected the amount of sediment reaching the channel, the deposition in the shallows, and the suspended sediment concentrations. The settling velocity chosen for use in validating the model was the value that best reproduced the shoaling pattern along the channel while remaining within the acceptable range of settling velocity values. Since the Trinity Bay area and locations upstream of Red Fish Reef experience very little bed erosion, the model is not sensitive to parameters that affect the erosion of the bed. The critical shear for erosion of the silts and cohesive material and the particle erosion constant for the cohesive material are varied and the model results are unaffected when the parameters are within the range of reasonable values.

Initial Model Results

The model suspended sediment concentration and distribution of channel shoaling for each of the water years are compared to the field data for suspended sediment concentration and the historic dredging records. Since sediment is an event driven process, the high flow water year will likely produce more shoaling and give a better indication of the paths of sediment transport due to the higher flow conditions and larger sediment loads. However, the low flow water year can give an indication of the other processes that may affect the shoaling in this area. When the flows are low, deposition can occur more easily. The shoaling pattern for both high and low flows is necessary to understand the overall picture of how the sediment behaves in the area . The suspended sediment concentrations are compared to historic field data during the time of the simulation at several locations. The rate of shoaling in the channel along Atkinson Island is compared to the 4 year historic rate of shoaling from the dredging records during the simulation period. Finally, the distribution of shoaling along the channel is compared to the 34 year historic pattern determined from the dredging records.

This initial validation process for the sediment model of the Houston Ship Channel and Trinity Bay area produced good agreement with suspended sediment concentrations and shoaling distribution along the channel. The shoaling rate within the channel for the high flow water year is much lower than the historical rate and the model also initially indicates shoaling along the shallows just outside of the channel in locations where it is not seen in the field. One feature not included in this initial model validation is the effect of navigation on the shoaling within the channel. The movement of a vessel has the capability to generate large shear stresses on the bed beyond the channel so that its effects extend out into the shallows. The vessel traffic in the Houston Ship Channel is likely to be a significant factor in the rate and magnitude of shoaling in the channel. With this in mind, direct modeling of vessel effects are included in the sediment model. The next section describes this process.

Sediment Transport Pattern

The Houston Ship Channel and Trinity Bay area is a depositional environment. The critical shear stress for erosion, which causes the bed material to erode from the bed and become suspended, is rarely exceeded with the typical flows and wind-induced wave effects except in shallow areas or when generated by moving vessels.

Figure 22 shows the maximum bed shear stress at each point over the entire year-long simulation of the high flow water year. These bed shears are due to the hydrodynamics and wind induced effects only - they do not include vessel effects. The figure is contoured between 0.1 Pa, the critical shear stress for deposition of the silts and critical shear for erosion of the cohesive material, and 0.67 Pa, the critical shear stress for erosion of the silts. Areas shaded in red are equal to or greater than 0.67 Pa and will experience erosion of the bed at some time during the year; it could occur once or repeatedly. All other areas will only experience deposition of the silts since the maximum shear stresses are below the critical shear stress for erosion, but can experience erosion of cohesive material at some point in the simulation. Although the areas shaded in green will hinder deposition more than those shaded in blue, the magnitude of deposition in these areas is dependent on the sediment supply reaching each location. The red areas near Morgan's Point and the upper section of Atkinson Island were generated during the high flow event near the start of the run (see Figure 17). The bed shears due to the hydrodynamics in this area never exceeded the critical shear stress for erosion of silts after that flow event.

The wind-induced waves can often have a large impact on the erosion of the bed. However, in this area that is not the case under typical conditions since the wind wave induced shear is included in Figure 22 and these open areas in the center of the bays did not experience erosive shears. This is supported by the field data as well. During the field data collection in December 2005, the winds typically ranged between 5 and 10 m/s (11-22 mph). Even with wind speeds of this magnitude, the suspended sediment concentrations in samples taken were not high – they rarely reached 100 mg/L. These values indicate that extremely high winds, such as hurricane force, would be necessary to generate erosion of the bed. This appears to confirm the shear stress calculations from the model simulations.

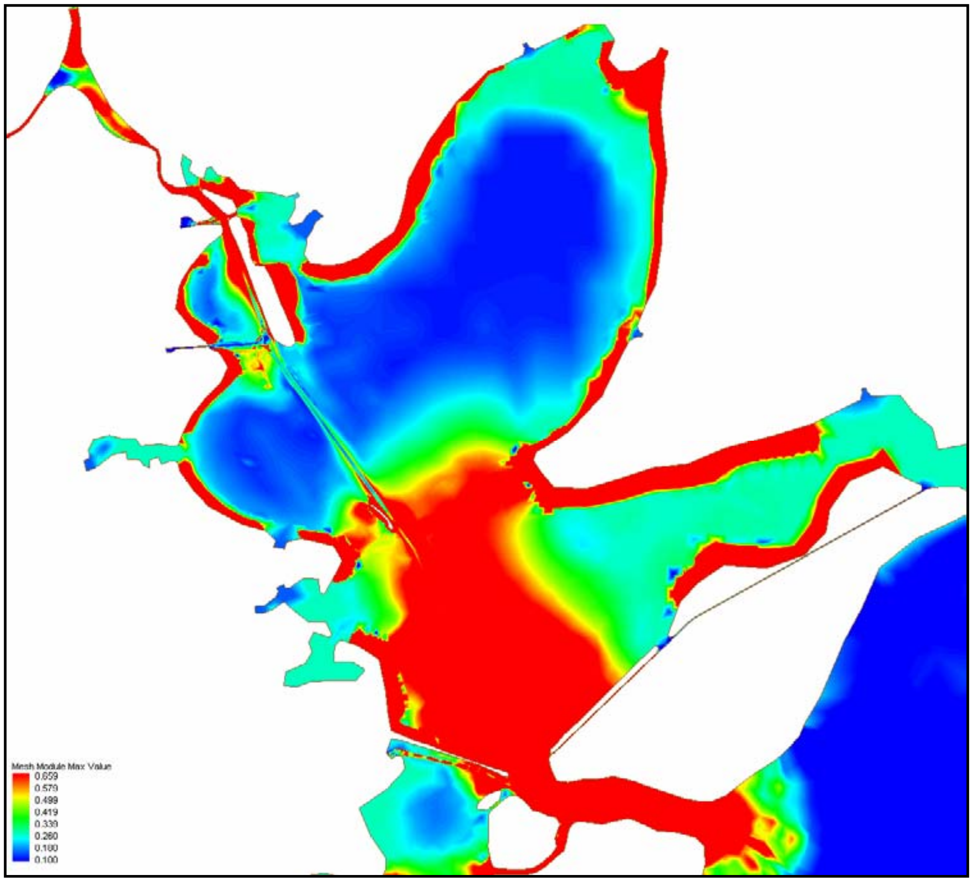

Figure 22. Maximum bed shears (Pa) generated during the high flow simulation.

Sources of Channel Shoaling

The shoaling that occurs within the model domain comes from several sources. The Trinity River and San Jacinto River introduce sediment to the system from upstream. The shallow edges of the bay can be eroded due to wave action, supplying sediment to be transported within the system. The impact from each of these sources of shoaling will vary along the channel and with varying flow conditions. In order to determine the importance of shoaling generated from each of the sources, the model is run independently with each source of channel shoaling and not including any effects due to the vessel movement.

Using the high flow water year (1995), the concentration of sediment from each of the river systems is removed to assess the significance of each. Both rivers' sediment concentration is removed to note the importance of bed erosion in the shallows. The river inflows are still included, just set to contain a sediment concentration of zero. These runs allow for the visualization of how and when various processes dominate the shoaling in the channel. Figure 23 shows the displacement along the ship channel at the end of the year-long run for the original case (with all sediment loads – light blue line), the case with only the San Jacinto sediment load (dark blue line), the case with only the Trinity sediment load (green line), and the case with no sediment loads - only boundary erosion (pink line). There are obvious differences in the overall amount of deposition and the pattern of deposition along the channel for each of the sediment load conditions. Without the loads from the San Jacinto River, the peak deposition occurs around Red Fish Reef. There is much less shoaling along Atkinson Island. The shoaling that is occurring in this upstream region is caused by the erosion of the boundary edges. The Trinity River loads move downstream through the bay and occasionally enter the channel near Red Fish Reef and Smith and Eagle Points. Once in the channel, the sediment will tend to drift upstream because of the upland direction of the residual currents until it settles to the bed. This time in suspension is determined from the settling velocity of the particles as well as their critical shear stress for deposition. The critical shear stress for erosion is rarely exceeded during these simulations, so once the grains reach the bed they will remain on the bed. It is apparent that the greatest influence on the shoaling along Atkinson Island is the San Jacinto River.

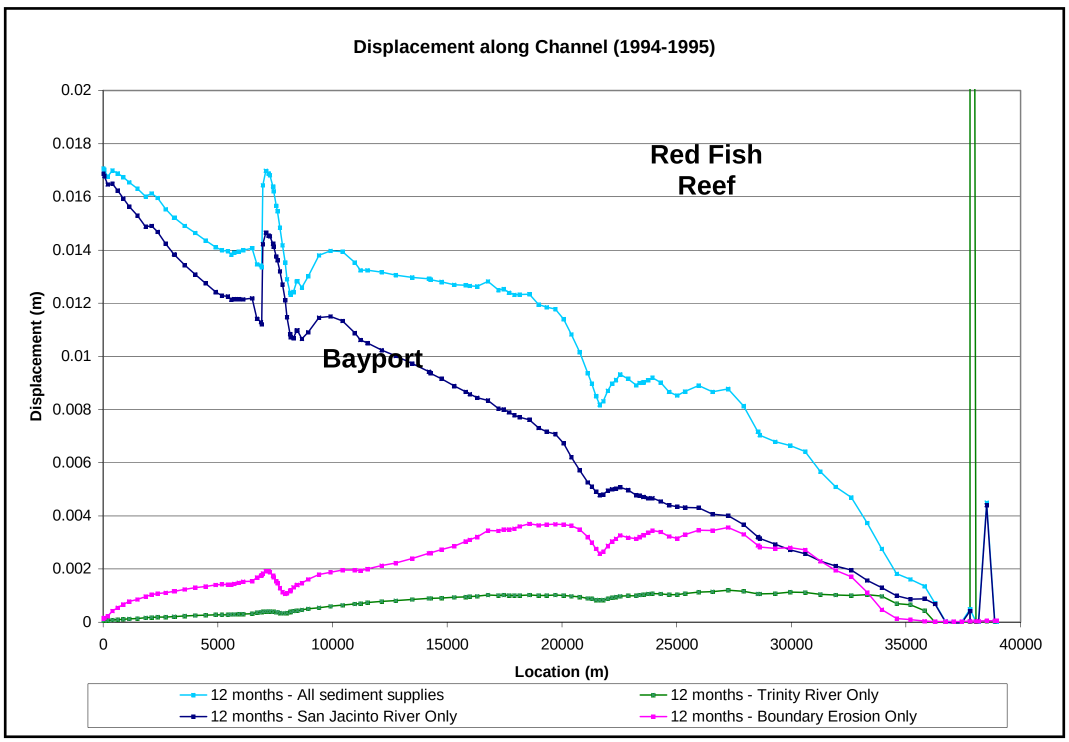

Figure 23. Bed displacement along the channel due to each sediment load source.

The sediment available for deposition in the Houston Ship Channel comes primarily from the San Jacinto River inflow and erosion of the bed. Because the residual currents have a net drift in the upstream direction, the suspended sediment that reaches the channel will also tend to drift upstream as it settles to the bed. The time and extent of the drift is determined by the settling velocity of the sediment and shear stresses generated by the flow. Figure 24 shows the suspended sediment concentrations and the bed displacement for a time very early in the simulation. At this point no significant sediment loads have entered the system and all of the sediment available for transport is due to erosion of the boundary edges. The drift of suspended sediment in the upstream direction is noticeable in the figure as is the tendency for sediment reaching the channel from this source to settle in the region of Red Fish Reef.

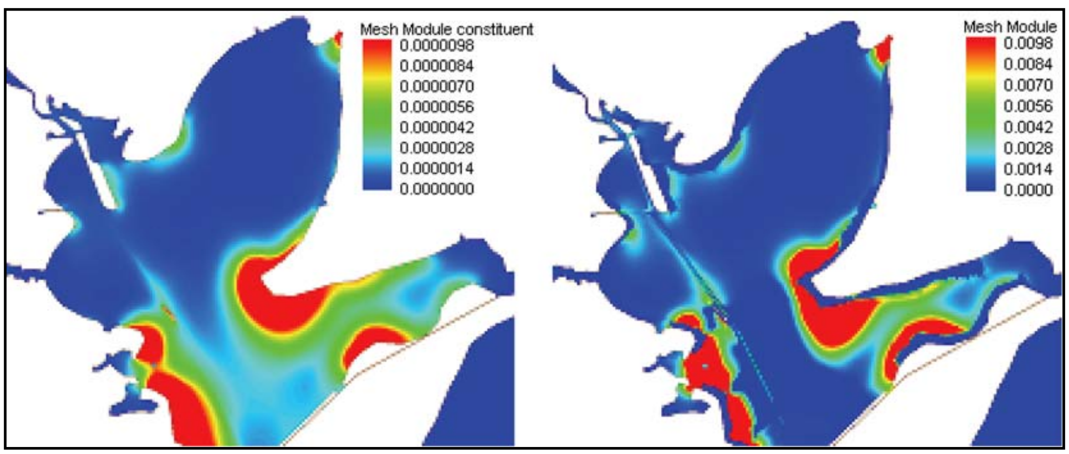

Figure 24.Suspended sediment concentration and bed displacement at 4 days of simulation.

As indicated above and in Figure 23, the sediment load from the San Jacinto River is the primary source of sediment to the Houston Ship Channel above Red Fish Reef. The flow rate from the San Jacinto River determines the distance that the suspended sediment will travel down the ship channel and the distance downstream that the deposition occurs during any given flow event. Higher flow events will push sediment further down the channel than lower flow events. Figure 25 is a plot of the deposition along the channel for the high flow water year at four different times during the year. The greatest increase in deposition occurs within the first 3 months which is in agreement with the time of highest flows as shown in Figure 17. The section of the channel upstream of Bayport has a large increase in deposition over the next 6 months, but less increase is evident in the channel downstream of Bayport. The distance between each of the lines indicates the amount of sediment that has fallen (deposited) over the course of 3 months. This figure illustrates the idea that the sediment supplied from the San Jacinto River deposits mostly in the area along Atkinson Island, upstream of Bayport. The largest increases in deposition over time are between Morgan's Point and Bayport. When suspended sediment from the San Jacinto River extends further downstream, less sediment is deposited than in the upper region which is why there is less of an increase in deposition over time, as shown in Figure 25. Details of the analysis of the transport patterns and timings are given in Appendix B.

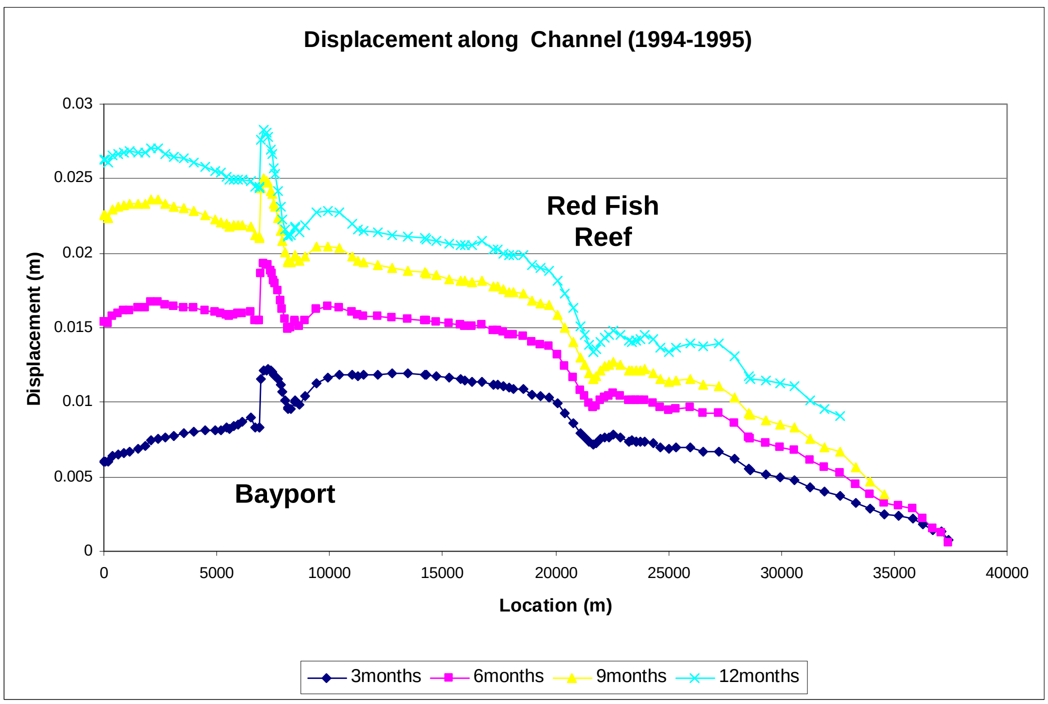

Figure 25. Distribution of bed displacement along the channel from Morgan's Point to Bolivar Roads at 3, 6, 9, and 12 months.

4 Vessel Impacts

During the initial sediment model validation the model indicates deposition along the channel in the shallows where it is not detected in the field (see Figure 26). It is likely that vessel traffic does not allow deposition in these reaches in nature. Therefore an investigation of navigation's impact on sedimentation in the shallows is undertaken. The Houston Ship Channel has an average of 50 to 60 deep-draft vessel passages a day (U.S. Coast Guard 2006). Since vessel movement can generate high shear stresses on the bed as well as create waves in shallower regions outside of the channel, the vessel traffic in the channel is likely to have a significant impact on the sedimentation rates and locations of shoaling.

An Adaptive Hydraulics (ADH) model of the domain was created to simulate a vessel traveling upstream along the channel, beginning downstream of Red Fish Reef and continuing to Barbour's Cut. The typical vessel represented in these simulations has a length of 232 m, width of 32.3 m, draft of 9.3 m, and speed of 4.5 m/s. The movement of the vessel generates a return current that moves out and around the vessel and returns to the channel behind the vessel. The return currents alone can be significant enough to cause erosion of the channel and the resulting long waves that move into the shallows can cause erosion of those areas as well. The ADH simulation generates the velocity pattern around the vessel caused by the return current and into the surrounding shallows. As the long wave generated by the vessel propagates into the shallows, it will form a bore. This occurs where the vessel speed is greater than the free surface wave speed. This wave speed is approximately $(gh)^{1/2}$. Here g is the acceleration associated with gravity and h is the water depth. In shallow water this free surface wave speed, or celerity, is less than in deeper water. These simulations are only appropriate for the areas immediately outside of the channel and beyond. The solutions directly in the channel are not accurate because the vessel propeller effects are not included and the model is hydrostatic.

Single Vessel

An ADH simulation of a single vessel is shown in Figure 27. This figure shows the contours of velocity around the vessel when it is along Atkinson Island (contoured between 0 and 1 m/s). The presence of islands near the channel generates a reflection and increases the drawdown and velocity. The high velocities extend to Atkinson Island and will cause erosion of any fine sediments located there. Observations from field data collection show that these islands are composed of very coarse material, indicating that the finer sediments have already been eroded away, confirming the model. The return current that is created by the moving vessel is indicated by the velocity vectors included in the figure. The shear stresses generated by the vessel movement are shown in Figure 28, contoured between 0.1 (the critical shear stress for deposition of the silts and erosion of the cohesives) and 0.67 Pa (the critical shear stress for erosion of the silts). Therefore, any shaded areas will not allow deposition of the silt and those areas in red will experience erosion of the bed. The bed shear is calculated from the velocity magnitude $\left(\tau_{bed} = \frac{1}{2}\rho C_f \|v\|^2\right)$, using a friction coefficient of 0.01 based on references by Maynord (2005).

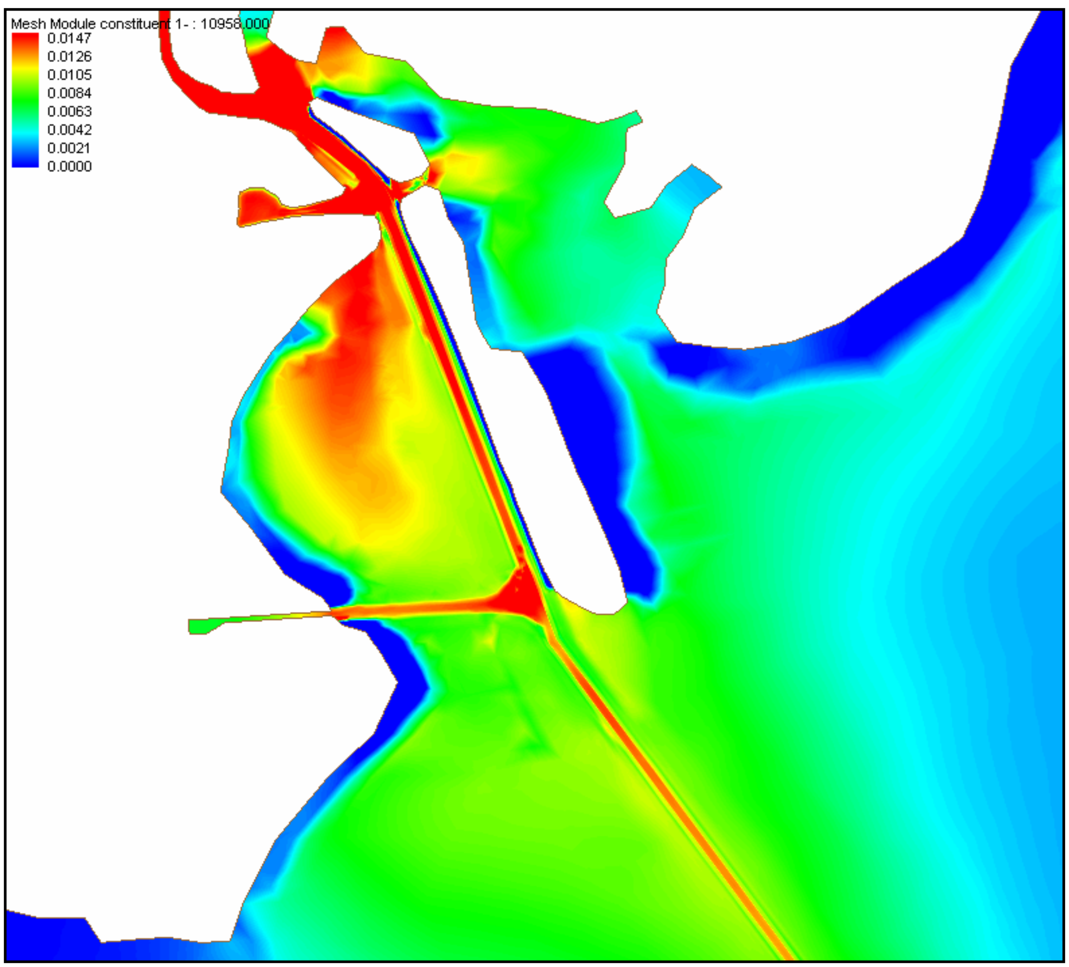

Figure 26. Magnitude of deposition (m) in the channel and in the surrounding shallows.

The maximum shear stress generated at each point in the domain for the entire simulation is shown in Figure 29. The extent to which erosion of the silts and cohesives may occur because of the vessels during some period of simulation is indicated by the areas shaded in red. All other shaded areas will cause erosion of the cohesive material and hinder deposition of the silts such that the suspended material will remain in suspension for a longer period because of the shear stresses on the bed.

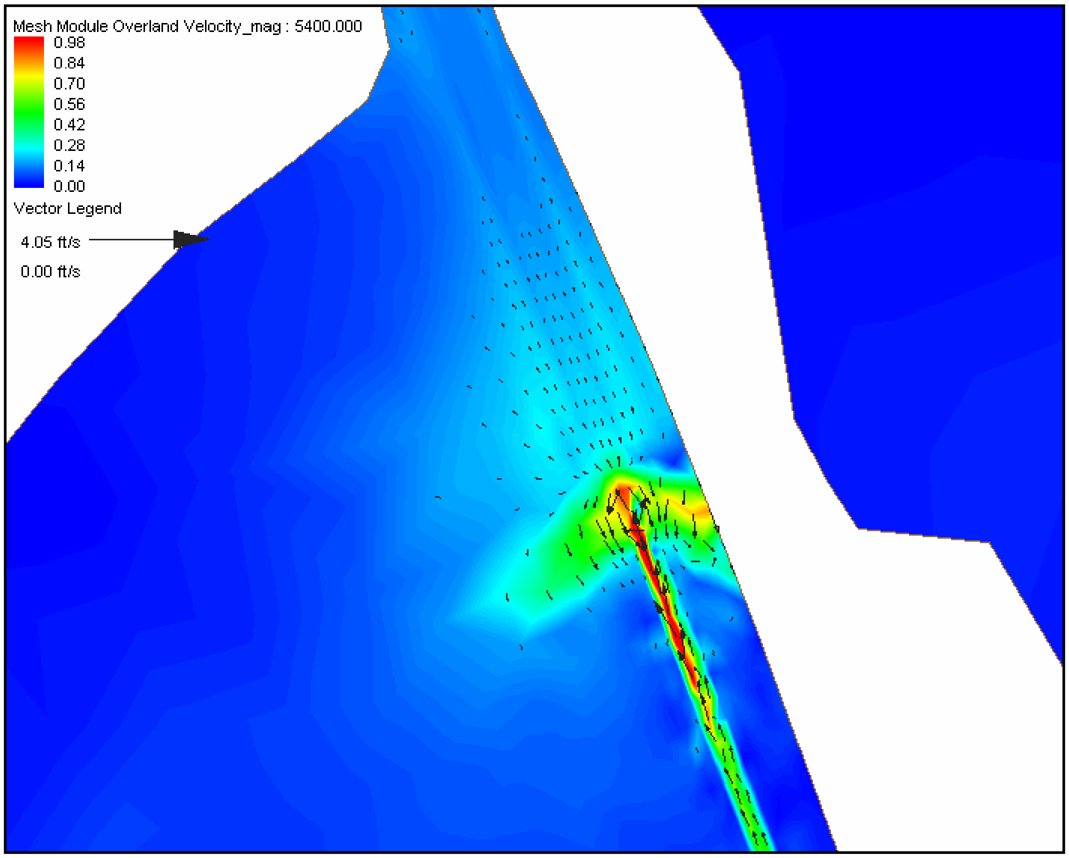

Figure 27. Velocity magnitude and direction around a moving vessel along Atkinson Island.

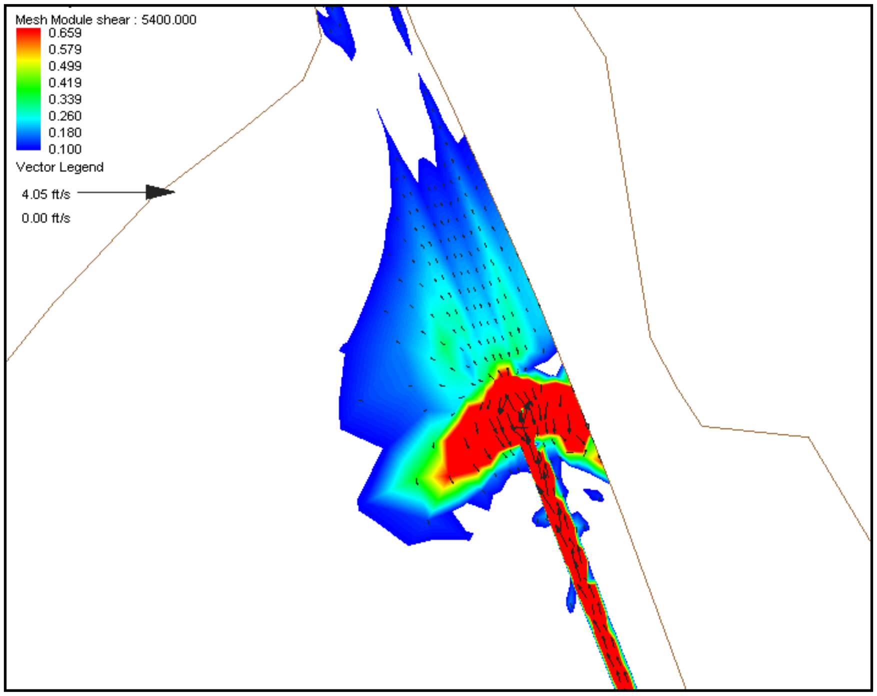

Figure 28. Bed shear stress generated by a moving vessel along Atkinson Island.

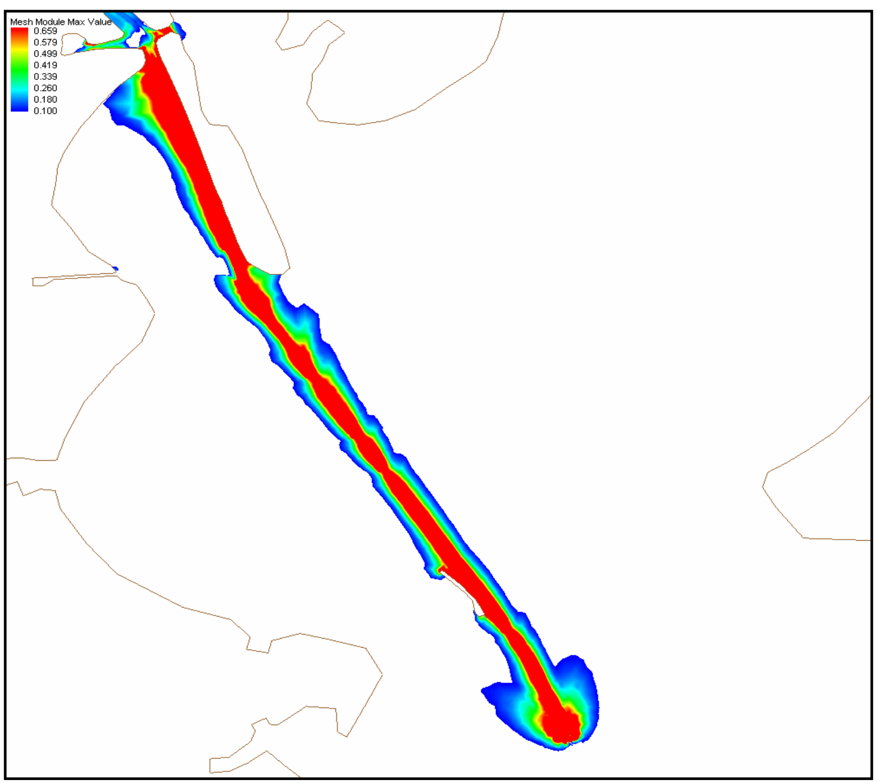

Figure 29. Maximum shear stress generated by the moving vessel over the entire simulation (contoured to show stresses greater than 0.1 Pa, the critical shear for deposition – red areas exceed the critical shear for erosion of 0.67 Pa).

Typical Day of Vessel Traffic

In order to quantify the impact of the vessel traffic on the shoaling in the Houston Ship Channel, a typical day of vessel traffic is repeated over the course of the year-long sediment simulations. The ADH simulations provide the vessel induced shear stress on the bed. This stress field can then be applied to the TABS-MDS sediment model so that the shear stresses due to the vessels are included with those generated by the flows and wind. The typical day of vessel traffic is determined by analyzing ship traffic data provided by Houston Pilots, the Port of Houston, Marine Exchange of the West Gulf, Vessel Traffic Services, and USACE Galveston District. Data from the 1st and 20th of each month in 2006 is analyzed for vessel beam, length, draft at transit, travel path, and time of travel.

Vessel speeds are unavailable, so they are computed based on vessel dimensions and the Schijf limiting speed equation. Displacement hull vessels have a maximum speed that they can attain. If a vessel is traveling near this speed, it can apply more power but its speed won't increase. Instead it just amplifies the forces acting against the vessel to balance thrust. This equation uses the ratio of the channel cross-sectional area to that of the vessel blockage area (product of draft and beam). The equation is given below

$$V_L = \sqrt{gh} * \sqrt{8 * COS^3\left(\pi/3 + \frac{ACOS}{3}\left(1 - \frac{1}{BR}\right)\right)}$$

where V_L = limiting speed, g = gravity, h = channel depth, and BR = blockage ratio. Although this gives the limiting speed, vessels often only travel at 85% of this speed since it is more efficient. The ADH vessel simulations used 85% of the Schijf limiting speed for each vessel. Since the vessel speeds are based on channel dimensions, the 45- X 530-ft channel sees vessel speeds ~6% higher than the 40- X 400-ft channel. This method of estimating ship speed does not take into consideration traffic issues that could result in slower speeds, but is reasonable for comparing plans.

The daily blockage averages and tonnages are compared over the year to determine any seasonal variation in vessel traffic; however, no variations are found. Figure 30 shows the blockage averages and Figure 31 shows the tonnages. Based on these analysis and travel paths, September 1st was determined to be an average day of vessel traffic and used in all simulations. This day includes 48 vessels with characteristics given in Table 6. Figure 32 shows the travel paths of all 48 vessels of this typical traffic day.

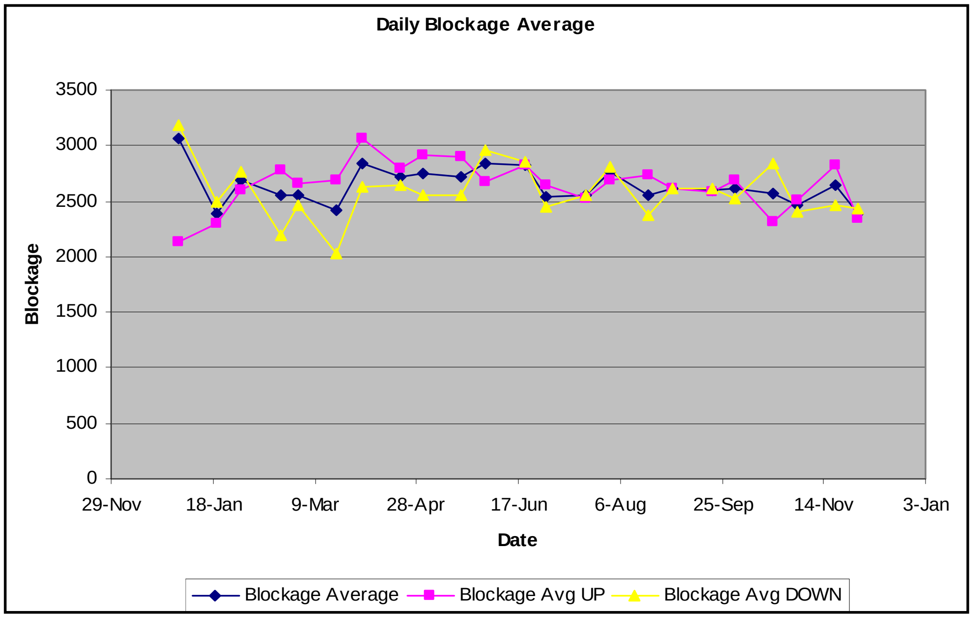

Figure 30. Daily blockage averages.

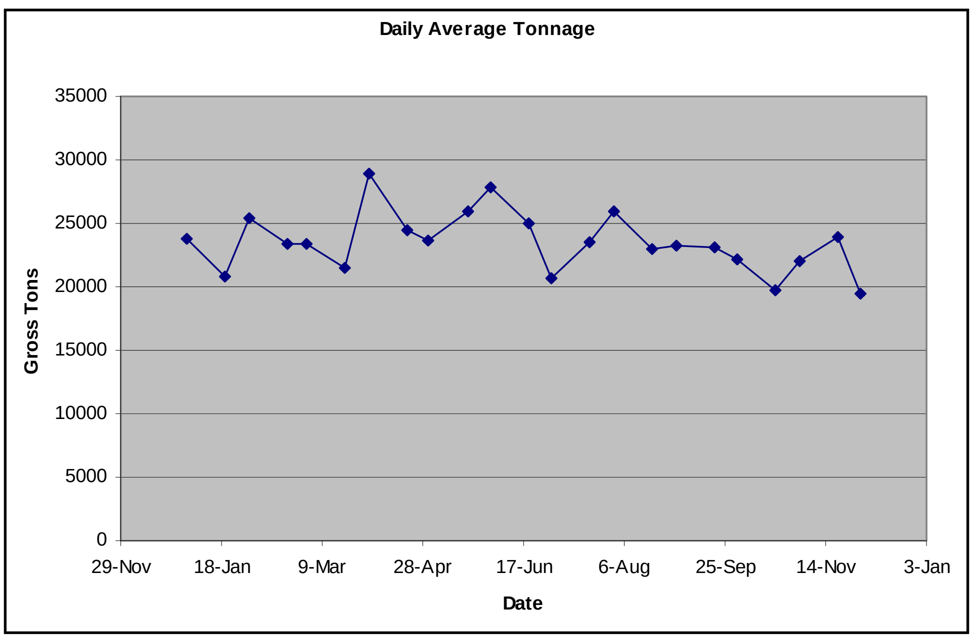

Figure 31. Daily tonnage averages.

Table 5. Vessel characteristics.

Parameter	Value
Draft	15 - 38 ft
Length	300 - 900 ft
Beam	50 - 140 ft
Speed	15 - 25 ft/s
Travel Path	Starting and ending at sea, Bayport, Barbour's Cut, and Baytown

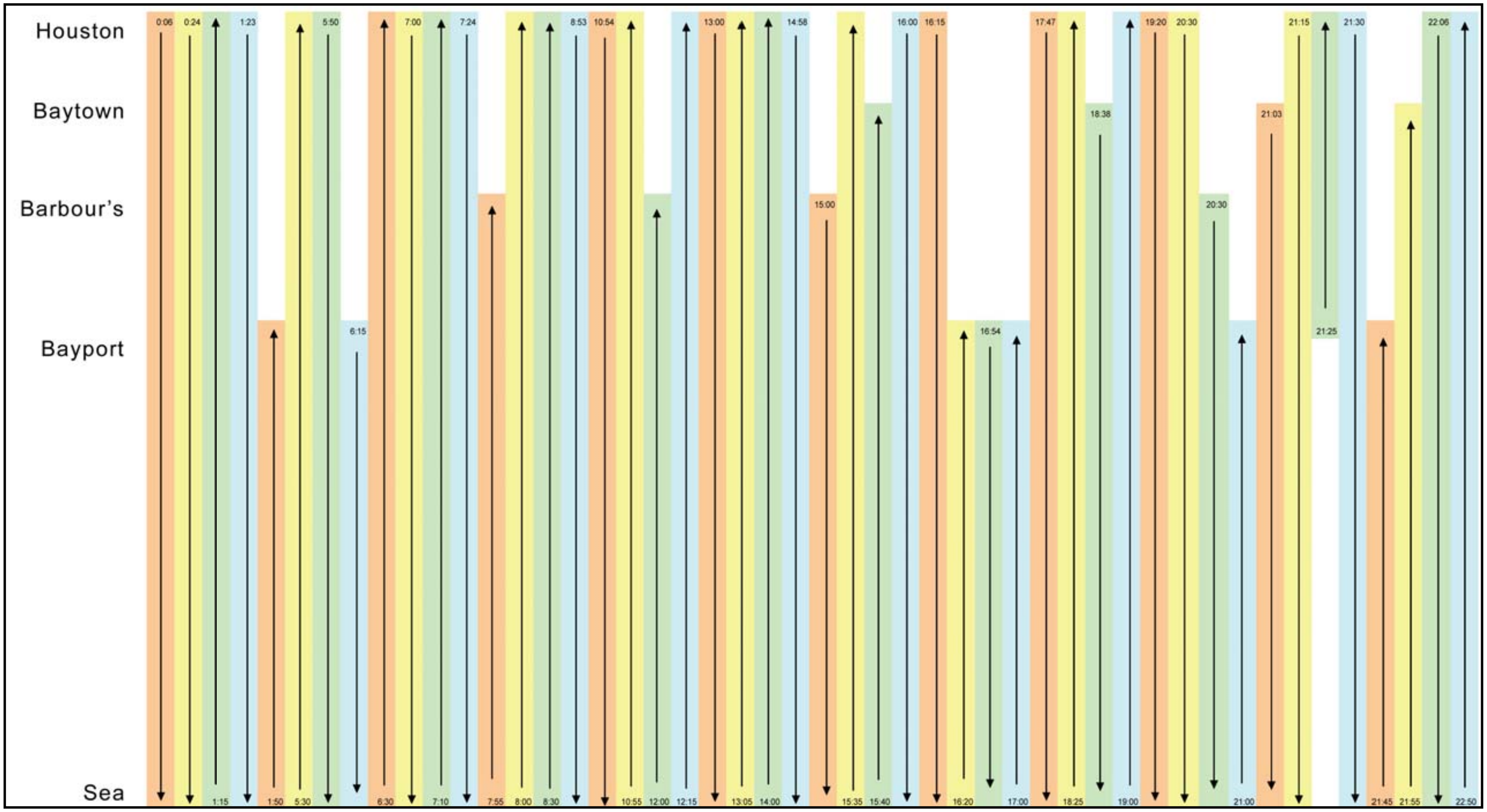

Figure 32. Typical day of vessel traffic.

Sediment Modeling with Vessel Effects

As with the previous sediment model simulations, the hydrodynamics and salinity are modeled initially and then used to drive the sediment transport simulations. The velocities generated from the ADH vessel simulations are used to calculate the shear stresses on the bed and applied daily in the year-long sediment simulations. The same hydrodynamics and sediment loads are used for these simulations as done previously.

Initial simulations indicate that the presence of the vessels does affect the sediment deposition in the shallows. Figure 33 shows the bed displacement with and without the inclusion of the vessels at a time early in the simulation. It is obvious that the vessel traffic prevents a large amount of sediment from depositing on the bed, especially in the shallow areas outside of the channel. The shear stresses generated by the vessels keep the sediment in suspension so that it is unable to settle to the bed.

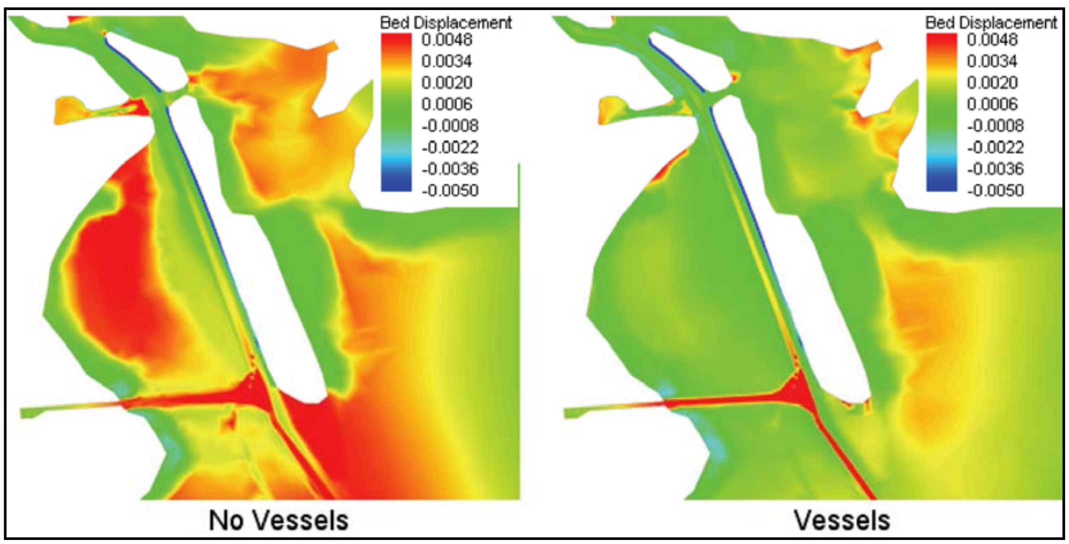

Figure 33. Bed displacement comparison.

5 Sediment Model Validation

A validated sediment model that includes the vessel effects for the Houston Ship Channel can be a very useful tool for use when attempting to determine the overall effectiveness of any proposed changes to the system. In the initial modeling effort, the vessel effects were not included and the results indicated some deficiencies in the shoaling pattern of the shallows. The initial vessel inclusion simulations indicated that these effects would provide better results in these areas. In an effort to further better the sediment model validation, the settling character of the sediment was adjusted so that the particles would simulate flocculation and deposit more like a cohesive/silt mixture. By making the settling nonlinear, the particles have a higher tendency to deposit in the channel. The sediment model validation procedure is then repeated with the inclusion of the vessels and this change in particle settling.

Suspended Sediment Comparison

For the validation time period, the suspended sediment samples were obtained from historic field sample sites compiled by the Texas Commission on Environmental Quality (TCEQ). There are 2 days during each of the simulated water years on which data are taken within the model domain. The locations of the field sample sites are shown in Figure 34. Table 6 gives the date and location of the sample, the field data value, the model computed value, and the difference between the two. The average difference in suspended sediment concentration between the field and model values is 21.4 mg/L. One point during the low flow water year had a significantly high suspended sediment concentration value (indicated in Table 6 with an asterisk). Since this value is much higher than the value at any of the nearby locations on the same date or any of the other samples overall, it is removed when the overall comparison of the model results to the field values is performed.

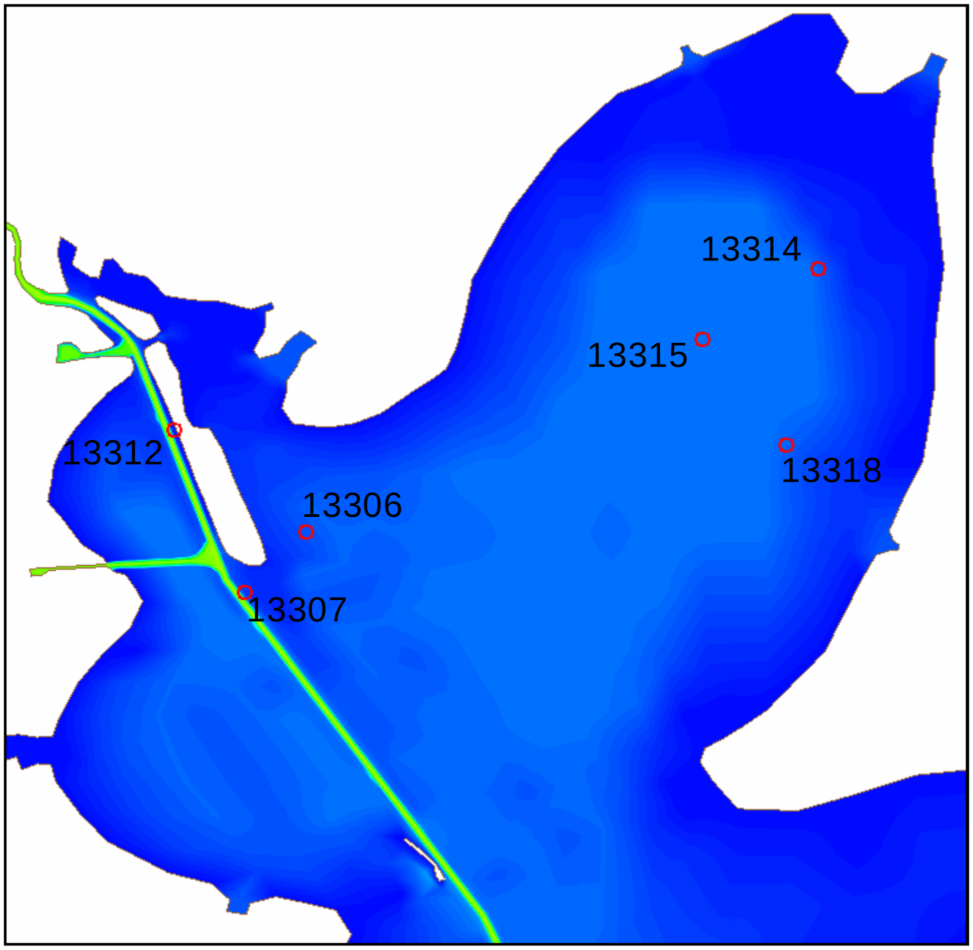

Figure 34. Suspended sediment sample locations.

Table 6. Suspended sediment comparison including vessel effects.

Date	Field/model, mg/L					
	TCEQ Point 13306	TCEQ Point 13307	TCEQ Point 13312	TCEQ Point 13314	TCEQ Point 13315	TCEQ Point 13318
1-31-95	28/48 (+20)	57/77 (+20)	16/159 (+143)	11/50 (+39)	29/50 (+21)	33/51 (+18)
4-25-95	16/26 (+10)	18/36 (+18)	6/51 (+45)	19/19 (+0)	17/18 (+1)	17/19 (+2)
1-10-96	13/31 (+18)	11/41 (+30)	10/52 (+42)	23/27 (+4)	266/28* (-238)	18/26 (+8)
4-9-96	20/27 (+7)	19/33 (+14)	9/43 (+34)	9/18 (+9)	24/20 (-4)	29/22 (-7)

Shoaling Rate Comparison

The historical shoaling rate for the upper half of the Houston Ship Channel, from Morgan's Point to Red Fish Reef, is shown in Figure 35. There is an obvious decline in the shoaling over this reach since the 1960's. The channel was first enlarged in the 1960's to the 40- x 400-ft condition and remained in this condition until the late 1990's. The latest period of dredging along Atkinson Island is used for comparison of the shoaling rate. This is the period used to generate the sediment load for the inflows and the comparison years. The period between the dredging was approximately four years (1994-1998) and the rate of shoaling was 8,035 yd^3/year/station (6,143 m^3/year/station). The model runs here are for only two of those years, a high flow water year (October 1994–September 1995) and a low flow water year (October 1995–September 1996).

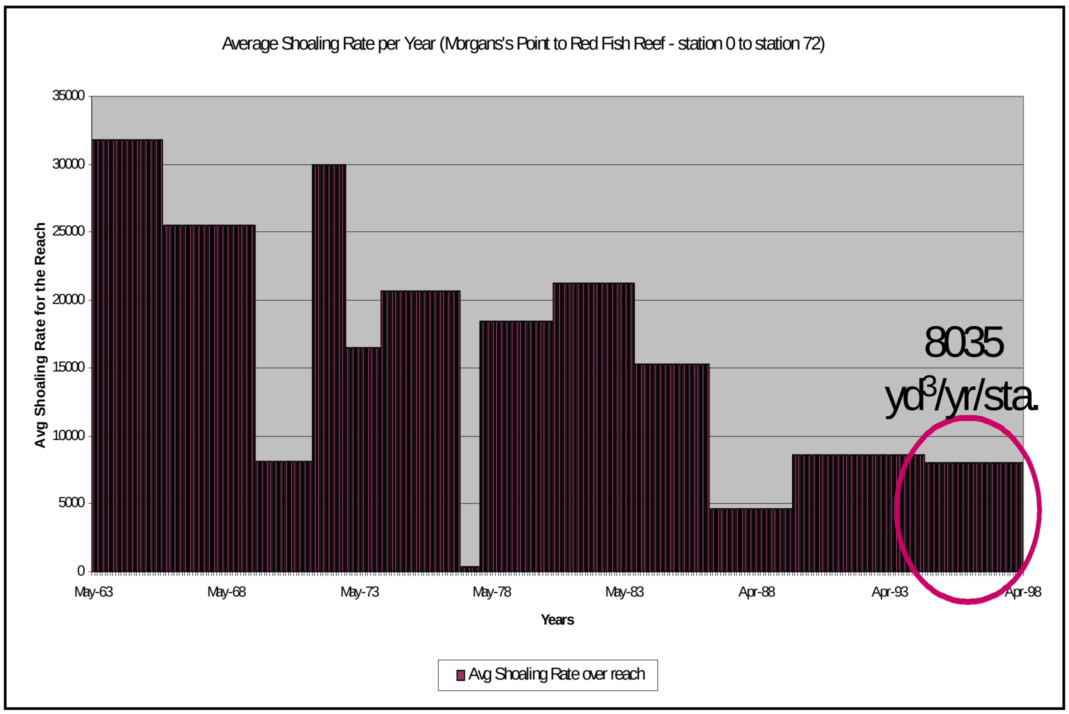

Figure 35. Average shoaling rate per year for the upper half of the Houston Ship Channel.

The model displacement results are plotted for several points along Atkinson Island and the yearly rate of displacement is similar for each. Figure 36 shows the locations and the displacement of two points for the high flow water year. The shoaling rate is computed by multiplying the displacement rate, station area of 400-ft (121.9-m) wide by 1000-ft (304.8-m) long, and a unit conversion factor. The model produced a shoaling rate of 1703 yd^3/year/station (1302 m^3/year/station) at the green location. The model gross deposition rate is about 20% of that found in the field. The final 2 years of the latest 4 year dredging cycle include several high flow periods similar in magnitude to the high flow water year. If the sediment model results were to be combined in such a manner, then the shoaling rate remains the same, as shown in Figure 37. Therefore, the overall difference in the rate of shoaling between the model and the field remains large. The model only accounts for about a quarter of the channel shoaling suggested by the dredging data. So there are sources or processes that the model does not acknowledge. This should be considered in making judgments using the model.

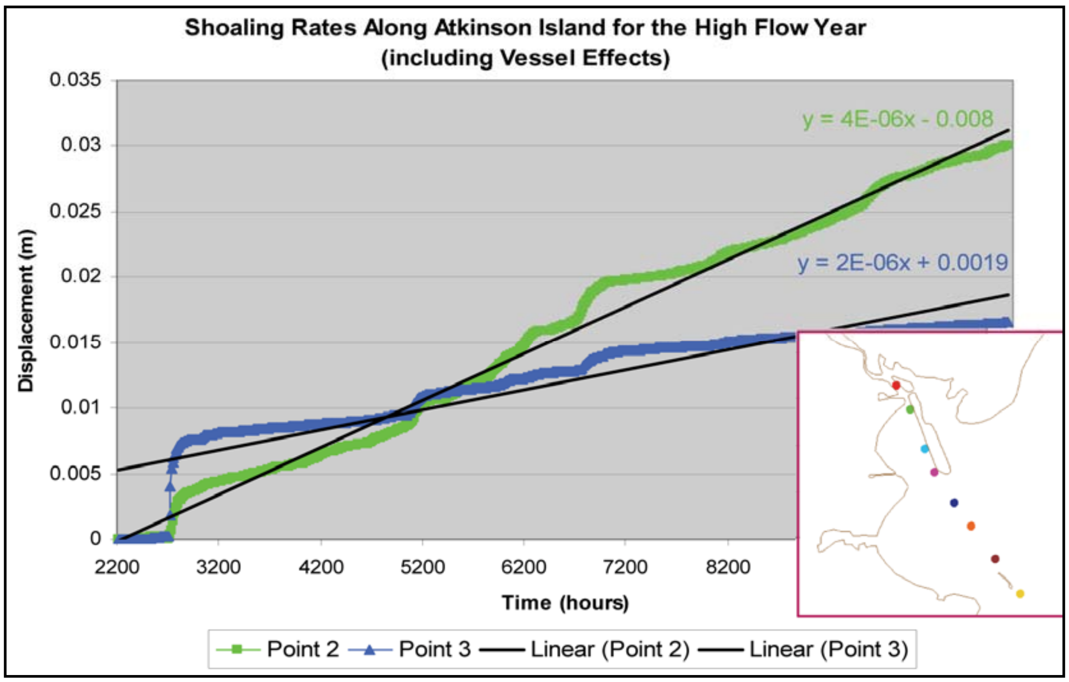

Figure 36. Model displacement rate for two points along Atkinson Island.

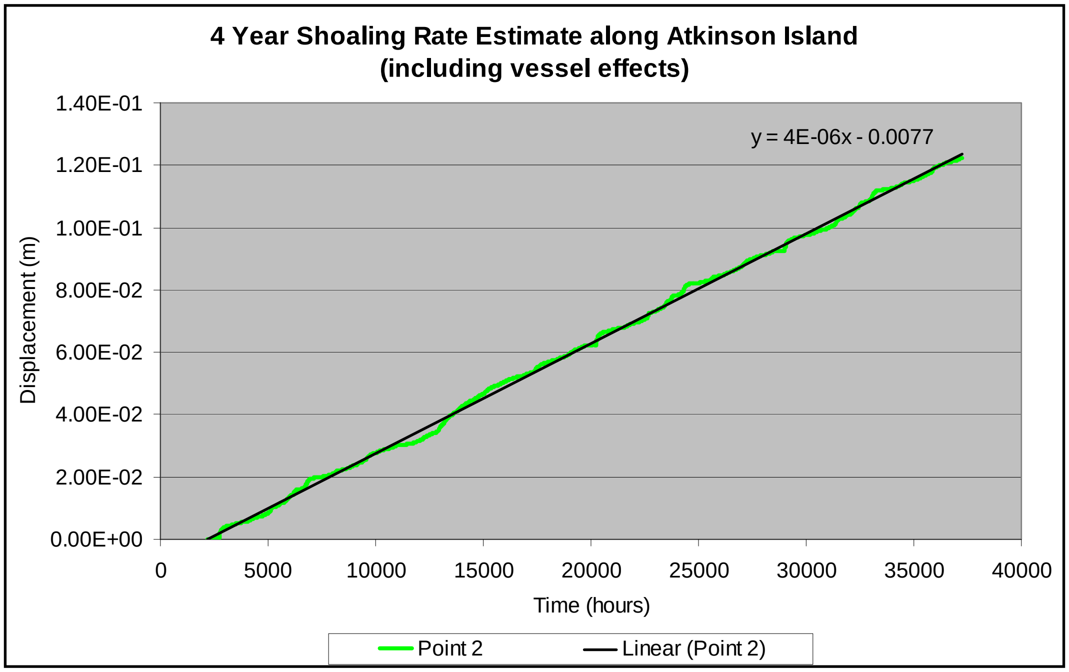

Figure 37. Estimated model displacement rate for one point along Atkinson Island over a 4-year period.

Shoaling Distribution Comparison

The volumetric shoaling rate along the channel centerline over the entire 34 years that the channel was in the 40- × 400-ft condition is shown in Figure 38 as the blue line. These data are normalized by the overall average because the purpose of this comparison is strictly to determine the pattern of distribution, not the magnitude. The pink line in the figure illustrates the normalized volumetric shoaling rate determined from the model with the inclusion of the vessel effects on the sedimentation. The overall comparison is good. The decline in the shoaling rate in the lower half of the channel is apparent in the model, as is the fairly constant rate in the upper region. However, the model shows more deposition near Morgan's Point and in the Bayport Flare than the 34 years of historic records indicate. The concept of sedimentation being an event driven process is important to remember when looking at the historic dredging records. When comparing the distribution of shoaling rates along the channel, 34 years of record are included in the field data, and Figure 35 shows a decline over time in the rate of shoaling in the upper half of the channel. Sedimentation is dominated by the magnitude of the flows and loads entering the system. Therefore, the patterns of shoaling apparent over a long time frame may have occurred due to a few strong events.

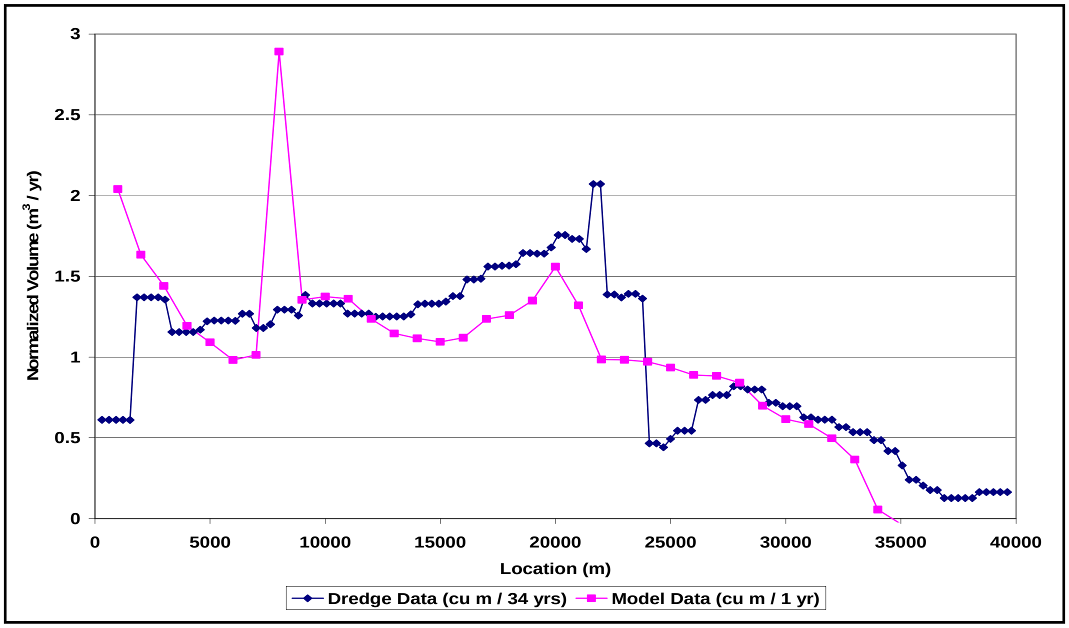

Figure 38. Normalized volumetric shoaling rate along the channel for the historical data and model results with vessel effects from Morgan's Point to Bolivar Roads.

Conclusions of the Model Validation

Now included in the model validation is the effect of navigation on the shoaling within the channel. Since the movement of vessels has the capability to generate large shear stresses on the bed, the shoaling is affected in areas outside of the channel and into shallow regions beyond. The validation process for the sediment model of the Houston Ship Channel and Trinity Bay area again produces good agreement with suspended sediment concentrations and shoaling distribution along the channel. The shoaling rate within the channel for the high flow water year is still much lower than the historic rate. Even when all four years (the high flow water year, the low flow water year, followed by two years of flows similar to those in the high flow year - see Figure 17) are considered, the rate remains low. However, the previous model results indicated shoaling along the shallows just outside of the channel in locations where it is not seen in the field. Once the vessel effects are included in the sediment model, these adjacent shallow areas do not see increased deposition, but rather behave as expected based on field observations. The distribution of deposition along the channel compares pretty well with the field.

6 Summary and Conclusions

This report documents the validation process of the sediment model for the Houston Ship Channel and Trinity Bay area. The validation included field data sampling and analyses, selection of simulation conditions, and comparison to field data. A further step was made in order to include the effects of vessel traffic on the sedimentation in the area.

The field data collection was necessary to define the nature of the bed material. The field data allowed for better understanding of the processes that move sediment in the area. Although the samples collected in December 2005 were taken under winds of 5-10 m/s, the suspended sediment concentrations in the bay were not high, indicating that wind-wave resuspension is not a primary means for sediment transport. This concept was supported by the shear stresses generated within the model and their magnitude being less than that required for erosion of the bed. Bed sediment samples allowed for the estimate of parameters that determine the erodibility and composition of the bed. The field data analysis provided for the definition of the bed layers and their properties as well as for the breakdown of sediment type being 50 percent silt and 50 percent cohesive material.

The sediment model validation of the Houston Ship Channel and Trinity Bay area is based on the comparison of the model's results to field data. The model simulated two water years during the latest dredging cycle before the channel enlargement began. The hydrodynamics for this time period and the sediment loads from the Trinity River and San Jacinto River were used to drive the model. The shoaling rate along Atkinson Island (where the largest increase in shoaling is occurring in the enlarged channel) based on the historical dredging records was compared to the rate of deposition determined from the model. The distribution of shoaling along the channel was also compared to the historic records, but only for the distribution, not magnitude, since the records include all 34 years in which the channel was in the pre-enlarged state. The records indicate an overall decline in the shoaling over the 34 years, so the conditions simulated in the model were expected to produce less shoaling than the average over the entire 34 years. Also considered in the validation were the suspended sediment concentrations in the area during the years simulated. The model results compared well in two of the three categories, but the model-generated shoaling rate is low compared to the historic records.

Because of the large number of deep-draft vessels traveling the Houston Ship Channel daily, the vessel traffic in the channel has a significant impact on the sedimentation rates and locations of shoaling. A vessel movement simulation was performed to determine the shear stresses generated by a moving vessel. The vessel causes stresses high enough to cause erosion of the bed and resuspension of sediment in the areas outside of the channel. These vessel simulations were made using a standard vessel size and speed. The impact of the vessels on the shoaling appears to be a significant factor, especially when considering the size of the enlarged channel and the increase in the speeds of the vessels in this channel. In order to improve the model validation, the vessel effects were included in the sediment model. A typical day of vessel traffic was determined and simulated with ADH in order to determine the shear stresses on the bed due to this traffic. These stresses were applied to the sediment transport model and repeated daily over the year long simulations. The suspended sediment concentrations and distribution of shoaling along the channel compared well to historic data. However, the overall shoaling rate in the channel remained low even with these included effects. The inclusion of the vessel effects did modify the shoaling in the shallows so that it better represented the field observations.

The model's low prediction of the shoaling volume may be due to several factors. Approximately half of the estimated sediment loads entering the system would have to settle into the channel in order to reproduce the dredging quantities. The sediment loads were only applied at the Trinity and San Jacinto Rivers and the data were taken from limited data and gage locations slightly upstream of their entrance into the modeled system. Therefore the sediment loads do not account for any ungaged streams or flow areas. Sensitivity testing of higher loads did not produce the necessary effects in the channel on the shallows to warrant a deviation from the known conditions. It is also possible that fluid mud layers form after high rain events or at other times. Conversations with individuals familiar with the area indicate that some areas appear to fill in at times, yet open up later. This is often indicative of fluid mud moving within the system and at some point it will settle out. Fluid mud formation can often form and disappear quickly making field validation of the even difficult.

Unfortunately field data collections for this study were unable to detect this type of load, so it could not be included in the model. Test simulations could be performed in an attempt to generate and transport this load, but without any known information about it, it is difficult to do and defend. There is also a possibility of dredge disposal escape contributing to the shoaling within the channel, but it is not likely that this load would account for the amount of sediment that the model is unable to predict. Field data collection of sediment loads entering the system upstream of Morgan's Point will be useful to develop a better applied load to the model. All of these things can be investigated and added to the model to make it more representative of the system being modeled.

The validation of the sediment model of the Houston Ship Channel area has provided a tool that can be used to study possible design changes to the channel and surrounding areas and investigate ways to limit the amount of deposition in the channel. This model can also be used to help individuals make decisions about locations of future dredge disposal sites so that there is less dredged material resuspended that moves back into the channel. The validated sediment model will be a useful tool to direct decisions to reduce dredging and dredging costs in the Houston-Galveston Ship Channels and Trinity Bay area.

References

Berger, R. C., R. T. McAdory, W. D. Martin, and J. H. Schmidt. 1995a. *Houston-Galveston Navigation Channels, Texas Project, Report 3, Three-dimensional hydrodynamic model verification.* Technical Report HL-92-7. Vicksburg, MS: U.S. Army Engineer Waterways Experiment Station.

Berger, R. C, R. T. McAdory, J. H. Schmidt, W. D. Martin, and L. H. Hauck. 1995b. *Houston-Galveston Navigation Channels, Texas Project, Report 4, Three-dimensional numerical modeling of hydrodynamics and salinity*. Technical Report HL-92-7. Vicksburg, MS: U. S. Army Engineer Waterways Experiment Station.

Carrillo, A. R., M. S. Sarruff, and R. C. Berger. 2002. *Effects of adding barge lanes along Houston Ship Channel through Galveston Bay, Texas.* ERDC/CHL TR-02-23. Vicksburg, MS: U.S. Army Engineer Research and Development Center.

Maynord, S. T. 2005. *Evaluation of bank recession in existing and proposed channels of the Sabine Neches Waterway*. Memorandum of Record, prepared for the U. S. Army Engineer District, Galveston. Vicksburg, MS: U. S. Army Engineer Research and Development Center, Coastal and Hydraulics Laboratory.

Tate, J. N., and R. C. Berger. 2006. *Houston-Galveston Navigation Channels, Texas Project: Navigation Channel Sedimentation Study, Phase 1.* ERDC/CHL TR-06-8, Vicksburg, MS: U.S. Army Engineer Research and Development Center, Coastal and Hydraulics Laboratory.

United States Coast Guard. 2006. *State of the Waterway-2005*. Vessel Traffic Service, Houston-Galveston. New Orleans, LA: U.S. Coast Guard, District 8.

Appendix A: Field Data Analysis

All field data and analysis results obtained from the samples taken during the period of 5-7 December 2005 are presented in this appendix.

Figure A1 and Table A1 give the point locations and names for all samples taken. The data are grouped by the date on which the sample was taken: A—December 5, B—December 6, and C—December 7. All data analysis results presented reference the samples by the point names as shown here. Table A2 gives the suspended sediment sample analysis results. Tables A3 to A30 give the bed sample analysis results for bulk density, moisture content, and percent organics.

The Vertical-Loop Sediment Water Tunnel (VOST) results are shown in Tables A32 to A39, with Table A31 giving the relationship between impeller voltage and shear stress. The erodibility constants can be determined from these results based on the change in concentration over time for a given shear stress applied. These results were not ideal and owing to the samples all failing due to pitting or sample casing exposure, general results were obtained from these tests as opposed to specific shear stresses for erosion and erosion rates at each sample location.

The final 26 tables (Tables A40 to A65) give the results of the Coulter Counter analysis for grain size distributions. These results include the mean grain size and percentages of sizes in the bed samples as well as a plot showing the distribution of grain sizes.

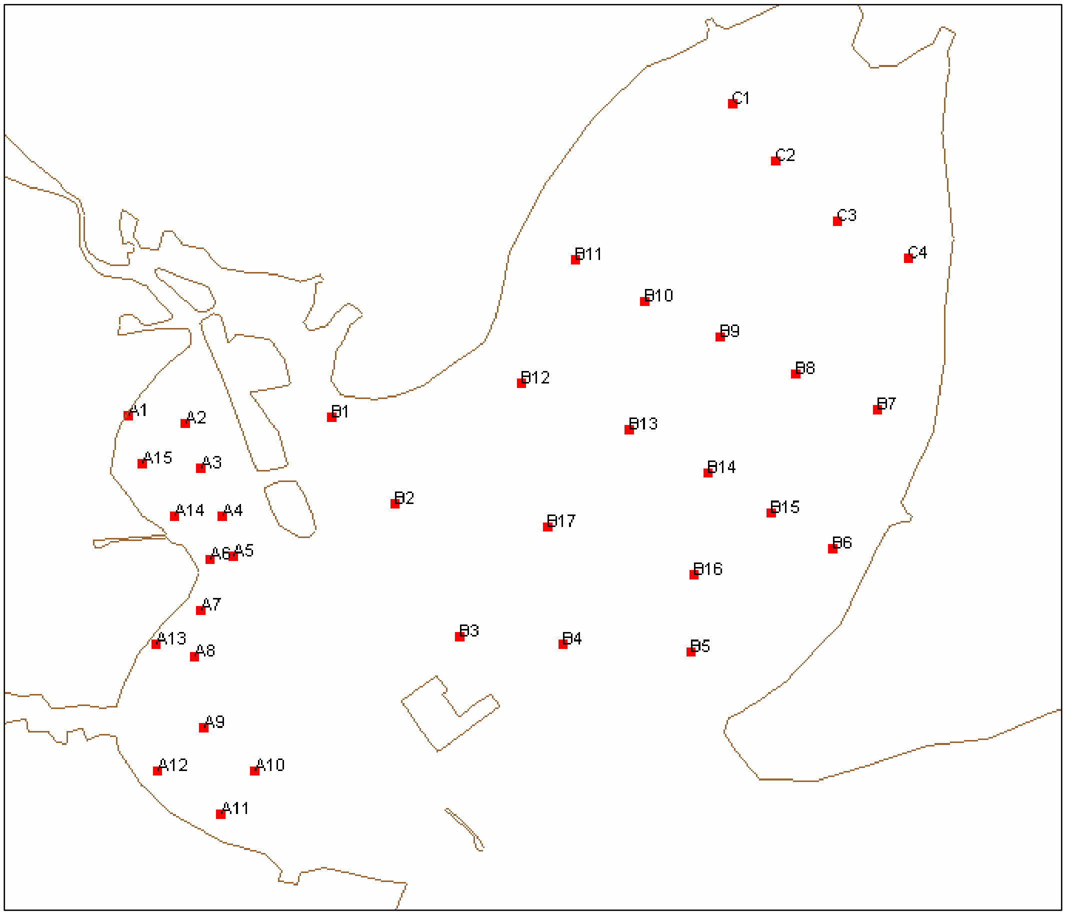

Figure A1. Field data point locations and names.

Table A1. Field data point locations and names.

Point Name	Date	Time Stamp	X-coordinate	Y-coordinate	Latitude	Longitude	Time (CST)
A1	12/5/2005	PC9:28:57	3235876.6	13805508	29.65	-95.00902	9:28:57
A2	12/5/2005	PC09:59:14	3242870.4	13804572	29.64677	-94.98711	9:59:14
A3	12/5/2005	PC10:23:15	3244674.1	13799102	29.63156	-94.98203	10:23:15
A4	12/5/2005	PC10:41:41	3247221	13793369	29.61557	-94.97464	10:41:41
A5	12/5/2005	PC10:58:06	3248587.5	13788646	29.60246	-94.97085	10:58:06
A6	12/5/2005	PC11:14:32	3245772.3	13788301	29.60177	-94.97974	11:14:32
A7	12/5/2005	PC11:29:00	3244647.4	13782200	29.58511	-94.98394	11:29:00
A8	12/5/2005	PC11:47:59	3243885.7	13776631	29.56988	-94.98694	11:47:59
A9	12/5/2005	PC12:09:18	3245117.7	13768105	29.54633	-94.98398	12:09:18
A10	12/5/2005	PC12:34:10	3251174	13762804	29.53118	-94.96552	12:34:10
A11	12/5/2005	PC12:48:28	3247154.2	13757657	29.51742	-94.97871	12:48:28
A12	12/5/2005	PC13:11:30	3239512.8	13762852	29.53242	-95.00217	13:11:30
A13	12/5/2005	PC13:37:35	3239295.5	13777972	29.57399	-95.00122	13:37:35
A14	12/5/2005	PC14:21:05	3241511.1	13793342	29.61603	-94.9926	14:21:05
A15	12/5/2005	PC14:42:50	3237699.5	13799754	29.63401	-95.0039	14:42:50
B1	12/6/2005	PC08:59:00	3260406.1	13805373	29.6473	-94.93185	8:59:00
B2	12/6/2005	PC09:28:16	3268090	13794924	29.61785	-94.90882	9:28:16
B3	12/6/2005	PC10:07:43	3275911.2	13778950	29.57319	-94.88599	10:07:43
B4	12/6/2005	PC11:20:55	3288163.9	13777958	29.56905	-94.84056	11:20:55
B5	12/6/2005	PC12:00:42	3303625.7	13777052	29.56527	-94.79907	12:00:42
B6	12/6/2005	PC12:26:13	3320656	13789520	29.59784	-94.74411	12:26:13
B7	12/6/2005	PC12:43:29	3326080.2	13806223	29.6432	-94.72513	12:43:29
B8	12/6/2005	PC13:02:47	3316164.9	13810534	29.65604	-94.75583	13:02:47
B9	12/6/2005	PC13:15:44	3307086.6	13814956	29.6691	-94.78389	13:15:44
B10	12/6/2005	PC13:53:15	3298071	13819186	29.68161	-94.81179	13:53:15
B11	12/6/2005	PC14:07:52	3289793.1	13824227	29.69628	-94.83728	14:07:52
B12	12/6/2005	PC14:32:20	3283152.6	13809417	29.65622	-94.85983	14:32:20
B13	12/6/2005	PC14:53:27	3296292.9	13803824	29.63957	-94.81911	14:53:27
B14	12/6/2005	PC15:11:50	3305703.1	13798696	29.62455	-94.79009	15:11:50
B15	12/6/2005	PC15:47:22	3313193.1	13793748	29.6102	-94.76709	15:47:22
B16	12/6/2005	PC16:03:02	3304033.7	13786396	29.5909	-94.79673	16:03:02
B17	12/6/2005	PC16:18:24	3286409.6	13792123	29.60838	-94.85151	16:18:24
C1	12/7/2005	PC09:23:33	3308707.8	13842940	29.74584	-94.77561	9:23:33
C2	12/7/2005	PC09:46:52	3313835.2	13835999	29.72626	-94.76025	9:46:52
C3	12/7/2005	PC10:22:56	3321262.9	13828756	29.70561	-94.7377	10:22:56
C4	12/7/2005	PC10:52:05	3329821.2	13824330	29.69259	-94.71127	10:52:05

Table A2. Field data suspended sediment analysis of concentration and salinity.

Point Name	Sample No.	Date	Depth	Vol mL	Weight, grams		Net	Conc mg/L	Salinity ppt
					Tare	Gross			
A2	10.21.41	5-Dec-05	3	100	0.0156	0.019	0.0034	34	26
A2	10.12.41	5-Dec-05	5	100	0.0157	0.019	0.0033	33	26
A3	10.30.25	5-Dec-05	3	100	0.0156	0.021	0.0054	54	27
A3	10.31.25	5-Dec-05	6	100	0.0167	0.0218	0.0051	51	26
A4	10.45.37	5-Dec-05	3	100	0.0157	0.0211	0.0054	54	26
A4	10.46.37	5-Dec-05	6	100	0.0153	0.0219	0.0066	66	27
A5	11.04.29	5-Dec-05	3	100	0.0171	0.0214	0.0043	43	26
A5	11.05.29	5-Dec-05	6	100	0.0175	0.0232	0.0057	57	25
A6	11.17.55	5-Dec-05	3	100	0.0154	0.0277	0.0123	123	26
A6	11.18.55	5-Dec-05	6	100	0.0155	0.0238	0.0083	83	25
A7	11.35.00	5-Dec-05	3	100	0.0154	0.0204	0.005	50	26
A8	12.00.13	5-Dec-05	3	100	0.0155	0.02	0.0045	45	26
A8	12.01.13	5-Dec-05	6	100	0.0154	0.0197	0.0043	43	26
A9	12.21.17	5-Dec-05	3	100	0.0174	0.0266	0.0092	92	24
A9	12.22.17	5-Dec-05	6	100	0.0175	0.0289	0.0114	114	24
A10	12.36.08	5-Dec-05	3	100	0.0154	0.0275	0.0121	121	26
A10	12.37.08	5-Dec-05	6	100	0.0156	0.0275	0.0119	119	26
A11	12.50.44	5-Dec-05	3	100	0.0158	0.0291	0.0133	133	26
A12	13.15.56	5-Dec-05	3	100	0.0158	0.0234	0.0076	76	25
A13	13.44.41	5-Dec-05	3	100	0.0158	0.019	0.0032	32	27
A14	14.23.29	5-Dec-05	3	100	0.0155	0.0198	0.0043	43	26
A15	14.47.46	5-Dec-05	3	100	0.0155	0.0183	0.0028	28	27
B1	9.05.30	6-Dec-05	3	100	0.0158	0.0176	0.0018	18	24
B2	9.34.45	6-Dec-05	3	100	0.0156	0.0206	0.005	50	26
B2	9.35.45	6-Dec-05	3	100	0.0155	0.0189	0.0034	34	28
B3	10.10.00	6-Dec-05	3	100	0.0156	0.0211	0.0055	55	27
B3	10.11.00	6-Dec-05	6	100	0.0155	0.0214	0.0059	59	27
B4	11.29.00	6-Dec-05	3	100	0.0154	0.0264	0.011	110	25
B4	11.30.00	6-Dec-05	6	100	0.0154	0.0262	0.0108	108	25
B5	12.05.00	6-Dec-05	3	100	0.0153	0.0234	0.0081	81	23
B6	12.29.55	6-Dec-05	3	100	0.016	0.0177	0.0017	17	23
B7	12.49.00	6-Dec-05	3	100	0.016	0.0179	0.0019	19	26
B8	1.05.00	6-Dec-05	3	100	0.0157	0.0189	0.0032	32	23
B8	13.06.00	6-Dec-05	6	100	0.0155	0.0189	0.0034	34	23
B9	13.20.00	6-Dec-05	3	100	0.0154	0.0185	0.0031	31	24
B9	13.21.00	6-Dec-05	6	100	0.0158	0.0185	0.0027	27	22
B10	13.56.00	6-Dec-05	3	100	0.0156	0.0201	0.0045	45	24
B10	13.57.00	6-Dec-05	6	100	0.0158	0.0212	0.0054	54	24
B11	14.12.30	6-Dec-05	3	100	0.0155	0.0177	0.0022	22	23

Point Name	Sample No.	Date	Depth	Vol mL	Weight, grams		Net	Conc mg/L	Salinity ppt
					Tare	Gross			
B12	14.35.00	6-Dec-05	3	100	0.0156	0.0187	0.0031	31	23
B12	14.36.00	6-Dec-05	6	100	0.0158	0.0195	0.0037	37	23
B13	14.58.00	6-Dec-05	3	100	0.0159	0.0216	0.0057	57	24
B13	14.59.00	6-Dec-05	6	100	0.0155	0.0213	0.0058	58	24
B14	15.24.00	6-Dec-05	3	100	0.0156	0.0211	0.0055	55	23
B14	15.25.00	6-Dec-05	6	100	0.0156	0.0214	0.0058	58	23
B15	15.51.00	6-Dec-05	3	100	0.0155	0.02	0.0045	45	23
B15	15.52.00	6-Dec-05	6	100	0.0156	0.0202	0.0046	46	23
B16	16.07.00	6-Dec-05	3	100	0.0156	0.0265	0.0109	109	23
B17	16.21.00	6-Dec-05	3	100	0.0158	0.0226	0.0068	68	24
B17	16.22.00	6-Dec-05	6	100	0.0159	0.0229	0.007	70	24
C1	9.28.00	7-Dec-05	3	100	0.0161	0.0178	0.0017	17	19
C2	9.50.00	7-Dec-05	3	100	0.0157	0.0191	0.0034	34	19
C2	9.51.00	7-Dec-05	6	100	0.0157	0.0193	0.0036	36	19
C3	10.26.00	7-Dec-05	3	100	0.0156	0.0161	0.0005	5	19
C4	10.55.00	7-Dec-05	3	100	0.0155	0.0168	0.0013	13	21

Table A3. Bed sample analysis results for A1.

Galveston Bay: Houston Ship Channel											
Length 29.5 cm											
Sample ID: 09:28:57 12/05/05 (A1)											
Visual 0.5 cm fluid mud											
	Not much difference in upper from lower. Judged more by color than density.										
	Sandy silty clay where the upper layer appears to be a little denser and less organic. Could be the sand.										
	Upper layer 4 cm and lower layer 25 cm.										
Procedure:											
1	Decanted surface water.										
2	Piped out fluid mud layer and combine with composite sample.										
3	Removed bottom cap.										
4	Applied positive pressure to push sample out bottom. Laid sample on a tray.										
Time	Crucible	Depth (ft)	Crucible Tare, grams	Wet Sed. + Crucible, grams	Dry Sed. + Crucible, grams	Wet Sed., grams	Dry Sed., grams	Fired Sed + Crucible, grams	Ash, grams	Moisture Content	% LOI
	27		12.4797	20.1622	17.6875	7.6825	5.2078	17.5922	5.1125	47.5191	1.8299
	31		11.5760	18.5774	16.2373	7.0014	4.6613	16.1242	4.5482	50.2027	2.4264
Pycno	Sample Layer	Temp. °C	Tare, grams	Bottle + Sed, grams	Bottle + Sediment + Water, grams	Density of Water	Pycnometer Bottle	Density, g/cm³			
204	.5 –4.5	24	27.3500	33.7861	55.7215	0.997	25.7013	1.7395			
205	4.5-29.5	24	28.3920	33.2676	55.1704	0.997	24.9413	1.6402			
208	.5 –4.5	24	27.3668	32.8343	54.5786	0.997	24.9842	1.7223			
209	4.5-29.5	24	27.9233	34.5205	56.0101	0.997	25.3639	1.7317			

Table A4. Bed sample analysis results for A2.

Galveston Bay: Houston Ship Channel											
Sample ID: 09:59:14 (A2)											
Visual: 0-0.8 cm brown (fluid mud) layer.											
	0.8-6 cm was the less dense material. Could only identify by feel.										
	6-29 cm was the more dense material. No obvious organic or debris layer.										
Procedure:											
1	Decanted surface water.										
2	Piped out fluid mud layer and combine with composite sample.										
3	Removed bottom cap.										
4	Applied positive pressure to push sample out bottom. Laid sample on a tray.										
Time	Crucible	Depth (ft)	Crucible Tare, grams	Wet Sed. + Crucible, grams	Dry Sed. + Crucible, grams	Wet Sed., grams	Dry Sed., grams	Fired Sed + Crucible, grams	Ash, grams	Moisture Content	% LOI
	12	.9-6 cm	9.3759	16.7321	12.4014	7.3562	3.0255	12.2325	2.8566	143.1400	5.5825
	13	7-29 cm	11.3108	18.9923	14.7949	7.6815	3.4841	14.585	3.2742	120.4730	6.0245
Pycno	Sample Layer	Temp. °C	Tare, grams	Bottle + Sed, grams	Bottle + Sediment + Water, grams	Density of Water	Pycnometer Bottle	Density, g/cm³			
204	.9-6 CM	24.5	27.3517	33.5619	54.5618	0.997	25.7013	1.339			
205	7-29 CM	24.5	28.3947	34.7275	55.4307	0.997	24.9413	1.517			

Table A5. Bed sample analysis results for A3.

Galveston Bay: Houston Ship Channel										
Sample ID: 10:23:15 (A3)										
Visual: 0.5 cm fluid mud.										
	4 cm upper layer.									
	22 cm lower layer.									
	Not much difference between layers.									
Procedure:										
1	Decanted surface water.									
2	Piped out fluid mud layer and combined with composite sample.									
3	Removed bottom cap.									
4	Applied positive pressure to push sample out bottom. Laid sample on a tray.									
Time	Crucible	Depth (ft)	Crucible Tare, grams	Wet Sed. + Crucible, grams	Dry Sed. + Crucible, grams	Wet Sed., grams	Dry Sed., grams	Fired Sed + Crucible, grams	Ash, grams	Moisture Content	% LOI
	4	.5-4	8.9948	15.3339	11.6967	6.3391	2.7019	11.5506	2.5558	134.6164	5.4073
	13	4-26 cm	11.3108	18.8293	15.1916	7.5185	3.8808	15.0044	3.6936	93.7358	4.8237
Pycno	Sample Layer	Temp. °C	Tare, grams	Bottle + Sed, grams	Bottle + Sediment + Water, grams	Density of Water	Pycnometer Bottle	Density, g/cm³			
204	.5-4	24	27.3478	32.0950	54.1709	0.997	25.7013	1.334			
205	4-26 cm	24	28.3903	34.1669	55.1334	0.997	24.9413	1.477			

Table A6. Bed sample analysis results for A4.

Galveston Bay: Houston Ship Channel										
Sample ID: 10:41:41 12/5/05 (A4)										
Length: 8.5 cm										
Visual: This was a sandy goop. I removed the mud portion with a spatula										
Procedure:										
1	Decanted surface water.									
2	Piped out fluid mud layer and combined with composite sample.									
3	Removed bottom cap.									
4	Applied positive pressure to push sample out bottom. Laid sample on a tray.									
Time	Crucible	Depth (ft)	Crucible Tare, grams	Wet Sed. + Crucible, grams	Dry Sed. + Crucible, grams	Wet Sed., grams	Dry Sed., grams	Fired Sed + Crucible, grams	Ash, grams	Moisture Content	% LOI
	4	0-8.5	8.9949	17.0252	13.0356	8.0303	4.0407	12.8838	3.8889	98.7354	3.7568
Pycno	Sample Layer	Temp. °C	Tare, grams	Bottle + Sed, grams	Bottle + Sediment + Water, grams	Density of Water	Pycnometer Bottle	Density, g/cm³			
209	0-8.5	24	27.9228	34.5663	55.2407	0.997	25.3639	1.436			

Table A7. Bed sample analysis results for A7.

Galveston Bay: Houston Ship Channel											
Sample ID: 11:29:00 12/5/05 (A7)											
Length: 14 cm											
Visual: Removed fluid mud with spatula.											
	Upper layer 4 cm long.										
	Lower layer 10 cm long.										
	Color and texture was the only way to determine layers, sandy.										
Procedure:											
1	Decanted surface water.										
2	Removed fluid mud layer and combined with composite sample.										
3	Removed bottom cap										
4	Applied positive pressure to push sample out bottom. Laid sample on a tray.										
Time	Crucible	Depth (ft)	Crucible Tare, grams	Wet Sed. + Crucible, grams	Dry Sed. + Crucible, grams	Wet Sed., grams	Dry Sed., grams	Fired Sed + Crucible, grams	Ash, grams	Moisture Content	% LOI
	13	0-4	11.3109	19.3509	16.8071	8.0400	5.4962	16.7071	5.3962	46.2829	1.8194
	12	38821.000	9.3755	17.6179	15.5841	8.2424	6.2086	15.507	6.1315	32.7578	1.2418
Pycno	Sample Layer	Temp. °C	Tare, grams	Bottle + Sed, grams	Bottle + Sediment + Water, grams	Density of Water	Pycnometer Bottle	Density, g/cm³			
206	0-4	24	28.3748	34.9677	56.1580	0.997	25.007	1.757			
208	4-14 cm	24	27.3663	34.7809	55.7411	0.997	24.984	1.872			

Table A8. Bed sample analysis results for A8.

Galveston Bay: Houston Ship Channel										
Length: 45 cm										
Sample ID: 11:47:59 12/5/05 (A8)										
Visual: 0.5 cm fluid mud										
	Upper layer 7 cm separated on its own. Appeared to be a sandy gel-like material.									
	Lower layer 38 cm long and sample held shape. Not as sandy as the upper layer.									
Procedure:										
1	Decanted surface water.									
2	Piped out fluid mud layer and combined with composite sample.									
3	Removed bottom cap.									
4	Applied positive pressure to push sample out bottom. Laid sample on a tray.									
Time	Crucible	Depth (ft)	Crucible Tare, grams	Wet Sed. + Crucible, grams	Dry Sed. + Crucible, grams	Wet Sed., grams	Dry Sed., grams	Fired Sed + Crucible, grams	Ash, grams	Moisture Content	% LOI
	30	BOT	11.1941	17.1832	14.3313	5.9891	3.1372	14.2023	3.0082	90.9059	4.1119
	15	TOP	13.3660	19.6134	16.0255	6.2474	2.6595	15.8975	2.5315	134.9088	4.8129
Pycno	Sample Layer	Temp. °C	Tare, grams	Bottle + Sed, grams	Bottle + Sediment + Water, grams	Density of Water	Pycnometer Bottle	Density, g/cm³			
209	7.5-45.5	24	27.9235	33.5488	55.0379	0.997	25.3639	1.476			
205	.5-7.5	24	28.3917	34.4189	54.9940	0.997	24.9413	1.400			

Table A9. Bed sample analysis results for A9.

Galveston Bay: Houston Ship Channel											
Sample ID: 12:09:18 (A9)											
Visual: 0-0.3 brown (fluid mud) layer											
	0.3-1 cm of low density material, unable to hold shape.										
	1-34.5 cm of sample denser material (holds shape).										
	Sample very volatile. Each time I put the 0.5-5 cm into the furnace it exploded.										
Procedure:											
1	Decanted surface water.										
2	Piped out fluid mud layer and combined with composite sample.										
3	Removed bottom cap.										
4	Applied positive pressure to push sample out bottom. Laid sample on a tray.										
Time	Crucible	Depth (ft)	Crucible Tare, grams	Wet Sed. + Crucible, grams	Dry Sed. + Crucible, grams	Wet Sed., grams	Dry Sed., grams	Fired Sed + Crucible, grams	Ash, grams	Moisture Content	% LOI
	4	.4-1.4 cm	8.9950	13.2436	10.2446	4.2486	1.2496	0	-8.995	239.9968	819.8303
	25	1.5-34.5 cm	10.4895	15.5896	12.4046	5.1001	1.9151	11.7413	1.2518	166.3099	34.6353
rerun	28	.4-1.4 cm	11.3850	17.7584	13.4064	6.3734	2.0214	12.7999	1.4149	215.2963	30.0040
rerun	31	1.5-34 cm	11.5757	21.0686	15.6787	9.4929	4.103	15.4207	3.845	131.3649	6.2881
Pycno	Sample Layer	Temp. °C	Tare, grams	Bottle + Sed, grams	Bottle + Sediment + Water, grams	Density of Water	Pycnometer Bottle	Density, g/cm³			
208	.3-1	24.5	27.3687	31.4494	52.993	0.997	24.9842	1.209			
209	1-34.5	24.5	27.9253	33.5130	54.5022	0.997	25.3639	1.296			

Table A10. Bed sample analysis results for A10.

Galveston Bay: Houston Ship Channel											
Sample ID: 12:34:10 (A10)											
Visual: 0.5 cm fluid mud.											
	10 cm layer upper layer.										
	11.5 cm lower sample.										
	Sample still had voids that were marked on sample tube. Water level 3 cm lower than indicated and sediment 4 cm lower.										
Procedure:											
1	Decanted surface water.										
2	Piped out fluid mud layer and combined with composite sample.										
3	Removed bottom cap.										
4	Applied positive pressure to push sample out bottom. Laid sample on a tray.										
Time	Crucible	Depth (ft)	Crucible Tare, grams	Wet Sed. + Crucible, grams	Dry Sed. + Crucible, grams	Wet Sed., grams	Dry Sed., grams	Fired Sed + Crucible, grams	Ash, grams	Moisture Content	% LOI
	12	.5-10 cm	9.3753	15.0249	11.1463	5.6496	1.771	10.9975	1.6222	219.0062	8.4020
	6	10-22 cm	9.0181	14.0836	11.1985	5.0655	2.1804	11.0745	2.0564	132.3198	5.6870
Pycno	Sample Layer	Temp. °C	Tare, grams	Bottle + Sed, grams	Bottle + Sediment + Water, grams	Density of Water	Pycnometer Bottle	Density, g/cm³			
209	.5-10	24	27.9222	33.5079	54.3960	0.997	25.3639	1.266			
208	10-22 cm	24	27.3648	32.3965	53.6512	0.997	24.9842	1.373			

Table A11. Bed sample analysis results for A12.

Galveston Bay: Houston Ship Channel											
Sample ID: 13:11:30 12/05/05 (A12)											
Length: 14 cm											
Visual: Used spatula to remove mud.											
	No real signs of layering.										
	Sample held shape. Sandy silty clay.										
Procedure:											
1	Decanted surface water.										
2	Scraped out fluid mud layer and combined with composite sample.										
3	Removed bottom cap.										
4	Applied positive pressure to push sample out bottom. Laid sample on a tray.										
Time	Crucible	Depth (ft)	Crucible Tare, grams	Wet Sed. + Crucible, grams	Dry Sed. + Crucible, grams	Wet Sed., grams	Dry Sed., grams	Fired Sed + Crucible, grams	Ash, grams	Moisture Content	% LOI
	6	0-14	9.0185	15.865	13.3288	6.8465	4.3103	13.2211	4.2026	58.8405	2.4987
Pycno	Sample Layer	Temp. °C	Tare, grams	Bottle + Sed, grams	Bottle + Sediment + Water, grams	Density of Water	Pycnometer Bottle	Density, g/cm³			
3	0-14	24	36.0598	45.7163	64.3870	0.9997	25.0277	1.520			

Table A12. Bed sample analysis results for A13.

Galveston Bay: Houston Ship Channel											
Sample ID: 13:37:35 12/5/05 (A13)											
Length: 24 cm											
Visual: 0.5 cm fluid mud.											
	Sample held shape. Mostly a sandy silty clay.										
	Color and texture determined the upper from the lower. Upper layer 4 cm.										
Procedure:											
1	Decanted surface water.										
2	Scraped out fluid mud layer and combined with composite sample.										
3	Removed bottom cap.										
4	Applied positive pressure to push sample out bottom. Laid sample on a tray.										
Time	Crucible	Depth (ft)	Crucible Tare, grams	Wet Sed. + Crucible, grams	Dry Sed. + Crucible, grams	Wet Sed., grams	Dry Sed., grams	Fired Sed + Crucible, grams	Ash, grams	Moisture Content	% LOI
	21	top	8.8948	15.7269	13.7778	6.8321	4.883	13.7039	4.8091	39.9160	1.5134
	17	bot	8.8840	16.9458	14.9113	8.0618	6.0273	14.8265	5.9425	33.7547	1.4069
Pycno	Sample Layer	Temp. °C	Tare, grams	Bottle + Sed, grams	Bottle + Sediment + Water, grams	Density of Water	Pycnometer Bottle	Density, g/cm^3			
4	.5-??	24	36.6178	44.7965	65.0390	0.997	24.7689	1.832			
6	??-24	24	36.5572	46.5710	65.7100	0.997	24.556	1.868			

Table A13. Bed sample analysis results for A15.

Galveston Bay: Houston Ship Channel											
Length: 19 cm											
Sample ID: 14:42:50 (A15)											
Visual: 0.5 cm fluid mud.											
	6 cm upper layer separated on its own.										
	12.5 cm lower sample held shape.										
	Clay silt.										
Procedure:											
1	Decanted surface water.										
2	Piped out fluid mud layer and combined with composite sample.										
3	Removed bottom cap.										
4	Applied positive pressure to push sample out bottom. Laid sample on a tray.										
Time	Crucible	Depth (ft)	Crucible Tare, grams	Wet Sed. + Crucible, grams	Dry Sed. + Crucible, grams	Wet Sed., grams	Dry Sed., grams	Fired Sed + Crucible, grams	Ash, grams	Moisture Content	% LOI
	20		10.5937	17.8418	13.1185	7.2481	2.5248	12.9059	2.3122	187.0762	8.4205
	26		10.9825	19.9901	15.4111	9.0076	4.4286	15.1851	4.2026	103.3961	5.1032
Pycno	Sample Layer	Temp. °C	Tare, grams	Bottle + Sed, grams	Bottle + Sediment + Water, grams	Density of Water	Pycnometer Bottle	Density, g/cm³			
208	.5-6.5	24	27.3662	37.4245	54.5894	0.997	24.9842	1.295			
209	6.5-19	24	27.9234	35.4187	55.6377	0.997	25.3639	1.474			

Table A14. Bed sample analysis results for B1.

Galveston Bay: Houston Ship Channel										
Length: 29 cm										
Sample ID: 08:59:00 12/6/05 (B1)										
Visual: Less than 0.5 cm fluid mud.										
	Sample appears to be a little sandy but still could determine the upper from the lower.									
	Upper layer 10.5 cm and lower 18.5 cm.									
	Sandy silty clay.									
Procedure:										
1	Decanted surface water.									
2	Piped out fluid mud layer and combined with composite sample.									
3	Removed bottom cap.									
4	Applied positive pressure to push sample out bottom. Laid sample on a tray.									
Time	Crucible	Depth (ft)	Crucible Tare, grams	Wet Sed. + Crucible, grams	Dry Sed. + Crucible, grams	Wet Sed., grams	Dry Sed., grams	Fired Sed + Crucible, grams	Ash, grams	Moisture Content	% LOI
	29		12.2822	20.3314	16.7977	8.0492	4.5155	16.6632	4.381	78.2571	2.9786
	30		11.1939	20.3306	16.9993	9.1367	5.8054	16.8342	5.6403	57.3828	2.8439
Pycno	Sample Layer	Temp. °C	Tare, grams	Bottle + Sed, grams	Bottle + Sediment + Water, grams	Density of Water	Pycnometer Bottle	Density, g/cm^3			
204	.5-11	24	27.3595	39.7120	57.3046	0.997	25.7013	1.533			
205	11-29.5	24	28.3943	37.9767	57.3127	0.997	24.9413	1.727			

Table A15. Bed sample analysis results for B2.

Galveston Bay: Houston Ship Channel										
Sample ID: 09:28:16 12/6/05 (B2)										
Length: 37 cm										
Visual: 0.5 cm fluid mud.										
	The rest of the sample appeared to be fairly consistent. Layers were determined more by feel than by visual inspection.									
	Upper layer 4 cm and the lower layer 33 cm.									
Procedure:										
1	Decanted surface water.									
2	Piped out fluid mud layer and combined with composite sample.									
3	Removed bottom cap.									
4	Applied positive pressure to push sample out bottom. Laid sample on a tray.									
Time	Crucible	Depth (ft)	Crucible Tare, grams	Wet Sed. + Crucible, grams	Dry Sed. + Crucible, grams	Wet Sed., grams	Dry Sed., grams	Fired Sed + Crucible, grams	Ash, grams	Moisture Content	% LOI
	25	TOP	10.4898	16.3948	12.7013	5.9050	2.2115	12.5551	2.0653	167.0133	6.6109
	26	BOT	10.9828	17.9834	14.3570	7.0006	3.3742	14.1565	3.1737	107.4744	5.9421
Pycno	Sample Layer	Temp. °C	Tare, grams	Bottle + Sed, grams	Bottle + Sediment + Water, grams	Density of Water	Pycnometer Bottle	Density, g/cm³			
206	.5-4.5	24	28.3754	33.9654	54.6506	0.997	25.007	1.312			
208	4.5-39.5	24	27.3664	34.0876	54.3955	0.997	24.9842	1.456			

Table A16. Bed sample analysis results for B3.

Galveston Bay: Houston Ship Channel											
Sample ID: 10:07:43 (B3)											
Visual: 0.8 cm fluid mud.											
	0.8-14.5 cm seems to be consistent with no obvious stratification or layering.										
	Sample held shape.										
Procedure:											
1	Decanted surface water.										
2	Piped out fluid mud layer and combined with composite sample.										
3	Removed bottom cap.										
4	Applied positive pressure to push sample out bottom. Laid sample on a tray.										
Time	Crucible	Depth (ft)	Crucible Tare, grams	Wet Sed. + Crucible, grams	Dry Sed. + Crucible, grams	Wet Sed., grams	Dry Sed., grams	Fired Sed + Crucible, grams	Ash, grams	Moisture Content	% LOI
	20	0.9-14.5 cm	10.5935	16.4138	13.2693	5.8203	2.6758	13.1212	2.5277	117.5163	5.5348
			0.0000	0	0	0.0000	0	0	0		
Pycno	Sample Layer	Temp. °C	Tare, grams	Bottle + Sed, grams	Bottle + Sediment + Water, grams	Density of Water	Pycnometer Bottle	Density, g/cm³			
208	.8-14.5	24	27.3687	33.0902	54.0535	0.997	24.9842	1.446			
205		0	0.0000	0.0000	0.0000	0	24.9413				

Table A17. Bed sample analysis results for B4.

Galveston Bay: Houston Ship Channel										
Length: 35 cm										
Sample ID: 11:20:55 12/6/05 (B4)										
Visual: 0.5 cm fluid mud.										
	3 cm upper layer.									
	31 cm lower layer.									
	Not a lot of difference in upper and lower layers. Upper appears to be a little denser and less organic than lower.									
	That could be the reason why. I ran the sample twice to be sure.									
Procedure:										
1	Decanted surface water.									
2	Piped out fluid mud layer and combined with composite sample.									
3	Removed bottom cap.									
4	Applied positive pressure to push sample out bottom. Laid sample on a tray.									
Time	Crucible	Depth (ft)	Crucible Tare, grams	Wet Sed. + Crucible, grams	Dry Sed. + Crucible, grams	Wet Sed., grams	Dry Sed., grams	Fired Sed + Crucible, grams	Ash, grams	Moisture Content	% LOI
	17	top	8.8838	13.8275	10.9097	4.9437	2.0259	10.7852	1.9014	144.0249	6.1454
	21	bot	8.8943	14.1085	10.8821	5.2142	1.9878	10.7179	1.8236	162.3101	8.2604
Pycno	Sample Layer	Temp. °C	Tare, grams	Bottle + Sed, grams	Bottle + Sediment + Water, grams	Density of Water	Pycnometer Bottle	Density, g/cm³			
204	3.5-34.5	24	27.3482	31.6442	54.0708	0.997	25.7013	1.339			
205	.5-3.5	24	28.3913	31.6260	54.0947	0.997	24.9413	1.345			
206	.5-3.5	24	28.3749	33.7280	54.6909	0.997	25.0070	1.345			
207	3.5-34.5	24	28.9407	34.5687	54.9441	0.997	24.7927	1.292			

Table A18. Bed sample analysis results for B5.

Galveston Bay: Houston Ship Channel											
Sample ID: 12:00:42 (B5)											
Visual: 0-0.5 cm fluid mud.											
	0.5-5 cm layer separated on its own. Unable to hold shape.										
	5-11.5 cm sample held shape.										
Procedure:											
1	Decanted surface water.										
2	Piped out fluid mud layer and combined with composite sample.										
3	Removed bottom cap.										
4	Applied positive pressure to push sample out bottom. Laid sample on a tray.										
Time	Crucible	Depth (ft)	Crucible Tare, grams	Wet Sed. + Crucible, grams	Dry Sed. + Crucible, grams	Wet Sed., grams	Dry Sed., grams	Fired Sed + Crucible, grams	Ash, grams	Moisture Content	% LOI
	21	0.5-5 cm	8.8940	12.9998	10.2389	4.1058	1.3449	10.1347	1.2407	205.2866	7.7478
	22	6-11.5 cm	8.7430	14.6487	11.4614	5.9057	2.7184	11.321	2.578	117.2491	5.1648
Pycno	Sample Layer	Temp. °C	Tare, grams	Bottle + Sed, grams	Bottle + Sediment + Water, grams	Density of Water	Pycnometer Bottle	Density, g/cm³			
204	.5-5	24	27.3517	33.1376	54.3476	0.997	25.7013	1.307			
209	5-11.5	24	27.9253	33.8979	54.9271	0.997	25.3639	1.398			

Table A19. Bed sample analysis results for B6.

Galveston Bay: Houston Ship Channel											
Sample ID: 12:26:13 12/06/05 (B6)											
Visual: 0.5 cm fluid mud, scraped off once sample was extracted.											
	Sample 11.5 cm no layers.										
Procedure:											
1	Removed bottom cap.										
2	Applied positive pressure to push sample out bottom. Laid sample on a tray.										
3	Scraped off mud layer and combined with composite sample.										
Time	Crucible	Depth (ft)	Crucible Tare, grams	Wet Sed. + Crucible, grams	Dry Sed. + Crucible, grams	Wet Sed., grams	Dry Sed., grams	Fired Sed + Crucible, grams	Ash, grams	Moisture Content	% LOI
	29	.5-12	12.2822	19.7568	17.3100	7.4746	5.0278	17.221	4.9388	48.6654	1.7702
Pycno	Sample Layer	Temp. °C	Tare, grams	Bottle + Sed, grams	Bottle + Sediment + Water, grams	Density of Water	Pycnometer Bottle	Density, g/cm³			
204	.5-12	24	27.3476	33.8565	55.6918	0.997	25.7013	1.713			

Table A20. Bed sample analysis results for B7.

Galveston Bay: Houston Ship Channel											
Sample ID: 12:43:29 (B7)											
Visual: 0-1 cm fluid mud.											
	1-4 cm of less dense material. Appears to be darker with an organic odor and a bit more stiff than previous samples.										
	4-16 cm is mostly sand with obvious layers of organics that appear as streaks. See photo.										
Procedure:											
1	Decanted surface water.										
2	Piped out fluid mud layer and combined with composite sample.										
3	Removed bottom cap.										
4	Applied positive pressure to push sample out bottom. Laid sample on a tray.										
Time	Crucible	Depth (ft)	Crucible Tare, grams	Wet Sed. + Crucible, grams	Dry Sed. + Crucible, grams	Wet Sed., grams	Dry Sed., grams	Fired Sed + Crucible, grams	Ash, grams	Moisture Content	% LOI
	3	1-4 cm	9.6523	15.1689	12.8473	5.5166	3.195	12.7543	3.102	72.6635	2.9108
	26	4-14 cm	10.9826	18.9608	17.2921	7.9782	6.3095	17.2466	6.264	26.4474	0.7211
Pycno	Sample Layer	Temp. °C	Tare, grams	Bottle + Sed, grams	Bottle + Sediment + Water, grams	Density of Water	Pycnometer Bottle	Density, g/cm³			
204	1-4 cm	24	27.3517	33.9003	55.3979	0.997	25.7013	1.582			
205	4-16cm	24	28.3947	34.5505	56.3374	0.997	24.9413	1.993			

Table A21. Bed sample analysis results for B9.

Galveston Bay: Houston Ship Channel											
Sample ID: 13:15:44 (B9)											
Length: 35.6 cm.											
Visual: Brown (fluid mud) layer is 0.6 cm.											
	The next 5 cm is the more jell like material. Once the sample was removed from the tube it didn't hold its shape and slumped.										
	The next 30 cm seemed to be consistent in density but at the 28 cm layer there appeared to be a little darker material that had a definite organic smell (hydrogen sulfides).										
Procedure:											
1	Decanted surface water.										
2	Piped out fluid mud layer and combined with composite sample.										
3	Removed bottom cap.										
4	Applied positive pressure to push sample out bottom. Laid sample on a tray.										
Time	Crucible	Depth (ft)	Crucible Tare, grams	Wet Sed. + Crucible, grams	Dry Sed. + Crucible, grams	Wet Sed., grams	Dry Sed., grams	Fired Sed + Crucible, grams	Ash, grams	Moisture Content	% LOI
	10	.7-5 cm	9.3228	18.0003	12.0485	8.6775	2.7257	11.86	2.5372	218.3586	6.9157
	15	6-28 cm	13.3661	20.4507	16.1067	7.0846	2.7406	15.9378	2.5717	158.5054	6.1629
Pycno	Sample Layer	Temp. °C	Tare, grams	Bottle + Sed, grams	Bottle + Sediment + Water, grams	Density of Water	Pycnometer Bottle	Density, g/cm³			
204	.7-5 cm	24.5	27.3517	32.4850	54.0021	0.9972	25.7013	1.245			
209	6-28 cm	24.5	27.9252	34.9471	54.8394	0.9972	25.3639	1.297			
205	6-28 cm	24.5	28.3947	32.6837	54.2417	0.9972	24.9413	1.291			

Table A22. Bed sample analysis results for B11.

Galveston Bay: Houston Ship Channel											
Sample ID: 14:07:52 (B11)											
Visual: 0-0.6 cm fluid mud.											
	0.6-5.5 cm showed signs of slumping and once dissected the less dense material separated from the more dense.										
	5.5-21 cm seemed consistent and held shape.										
Procedure:											
1	Decanted surface water.										
2	Piped out fluid mud layer and combined with composite sample.										
3	Removed bottom cap.										
4	Applied positive pressure to push sample out bottom. Laid sample on a tray.										
Time	Crucible	Depth (ft)	Crucible Tare, grams	Wet Sed. + Crucible, grams	Dry Sed. + Crucible, grams	Wet Sed., grams	Dry Sed., grams	Fired Sed + Crucible, grams	Ash, grams	Moisture Content	% LOI
	6	0.6-5.5 cm	9.0183	17.2026	13.2107	8.1843	4.1924	13.0535	4.0352	95.2175	3.7496
	27	5.5-21 cm	12.4793	19.8196	16.5698	7.3403	4.0905	16.4246	3.9453	79.4475	3.5497
Pycno	Sample Layer	Temp. °C	Tare, grams	Bottle + Sed, grams	Bottle + Sediment + Water, grams	Density of Water	Pycnometer Bottle	Density, g/cm^3			
204	.6-5.5	24	27.3517	33.5743	55.0435	0.997	25.7013	1.493			
205	5.5-21	24	28.3947	35.2966	55.9359	0.997	24.9413	1.628			

Table A23. Bed sample analysis results for B12.

Galveston Bay: Houston Ship Channel											
Sample ID: 14:32:20 12/6/05 (B12)											
Length: 35 cm											
Visual: 0.5 cm fluid mud.											
	1 cm of less dense material, no sample taken.										
	33.5 cm sample.										
Procedure:											
1	Decanted surface water.										
2	Piped out fluid mud layer and combined with composite sample.										
3	Removed bottom cap.										
4	Applied positive pressure to push sample out bottom. Laid sample on a tray.										
Time	Crucible	Depth (ft)	Crucible Tare, grams	Wet Sed. + Crucible, grams	Dry Sed. + Crucible, grams	Wet Sed., grams	Dry Sed., grams	Fired Sed + Crucible, grams	Ash, grams	Moisture Content	% LOI
	25		10.4896	20.7803	14.3330	10.2907	3.8434	14.0318	3.5422	167.7499	7.8368
Pycno	Sample Layer	Temp. °C	Tare, grams	Bottle + Sed, grams	Bottle + Sediment + Water, grams	Density of Water	Pycnometer Bottle	Density, g/cm³			
204	1-33.5	24	27.3497	32.8042	54.3089	0.997	25.7013	1.320			

Table A24. Bed sample analysis results for B14.

Galveston Bay: Houston Ship Channel											
Sample ID: 15:11:50 12/6/05 (B14)											
Visual: No standing water on sample. Sample didn't extract like others.											
	The sample appears to be more gel-like than the others.										
	Length: 11 cm.										
Procedure:											
1	Removed bottom cap.										
2	Applied positive pressure to push sample out bottom. Laid sample on a tray.										
3	Scraped out mud layer and combined with composite sample.										
Time	Crucible	Depth (ft)	Crucible Tare, grams	Wet Sed. + Crucible, grams	Dry Sed. + Crucible, grams	Wet Sed., grams	Dry Sed., grams	Fired Sed + Crucible, grams	Ash, grams	Moisture Content	% LOI
	20	0-11	10.5938	18.8908	13.0334	8.2970	2.4396	12.7799	2.1861	240.0967	10.3910
Pycno	Sample Layer	Temp. °C	Tare, grams	Bottle + Sed, grams	Bottle + Sediment + Water, grams	Density of Water	Pycnometer Bottle	Density, g/cm³			
205	0-11	24	28.3916	35.7281	54.5996	0.997	24.941	1.220			

Table A25. Bed sample analysis results for B16.

Galveston Bay: Houston Ship Channel											
Sample ID: 16:03:02 12/6/05 (B16)											
Length: 27.5 cm											
Visual: 0.5 cm fluid mud.											
	Upper layer 12 cm. This layer was unable to hold shape, more of a soft gel.										
	Lower layer 15 cm, sample held shape.										
Procedure:											
1	Decanted surface water.										
2	Piped out fluid mud layer and combined with composite sample.										
3	Removed bottom cap.										
4	Applied positive pressure to push sample out bottom. Laid sample on a tray.										
Time	Crucible	Depth (ft)	Crucible Tare, grams	Wet Sed. + Crucible, grams	Dry Sed. + Crucible, grams	Wet Sed., grams	Dry Sed., grams	Fired Sed + Crucible, grams	Ash, grams	Moisture Content	% LOI
	8	.5-12.5	11.1129	19.8863	14.1216	8.7734	3.0087	13.9308	2.8179	191.6010	6.3416
	28	12.5-27.5	11.3876	18.1792	14.3866	6.7916	2.999	14.2498	2.8622	126.4622	4.5615
Pycno	Sample Layer	Temp. °C	Tare, grams	Bottle + Sed, grams	Bottle + Sediment + Water, grams	Density of Water	Pycnometer Bottle	Density, g/cm³			
8	.5-12.5	24	36.3900	43.5369	62.6600	0.997	24.7872	1.275			
204	12.5-27.5	24	27.3485	34.3621	55.0894	0.997	25.7013	1.428			

Table A26. Bed sample analysis results for B17.

Galveston Bay: Houston Ship Channel											
Sample ID: 16:18:24 (B17)											
Visual: Sample had no standing water; therefore there was no brown layer greater than a cap.											
	0-13.5 cm was the less dense material and was quite obvious by its inability to maintain shape.										
	13.5-25 cm was consistent and held shape.										
Procedure:											
1	Decanted surface water.										
2	Piped out fluid mud layer and combined with composite sample.										
3	Removed bottom cap.										
4	Applied positive pressure to push sample out bottom. Laid sample on a tray.										
Time	Crucible	Depth (ft)	Crucible Tare, grams	Wet Sed. + Crucible, grams	Dry Sed. + Crucible, grams	Wet Sed., grams	Dry Sed., grams	Fired Sed + Crucible, grams	Ash, grams	Moisture Content	% LOI
	9	0-13.5 cm	8.7656	15.338	11.0267	6.5724	2.2611	10.773	2.0074	190.6727	11.2202
	29	13.5-25 cm	12.2819	18.2014	14.625	5.9195	2.3431	14.4013	2.1194	152.6354	9.5472
Pycno	Sample Layer	Temp. °C	Tare, grams	Bottle + Sed, grams	Bottle + Sediment + Water, grams	Density of Water	Pycnometer Bottle	Density, g/cm^3			
205	0-13.5	21	28.3947	34.7465	54.6459	0.998	24.9413	1.270			
208	13.5-25	21	27.3687	33.3882	53.8139	0.998	24.9842	1.332			

Table A27. Bed sample analysis results for C1.

Galveston Bay: Houston Ship Channel											
Sample ID: 9:23:33 (C1)											
Visual: 0.5 cm fluid mud.											
	6 cm layer separated on its own. Unable to hold shape.										
	Sample held shape. Sandy clay										
Procedure:											
1	Decanted surface water.										
2	Piped out fluid mud layer and combined with composite sample.										
3	Removed bottom cap.										
4	Applied positive pressure to push sample out bottom. Laid sample on a tray.										
Time	Crucible	Depth (ft)	Crucible Tare, grams	Wet Sed. + Crucible, grams	Dry Sed. + Crucible, grams	Wet Sed., grams	Dry Sed., grams	Fired Sed + Crucible, grams	Ash, grams	Moisture Content	% LOI
	8		11.1128	21.4141	16.3005	10.3013	5.1877	16.1013	4.9885	98.5716	3.8399
	15		13.3659	21.8939	18.3322	8.5280	4.9663	18.1664	4.8005	71.7174	3.3385
Pycno	Sample Layer	Temp. °C	Tare, grams	Bottle + Sed, grams	Bottle + Sediment + Water, grams	Density of Water	Pycnometer Bottle	Density, g/cm³			
208	.5-6.5	24	27.3710	35.5416	54.8197	0.997	24.9842	1.447			
209	6.5-??	24	27.9252	38.0142	56.8489	0.997	25.3639	1.559			

Table A28. Bed sample analysis results for C2.

Galveston Bay: Houston Ship Channel											
Sample ID: 09:46:52 Collected 12/7/05 (C2)											
Visual: Brown layer (fluff) 0.8 cm.											
	What appears to be a gray layer 3 cm.										
	Gray/black layer 23 cm.										
Procedure:											
1	Decanted surface water.										
2	Piped out fluid mud layer and combined with composite sample.										
3	Removed bottom cap.										
4	Applied positive pressure to push sample out bottom. Laid sample on a tray.										
Time	Crucible	Depth (ft)	Crucible Tare, grams	Wet Sed. + Crucible, grams	Dry Sed. + Crucible, grams	Wet Sed., grams	Dry Sed., grams	Fired Sed + Crucible, grams	Ash, grams	Moisture Content	% LOI
09:46:52	208	1.349	8.9207	16.9333	12.1756	8.0126	3.2549	11.2463	2.3256	146.1704	28.5508
09:46:52	205	1.313	8.8183	15.7645	11.5725	6.9462	2.7542	11.4298	2.6115	152.2039	5.1812
Pycno	Sample Layer	Temp. °C	Tare, grams	Bottle + Sed, grams	Bottle + Sediment + Water, grams	Density of Water	Pycnometer Bottle	Density, g/cm³			
208	2-20cm	23.5	27.3692	31.7076	53.4186	0.9974	24.984	1.349			
205	0-2cm	23.5	28.3985	34.7810	54.8074	0.9974	24.941	1.313			

Table A29. Bed sample analysis results for C3.

Galveston Bay: Houston Ship Channel											
Sample ID: 10:22:56 (C3)											
Visual: 0-1 cm brown (fluid mud) layer.											
	1-8 cm less dense material that seems to separate itself from the remainder of sample.										
	8-23 cm of sample tended to be denser and held its shape. At the 28 cm layer appeared to be an organic layer of brush (sticks, grass, leaves) and some shale.										
	Length of sample is 36 cm.										
Procedure:											
1	Decanted surface water.										
2	Piped out fluid mud layer and combined with composite sample.										
3	Removed bottom cap.										
4	Applied positive pressure to push sample out bottom. Laid sample on a tray.										
Time	Crucible	Depth (ft)	Crucible Tare, grams	Wet Sed. + Crucible, grams	Dry Sed. + Crucible, grams	Wet Sed., grams	Dry Sed., grams	Fired Sed + Crucible, grams	Ash, grams	Moisture Content	% LOI
102256	8	1.5-8 cm	11.1127	18.9773	14.5718	7.8646	3.4591	14.3884	3.2757	127.3597	5.3020
102256	30	9-23 cm	11.1940	22.9553	18.1765	11.7613	6.9825	17.9542	6.7602	68.4397	3.1837
Pycno	Sample Layer	Temp. °C	Tare, grams	Bottle + Sed, grams	Bottle + Sediment + Water, grams	Density of Water	Pycnometer Bottle	Density, g/cm³			
208	1.5-8 cm	24.5	27.3687	31.9322	53.5226	0.9972	24.9842	1.369			
205	9-23 cm	24.5	28.3935	34.7286	55.3927	0.9972	24.9413	1.502			

Table A30. Bed sample analysis results for oxidized layer.

Galveston Bay: Houston Ship Channel											
Sample ID: Brown fluff (oxidized layer).											
Visual: This is the composite sample of the thin brown layer collected from all the samples containing this layer.											
Procedure:											
1	Decanted surface water.										
2	Mixed sample.										
3	Tested, same system that follows Step 4 on A29.										
Time	Crucible	Depth (ft)	Crucible Tare, grams	Wet Sed. + Crucible, grams	Dry Sed. + Crucible, grams	Wet Sed., grams	Dry Sed., grams	Fired Sed + Crucible, grams	Ash, grams	Moisture Content	% LOI
17	0-1 cm	8.8839	14.3082	10.5547	5.4243	1.6708	10.4407	1.5568	224.6529	6.8231	6.8231
Pycno	Sample Layer	Temp. °C	Tare, grams	Bottle + Sed, grams	Bottle + Sediment + Water, grams	Density of Water	Pycnometer Bottle	Density, g/cm³			
204		21	27.3517	32.5356	53.9722	0.997	25.7013	1.234			

Table A31. Impeller voltage – shear stress relationship.

Voltage	Stress (Pa)
2	0.2
3	0.35
4	0.5
5	0.67
6	0.83
7	0.98
8	1.14
9	1.29
10	1.45
11	1.6

Table A32. VOST Results for A2.

Project Name: Houston Ship Channel						
Date of Project:						
Sample I.D.: 095914 TOP (A2)						
Bottle	Impeller Voltage	Optical Back Scatter Voltage	Time (min)	Vol. (mL)	Net Wt. (g)	Conc. (g/L)
21	2	-0.107	20	100	0	0.0000
22	2	-0.112	30	100	0.0001	0.0010
23	2	-0.112	40	100	0.0001	0.0010
24	2	-0.108	50	100	0	0.0000
25	2	-0.112	60	100	0	0.0000
26	5	-0.128	20	100	0.001	0.0100
27	5	-0.130	30	100	0	0.0000
28	5	-0.130	40	100	0.0002	0.0020
29	5	-0.131	50	100	0.0001	0.0010
30	5	-0.129	60	100	0	0.0000
1	7	-0.144	20	100	0.0002	0.0020
2	7	-0.146	30	100	0.0002	0.0020
3	7	-0.146	40	100	0.0003	0.0030
14	7	-0.139	50	100	0.0002	0.0020
15	7	-0.138	60	100	0.0003	0.0030
16	8	-0.115	20	100	0.0002	0.0020
17	8	-0.099	30	100	0.0002	0.0020
18	8	-0.143	40	100	0.0003	0.0030

Table A33. VOST results for B9.

Project Name: Houston Ship Channel						
Date of Project:						
Sample I.D.:131544 TOP (B9)						
Bottle	Impeller Voltage	Optical Back Scatter Voltage	Time (min)	Vol. (mL)	Net Wt. (g)	Conc. (g/L)
1	2	0.366	20	100	0.0001	0.0010
2	2	0.379	30	100	0	0.0000
3	2	0.395	40	100	0.0001	0.0010
4	2	0.408	50	100	0.0002	0.0020
5	2	0.427	60	100	0.0001	0.0010
6	5	0.34	20	100	0	0.0000
7	5	0.34	30	100	0.0002	0.0020
8	5	0.339	40	100	0.0002	0.0020
9	5	0.333	50	100	0.0002	0.0020
10	5	0.335	60	100	0.0002	0.0020
11	7	0.355	20	100	0.0003	0.0030
12	7		30	100	0.0004	0.0040
13	7	0.37	40	100	0.0003	0.0030
14	7	0.369	50	100	0.0004	0.0040
15	7	0.369	60	100	0.0002	0.0020
16	8	0.369	20	100	0.0003	0.0030
17	8	0.369	30	100	0.0007	0.0070
18	8	0.371	40	100	0.0006	0.0060
19	8	0.374	50	100	0.0008	0.0080
20	8	0.372	60	100	0.0007	0.0070

Table A34. VOST results for B16.

Project Name: Houston Ship Channel						
Date of Project:						
Sample I.D.: 160302 TOP (B16)						
Bottle	Impeller Voltage	Optical Back Scatter Voltage	Time (min)	Vol. (mL)	Net Wt. (g)	Conc. (g/L)
1	2	0.228	20	100	0	0.0000
2	2	0.290	30	100	0	0.0000
3	2	0.290	40	100	0	0.0000
4	2	0.287	50	100	0	0.0000
5	2	0.289	60	100	0.0001	0.0010
6	5	0.283	20	100	0	0.0000
7	5	0.281	30	100	0.0001	0.0010
8	5	0.280	40	100	0.0001	0.0010
9	5	0.280	50	100	0	0.0000
10	5	0.280	60	100	0	0.0000
11	7	0.275	20	100	0.0002	0.0020
12	7	0.268	30	100	0.0001	0.0010
13	7	0.254	40	100	0.0001	0.0010
14	7	0.079	50	100	0.0001	0.0010
15	7	0.379	60	100	0.0001	0.0010
16	8	0.080	20	100	0.0003	0.0030
17	8	-0.115	30	100	0.0004	0.0040
18	8	-0.116	40	100	0.0007	0.0070
19	8	-0.120	50	100	0.0013	0.0130

Table A35. VOST results for B17 top.

Project Name: Houston Ship Channel						
Date of Project:						
Sample I.D.: 161824 TOP (B17)						
Bottle	Impeller Voltage	Optical Back Scatter Voltage	Time (min)	Vol. (mL)	Net Wt. (g)	Conc. (g/L)
1	2	0.402	20	100	0.0002	0.0020
2	2	0.420	30	100	0.0002	0.0020
3	2	0.439	40	100	0.0001	0.0010
4	2	0.575	50	100	0.0002	0.0020
5	2	0.600	60	100	0	0.0000
6	5	0.359	20	100	0.0001	0.0010
7	5	0.356	30	100	0.0001	0.0010
8	5	0.367	40	100	0.0002	0.0020
9	5	0.370	50	100	0.0001	0.0010
10	5	0.375	60	100	0.0001	0.0010
11	7	0.330	20	100	0.0002	0.0020
12	7	0.369	30	100	0.0002	0.0020
13	7	0.367	40	100	0.0002	0.0020
14	7	0.340	50	100	0.0002	0.0020
15	7	0.338	60	100	0.0002	0.0020
16	8	0.356	20	100	0.0001	0.0010
17	8	0.356	30	100	0.0001	0.0010
18	8	0.354	40	100	0.0003	0.0030
19	8	0.347	50	100	0.0002	0.0020
20	8	0.358	60	100	0.0002	0.0020
21	9	0.354	20	100	0.0002	0.0020
22	9	0.357	30	100	0.0002	0.0020
23	9	0.360	40	100	0.0002	0.0020
24	9	0.360	50	100	0.0003	0.0030
25	9	0.360	60	100	0.0002	0.0020
26	10	0.367	20	100	0.0004	0.0040
27	10	0.380	30	100	0.0004	0.0040
28	10	0.395	40	100	0.0005	0.0050
29	10	0.380	50	100	0.0005	0.0050
30	10	0.385	60	100	0.0005	0.0050

Table A36. VOST results for B17 bottom.

Project Name: Houston Ship Channel						
Date of Project: 12/6/05						
Sample I.D.:161824 Bottom (B17)						
Bottle	Impeller Voltage	Optical Back Scatter Voltage	Time (min)	Vol. (mL)	Net Wt. (g)	Conc. (g/L)
1	2	0.377	20	100	0.0001	0.0010
2	2	0.378	30	100	0.0001	0.0010
3	2	0.366	40	100	0.0001	0.0010
4	2	0.379	50	100	0.0002	0.0020
5	2	0.389	60	100	0.0001	0.0010
6	5	0.264	20	100	0.0004	0.0040
7	5	0.268	30	100	0.0003	0.0030
8	5	0.272	40	100	0.0002	0.0020
9	5	0.275	50	100	0.0004	0.0040
10	5	0.234	60	100	0.0003	0.0030
11	7	0.218	20	100	0.0005	0.0050
12	7	0.218	30	100	0.0005	0.0050
13	7	0.22	40	100	0.0004	0.0040
14	7	0.219	50	100	0.0004	0.0040
15	7	0.219	60	100	0.0003	0.0030
16	10	0.228	20	100	0.0004	0.0040
17	10	0.229	30	100	0.0004	0.0040
18	10	0.229	40	100	0.0004	0.0040
19	10	0.23	50	100	0.0005	0.0050
20	10	0.23	60	100	0.0006	0.0060
21	15	1.165	20	100	0.0131	0.1310

Table A37. VOST results for C1.

Project Name: Houston Ship Channel						
Date of Project:						
Sample I.D.: 092333 TOP (C1)						
Bottle	Impeller Voltage	Optical Back Scatter Voltage	Time (min)	Vol. (mL)	Net Wt. (g)	Conc. (g/L)
1	2	-0.115	20	100	0.0001	0.0010
2	2	-0.103	30	100	0	0.0000
3	2	-0.100	40	100	0	0.0000
4	2	-0.101	50	100	0.0001	0.0010
5	2	-0.099	60	100	0.0001	0.0010
6	5	-0.133	20	100	0.0001	0.0010
7	5	-0.127	30	100	0.0001	0.0010
8	5	-0.137	40	100	0	0.0000
9	5	-0.130	50	100	0.0001	0.0010
10	5	-0.129	60	100	0.0001	0.0010
11	7	-0.131	20	100	0.0001	0.0010
12	7	-0.139	30	100	0.0001	0.0010
13	7	-0.138	40	100	0.0003	0.0030
14	7	-0.139	50	100	0.0002	0.0020
15	7	-0.138	60	100	0.0003	0.0030
16	8	-0.115	20	100	0.0002	0.0020
17	8	-0.099	30	100	0.0002	0.0020
18	8	-0.143	40	100	0.0003	0.0030

Table A38. VOST results for C3.

Project Name: Houston Ship Channel						
Date of Project:						
Sample I.D.:102256 TOP (C3)						
Bottle	Impeller Voltage	Optical Back Scatter Voltage	Time (min)	Vol. (mL)	Net Wt. (g)	Conc. (g/L)
1	2	0.178	20	100	0.0001	0.0010
2	2	0.182	30	100	0.0001	0.0010
3	2	0.188	40	100	0	0.0000
4	2	0.19	50	100	0	0.0000
5	2	0.194	60	100	0	0.0000
6	5	0.226	20	100	0	0.0000
7	5	0.228	30	100	0	0.0000
8	5	0.238	40	100	0	0.0000
9	5	0.253	50	100	0	0.0000
10	5	0.265	60	100	0.0001	0.0010
11	7	0.345	20	100	0.0001	0.0010
12	7	0.352	30	100	0.0002	0.0020
13	7	0.389	40	100	0.0002	0.0020
14	7	0.41	50	100	0.0004	0.0040
15	7	0.39	60	100	0.0004	0.0040
16	8	0.55	20	100	0.0004	0.0040
17	8	0.548	30	100	0.0003	0.0030
18	8	0.552	40	100	0.0003	0.0030
19	8	0.545	50	100	0.0003	0.0030
20	8	0.545	60	100	0.0003	0.0030
21	9	0.543	20	100	0.0003	0.0030
22	9	0.545	30	100	0.0004	0.0040
23	9	0.546	40	100	0.0004	0.0040
24	9	0.571	50	100	0.0003	0.0030
25	9	0.573	60	100	0.0004	0.0040
26	10	0.57	20	100	0.0004	0.0040
27	10	0.62	30	100	0.0005	0.0050
28	10	0.631	40	100	0.0006	0.0060
29	10	0.364	50	100	0.0005	0.0050

Table A39. VOST results for the oxidized layer (first test – tested twice).

Project Name: Houston Ship Channel							
Date of Project:							
Sample I.D.: Fluff (oxidized layer)							
Bottle	Impeller Voltage	Optical Back Scatter Voltage	Time (min)	Vol. (mL)	Net Wt. (g)	Conc. (g/L)	Comments
1	2	-0.112	20	100	0	0.0000	
2	2	-0.119	30	100	0	0.0000	
3	2	-0.119	40	100	0	0.0000	
4	2	-0.126	50	100	0	0.0000	
5	2	-0.127	60	100	0.0002	0.0020	
6	5	-0.143	20	100	0.0002	0.0020	
7	5	-0.143	30	100	0.0002	0.0020	
8	5	-0.144	40	100	0.0002	0.0020	Little pot holes
9	5	-0.144	50	100	0.0002	0.0020	
10	5	-0.145	60	100	0.0002	0.0020	
11	7	-0.150	20	100	0.0001	0.0010	More pot holes
12	7	-0.151	30	100	0.0001	0.0010	
13	7	-0.151	40	100	0.0001	0.0010	
14	7	-0.151	50	100	0.0001	0.0010	
15	7	-0.152	60	100	0.0001	0.0010	Even more pot holes
16	8	-0.151	20	100	0.0003	0.0030	Eroding around rim
17	8	-0.151	30	100	0.0003	0.0030	
18	8	-0.152	40	100	0.0004	0.0040	
19	8	-0.152	50	100	0.0006	0.0060	
20	8	-0.150	60	100	0.0005	0.0050	

Table A39. VOST results for the oxidized layer (second test – tested twice).

Project Name: Houston Ship Channel							
Date of Project:							
Sample I.D.: Fluff (oxidized layer)							
Bottle	Impeller Voltage	Optical Back Scatter Voltage	Time (min)	Vol. (mL)	Net Wt. (g)	Conc. (g/L)	Comments
1	2	-0.107	20	100	0.0001	0.0010	
2	2	-0.100	30	100	0	0.0000	
3	2	-0.103	40	100	0.0002	0.0020	
4	2	-0.103	50	100	0.0001	0.0010	
5	2	-0.125	60	100	0.0001	0.0010	
6	5	-0.137	20	100	0.0001	0.0010	
7	5	-0.138	30	100	0.0002	0.0020	Little pot holes
8	5	-0.137	40	100	0.0002	0.0020	
9	5	-0.136	50	100	0.0001	0.0010	
10	5	-0.137	60	100	0.0001	0.0010	
11	7	-0.149	20	100	0.0001	0.0010	Sample seems to be dissolving
12	7	-0.149	30	100	0.0001	0.0010	
13	7	-0.149	40	100	0.0001	0.0010	
14	7	-0.151	50	100	0.0001	0.0010	
15	7	-0.149	60	100	0.0002	0.0020	
16	8	-0.145	20	100	0.0002	0.0020	
17	8	-0.141	30	100	0.0002	0.0020	Rim exposed

Table A40. Grain size distribution from Coulter Counter for A1.

COULTER® LS	9:52 28 Mar 2006		
File name:	092857.$04 (A1)		
From	0.375	95% Conf. Limits:	0
To	948.2	95% Conf. Limits:	159.8
Volume	100 mL	S.D.:	52.68
Mean:	56.5	Variance:	2776
Median:	47.32	C.V.:	93.25
D(3,2):	6.791	Skewness:	1.068
Mean/Median Ratio:	1.194	Kurtosis:	1.805
Mode:	96.49	Specific Surf. Area	8835
Volume, %	092857.$04 Particle Diameter µm <	092857.$05 Particle Diameter µm <	092857.$03 Particle Diameter µm <
10	2.544	2.398	2.381
25	7.349	6.746	6.69
50	47.32	42.77	42.73
75	92.81	88.21	89.03
90	127.3	120.5	123
	092857.$04	092857.$05	092857.$03
Channel Diameter (Lower) µm	Diff. Volume %	Diff. Volume %	Diff. Volume %
0.375	0.07	0.073	0.076
0.412	0.124	0.13	0.134
0.452	0.182	0.191	0.197
0.496	0.257	0.269	0.277
0.545	0.316	0.332	0.341
0.598	0.366	0.384	0.394
0.657	0.408	0.429	0.439
0.721	0.448	0.471	0.48
0.791	0.479	0.504	0.512
0.869	0.501	0.528	0.535
0.953	0.517	0.546	0.551
1.047	0.532	0.563	0.566
1.149	0.549	0.583	0.583
1.261	0.568	0.604	0.603
1.385	0.591	0.63	0.628
1.52	0.622	0.663	0.661
1.669	0.663	0.708	0.706
1.832	0.715	0.763	0.762
2.01	0.776	0.829	0.829
2.207	0.847	0.904	0.905
2.423	0.925	0.986	0.989

2.66	1.01	1.07	1.08
2.92	1.09	1.16	1.17
3.206	1.18	1.25	1.26
3.519	1.26	1.34	1.34
3.862	1.33	1.41	1.42
4.241	1.4	1.47	1.48
4.656	1.45	1.52	1.53
5.111	1.48	1.56	1.57
5.611	1.5	1.58	1.58
6.158	1.51	1.58	1.58
6.761	1.49	1.56	1.56
7.421	1.46	1.53	1.52
8.147	1.41	1.48	1.47
8.944	1.35	1.41	1.39
9.819	1.27	1.33	1.31
10.78	1.19	1.24	1.22
11.83	1.1	1.14	1.12
12.99	1.02	1.06	1.04
14.26	0.961	1	0.981
15.65	0.929	0.971	0.963
17.18	0.924	0.975	0.976
18.86	0.939	1	1
20.7	0.964	1.04	1.03
22.73	0.997	1.08	1.04
24.95	1.04	1.12	1.06
27.38	1.12	1.17	1.13
30.07	1.24	1.27	1.26
33	1.43	1.43	1.47
36.24	1.66	1.66	1.74
39.77	1.93	1.94	2.02
43.66	2.21	2.25	2.3
47.93	2.48	2.57	2.54
52.63	2.76	2.88	2.77
57.77	3.05	3.17	3.03
63.41	3.4	3.47	3.34
69.62	3.81	3.79	3.71
76.43	4.23	4.11	4.09
83.9	4.58	4.41	4.38
92.09	4.76	4.59	4.51
101.1	4.67	4.57	4.42
111	4.28	4.26	4.07
121.8	3.64	3.64	3.5

133.7	2.84	2.77	2.77
146.8	2.02	1.8	1.98
161.2	1.3	0.905	1.23
176.8	0.74	0.314	0.616
194.2	0.384	0.056	0.221
213.2	0.202	0.004	0.046
234.1	0.131	0	0.004
256.8	0.115	0	6.50E-05
282.1	0.113	0	0
309.6	0.098	0	0
339.8	0.061	0	0
373.1	0.025	0	0
409.6	0.005	0	0
449.7	0.0037	0	0

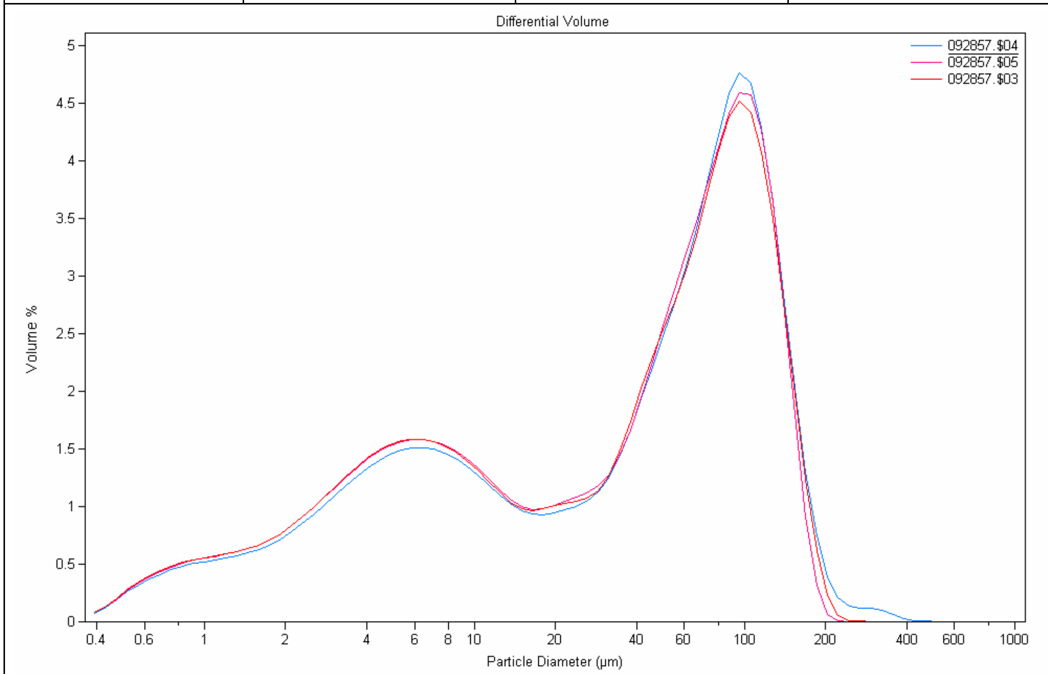

Table A41. Grain size distribution from Coulter Counter for A2.

COULTER LS	3/27/2006 14:17		
File name:	095914.$04 (A2)		
From	0.375	95% Conf. Limits:	0
To	948.2	95% Conf. Limits:	16.58
Volume	100 mL	S.D.:	5.046
Mean:	6.691	Variance:	25.46
Median:	5.444	C.V.:	75.42
D(3,2):	2.893	Skewness:	0.924
Mean/Median Ratio:	1.229	Kurtosis:	0.172
Mode:	7.083	Specific Surf. Area	20738
Volume %	095914.$04 Particle Diameter µm <	095914.$05 Particle Diameter µm <	095914.$06 Particle Diameter µm <
10	1.118	0.829	0.822
25	2.669	2.47	2.442
50	5.444	5.058	4.993
75	9.644	8.89	8.847
90	14.37	13.05	12.93
	095914.$04	095914.$05	095914.$06
Channel Diameter (Lower) µm	Diff. Volume %	Diff. Volume %	Diff. Volume %
0.375	0.185	0.339	0.344
0.412	0.327	0.63	0.638
0.452	0.477	1.01	1.02
0.496	0.669	1.3	1.31
0.545	0.817	1.49	1.51
0.598	0.934	1.58	1.6
0.657	1.03	1.56	1.58
0.721	1.11	1.46	1.48
0.791	1.17	1.3	1.31
0.869	1.2	1.09	1.11
0.953	1.22	0.899	0.911
1.047	1.23	0.753	0.764
1.149	1.25	0.689	0.7
1.261	1.28	0.726	0.737
1.385	1.33	0.868	0.882
1.52	1.4	1.11	1.12
1.669	1.51	1.42	1.44
1.832	1.65	1.76	1.78
2.01	1.83	2.1	2.12
2.207	2.03	2.39	2.42
2.423	2.25	2.64	2.67

2.66	2.5	2.83	2.87
2.92	2.75	3	3.03
3.206	3	3.16	3.2
3.519	3.24	3.33	3.36
3.862	3.46	3.5	3.53
4.241	3.66	3.68	3.7
4.656	3.83	3.84	3.84
5.111	3.97	3.98	3.96
5.611	4.06	4.09	4.05
6.158	4.12	4.17	4.11
6.761	4.14	4.22	4.14
7.421	4.13	4.23	4.15
8.147	4.07	4.16	4.1
8.944	3.96	4	3.98
9.819	3.8	3.76	3.79
10.78	3.61	3.52	3.57
11.83	3.39	3.3	3.34
12.99	3.17	3.09	3.07
14.26	2.93	2.81	2.71
15.65	2.66	2.35	2.21
17.18	2.25	1.45	1.39
18.86	1.51	0.417	0.423
20.7	0.706	0.026	0.028
22.73	0.156	0	0
24.95	0.014	0	0

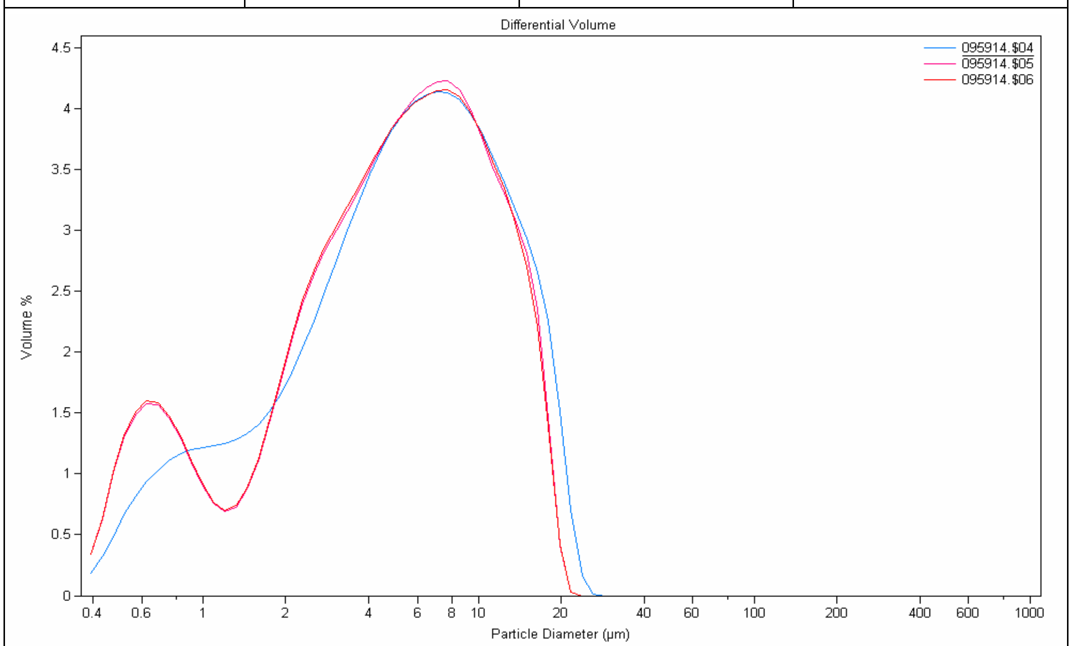

Table A42. Grain size distribution from Coulter Counter for A2 bottom.

COULTER LS	3/30/2006 13:19		
File name:	095914b.$04 (A2 bottom)		
From	0.375	95% Conf. Limits:	0
To	948.2	95% Conf. Limits:	56.37
Volume	100 mL	S.D.:	19.78
Mean:	17.6	Variance:	391.1
Median:	8.997	C.V.:	112.3
D(3,2):	4.27	Skewness:	1.602
Mean/Median Ratio:	1.957	Kurtosis:	1.899
Mode:	7.083	Specific Surf. Area	14053
Volume %	095914b.$04 Particle Diameter µm <	095914b.$05 Particle Diameter µm <	095914b.$06 Particle Diameter µm <
10	1.705	1.697	1.693
25	3.92	3.897	3.882
50	8.997	8.927	8.888
75	24.44	24.17	24.06
90	49.42	48.91	48.1
	095914b.$04	095914b.$05	095914b.$06
Channel Diameter (Lower) µm	Diff. Volume %	Diff. Volume %	Diff. Volume %
0.375	0.096	0.097	0.097
0.412	0.171	0.172	0.172
0.452	0.25	0.252	0.253
0.496	0.354	0.357	0.358
0.545	0.439	0.442	0.443
0.598	0.511	0.514	0.515
0.657	0.575	0.579	0.58
0.721	0.637	0.641	0.642
0.791	0.689	0.693	0.695
0.869	0.732	0.736	0.737
0.953	0.769	0.773	0.775
1.047	0.807	0.811	0.813
1.149	0.85	0.854	0.856
1.261	0.898	0.902	0.905
1.385	0.954	0.959	0.962
1.52	1.02	1.03	1.03
1.669	1.11	1.11	1.12
1.832	1.21	1.22	1.22
2.01	1.33	1.34	1.35
2.207	1.47	1.48	1.48
2.423	1.62	1.63	1.64

2.66	1.78	1.79	1.8
2.92	1.95	1.96	1.97
3.206	2.12	2.13	2.14
3.519	2.29	2.3	2.31
3.862	2.45	2.46	2.47
4.241	2.59	2.6	2.61
4.656	2.72	2.73	2.74
5.111	2.82	2.83	2.84
5.611	2.89	2.9	2.91
6.158	2.94	2.95	2.95
6.761	2.96	2.96	2.97
7.421	2.94	2.95	2.95
8.147	2.9	2.9	2.9
8.944	2.82	2.82	2.82
9.819	2.71	2.72	2.72
10.78	2.58	2.59	2.59
11.83	2.45	2.46	2.46
12.99	2.32	2.33	2.34
14.26	2.22	2.23	2.24
15.65	2.15	2.16	2.16
17.18	2.11	2.12	2.11
18.86	2.1	2.09	2.08
20.7	2.09	2.08	2.06
22.73	2.08	2.07	2.04
24.95	2.06	2.06	2.03
27.38	2.04	2.04	2.04
30.07	2	2.01	2.05
33	1.97	1.98	2.05
36.24	1.94	1.95	2.03
39.77	1.94	1.92	1.99
43.66	1.95	1.91	1.94
47.93	1.96	1.9	1.87
52.63	1.96	1.89	1.81
57.77	1.9	1.83	1.72
63.41	1.72	1.68	1.58
69.62	1.42	1.4	1.34
76.43	0.973	0.98	0.978
83.9	0.499	0.51	0.538
92.09	0.16	0.166	0.19
101.1	0.025	0.027	0.033
111	0.001	0.001	0.002

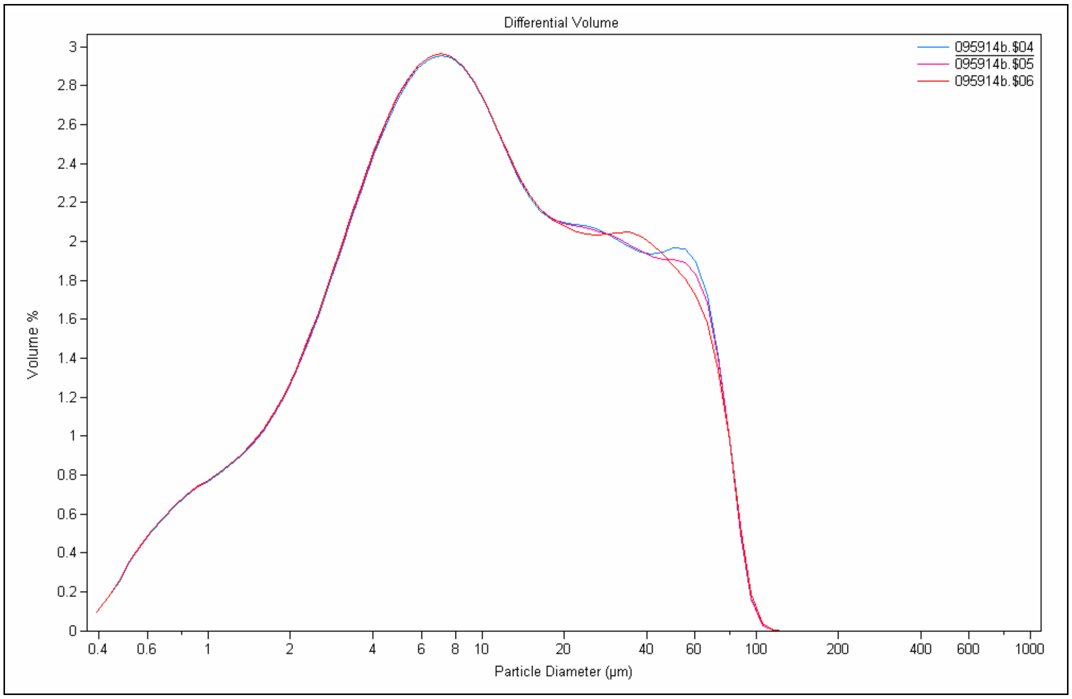

Differential Volume
095914b.$04
095914b.$05
095914b.$06
Volume %
Particle Diameter (µm)
0
0.2
0.4
0.6
0.8
1
1.2
1.4
1.6
1.8
2
2.2
2.4
2.6
2.8
3
0.4
0.6
1
2
4
6
8
10
20
40
60
100
200
400
600
1000

Table A43. Grain size distribution from Coulter Counter for A3.

COULTER LS	3/28/2006 14:28		
File name:	102315.$06 (A3)		
From	0.375	95% Conf. Limits:	0
To	948.2	95% Conf. Limits:	18.01
Volume	100 mL	S.D.:	5.483
Mean:	7.262	Variance:	30.06
Median:	5.962	C.V.:	75.5
D(3,2):	2.864	Skewness:	0.844
Mean/Median Ratio:	1.218	Kurtosis:	-0.0808
Mode:	7.776	Specific Surf. Area	20946
Volume %	102305.$06 Particle Diameter µm <	102305.$05 Particle Diameter µm <	102305.$04 Particle Diameter µm <
10	0.993	0.992	1.001
25	2.869	2.87	2.895
50	5.962	5.972	6.032
75	10.56	10.54	10.68
90	15.77	15.72	16.07
	102305.$06	102305.$05	102305.$04
Channel Diameter (Lower) µm	Diff. Volume %	Diff. Volume %	Diff. Volume %
0.375	0.248	0.249	0.248
0.412	0.463	0.465	0.462
0.452	0.749	0.752	0.747
0.496	0.978	0.981	0.974
0.545	1.15	1.15	1.14
0.598	1.25	1.25	1.24
0.657	1.28	1.28	1.27
0.721	1.25	1.25	1.24
0.791	1.17	1.17	1.16
0.869	1.06	1.06	1.05
0.953	0.947	0.941	0.93
1.047	0.848	0.839	0.829
1.149	0.789	0.78	0.77
1.261	0.789	0.78	0.77
1.385	0.856	0.847	0.837
1.52	0.99	0.983	0.973
1.669	1.18	1.18	1.17
1.832	1.41	1.41	1.4
2.01	1.66	1.66	1.65
2.207	1.91	1.91	1.9
2.423	2.14	2.15	2.13

2.66	2.35	2.36	2.34
2.92	2.54	2.55	2.53
3.206	2.74	2.73	2.72
3.519	2.93	2.92	2.9
3.862	3.14	3.12	3.1
4.241	3.35	3.33	3.3
4.656	3.56	3.54	3.51
5.111	3.76	3.75	3.71
5.611	3.93	3.94	3.89
6.158	4.07	4.09	4.05
6.761	4.16	4.19	4.15
7.421	4.19	4.23	4.2
8.147	4.15	4.18	4.17
8.944	4.05	4.05	4.06
9.819	3.88	3.87	3.88
10.78	3.7	3.67	3.67
11.83	3.52	3.51	3.47
12.99	3.37	3.39	3.32
14.26	3.27	3.34	3.27
15.65	3.16	3.25	3.23
17.18	2.92	2.99	3.08
18.86	2.4	2.38	2.6
20.7	1.38	1.25	1.54
22.73	0.36	0.275	0.411
24.95	0.02	0.012	0.024

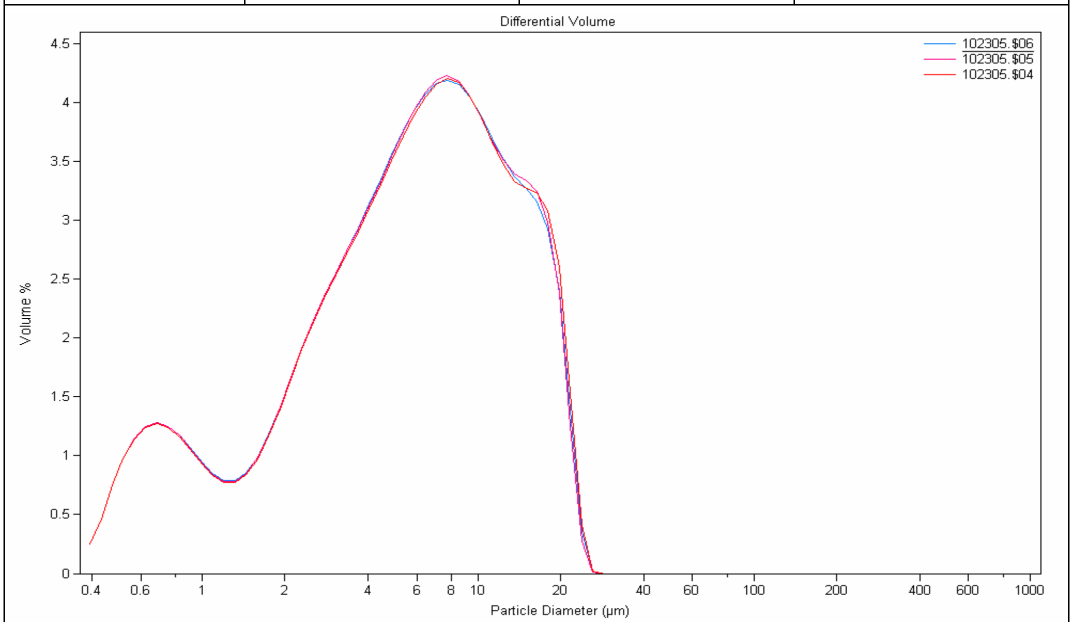

Table A44. Grain size distribution from Coulter Counter for A7.

COULTER LS	3/28/2006 10:15		
File name:	112900.$03 (A7)		
From	0.375	95% Conf. Limits:	0
To	948.2	95% Conf. Limits:	130.8
Volume	100 mL	S.D.:	40.21
Mean:	51.99	Variance:	1617
Median:	50.82	C.V.:	77.34
D(3,2):	9.104	Skewness:	0.679
Mean/Median Ratio:	1.023	Kurtosis:	0.168
Mode:	66.44	Specific Surf. Area	6590
Volume %	112900.$03 Particle Diameter µm <	112900.$02 Particle Diameter µm <	112900.$01 Particle Diameter µm <
10	3.741	3.836	3.974
25	12.74	13.39	14.19
50	50.82	51.56	52.7
75	76.83	78.05	80.07
90	105.6	106.7	110.1
	112900.$03	112900.$02	112900.$01
Channel Diameter (Lower) µm	Diff. Volume %	Diff. Volume %	Diff. Volume %
0.375	0.045	0.044	0.043
0.412	0.079	0.078	0.076
0.452	0.116	0.115	0.112
0.496	0.165	0.163	0.158
0.545	0.205	0.201	0.196
0.598	0.238	0.234	0.228
0.657	0.268	0.264	0.257
0.721	0.297	0.292	0.284
0.791	0.32	0.315	0.306
0.869	0.339	0.333	0.323
0.953	0.353	0.347	0.337
1.047	0.367	0.36	0.349
1.149	0.382	0.374	0.362
1.261	0.397	0.389	0.376
1.385	0.414	0.405	0.391
1.52	0.435	0.425	0.409
1.669	0.462	0.451	0.435
1.832	0.497	0.484	0.466
2.01	0.537	0.522	0.503
2.207	0.584	0.567	0.546
2.423	0.637	0.619	0.596

2.66	0.697	0.676	0.653
2.92	0.761	0.738	0.713
3.206	0.827	0.802	0.776
3.519	0.893	0.867	0.839
3.862	0.958	0.931	0.902
4.241	1.02	0.991	0.962
4.656	1.08	1.05	1.02
5.111	1.13	1.1	1.07
5.611	1.17	1.14	1.11
6.158	1.2	1.17	1.14
6.761	1.22	1.19	1.16
7.421	1.23	1.2	1.18
8.147	1.23	1.2	1.18
8.944	1.22	1.19	1.17
9.819	1.19	1.17	1.15
10.78	1.17	1.15	1.13
11.83	1.13	1.12	1.1
12.99	1.1	1.08	1.07
14.26	1.07	1.05	1.04
15.65	1.04	1.03	1.02
17.18	1.02	1.02	1.01
18.86	1.01	1.02	1.01
20.7	1.02	1.02	1.01
22.73	1.03	1.02	1.01
24.95	1.07	1.05	1.03
27.38	1.18	1.14	1.12
30.07	1.38	1.36	1.32
33	1.75	1.73	1.69
36.24	2.3	2.3	2.25
39.77	3.02	3.03	2.97
43.66	3.87	3.86	3.8
47.93	4.71	4.68	4.6
52.63	5.41	5.35	5.26
57.77	5.84	5.78	5.69
63.41	5.94	5.91	5.83
69.62	5.72	5.74	5.69
76.43	5.25	5.33	5.33
83.9	4.62	4.76	4.82
92.09	3.93	4.11	4.22
101.1	3.24	3.45	3.57
111	2.6	2.81	2.92
121.8	2.01	2.19	2.27

133.7	1.48	1.6	1.67
146.8	1.02	1.04	1.13
161.2	0.638	0.566	0.683
176.8	0.336	0.227	0.356
194.2	0.135	0.057	0.156
213.2	0.033	0.007	0.063
234.1	0.004	0.0025	0.033
256.8	0.001	0	0.032
282.1	0	0	0.043
309.6	0	0	0.054
339.8	0	0	0.06
373.1	0	0	0.06
409.6	0	0	0.055
449.7	0	0	0.044
493.6	0	0	0.027
541.9	0	0	0.01
594.9	0	0	0.002
653	0	0	0.0011

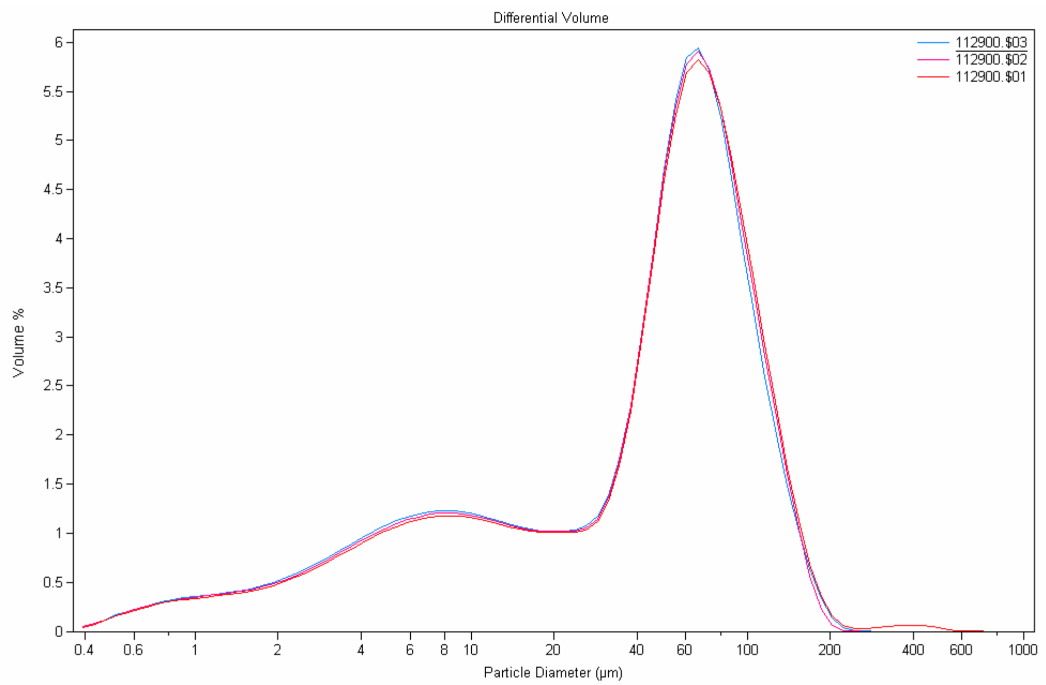

Table A45. Grain size distribution from Coulter Counter for A8.

COULTER LS	9:19 28 Mar 2006		
File name:	114759.$06 (A8)		
From	0.375	95% Conf. Limits:	0
To	948.2	95% Conf. Limits:	18.64
Volume	100 mL	S.D.:	5.703
Mean:	7.459	Variance:	32.53
Median:	6.05	C.V.:	76.47
D(3,2):	2.858	Skewness:	0.839
Mean/Median Ratio:	1.233	Kurtosis:	-0.153
Mode:	8.536	Specific Surf. Area	20994
Volume %	114759.$06 Particle Diameter µm <	114759.$04 Particle Diameter µm <	114759.$02 Particle Diameter µm <
10	0.965	0.973	0.993
25	2.884	2.889	2.92
50	6.05	6.049	6.092
75	10.87	10.81	10.84
90	16.48	16.34	16.29
	114759.$06	114759.$04	114759.$02
Channel Diameter (Lower) µm	Diff. Volume %	Diff. Volume %	Diff. Volume %
0.375	0.264	0.261	0.253
0.412	0.492	0.486	0.471
0.452	0.794	0.785	0.762
0.496	1.03	1.02	0.992
0.545	1.2	1.19	1.16
0.598	1.3	1.29	1.26
0.657	1.32	1.31	1.28
0.721	1.27	1.27	1.25
0.791	1.17	1.17	1.16
0.869	1.04	1.04	1.04
0.953	0.898	0.901	0.906
1.047	0.779	0.785	0.795
1.149	0.708	0.716	0.729
1.261	0.703	0.712	0.725
1.385	0.774	0.782	0.792
1.52	0.92	0.927	0.929
1.669	1.13	1.13	1.13
1.832	1.39	1.39	1.37
2.01	1.66	1.66	1.63
2.207	1.93	1.92	1.89
2.423	2.17	2.17	2.13

2.66	2.39	2.38	2.35
2.92	2.58	2.58	2.54
3.206	2.76	2.76	2.72
3.519	2.93	2.93	2.9
3.862	3.1	3.1	3.08
4.241	3.26	3.27	3.27
4.656	3.43	3.45	3.46
5.111	3.59	3.61	3.65
5.611	3.75	3.78	3.83
6.158	3.89	3.92	3.99
6.761	4.02	4.04	4.12
7.421	4.1	4.12	4.18
8.147	4.1	4.13	4.15
8.944	4.01	4.04	4.04
9.819	3.83	3.87	3.84
10.78	3.59	3.66	3.63
11.83	3.38	3.45	3.46
12.99	3.26	3.3	3.36
14.26	3.26	3.25	3.36
15.65	3.32	3.23	3.38
17.18	3.27	3.12	3.26
18.86	2.84	2.71	2.76
20.7	1.8	1.77	1.59
22.73	0.549	0.577	0.399
24.95	0.037	0.042	0.021

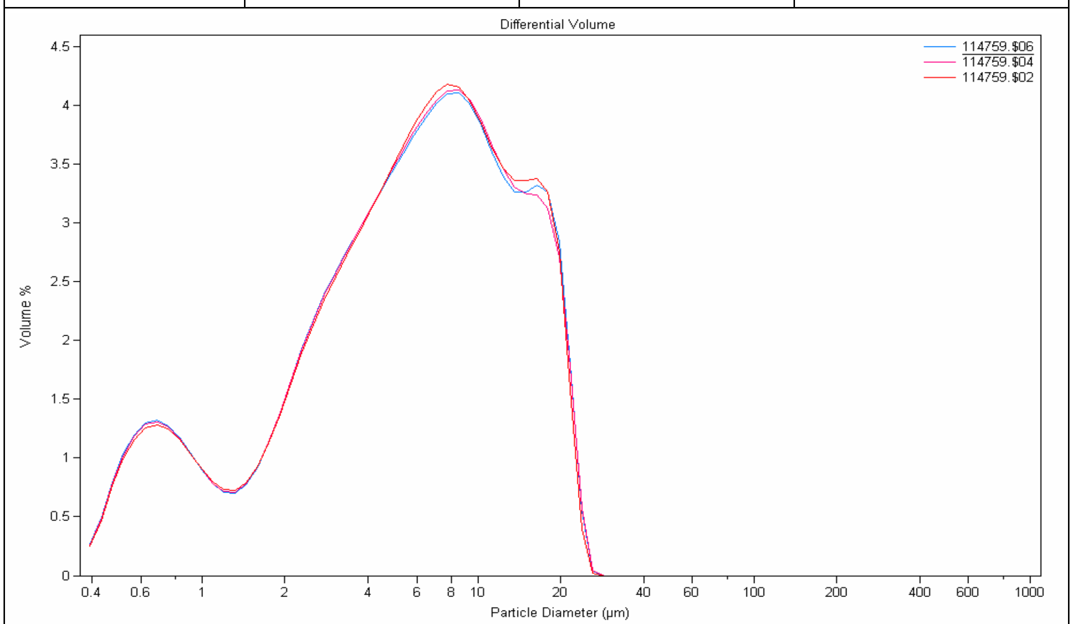

Table A46. Grain size distribution from Coulter counter for A9.

COULTER LS	3/28/2006 14:41		
File name:	120918.$04 (A9)		
From	0.375	95% Conf. Limits:	0
To	948.2	95% Conf. Limits:	21.89
Volume	100 mL	S.D.:	6.706
Mean:	8.749	Variance:	44.98
Median:	7.008	C.V.:	76.66
D(3,2):	3.385	Skewness:	0.926
Mean/Median Ratio:	1.248	Kurtosis:	0.049
Mode:	8.536	Specific Surf. Area	17724
Volume %	120918.$04 Particle Diameter µm <	120918.$05 Particle Diameter µm <	120918.$06 Particle Diameter µm <
10	1.351	1.317	1.31
25	3.531	3.474	3.459
50	7.008	6.895	6.884
75	12.44	12.12	12.11
90	19.54	18.86	18.92
	120918.$04	120918.$05	120918.$06
Channel Diameter (Lower) µm	Diff. Volume %	Diff. Volume %	Diff. Volume %
0.375	0.186	0.189	0.19
0.412	0.348	0.354	0.356
0.452	0.565	0.575	0.578
0.496	0.742	0.754	0.758
0.545	0.874	0.889	0.893
0.598	0.958	0.974	0.979
0.657	0.993	1.01	1.01
0.721	0.982	1	1
0.791	0.933	0.949	0.952
0.869	0.857	0.872	0.874
0.953	0.771	0.784	0.786
1.047	0.693	0.705	0.707
1.149	0.641	0.653	0.656
1.261	0.631	0.643	0.646
1.385	0.67	0.684	0.688
1.52	0.763	0.78	0.785
1.669	0.906	0.926	0.933
1.832	1.09	1.12	1.12
2.01	1.31	1.33	1.35
2.207	1.54	1.57	1.58
2.423	1.77	1.8	1.82

2.66	2	2.04	2.05
2.92	2.23	2.26	2.27
3.206	2.46	2.49	2.49
3.519	2.68	2.72	2.72
3.862	2.92	2.94	2.94
4.241	3.15	3.18	3.17
4.656	3.38	3.41	3.4
5.111	3.61	3.64	3.63
5.611	3.81	3.86	3.84
6.158	3.99	4.04	4.04
6.761	4.14	4.19	4.19
7.421	4.23	4.29	4.29
8.147	4.25	4.31	4.31
8.944	4.19	4.24	4.24
9.819	4.05	4.08	4.07
10.78	3.84	3.85	3.83
11.83	3.57	3.58	3.54
12.99	3.3	3.3	3.27
14.26	3.06	3.07	3.04
15.65	2.91	2.95	2.93
17.18	2.92	2.98	2.97
18.86	3.02	3.06	3.06
20.7	3.09	3.05	3.07
22.73	2.83	2.62	2.67
24.95	1.71	1.17	1.19
27.38	0.434	0.107	0.11
30.07	0.022	0	0

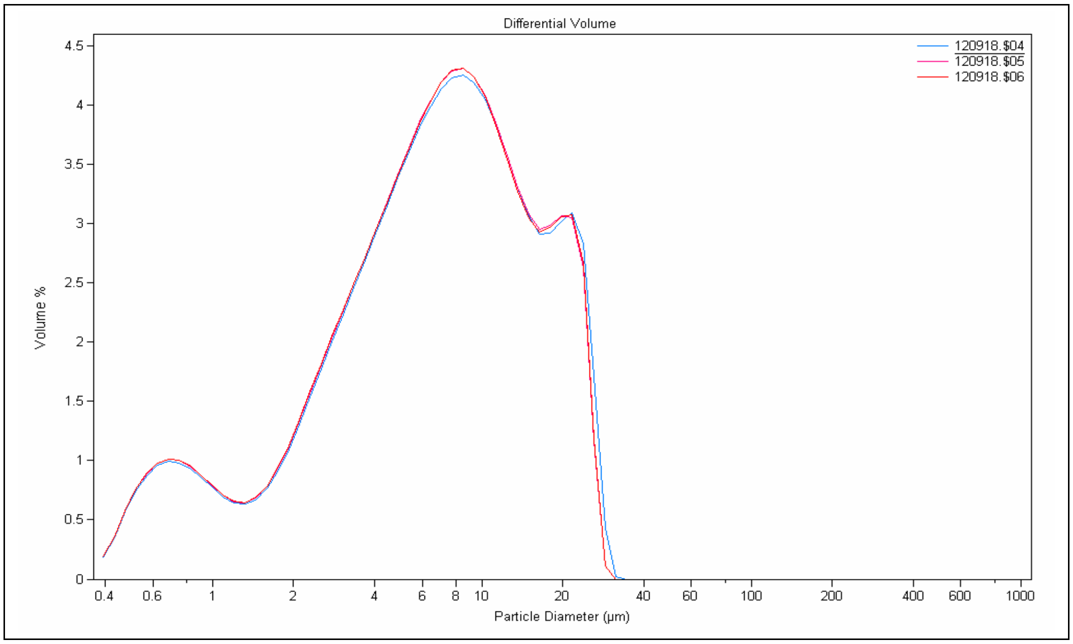
Differential Volume
120918.$04
120918.$05
120918.$06
Volume %
Particle Diameter (µm)
0
0.5
1
1.5
2
2.5
3
3.5
4
4.5
0.4
0.6
1
2
4
6
8
10
20
40
60
100
200
400
600
1000

Table A47. Grain size distribution from Coulter Counter for A9 bottom.

COULTER LS	3/30/2006 10:50		
File name:	120918b.$04 (A9 bottom)		
From	0.375	95% Conf. Limits:	0
To	948.2	95% Conf. Limits:	42.49
Volume	100 mL	S.D.:	14.94
Mean:	13.21	Variance:	223.2
Median:	6.865	C.V.:	113.1
D(3,2):	3.423	Skewness:	1.63
Mean/Median Ratio:	1.924	Kurtosis:	1.91
Mode:	5.878	Specific Surf. Area	17530
Volume %	120918b.$04 Particle Diameter µm <	120918b.$05 Particle Diameter µm <	120918b.$06 Particle Diameter µm <
10	1.291	1.29	1.287
25	2.99	2.984	2.976
50	6.865	6.856	6.852
75	17.75	17.81	17.84
90	37.8	37.72	37.69
	120918b.$04	120918b.$05	120918b.$06
Channel Diameter (Lower) µm	Diff. Volume %	Diff. Volume %	Diff. Volume %
0.375	0.135	0.135	0.136
0.412	0.24	0.24	0.241
0.452	0.353	0.353	0.353
0.496	0.5	0.5	0.501
0.545	0.62	0.62	0.621
0.598	0.722	0.722	0.724
0.657	0.813	0.814	0.816
0.721	0.901	0.902	0.904
0.791	0.975	0.976	0.979
0.869	1.03	1.04	1.04
0.953	1.09	1.09	1.09
1.047	1.13	1.14	1.14
1.149	1.19	1.19	1.19
1.261	1.24	1.25	1.25
1.385	1.31	1.31	1.32
1.52	1.38	1.39	1.39
1.669	1.48	1.48	1.49
1.832	1.59	1.59	1.6
2.01	1.71	1.72	1.72
2.207	1.85	1.86	1.86
2.423	2	2.01	2.01

2.66	2.16	2.17	2.17
2.92	2.33	2.33	2.33
3.206	2.48	2.48	2.48
3.519	2.63	2.63	2.63
3.862	2.76	2.76	2.76
4.241	2.87	2.87	2.86
4.656	2.95	2.95	2.95
5.111	3.01	3.01	3
5.611	3.04	3.03	3.02
6.158	3.03	3.03	3.02
6.761	2.99	2.99	2.98
7.421	2.93	2.93	2.92
8.147	2.83	2.83	2.82
8.944	2.71	2.71	2.7
9.819	2.56	2.56	2.55
10.78	2.4	2.4	2.4
11.83	2.25	2.24	2.24
12.99	2.12	2.1	2.1
14.26	2.03	2	2
15.65	1.98	1.94	1.95
17.18	1.97	1.93	1.94
18.86	1.98	1.95	1.96
20.7	1.96	1.96	1.97
22.73	1.91	1.94	1.96
24.95	1.82	1.89	1.9
27.38	1.75	1.82	1.82
30.07	1.71	1.76	1.76
33	1.75	1.74	1.74
36.24	1.84	1.77	1.78
39.77	1.93	1.84	1.85
43.66	1.96	1.89	1.89
47.93	1.86	1.84	1.83
52.63	1.58	1.63	1.62
57.77	1.04	1.12	1.11
63.41	0.476	0.531	0.529
69.62	0.104	0.119	0.119
76.43	0.01	0.011	0.012

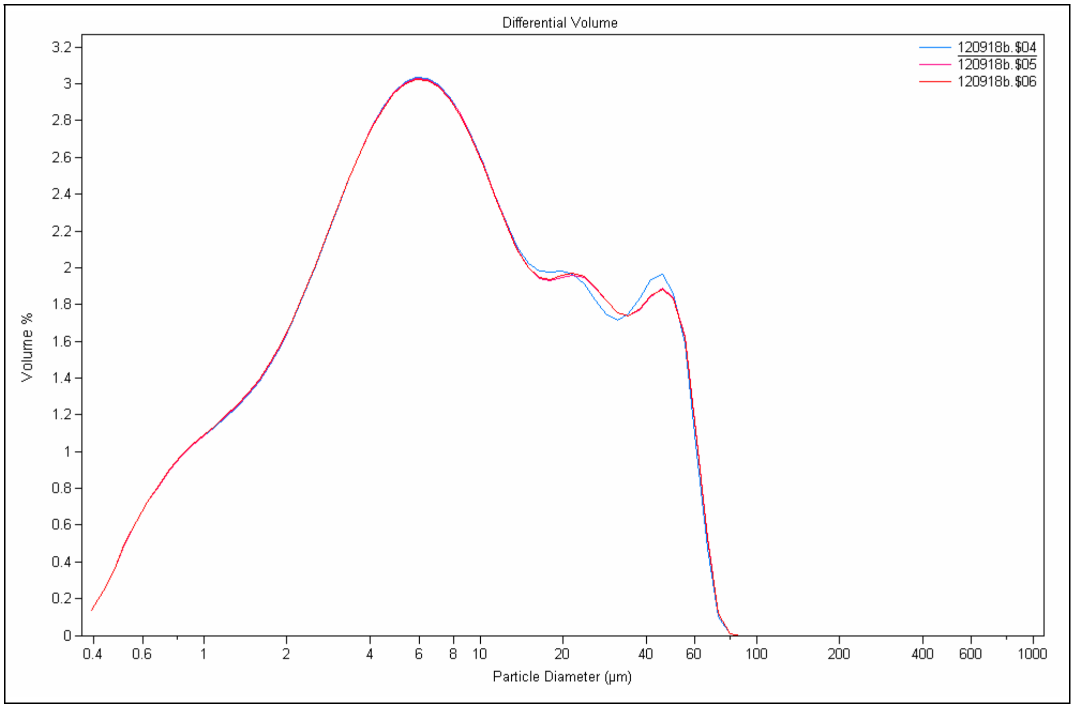
Differential Volume
120918b.$04
120918b.$05
120918b.$06
Volume %
3.2
3
2.8
2.6
2.4
2.2
2
1.8
1.6
1.4
1.2
1
0.8
0.6
0.4
0.2
0
0.4
0.6
1
2
4
6
8
10
20
40
60
100
200
400
600
1000
Particle Diameter (μm)

Table A48. Grain size distribution from Coulter Counter for A10.

COULTER LS	3/27/2006 13:52		
File name:	123410.$01 (A10)		
From	0.375	95% Conf. Limits:	0
To	948.2	95% Conf. Limits:	22.78
Volume	100 mL	S.D.:	6.813
Mean:	9.431	Variance:	46.41
Median:	7.956	C.V.:	72.24
D(3,2):	3.619	Skewness:	0.718
Mean/Median Ratio:	1.185	Kurtosis:	-0.36
Mode:	9.371	Specific Surf. Area	16580
Volume %	123410.$01 Particle Diameter µm <	123410.$02 Particle Diameter µm <	123410.$03 Particle Diameter µm <
10	1.491	1.458	1.441
25	3.914	3.86	3.833
50	7.956	7.89	7.864
75	13.8	13.71	13.7
90	20.06	19.9	20.01
	123410.$01	123410.$02	123410.$03
Channel Diameter (Lower) µm	Diff. Volume %	Diff. Volume %	Diff. Volume %
0.375	0.176	0.178	0.181
0.412	0.328	0.334	0.338
0.452	0.533	0.541	0.549
0.496	0.698	0.71	0.719
0.545	0.823	0.837	0.847
0.598	0.901	0.916	0.927
0.657	0.934	0.949	0.96
0.721	0.922	0.938	0.946
0.791	0.875	0.89	0.896
0.869	0.802	0.815	0.819
0.953	0.719	0.73	0.732
1.047	0.643	0.651	0.652
1.149	0.592	0.597	0.598
1.261	0.578	0.581	0.583
1.385	0.609	0.611	0.615
1.52	0.689	0.691	0.698
1.669	0.813	0.816	0.827
1.832	0.973	0.979	0.993
2.01	1.16	1.17	1.18
2.207	1.35	1.37	1.38
2.423	1.54	1.56	1.58

2.66	1.73	1.76	1.77
2.92	1.91	1.95	1.95
3.206	2.09	2.13	2.13
3.519	2.28	2.32	2.31
3.862	2.47	2.51	2.5
4.241	2.69	2.72	2.71
4.656	2.92	2.94	2.93
5.111	3.17	3.18	3.17
5.611	3.43	3.42	3.42
6.158	3.68	3.67	3.67
6.761	3.92	3.9	3.9
7.421	4.12	4.1	4.1
8.147	4.27	4.25	4.24
8.944	4.35	4.33	4.31
9.819	4.35	4.34	4.31
10.78	4.27	4.27	4.23
11.83	4.14	4.13	4.09
12.99	3.97	3.96	3.93
14.26	3.8	3.8	3.76
15.65	3.69	3.69	3.64
17.18	3.68	3.69	3.62
18.86	3.68	3.69	3.62
20.7	3.57	3.56	3.52
22.73	3.05	3.01	3.04
24.95	1.7	1.55	1.69
27.38	0.382	0.278	0.37
30.07	0.017	0.008	0.015

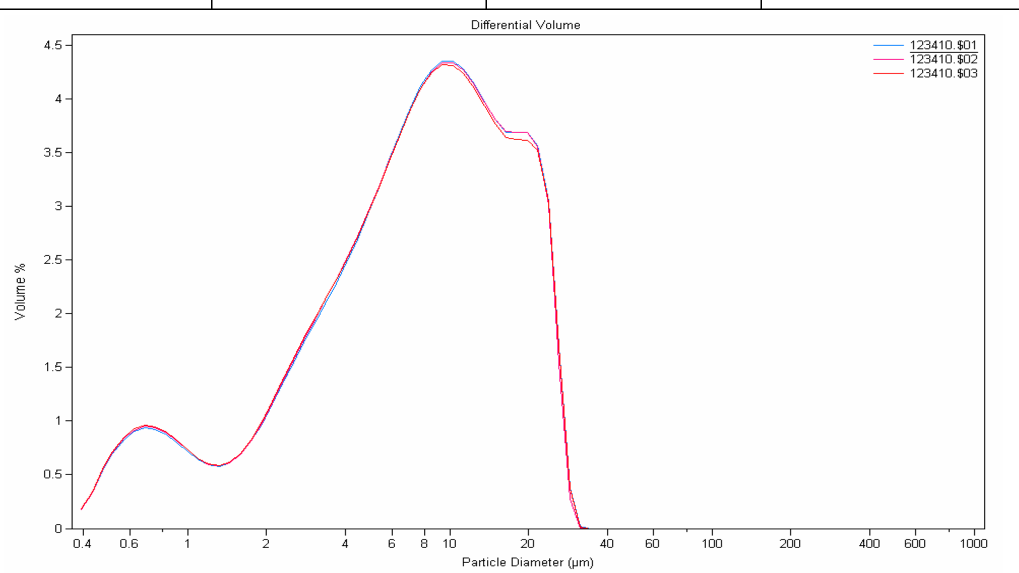

Table A49. Grain size distribution from Coulter Counter for A13.

COULTER LS	8:43 28 Mar 2006		
File name:	133735.$01 (A13)		
From	0.375	95% Conf. Limits:	0
To	948.2	95% Conf. Limits:	144.1
Volume	100 mL	S.D.:	45.89
Mean:	54.19	Variance:	2106
Median:	49.1	C.V.:	84.68
D(3,2):	8.114	Skewness:	1.036
Mean/Median Ratio:	1.104	Kurtosis:	1.617
Mode:	60.52	Specific Surf. Area	7394
Volume %	133735.$01 Particle Diameter µm <	133735.$02 Particle Diameter µm <	133735.$03 Particle Diameter µm <
10	3.182	3.052	3.01
25	10.76	9.952	9.739
50	49.1	47.63	47.29
75	81.22	78.82	78.72
90	116.2	113.2	112.4
	133735.$01	133735.$02	133735.$03
Channel Diameter (Lower) µm	Diff. Volume %	Diff. Volume %	Diff. Volume %
0.375	0.055	0.057	0.057
0.412	0.098	0.101	0.101
0.452	0.144	0.148	0.149
0.496	0.204	0.209	0.211
0.545	0.251	0.259	0.26
0.598	0.292	0.3	0.303
0.657	0.328	0.337	0.34
0.721	0.362	0.372	0.375
0.791	0.388	0.4	0.404
0.869	0.409	0.421	0.425
0.953	0.424	0.438	0.442
1.047	0.438	0.453	0.458
1.149	0.453	0.469	0.475
1.261	0.467	0.485	0.491
1.385	0.485	0.504	0.511
1.52	0.506	0.528	0.536
1.669	0.536	0.56	0.569
1.832	0.573	0.6	0.61
2.01	0.617	0.647	0.658
2.207	0.668	0.701	0.713
2.423	0.726	0.763	0.776

2.66	0.791	0.83	0.845
2.92	0.858	0.901	0.916
3.206	0.927	0.972	0.988
3.519	0.994	1.04	1.06
3.862	1.06	1.11	1.12
4.241	1.12	1.17	1.18
4.656	1.17	1.22	1.23
5.111	1.2	1.25	1.27
5.611	1.23	1.28	1.29
6.158	1.25	1.29	1.3
6.761	1.25	1.29	1.3
7.421	1.24	1.28	1.28
8.147	1.21	1.25	1.25
8.944	1.18	1.21	1.21
9.819	1.13	1.16	1.15
10.78	1.08	1.1	1.09
11.83	1.02	1.03	1.02
12.99	0.962	0.966	0.954
14.26	0.92	0.919	0.907
15.65	0.898	0.896	0.888
17.18	0.891	0.892	0.894
18.86	0.887	0.897	0.907
20.7	0.883	0.902	0.916
22.73	0.897	0.923	0.933
24.95	0.971	1	1
27.38	1.16	1.19	1.18
30.07	1.5	1.53	1.52
33	2	2.04	2.04
36.24	2.63	2.68	2.7
39.77	3.3	3.36	3.39
43.66	3.9	3.98	4
47.93	4.36	4.44	4.43
52.63	4.65	4.71	4.66
57.77	4.77	4.81	4.72
63.41	4.76	4.75	4.67
69.62	4.66	4.6	4.56
76.43	4.49	4.39	4.4
83.9	4.26	4.13	4.18
92.09	3.98	3.82	3.89
101.1	3.62	3.44	3.5
111	3.17	2.98	3
121.8	2.63	2.44	2.43

133.7	2.03	1.85	1.81
146.8	1.43	1.28	1.23
161.2	0.908	0.812	0.759
176.8	0.525	0.488	0.44
194.2	0.295	0.297	0.26
213.2	0.181	0.197	0.173
234.1	0.131	0.138	0.127
256.8	0.102	0.087	0.089
282.1	0.067	0.041	0.048
309.6	0.03	0.01	0.016
339.8	0.006	0.001	0.002
373.1	0.001	1.80E-05	0.0011

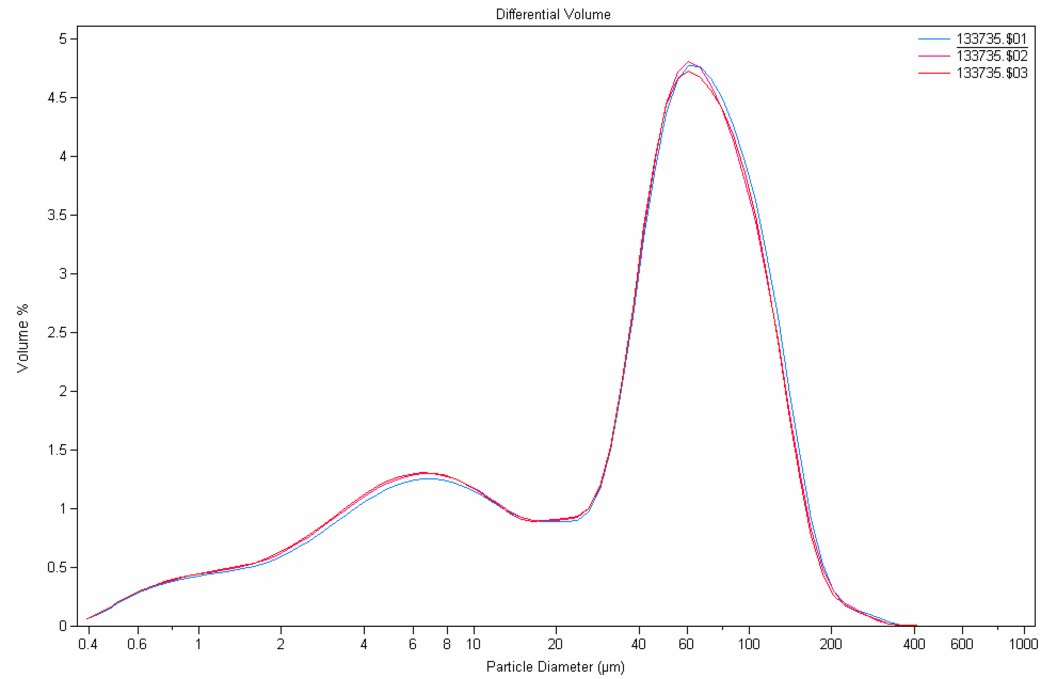

Table A50. Grain size distribution from Coulter Counter for A15.

COULTER LS	3/27/2006 13:32		
File name:	144250.$01 (A15)		
From	0.375	95% Conf. Limits:	0
To	948.2	95% Conf. Limits:	17.41
Volume	100 mL	S.D.:	5.196
Mean:	7.221	Variance:	27
Median:	6.152	C.V.:	71.95
D(3,2):	2.951	Skewness:	0.751
Mean/Median Ratio:	1.174	Kurtosis:	-0.22
Mode:	8.536	Specific Surf. Area	20334
Volume %	144250.$01 Particle Diameter μm <	144250.$02 Particle Diameter μm <	144250.$03 Particle Diameter μm <
10	1.042	1.028	1.018
25	3.032	2.993	2.96
50	6.152	6.078	6.018
75	10.47	10.38	10.29
90	15.15	15.07	14.94
	144250.$01	144250.$02	144250.$03
Channel Diameter (Lower) μm	Diff. Volume %	Diff. Volume %	Diff. Volume %
0.375	0.247	0.25	0.253
0.412	0.46	0.466	0.471
0.452	0.743	0.752	0.759
0.496	0.964	0.977	0.986
0.545	1.12	1.14	1.15
0.598	1.21	1.23	1.24
0.657	1.23	1.24	1.25
0.721	1.18	1.2	1.21
0.791	1.09	1.1	1.11
0.869	0.965	0.976	0.985
0.953	0.834	0.844	0.853
1.047	0.726	0.735	0.745
1.149	0.666	0.674	0.685
1.261	0.669	0.677	0.69
1.385	0.744	0.754	0.769
1.52	0.889	0.901	0.92
1.669	1.09	1.11	1.13
1.832	1.34	1.36	1.38
2.01	1.6	1.62	1.65
2.207	1.85	1.88	1.91
2.423	2.09	2.12	2.14

2.66	2.3	2.34	2.36
2.92	2.5	2.54	2.56
3.206	2.7	2.74	2.76
3.519	2.9	2.94	2.96
3.862	3.12	3.16	3.18
4.241	3.35	3.38	3.4
4.656	3.59	3.6	3.63
5.111	3.82	3.83	3.85
5.611	4.04	4.04	4.06
6.158	4.24	4.23	4.24
6.761	4.4	4.38	4.38
7.421	4.5	4.48	4.46
8.147	4.52	4.48	4.46
8.944	4.43	4.39	4.37
9.819	4.26	4.2	4.19
10.78	4.04	3.98	3.97
11.83	3.8	3.75	3.73
12.99	3.6	3.56	3.54
14.26	3.39	3.35	3.33
15.65	3.11	3.07	3.04
17.18	2.78	2.74	2.66
18.86	2.07	2.01	1.89
20.7	0.766	0.733	0.655
22.73	0.06	0.057	0.048

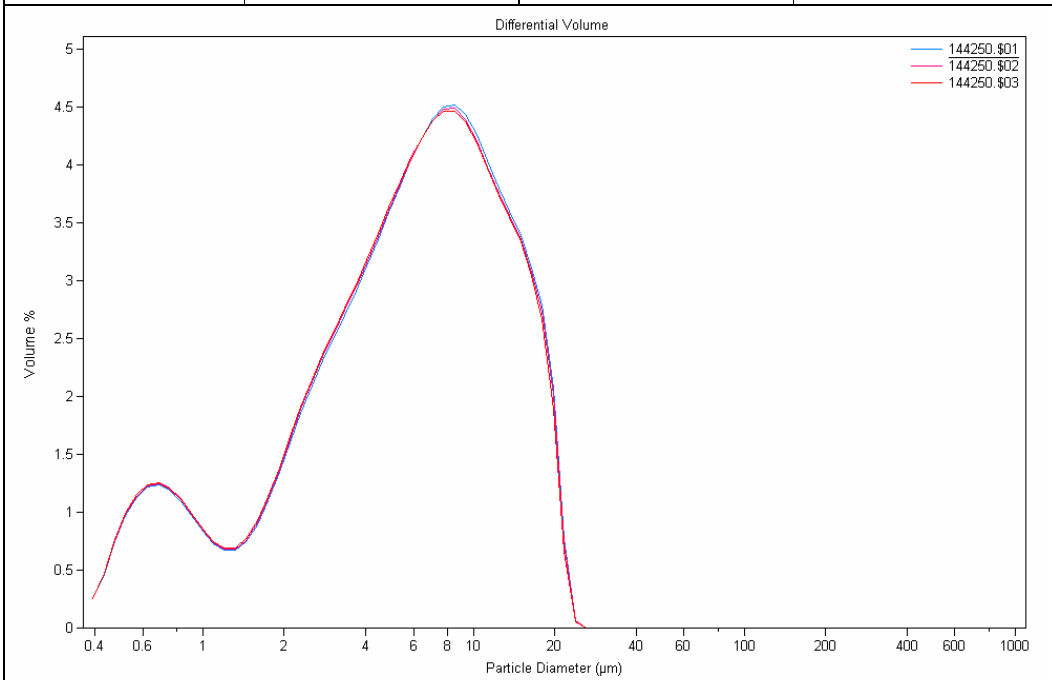

Table A51. Grain size distribution from Coulter Counter for B1.

COULTER LS	3/28/2006 10:05		
File name:	085900.$05 (B1)		
From	0.375	95% Conf. Limits:	0
To	948.2	95% Conf. Limits:	17.6
Volume	100 mL	S.D.:	5.303
Mean:	7.204	Variance:	28.13
Median:	5.951	C.V.:	73.62
D(3,2):	3.133	Skewness:	0.84
Mean/Median Ratio:	1.211	Kurtosis:	-0.0623
Mode:	7.776	Specific Surf. Area	19153
Volume %	085900.$05 Particle Diameter µm <	085900.$04 Particle Diameter µm <	085900.$03 Particle Diameter µm <
10	1.239	1.243	1.248
25	2.935	2.939	2.964
50	5.951	5.953	6.011
75	10.44	10.41	10.49
90	15.37	15.26	15.33
	085900.$05	085900.$04	085900.$03
Channel Diameter (Lower) µm	Diff. Volume %	Diff. Volume %	Diff. Volume %
0.375	0.154	0.152	0.152
0.412	0.272	0.27	0.269
0.452	0.398	0.395	0.393
0.496	0.561	0.557	0.555
0.545	0.691	0.685	0.683
0.598	0.796	0.791	0.788
0.657	0.886	0.88	0.877
0.721	0.968	0.963	0.959
0.791	1.03	1.03	1.02
0.869	1.07	1.07	1.07
0.953	1.1	1.1	1.1
1.047	1.13	1.13	1.12
1.149	1.16	1.16	1.16
1.261	1.2	1.2	1.19
1.385	1.25	1.25	1.24
1.52	1.32	1.32	1.31
1.669	1.41	1.42	1.4
1.832	1.54	1.54	1.52
2.01	1.69	1.69	1.67
2.207	1.87	1.87	1.84
2.423	2.07	2.07	2.04

2.66	2.29	2.29	2.26
2.92	2.53	2.53	2.5
3.206	2.78	2.78	2.74
3.519	3.02	3.02	2.99
3.862	3.26	3.26	3.23
4.241	3.48	3.49	3.46
4.656	3.69	3.69	3.67
5.111	3.87	3.88	3.86
5.611	4.01	4.03	4.01
6.158	4.12	4.14	4.13
6.761	4.19	4.21	4.21
7.421	4.22	4.25	4.25
8.147	4.21	4.24	4.26
8.944	4.14	4.18	4.2
9.819	4.02	4.06	4.09
10.78	3.84	3.88	3.93
11.83	3.64	3.68	3.73
12.99	3.47	3.49	3.55
14.26	3.3	3.29	3.36
15.65	3.12	3.07	3.14
17.18	2.84	2.76	2.81
18.86	2.05	1.97	2
20.7	1.05	1.01	1.01
22.73	0.249	0.237	0.238
24.95	0.026	0.025	0.025

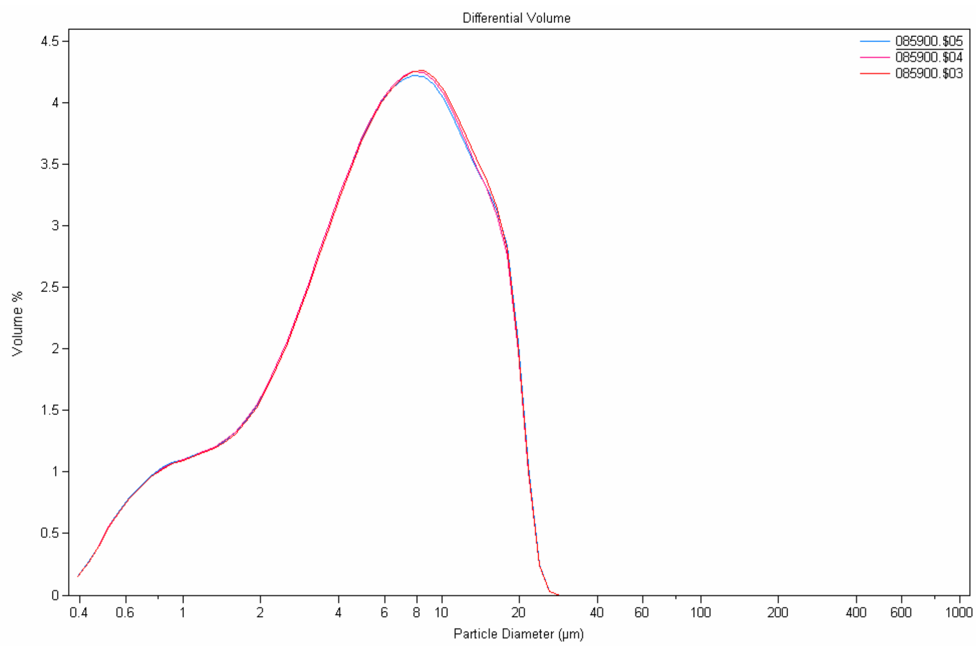

Table A52. Grain size distribution from Coulter Counter for B2.

COULTER LS	9:06 28 Mar 2006		
File name:	092816.$01 (B2)		
From	0.375	95% Conf. Limits:	0
To	948.2	95% Conf. Limits:	22.64
Volume	100 mL	S.D.:	7.07
Mean:	8.783	Variance:	49.98
Median:	6.742	C.V.:	80.49
D(3,2):	3.431	Skewness:	1.026
Mean/Median Ratio:	1.303	Kurtosis:	0.318
Mode:	7.776	Specific Surf. Area	17489
Volume %	092816.$01 Particle Diameter µm <	092816.$04 Particle Diameter µm <	092816.$06 Particle Diameter µm <
10	1.355	1.32	1.312
25	3.241	3.159	3.136
50	6.742	6.645	6.605
75	12.68	12.69	12.62
90	19.89	20.11	19.86
	092816.$01	092816.$04	092816.$06
Channel Diameter (Lower) µm	Diff. Volume %	Diff. Volume %	Diff. Volume %
0.375	0.135	0.14	0.141
0.412	0.24	0.249	0.251
0.452	0.352	0.364	0.368
0.496	0.497	0.514	0.519
0.545	0.611	0.632	0.638
0.598	0.707	0.731	0.737
0.657	0.789	0.815	0.822
0.721	0.865	0.893	0.9
0.791	0.924	0.954	0.96
0.869	0.966	0.996	1
0.953	0.998	1.03	1.03
1.047	1.03	1.06	1.06
1.149	1.06	1.09	1.09
1.261	1.09	1.13	1.13
1.385	1.14	1.17	1.18
1.52	1.2	1.24	1.24
1.669	1.29	1.32	1.33
1.832	1.4	1.44	1.45
2.01	1.53	1.57	1.58
2.207	1.69	1.73	1.74
2.423	1.87	1.91	1.92

2.66	2.07	2.1	2.12
2.92	2.28	2.31	2.33
3.206	2.5	2.53	2.55
3.519	2.72	2.74	2.76
3.862	2.93	2.94	2.96
4.241	3.14	3.14	3.15
4.656	3.32	3.31	3.31
5.111	3.48	3.45	3.45
5.611	3.61	3.57	3.56
6.158	3.71	3.65	3.64
6.761	3.78	3.71	3.7
7.421	3.81	3.73	3.71
8.147	3.8	3.71	3.69
8.944	3.75	3.66	3.65
9.819	3.68	3.57	3.57
10.78	3.56	3.46	3.47
11.83	3.43	3.32	3.35
12.99	3.28	3.17	3.22
14.26	3.15	3.05	3.1
15.65	3.04	2.97	3.03
17.18	2.98	2.95	2.98
18.86	2.91	2.93	2.93
20.7	2.78	2.86	2.81
22.73	2.52	2.63	2.55
24.95	1.92	2.02	1.9
27.38	1.08	1.13	1.03
30.07	0.36	0.371	0.319
33	0.058	0.059	0.047
36.24	0.003	0.002	0.002

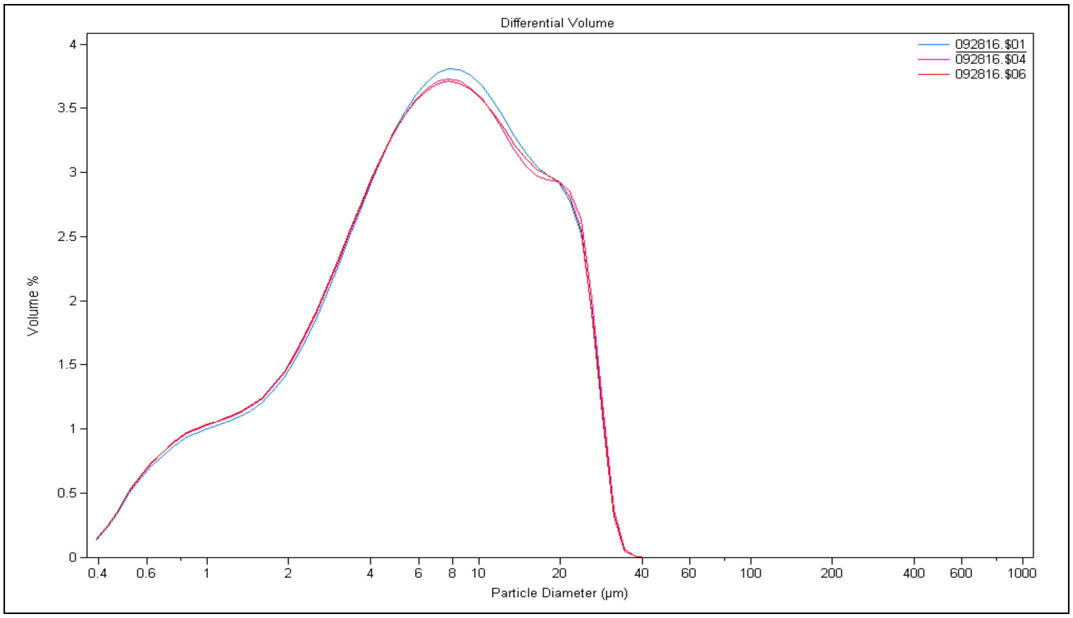
Differential Volume
092816.$01
092816.$04
092816.$06
Volume %
0
0.5
1
1.5
2
2.5
3
3.5
4
0.4
0.6
1
2
4
6
8
10
20
40
60
100
200
400
600
1000
Particle Diameter (µm)

Table A53. Grain size distribution from Coulter Counter for B3 bottom.

COULTER LS	3/30/2006 13:54		
File name:	100743b.$01 (B3 bottom)		
From	0.375	95% Conf. Limits:	0
To	948.2	95% Conf. Limits:	58.54
Volume	100 mL	S.D.:	20.79
Mean:	17.8	Variance:	432.1
Median:	8.794	C.V.:	116.8
D(3,2):	4.079	Skewness:	1.692
Mean/Median Ratio:	2.024	Kurtosis:	2.209
Mode:	7.083	Specific Surf. Area	14710
Volume %	100743b.$01 Particle Diameter µm <	100743b.$02 Particle Diameter µm <	100743b.$03 Particle Diameter µm <
10	1.577	1.552	1.533
25	3.756	3.695	3.655
50	8.794	8.627	8.515
75	23.72	23.1	22.66
90	51.09	49.47	49.07
	100743b.$01	100743b.$02	100743b.$03
Channel Diameter (Lower) µm	Diff. Volume %	Diff. Volume %	Diff. Volume %
0.375	0.108	0.11	0.111
0.412	0.191	0.195	0.198
0.452	0.281	0.286	0.29
0.496	0.397	0.405	0.411
0.545	0.492	0.501	0.508
0.598	0.572	0.582	0.591
0.657	0.642	0.654	0.664
0.721	0.71	0.722	0.733
0.791	0.765	0.779	0.791
0.869	0.809	0.824	0.836
0.953	0.846	0.861	0.873
1.047	0.881	0.897	0.909
1.149	0.921	0.937	0.949
1.261	0.963	0.98	0.993
1.385	1.01	1.03	1.04
1.52	1.08	1.09	1.11
1.669	1.16	1.18	1.19
1.832	1.25	1.27	1.29
2.01	1.37	1.39	1.4
2.207	1.49	1.52	1.53
2.423	1.64	1.66	1.68

2.66	1.79	1.82	1.83
2.92	1.95	1.98	2
3.206	2.11	2.14	2.16
3.519	2.27	2.3	2.32
3.862	2.42	2.45	2.47
4.241	2.56	2.59	2.61
4.656	2.68	2.7	2.72
5.111	2.77	2.8	2.81
5.611	2.85	2.87	2.88
6.158	2.89	2.91	2.92
6.761	2.91	2.92	2.93
7.421	2.9	2.91	2.92
8.147	2.86	2.87	2.87
8.944	2.79	2.8	2.8
9.819	2.7	2.7	2.7
10.78	2.58	2.59	2.59
11.83	2.46	2.46	2.46
12.99	2.34	2.34	2.34
14.26	2.25	2.25	2.23
15.65	2.19	2.18	2.16
17.18	2.14	2.13	2.12
18.86	2.1	2.08	2.09
20.7	2.04	2.01	2.04
22.73	1.96	1.93	1.96
24.95	1.87	1.85	1.86
27.38	1.81	1.79	1.77
30.07	1.78	1.77	1.72
33	1.78	1.8	1.71
36.24	1.8	1.84	1.75
39.77	1.82	1.87	1.82
43.66	1.82	1.87	1.87
47.93	1.82	1.84	1.89
52.63	1.81	1.79	1.85
57.77	1.79	1.71	1.76
63.41	1.72	1.6	1.59
69.62	1.56	1.42	1.35
76.43	1.28	1.14	1.05
83.9	0.809	0.721	0.638
92.09	0.351	0.314	0.272
101.1	0.074	0.066	0.056
111	0.006	0.006	0.005

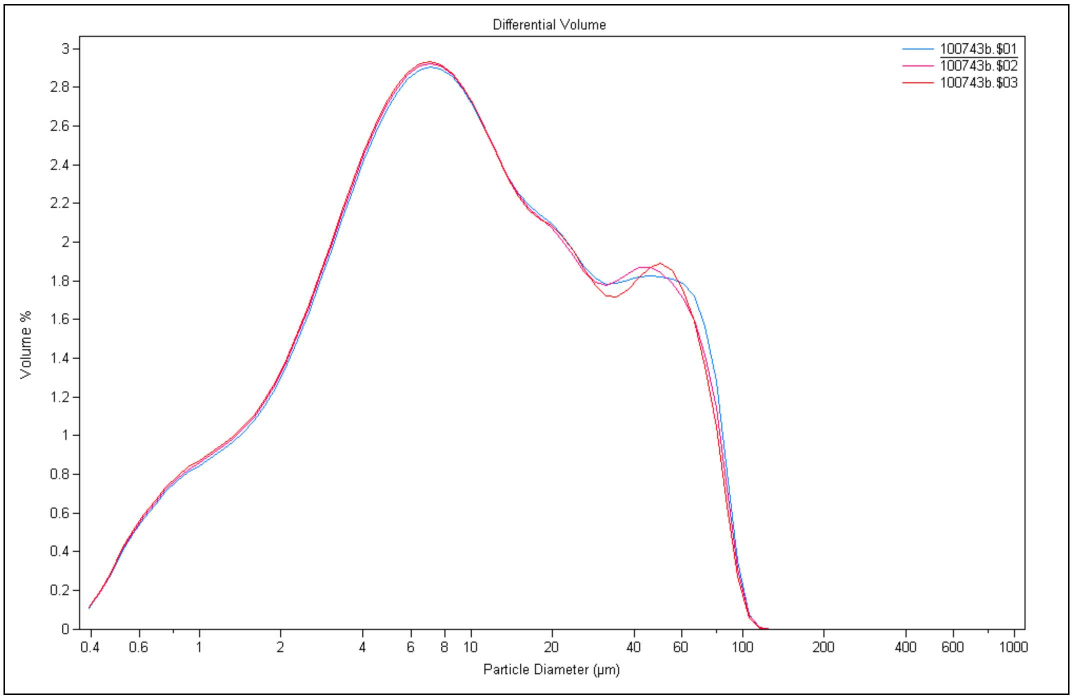
Differential Volume
Volume %
Particle Diameter (µm)
100743b.$01
100743b.$02
100743b.$03
0
0.2
0.4
0.6
0.8
1
1.2
1.4
1.6
1.8
2
2.2
2.4
2.6
2.8
3
0.4
0.6
1
2
4
6
8
10
20
40
60
100
200
400
600
1000

Table A54. Grain size distribution from Coulter Counter for B4.

COULTER LS	9:29 28 Mar 2006		
File name:	112055.$03 (B4)		
From	0.375	95% Conf. Limits:	0
To	948.2	95% Conf. Limits:	24.18
Volume	100 mL	S.D.:	7.457
Mean:	9.562	Variance:	55.61
Median:	7.558	C.V.:	77.98
D(3,2):	3.605	Skewness:	0.864
Mean/Median Ratio:	1.265	Kurtosis:	-0.0996
Mode:	10.29	Specific Surf. Area	16645
Volume %	112054.$03 Particle Diameter µm <	112054.$01 Particle Diameter µm <	112054.$02 Particle Diameter µm <
10	1.393	1.407	1.401
25	3.515	3.554	3.535
50	7.558	7.639	7.602
75	14.23	14.3	14.3
90	21.17	21.25	21.26
	112054.$03	112054.$01	112054.$02
Channel Diameter (Lower) µm	Diff. Volume %	Diff. Volume %	Diff. Volume %
0.375	0.133	0.13	0.132
0.412	0.236	0.232	0.234
0.452	0.346	0.34	0.343
0.496	0.488	0.48	0.484
0.545	0.601	0.591	0.596
0.598	0.694	0.684	0.689
0.657	0.774	0.763	0.768
0.721	0.847	0.836	0.841
0.791	0.902	0.892	0.896
0.869	0.939	0.929	0.933
0.953	0.964	0.955	0.958
1.047	0.984	0.976	0.979
1.149	1.01	0.998	1
1.261	1.03	1.02	1.02
1.385	1.06	1.05	1.05
1.52	1.1	1.09	1.1
1.669	1.17	1.16	1.16
1.832	1.25	1.24	1.25
2.01	1.36	1.35	1.35
2.207	1.49	1.47	1.48
2.423	1.64	1.62	1.63

2.66	1.81	1.79	1.8
2.92	2	1.98	1.99
3.206	2.2	2.17	2.19
3.519	2.4	2.37	2.39
3.862	2.61	2.58	2.59
4.241	2.81	2.78	2.79
4.656	2.99	2.97	2.98
5.111	3.16	3.14	3.15
5.611	3.31	3.3	3.3
6.158	3.45	3.44	3.44
6.761	3.56	3.56	3.55
7.421	3.64	3.65	3.64
8.147	3.69	3.71	3.69
8.944	3.72	3.75	3.72
9.819	3.72	3.76	3.73
10.78	3.71	3.75	3.71
11.83	3.67	3.71	3.68
12.99	3.62	3.66	3.63
14.26	3.58	3.61	3.59
15.65	3.55	3.57	3.56
17.18	3.53	3.54	3.54
18.86	3.49	3.49	3.5
20.7	3.35	3.35	3.37
22.73	3.05	3.06	3.08
24.95	2.38	2.41	2.42
27.38	1.39	1.44	1.43
30.07	0.509	0.538	0.53
33	0.091	0.098	0.096
36.24	0.005	0.006	0.006

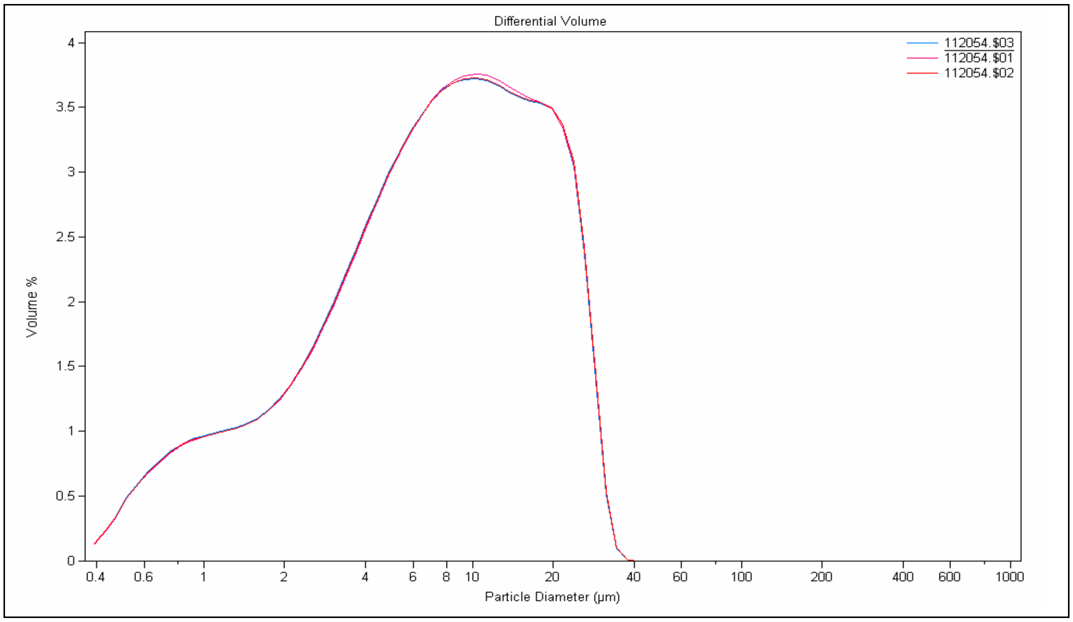
Differential Volume
112054.$03
112054.$01
112054.$02
Volume %
0
0.5
1
1.5
2
2.5
3
3.5
4
0.4
0.6
1
2
4
6
8
10
20
40
60
100
200
400
600
1000
Particle Diameter (µm)

Table A55. Grain size distribution from Coulter Counter for B5.

COULTER LS	3/28/2006 10:23		
File name:	120042.$03 (B5)		
From	0.375	95% Conf. Limits:	0
To	948.2	95% Conf. Limits:	20.97
Volume	100 mL	S.D.:	6.344
Mean:	8.535	Variance:	40.24
Median:	7.045	C.V.:	74.32
D(3,2):	3.404	Skewness:	0.91
Mean/Median Ratio:	1.212	Kurtosis:	0.147
Mode:	8.536	Specific Surf. Area	17625
Volume %	120042.$03 Particle Diameter µm <	120042.$02 Particle Diameter µm <	120042.$01 Particle Diameter µm <
10	1.367	1.412	1.543
25	3.618	3.704	3.939
50	7.045	7.155	7.543
75	12.07	12.21	12.99
90	18.36	18.41	19.92
	120042.$03	120042.$02	120042.$01
Channel Diameter (Lower) µm	Diff. Volume %	Diff. Volume %	Diff. Volume %
0.375	0.185	0.179	0.166
0.412	0.346	0.335	0.31
0.452	0.561	0.545	0.504
0.496	0.736	0.715	0.663
0.545	0.868	0.844	0.784
0.598	0.952	0.927	0.863
0.657	0.987	0.963	0.899
0.721	0.977	0.955	0.895
0.791	0.928	0.909	0.856
0.869	0.852	0.837	0.793
0.953	0.765	0.754	0.719
1.047	0.685	0.677	0.65
1.149	0.631	0.624	0.601
1.261	0.616	0.607	0.585
1.385	0.649	0.637	0.609
1.52	0.734	0.715	0.677
1.669	0.869	0.841	0.789
1.832	1.04	1.01	0.936
2.01	1.25	1.2	1.11
2.207	1.47	1.42	1.3
2.423	1.69	1.64	1.51

2.66	1.92	1.86	1.72
2.92	2.15	2.09	1.93
3.206	2.38	2.33	2.17
3.519	2.62	2.58	2.42
3.862	2.88	2.84	2.69
4.241	3.14	3.12	2.97
4.656	3.42	3.41	3.27
5.111	3.69	3.69	3.57
5.611	3.95	3.95	3.86
6.158	4.18	4.19	4.11
6.761	4.37	4.38	4.32
7.421	4.48	4.5	4.46
8.147	4.51	4.54	4.5
8.944	4.43	4.48	4.46
9.819	4.27	4.33	4.32
10.78	4.04	4.12	4.12
11.83	3.78	3.87	3.9
12.99	3.52	3.62	3.68
14.26	3.29	3.38	3.46
15.65	3.1	3.17	3.25
17.18	2.97	3.01	3.01
18.86	2.83	2.84	2.76
20.7	2.62	2.61	2.53
22.73	2.18	2.18	2.29
24.95	1.2	1.25	1.98
27.38	0.266	0.307	1.44
30.07	0.011	0.016	0.546
33	0	0	0.045

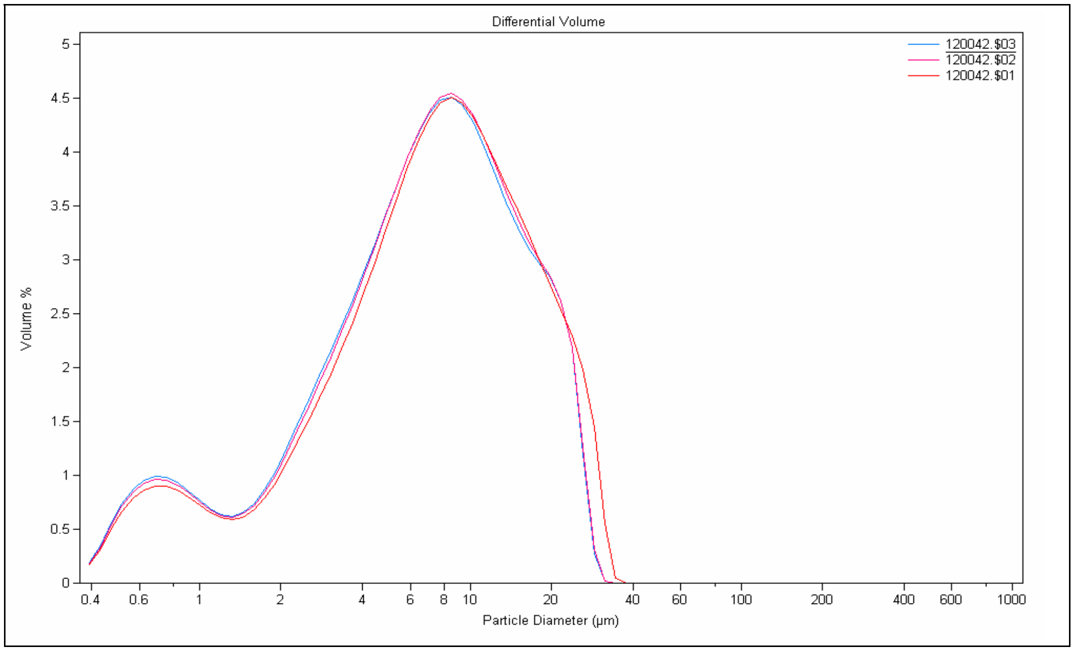
Differential Volume
120042.$03
120042.$02
120042.$01
Volume %
5
4.5
4
3.5
3
2.5
2
1.5
1
0.5
0
0.4
0.6
1
2
4
6
8
10
20
40
60
100
200
400
600
1000
Particle Diameter (µm)

Table A56. Grain size distribution from Coulter Counter for B5 bottom.

COULTER LS	3/30/2006 10:38		
File name:	120042b.$04 (B5 bottom)		
From	0.375	95% Conf. Limits:	0
To	948.2	95% Conf. Limits:	79.96
Volume	100 mL	S.D.:	29.42
Mean:	22.3	Variance:	865.4
Median:	8.986	C.V.:	131.9
D(3,2):	4.321	Skewness:	1.757
Mean/Median Ratio:	2.482	Kurtosis:	1.956
Mode:	7.776	Specific Surf. Area	13884
Volume %	**120042b.$04 Particle Diameter µm <**	**120042b.$05 Particle Diameter µm <**	**120042b.$06 Particle Diameter µm <**
10	1.724	1.71	1.699
25	4.09	4.061	4.041
50	8.986	8.871	8.816
75	24.2	24.1	24.13
90	77.3	76.83	75.58
	120042b.$04	120042b.$05	120042b.$06
Channel Diameter (Lower) µm	**Diff. Volume %**	**Diff. Volume %**	**Diff. Volume %**
0.375	0.1	0.101	0.102
0.412	0.178	0.18	0.181
0.452	0.262	0.264	0.265
0.496	0.37	0.373	0.375
0.545	0.457	0.461	0.464
0.598	0.53	0.535	0.538
0.657	0.594	0.599	0.603
0.721	0.654	0.66	0.664
0.791	0.701	0.708	0.712
0.869	0.737	0.744	0.749
0.953	0.765	0.773	0.778
1.047	0.792	0.799	0.805
1.149	0.822	0.829	0.836
1.261	0.854	0.862	0.869
1.385	0.894	0.902	0.909
1.52	0.946	0.954	0.962
1.669	1.02	1.02	1.03
1.832	1.11	1.11	1.12
2.01	1.21	1.22	1.23
2.207	1.34	1.35	1.36
2.423	1.49	1.5	1.51

2.66	1.65	1.66	1.67
2.92	1.83	1.85	1.85
3.206	2.02	2.03	2.04
3.519	2.22	2.23	2.23
3.862	2.41	2.42	2.43
4.241	2.59	2.61	2.61
4.656	2.76	2.78	2.79
5.111	2.91	2.93	2.94
5.611	3.03	3.06	3.06
6.158	3.12	3.15	3.16
6.761	3.17	3.21	3.22
7.421	3.18	3.22	3.24
8.147	3.15	3.19	3.21
8.944	3.07	3.1	3.12
9.819	2.95	2.97	2.98
10.78	2.78	2.79	2.79
11.83	2.59	2.57	2.56
12.99	2.39	2.34	2.3
14.26	2.23	2.14	2.07
15.65	2.12	2	1.91
17.18	2.05	1.93	1.84
18.86	1.99	1.91	1.85
20.7	1.87	1.88	1.89
22.73	1.68	1.78	1.88
24.95	1.43	1.61	1.76
27.38	1.2	1.38	1.52
30.07	1.06	1.17	1.23
33	1.02	1.01	0.954
36.24	1.06	0.929	0.764
39.77	1.12	0.886	0.679
43.66	1.11	0.856	0.693
47.93	1.05	0.846	0.799
52.63	0.989	0.906	1
57.77	1.05	1.1	1.31
63.41	1.31	1.48	1.72
69.62	1.76	2.01	2.16
76.43	2.28	2.51	2.5
83.9	2.58	2.72	2.57
92.09	2.44	2.44	2.23
101.1	1.77	1.6	1.51
111	0.896	0.697	0.709
121.8	0.266	0.144	0.189

133.7	0.038	0.012	0.024
146.8	0.001	0	0.001

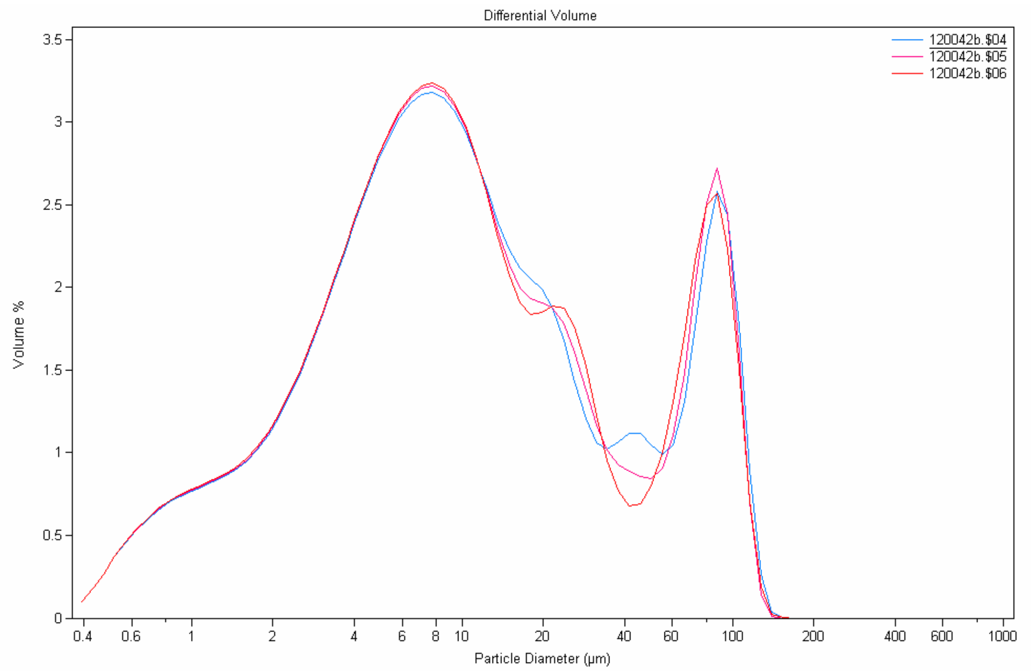

Table A57. Grain size distribution from Coulter Counter for B7 bottom.

COULTER LS	9:27 30 Mar 2006		
File name:	124329-b.$01 (B7 bottom)		
From	0.375	95% Conf. Limits:	40.2
To	948.2	95% Conf. Limits:	289.6
Volume	100 mL	S.D.:	63.62
Mean:	164.9	Variance:	4048
Median:	163.8	C.V.:	38.58
D(3,2):	25.81	Skewness:	-0.425
Mean/Median Ratio:	1.007	Kurtosis:	1.633
Mode:	168.8	Specific Surf. Area	2325
Volume %	124329-b.$01 Particle Diameter µm <	124329-b.$02 Particle Diameter µm <	124329-b.$03 Particle Diameter µm <
10	115	121.6	123.6
25	137.7	141	143.2
50	163.8	164.3	166.6
75	196	192.1	194.5
90	238.7	236.7	241.3
	124329-b.$01	124329-b.$02	124329-b.$03
Channel Diameter (Lower) µm	Diff. Volume %	Diff. Volume %	Diff. Volume %
0.375	0.005	0.016	0.011
0.412	0.01	0.03	0.022
0.452	0.017	0.05	0.037
0.496	0.023	0.069	0.051
0.545	0.03	0.087	0.064
0.598	0.037	0.102	0.077
0.657	0.045	0.117	0.089
0.721	0.053	0.129	0.101
0.791	0.064	0.141	0.112
0.869	0.078	0.151	0.124
0.953	0.096	0.16	0.136
1.047	0.119	0.17	0.149
1.149	0.148	0.181	0.164
1.261	0.183	0.194	0.182
1.385	0.226	0.209	0.203
1.52	0.274	0.228	0.227
1.669	0.328	0.251	0.254
1.832	0.385	0.279	0.284
2.01	0.442	0.31	0.316
2.207	0.496	0.344	0.349
2.423	0.541	0.38	0.381

2.66	0.572	0.414	0.408
2.92	0.581	0.443	0.428
3.206	0.566	0.463	0.437
3.519	0.52	0.471	0.43
3.862	0.446	0.46	0.407
4.241	0.346	0.43	0.364
4.656	0.234	0.378	0.304
5.111	0.124	0.307	0.229
5.611	0.034	0.223	0.151
6.158	0.002	0.136	0.074
6.761	0	0.048	0.017
7.421	0	0.004	0.001

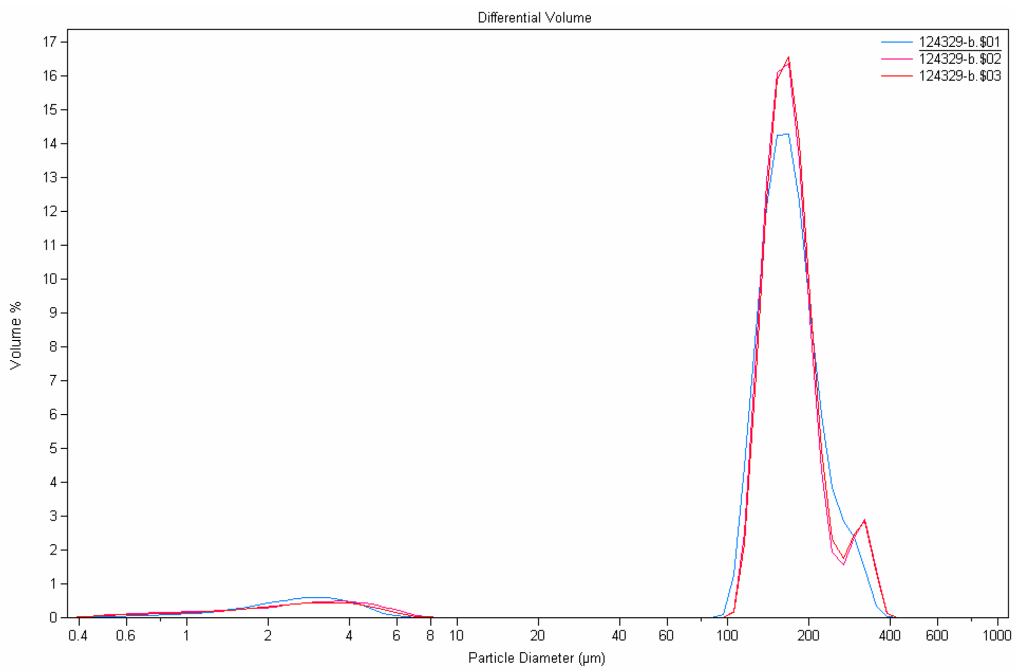

Table A58. Grain size distribution from Coulter Counter for B9 bottom.

COULTER LS	3/30/2006 13:33		
File name:	131544b.$01 (B9 bottom)		
From	0.375	95% Conf. Limits:	0
To	948.2	95% Conf. Limits:	41.16
Volume	100 mL	S.D.:	14.22
Mean:	13.29	Variance:	202.3
Median:	8.315	C.V.:	107.1
D(3,2):	3.771	Skewness:	1.977
Mean/Median Ratio:	1.598	Kurtosis:	4.054
Mode:	8.536	Specific Surf. Area	15911
Volume %	131544b.$01 Particle Diameter µm <	131544b.$02 Particle Diameter µm <	131544b.$03 Particle Diameter µm <
10	1.521	1.472	1.452
25	3.815	3.72	3.677
50	8.315	8.084	8.009
75	17.35	16.73	16.59
90	32.12	30.32	30.36
	131544b.$01	131544b.$02	131544b.$03
Channel Diameter (Lower) µm	Diff. Volume %	Diff. Volume %	Diff. Volume %
0.375	0.155	0.159	0.161
0.412	0.29	0.297	0.302
0.452	0.472	0.484	0.491
0.496	0.622	0.638	0.647
0.545	0.737	0.757	0.767
0.598	0.816	0.837	0.848
0.657	0.856	0.879	0.89
0.721	0.861	0.885	0.895
0.791	0.837	0.861	0.87
0.869	0.794	0.817	0.825
0.953	0.744	0.766	0.773
1.047	0.701	0.722	0.728
1.149	0.68	0.7	0.706
1.261	0.69	0.711	0.717
1.385	0.739	0.761	0.768
1.52	0.827	0.851	0.86
1.669	0.951	0.977	0.989
1.832	1.1	1.13	1.15
2.01	1.27	1.3	1.32
2.207	1.45	1.48	1.5
2.423	1.62	1.66	1.68

2.66	1.79	1.83	1.85
2.92	1.94	1.99	2.01
3.206	2.1	2.15	2.17
3.519	2.26	2.31	2.33
3.862	2.42	2.48	2.5
4.241	2.59	2.66	2.67
4.656	2.77	2.83	2.84
5.111	2.94	3	3.01
5.611	3.11	3.16	3.17
6.158	3.26	3.3	3.31
6.761	3.38	3.42	3.41
7.421	3.47	3.49	3.48
8.147	3.5	3.51	3.49
8.944	3.47	3.47	3.44
9.819	3.38	3.38	3.35
10.78	3.25	3.26	3.23
11.83	3.12	3.13	3.11
12.99	2.99	3.02	3.02
14.26	2.9	2.92	2.94
15.65	2.84	2.84	2.86
17.18	2.79	2.76	2.76
18.86	2.72	2.68	2.63
20.7	2.57	2.54	2.46
22.73	2.35	2.34	2.25
24.95	2.05	2.04	1.97
27.38	1.74	1.69	1.68
30.07	1.53	1.44	1.46
33	1.46	1.34	1.35
36.24	1.4	1.31	1.25
39.77	1.28	1.27	1.15
43.66	1.12	1.13	1.06
47.93	0.934	0.955	0.934
52.63	0.836	0.875	0.859
57.77	0.935	0.876	0.907
63.41	0.954	0.673	0.81
69.62	0.518	0.234	0.334
76.43	0.093	0.017	0.028
83.9	0.003	0	0

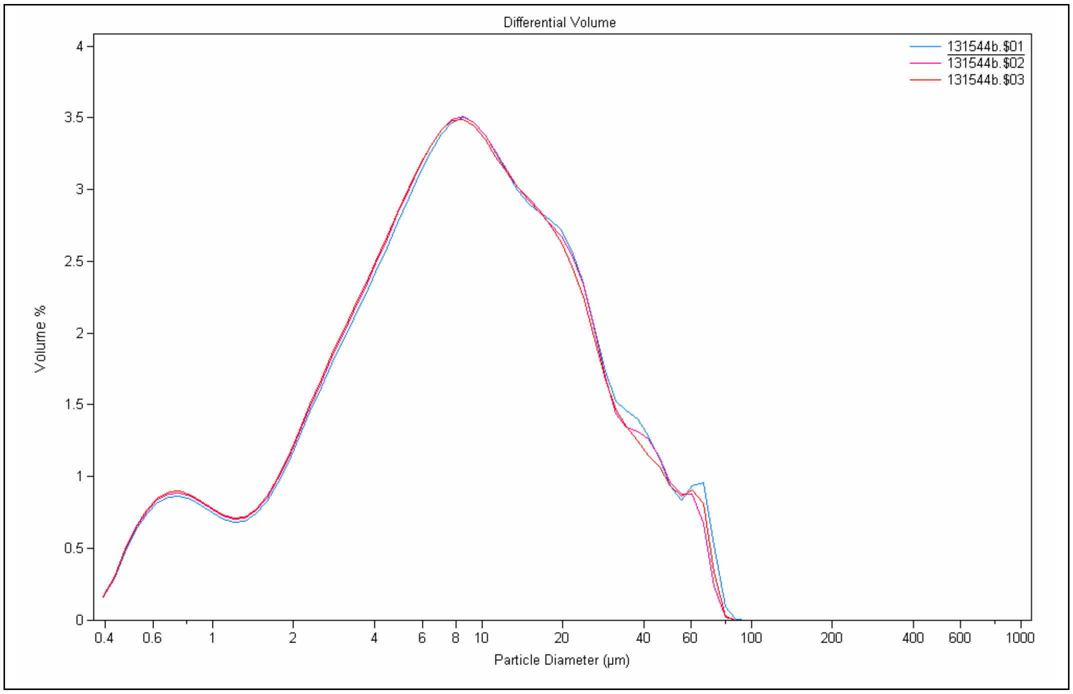
Differential Volume
131544b.$01
131544b.$02
131544b.$03
Volume %
4
3.5
3
2.5
2
1.5
1
0.5
0
0.4
0.6
1
2
4
6
8
10
20
40
60
100
200
400
600
1000
Particle Diameter (μm)

Table A59. Grain size distribution from Coulter Counter for B11 bottom.

COULTER LS	3/30/2006 10:14		
File name:	140752b.$01 (B11 bottom)		
From	0.375	95% Conf. Limits:	0
To	948.2	95% Conf. Limits:	132
Volume	100 mL	S.D.:	46.12
Mean:	41.61	Variance:	2127
Median:	18.65	C.V.:	110.8
D(3,2):	5.097	Skewness:	1.095
Mean/Median Ratio:	2.231	Kurtosis:	0.0657
Mode:	116.3	Specific Surf. Area	11771
Volume %	**140752b.$01 Particle Diameter µm <**	**140752b.$02 Particle Diameter µm <**	**140752b.$03 Particle Diameter µm <**
10	1.805	1.783	1.764
25	5.174	5.094	5.047
50	18.65	18.23	18.04
75	72.12	71.67	72.11
90	116.8	117.1	115.8
	140752b.$01	140752b.$02	140752b.$03
Channel Diameter (Lower) µm	**Diff. Volume %**	**Diff. Volume %**	**Diff. Volume %**
0.375	0.1	0.102	0.103
0.412	0.178	0.181	0.183
0.452	0.261	0.265	0.268
0.496	0.368	0.374	0.379
0.545	0.455	0.462	0.468
0.598	0.527	0.535	0.541
0.657	0.589	0.598	0.605
0.721	0.647	0.656	0.663
0.791	0.692	0.701	0.709
0.869	0.723	0.733	0.741
0.953	0.745	0.754	0.762
1.047	0.761	0.77	0.778
1.149	0.778	0.786	0.794
1.261	0.794	0.802	0.809
1.385	0.813	0.82	0.828
1.52	0.837	0.844	0.852
1.669	0.874	0.881	0.888
1.832	0.922	0.929	0.937
2.01	0.981	0.989	0.997
2.207	1.05	1.06	1.07
2.423	1.13	1.14	1.15

2.66	1.22	1.23	1.24
2.92	1.32	1.33	1.34
3.206	1.42	1.44	1.44
3.519	1.51	1.54	1.54
3.862	1.61	1.63	1.64
4.241	1.69	1.72	1.72
4.656	1.77	1.8	1.8
5.111	1.83	1.86	1.86
5.611	1.88	1.91	1.9
6.158	1.91	1.94	1.93
6.761	1.93	1.95	1.95
7.421	1.93	1.95	1.94
8.147	1.92	1.93	1.92
8.944	1.89	1.9	1.89
9.819	1.85	1.86	1.85
10.78	1.8	1.81	1.8
11.83	1.75	1.76	1.75
12.99	1.71	1.72	1.71
14.26	1.69	1.69	1.7
15.65	1.68	1.66	1.69
17.18	1.68	1.62	1.67
18.86	1.67	1.58	1.63
20.7	1.65	1.53	1.56
22.73	1.61	1.5	1.49
24.95	1.55	1.49	1.45
27.38	1.5	1.52	1.46
30.07	1.47	1.56	1.51
33	1.47	1.6	1.58
36.24	1.5	1.63	1.63
39.77	1.56	1.64	1.63
43.66	1.67	1.66	1.62
47.93	1.8	1.72	1.65
52.63	1.96	1.85	1.75
57.77	2.14	2.05	1.97
63.41	2.33	2.29	2.28
69.62	2.51	2.53	2.61
76.43	2.68	2.71	2.88
83.9	2.85	2.84	3.03
92.09	3.02	2.94	3.08
101.1	3.16	3.02	3.05
111	3.19	3.04	2.96
121.8	2.98	2.89	2.75

133.7	2.48	2.48	2.35
146.8	1.74	1.82	1.75
161.2	0.922	1.02	1.01
176.8	0.327	0.387	0.402
194.2	0.058	0.073	0.079
213.2	0.004	0.006	0.006

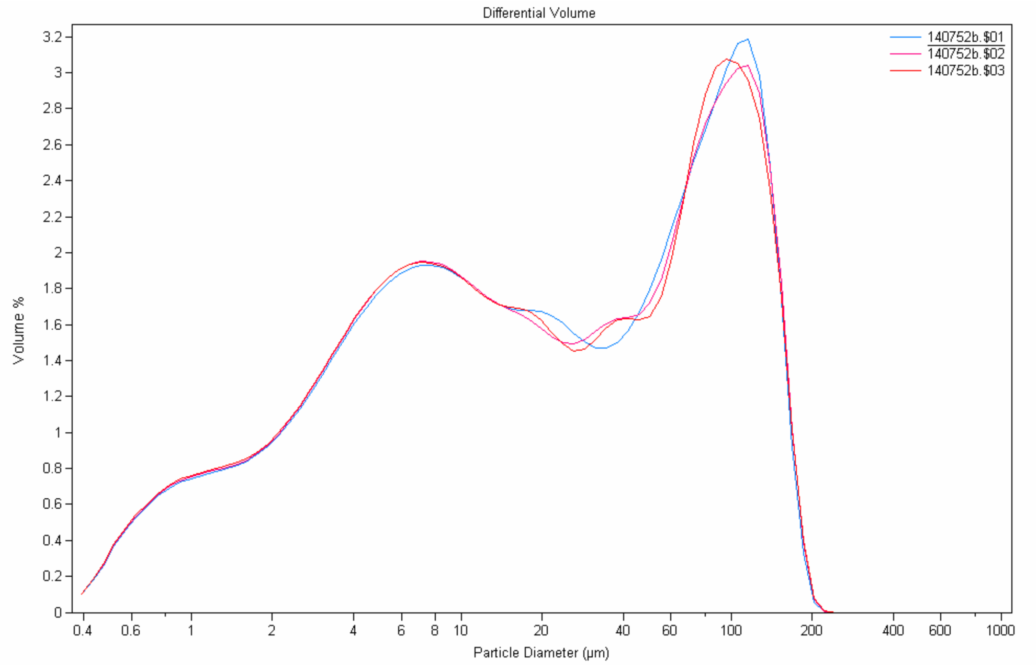

Table A60. Grain size distribution from Coulter Counter for B16.

COULTER LS	3/27/2006 13:39		
File name:	160302.$01 (B16)		
From	0.375	95% Conf. Limits:	0
To	948.2	95% Conf. Limits:	20.42
Volume	100 mL	S.D.:	6.231
Mean:	8.213	Variance:	38.82
Median:	6.646	C.V.:	75.87
D(3,2):	3.188	Skewness:	0.852
Mean/Median Ratio:	1.236	Kurtosis:	-0.122
Mode:	8.536	Specific Surf. Area	18823
Volume %	160302.$01 Particle Diameter µm <	160302.$02 Particle Diameter µm <	160302.$03 Particle Diameter µm <
10	1.197	1.194	1.193
25	3.252	3.245	3.246
50	6.646	6.64	6.659
75	11.9	11.96	12.03
90	18.09	18.18	18.42
	160302.$01	160302.$02	160302.$03
Channel Diameter (Lower) µm	Diff. Volume %	Diff. Volume %	Diff. Volume %
0.375	0.207	0.208	0.209
0.412	0.386	0.388	0.39
0.452	0.626	0.629	0.632
0.496	0.819	0.822	0.826
0.545	0.963	0.966	0.97
0.598	1.05	1.05	1.06
0.657	1.09	1.09	1.09
0.721	1.07	1.07	1.07
0.791	1.01	1.01	1.01
0.869	0.922	0.922	0.92
0.953	0.825	0.824	0.82
1.047	0.741	0.74	0.733
1.149	0.69	0.688	0.68
1.261	0.687	0.685	0.676
1.385	0.741	0.739	0.731
1.52	0.854	0.854	0.846
1.669	1.02	1.02	1.02
1.832	1.23	1.24	1.23
2.01	1.47	1.47	1.47
2.207	1.71	1.72	1.72
2.423	1.95	1.96	1.96

2.66	2.17	2.18	2.19
2.92	2.39	2.4	2.4
3.206	2.59	2.6	2.6
3.519	2.78	2.79	2.79
3.862	2.98	2.99	2.98
4.241	3.18	3.18	3.17
4.656	3.38	3.38	3.35
5.111	3.57	3.56	3.53
5.611	3.75	3.73	3.7
6.158	3.91	3.88	3.86
6.761	4.03	4	3.98
7.421	4.11	4.07	4.06
8.147	4.13	4.09	4.08
8.944	4.07	4.03	4.03
9.819	3.94	3.91	3.9
10.78	3.75	3.73	3.7
11.83	3.54	3.53	3.48
12.99	3.37	3.36	3.29
14.26	3.26	3.26	3.18
15.65	3.26	3.28	3.2
17.18	3.3	3.34	3.32
18.86	3.24	3.3	3.37
20.7	2.85	2.91	3.07
22.73	1.82	1.85	2.02
24.95	0.547	0.546	0.622
27.38	0.036	0.035	0.041

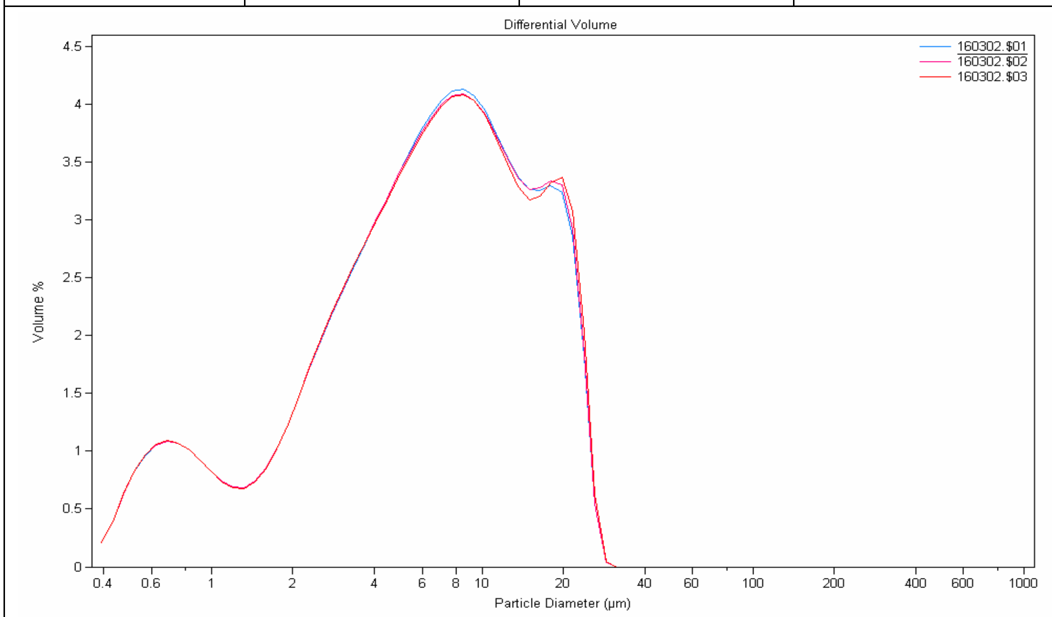

Table A61. Grain size distribution from Coulter Counter for B17 bottom.

COULTER LS	3/30/2006 11:02		
File name:	161824b.$04 (B17 bottom)		
From	0.375	95% Conf. Limits:	0
To	948.2	95% Conf. Limits:	50.62
Volume	100 mL	S.D.:	18.08
Mean:	15.18	Variance:	326.8
Median:	8.18	C.V.:	119.1
D(3,2):	3.668	Skewness:	2.013
Mean/Median Ratio:	1.856	Kurtosis:	3.705
Mode:	7.776	Specific Surf. Area	16358
Volume %	**161824b.$04 Particle Diameter µm <**	**161824b.$05 Particle Diameter µm <**	**161824b.$06 Particle Diameter µm <**
10	1.414	1.402	1.386
25	3.69	3.665	3.634
50	8.18	8.119	8.047
75	18.67	18.61	18.4
90	41.86	41.6	40.85
	161824b.$04	161824b.$05	161824b.$06
Channel Diameter (Lower) µm	**Diff. Volume %**	**Diff. Volume %**	**Diff. Volume %**
0.375	0.17	0.172	0.173
0.412	0.319	0.322	0.324
0.452	0.518	0.523	0.527
0.496	0.681	0.687	0.692
0.545	0.806	0.812	0.819
0.598	0.888	0.895	0.902
0.657	0.928	0.934	0.942
0.721	0.927	0.934	0.942
0.791	0.894	0.899	0.908
0.869	0.838	0.843	0.851
0.953	0.775	0.778	0.786
1.047	0.719	0.722	0.73
1.149	0.688	0.69	0.697
1.261	0.691	0.694	0.701
1.385	0.737	0.741	0.748
1.52	0.827	0.832	0.839
1.669	0.956	0.963	0.971
1.832	1.12	1.12	1.13
2.01	1.29	1.3	1.31
2.207	1.48	1.49	1.5
2.423	1.65	1.67	1.68

2.66	1.82	1.84	1.85
2.92	1.99	2	2.01
3.206	2.14	2.15	2.17
3.519	2.3	2.31	2.33
3.862	2.47	2.47	2.49
4.241	2.63	2.64	2.65
4.656	2.79	2.8	2.82
5.111	2.95	2.96	2.97
5.611	3.09	3.1	3.11
6.158	3.2	3.22	3.23
6.761	3.28	3.3	3.31
7.421	3.31	3.33	3.34
8.147	3.28	3.29	3.3
8.944	3.19	3.19	3.2
9.819	3.05	3.03	3.04
10.78	2.89	2.86	2.85
11.83	2.76	2.71	2.69
12.99	2.66	2.61	2.58
14.26	2.59	2.55	2.53
15.65	2.54	2.52	2.52
17.18	2.47	2.48	2.51
18.86	2.37	2.4	2.44
20.7	2.24	2.26	2.28
22.73	2.09	2.06	2.04
24.95	1.89	1.81	1.77
27.38	1.59	1.51	1.48
30.07	1.27	1.26	1.25
33	1.14	1.21	1.21
36.24	1.28	1.37	1.37
39.77	1.59	1.6	1.62
43.66	1.8	1.7	1.76
47.93	1.55	1.4	1.41
52.63	0.891	0.821	0.668
57.77	0.595	0.661	0.43
63.41	1.04	1.2	1.04
69.62	1.7	1.78	1.84
76.43	1.3	1.24	1.32
83.9	0.369	0.322	0.338
92.09	0.021	0.017	0.017

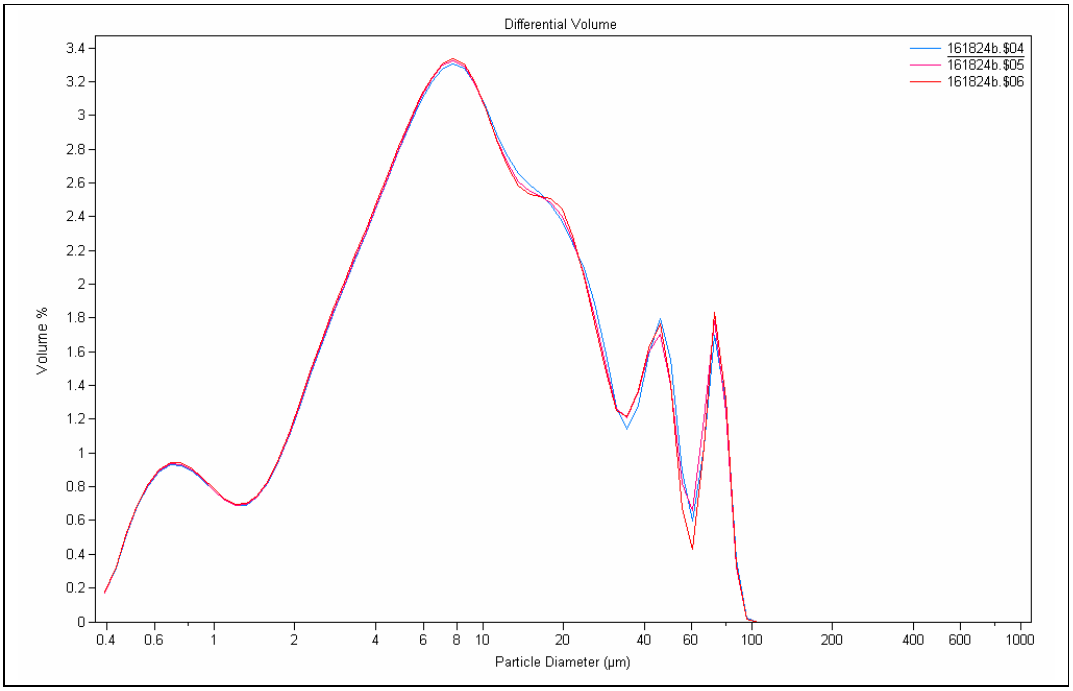
Differential Volume
161824b.$04
161824b.$05
161824b.$06
Volume %
0
0.2
0.4
0.6
0.8
1
1.2
1.4
1.6
1.8
2
2.2
2.4
2.6
2.8
3
3.2
3.4
0.4
0.6
1
2
4
6
8
10
20
40
60
100
200
400
600
1000
Particle Diameter (µm)

Table A62. Grain size distribution from Coulter Counter for C1.

COULTER LS	3/27/2006 11:07		
File name:	092333.$01 (C1)		
From	0.375	95% Conf. Limits:	0
To	948.2	95% Conf. Limits:	19.98
Volume	100 mL	S.D.:	5.961
Mean:	8.297	Variance:	35.54
Median:	7.064	C.V.:	71.84
D(3,2):	3.298	Skewness:	0.574
Mean/Median Ratio:	1.175	Kurtosis:	-0.716
Mode:	16.4	Specific Surf. Area	18190
Volume %	Particle Diameter µm <		
10	1.226		
16	1.949		
25	3.201		
50	7.064		
75	12.73		
84	15.42		
90	17.4		
95	19.37		
Channel Diameter (Lower) µm	Diff. Volume %		
0.375	0.158		
0.412	0.28		
0.452	0.409		
0.496	0.577		
0.545	0.71		
0.598	0.818		
0.657	0.909		
0.721	0.991		
0.791	1.05		
0.869	1.09		
0.953	1.11		
1.047	1.12		
1.149	1.13		
1.261	1.15		
1.385	1.17		
1.52	1.2		
1.669	1.25		
1.832	1.33		
2.01	1.43		
2.207	1.55		
2.423	1.7		

2.66	1.86		
2.92	2.04		
3.206	2.24		
3.519	2.44		
3.862	2.64		
4.241	2.83		
4.656	3.03		
5.111	3.21		
5.611	3.38		
6.158	3.52		
6.761	3.65		
7.421	3.78		
8.147	3.89		
8.944	3.98		
9.819	4.05		
10.78	4.1		
11.83	4.16		
12.99	4.31		
14.26	4.49		
15.65	4.66		
17.18	4.61		
18.86	3.55		
20.7	1.91		
22.73	0.467		
24.95	0.051		

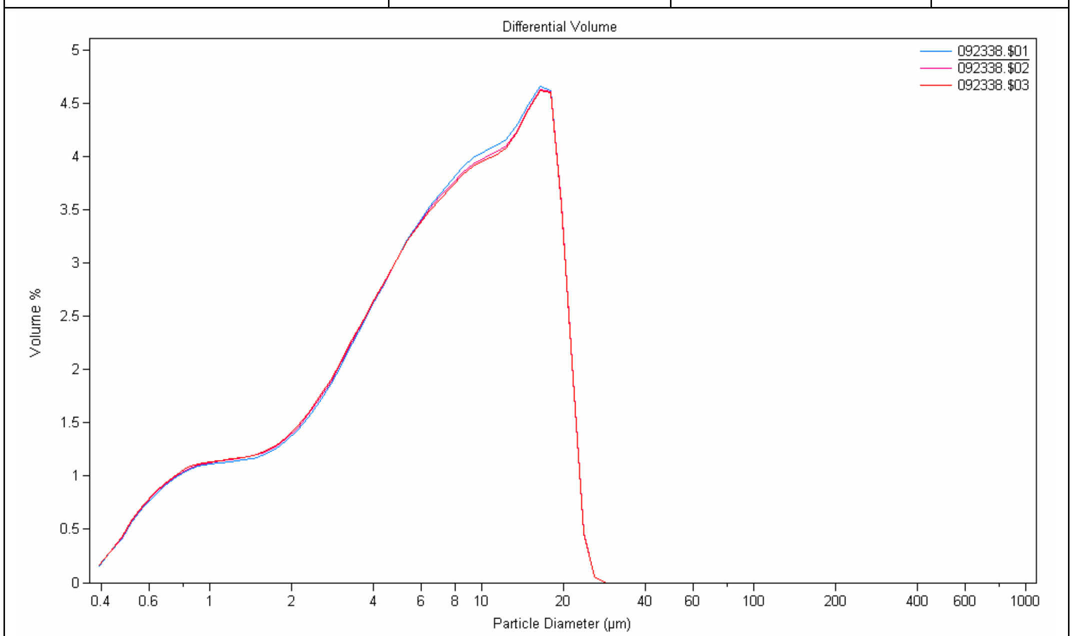

Table A63. Grain size distribution from Coulter Counter for C1 bottom.

COULTER LS	3/30/2006 10:04		
File name:	092338b.$07 (C1 bottom)		
From	0.375	95% Conf. Limits:	0
To	948.2	95% Conf. Limits:	311.4
Volume	100 mL	S.D.:	119.6
Mean:	76.94	Variance:	14304
Median:	21.52	C.V.:	155.4
D(3,2):	5.327	Skewness:	2.097
Mean/Median Ratio:	3.576	Kurtosis:	3.961
Mode:	26.14	Specific Surf. Area	11264
Volume %	**092338b.$07 Particle Diameter µm <**	**092338b.$08 Particle Diameter µm <**	**092338b.$09 Particle Diameter µm <**
10	1.84	1.847	1.833
25	5.424	5.463	5.403
50	21.52	21.84	21.45
75	86.87	92.1	87.19
90	265.9	281.7	276.8
	092338b.$07	092338b.$08	092338b.$09
Channel Diameter (Lower) µm	**Diff. Volume %**	**Diff. Volume %**	**Diff. Volume %**
0.375	0.091	0.09	0.091
0.412	0.161	0.16	0.162
0.452	0.236	0.235	0.238
0.496	0.335	0.334	0.337
0.545	0.416	0.414	0.419
0.598	0.485	0.483	0.488
0.657	0.547	0.545	0.55
0.721	0.606	0.604	0.609
0.791	0.656	0.654	0.659
0.869	0.695	0.693	0.698
0.953	0.727	0.725	0.73
1.047	0.756	0.753	0.758
1.149	0.786	0.783	0.788
1.261	0.814	0.811	0.816
1.385	0.844	0.841	0.846
1.52	0.878	0.875	0.88
1.669	0.92	0.917	0.923
1.832	0.97	0.967	0.973
2.01	1.03	1.02	1.03
2.207	1.09	1.08	1.09
2.423	1.15	1.15	1.16

2.66	1.22	1.21	1.22
2.92	1.29	1.28	1.29
3.206	1.35	1.35	1.36
3.519	1.42	1.41	1.42
3.862	1.47	1.46	1.47
4.241	1.52	1.51	1.52
4.656	1.56	1.54	1.55
5.111	1.59	1.57	1.58
5.611	1.61	1.59	1.6
6.158	1.62	1.6	1.6
6.761	1.62	1.61	1.61
7.421	1.62	1.61	1.6
8.147	1.62	1.6	1.6
8.944	1.62	1.6	1.59
9.819	1.62	1.6	1.59
10.78	1.62	1.6	1.6
11.83	1.64	1.62	1.62
12.99	1.68	1.66	1.67
14.26	1.74	1.72	1.75
15.65	1.8	1.79	1.84
17.18	1.87	1.87	1.93
18.86	1.94	1.94	2
20.7	1.99	1.99	2.03
22.73	2.02	2.01	2.02
24.95	2.04	2	1.98
27.38	2.03	1.97	1.92
30.07	2	1.92	1.86
33	1.94	1.86	1.81
36.24	1.86	1.79	1.77
39.77	1.75	1.73	1.74
43.66	1.64	1.67	1.71
47.93	1.54	1.59	1.68
52.63	1.44	1.5	1.63
57.77	1.36	1.39	1.54
63.41	1.29	1.28	1.41
69.62	1.24	1.18	1.23
76.43	1.21	1.12	1.05
83.9	1.21	1.11	0.937
92.09	1.22	1.16	0.928
101.1	1.24	1.23	1.03
111	1.23	1.28	1.18
121.8	1.2	1.25	1.27

133.7	1.15	1.12	1.21
146.8	1.1	0.958	1.03
161.2	1.1	0.862	0.888
176.8	1.15	0.911	0.917
194.2	1.26	1.13	1.16
213.2	1.42	1.46	1.54
234.1	1.56	1.77	1.83
256.8	1.65	1.91	1.84
282.1	1.65	1.83	1.53
309.6	1.55	1.6	1.12
339.8	1.4	1.34	0.84
373.1	1.21	1.16	0.797
409.6	1.02	1.08	0.976
449.7	0.837	1.04	1.25
493.6	0.651	0.928	1.38
541.9	0.41	0.636	1.07
594.9	0.183	0.289	0.522
653	0.039	0.062	0.116
716.9	0.004	0.005	0.01

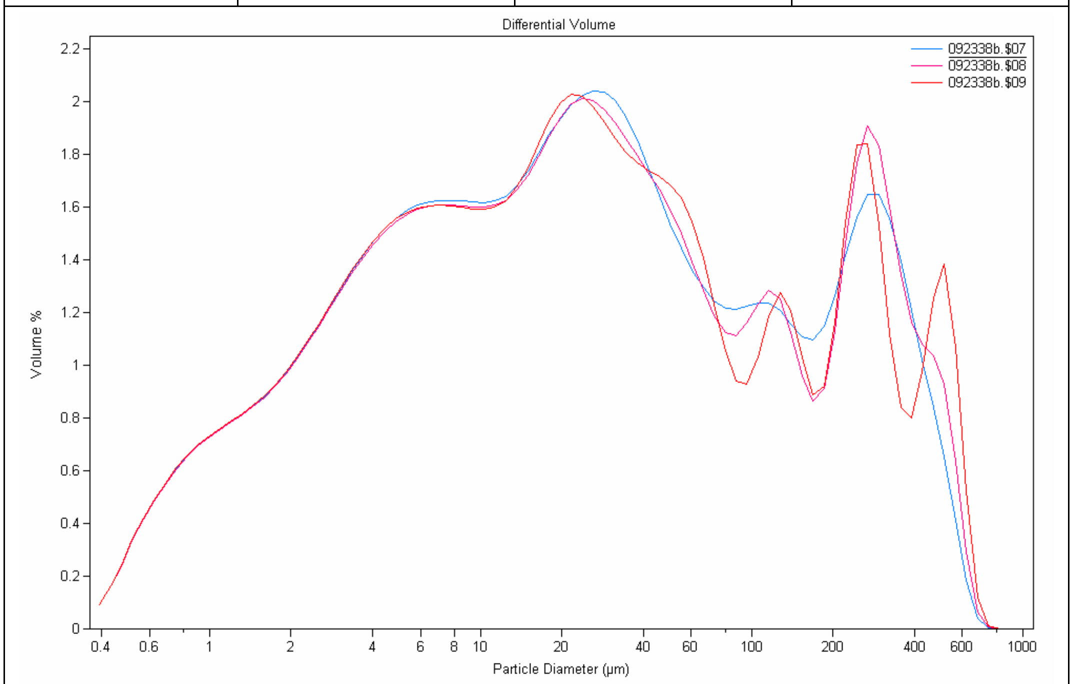

Table A64. Grain size distribution from Coulter Counter for C3 bottom.

COULTER LS	3/30/2006 13:45		
File name:	102256b.$01 (C3 bottom)		
From	0.375	95% Conf. Limits:	0
To	948.2	95% Conf. Limits:	260.7
Volume	100 mL	S.D.:	100.5
Mean:	63.66	Variance:	10101
Median:	27.8	C.V.:	157.9
D(3,2):	6.133	Skewness:	3.168
Mean/Median Ratio:	2.29	Kurtosis:	11.69
Mode:	50.23	Specific Surf. Area	9783
Volume %	**102256b.$01 Particle Diameter µm <**	**102256b.$02 Particle Diameter µm <**	**102256b.$03 Particle Diameter µm <**
10	2.234	2.207	2.248
25	6.498	6.476	6.696
50	27.8	28.1	30.18
75	74.76	75.66	82.38
90	155.5	156.9	193.1
	102256b.$01	102256b.$02	102256b.$03
Channel Diameter (Lower) µm	**Diff. Volume %**	**Diff. Volume %**	**Diff. Volume %**
0.375	0.072	0.072	0.071
0.412	0.127	0.129	0.126
0.452	0.187	0.189	0.186
0.496	0.265	0.269	0.264
0.545	0.33	0.334	0.328
0.598	0.386	0.39	0.383
0.657	0.436	0.441	0.433
0.721	0.485	0.491	0.482
0.791	0.527	0.533	0.524
0.869	0.561	0.568	0.558
0.953	0.59	0.598	0.587
1.047	0.618	0.626	0.615
1.149	0.646	0.655	0.644
1.261	0.676	0.685	0.673
1.385	0.707	0.717	0.704
1.52	0.744	0.753	0.74
1.669	0.788	0.797	0.783
1.832	0.838	0.848	0.833
2.01	0.896	0.905	0.888
2.207	0.959	0.967	0.949
2.423	1.03	1.03	1.01

2.66	1.1	1.1	1.08
2.92	1.17	1.18	1.15
3.206	1.25	1.25	1.22
3.519	1.32	1.31	1.28
3.862	1.38	1.38	1.34
4.241	1.44	1.43	1.39
4.656	1.49	1.48	1.44
5.111	1.53	1.51	1.47
5.611	1.56	1.54	1.49
6.158	1.58	1.55	1.51
6.761	1.59	1.56	1.51
7.421	1.59	1.56	1.51
8.147	1.58	1.55	1.5
8.944	1.56	1.53	1.49
9.819	1.54	1.51	1.48
10.78	1.51	1.5	1.47
11.83	1.49	1.49	1.46
12.99	1.48	1.48	1.46
14.26	1.49	1.5	1.47
15.65	1.52	1.54	1.5
17.18	1.58	1.59	1.54
18.86	1.65	1.65	1.57
20.7	1.74	1.71	1.6
22.73	1.81	1.76	1.65
24.95	1.88	1.82	1.72
27.38	1.95	1.91	1.83
30.07	2.03	2.03	1.99
33	2.14	2.18	2.18
36.24	2.29	2.35	2.36
39.77	2.45	2.49	2.5
43.66	2.58	2.57	2.56
47.93	2.66	2.59	2.55
52.63	2.64	2.55	2.48
57.77	2.54	2.47	2.38
63.41	2.37	2.37	2.26
69.62	2.2	2.27	2.16
76.43	2.06	2.17	2.08
83.9	1.97	2.09	2.01
92.09	1.95	2.01	1.96
101.1	1.95	1.94	1.91
111	1.95	1.88	1.85
121.8	1.89	1.82	1.75

133.7	1.76	1.73	1.6
146.8	1.54	1.58	1.41
161.2	1.28	1.35	1.19
176.8	1.02	1.09	0.969
194.2	0.813	0.849	0.79
213.2	0.682	0.671	0.664
234.1	0.62	0.56	0.585
256.8	0.596	0.491	0.525
282.1	0.57	0.429	0.451
309.6	0.514	0.348	0.356
339.8	0.431	0.27	0.27
373.1	0.376	0.251	0.236
409.6	0.376	0.324	0.288
449.7	0.464	0.533	0.446
493.6	0.596	0.811	0.697
541.9	0.573	0.835	0.951
594.9	0.365	0.542	1.09
653	0.099	0.147	1.03
716.9	0.012	0.018	0.772
786.9	0	0	0.529
863.9	0	0	0.266

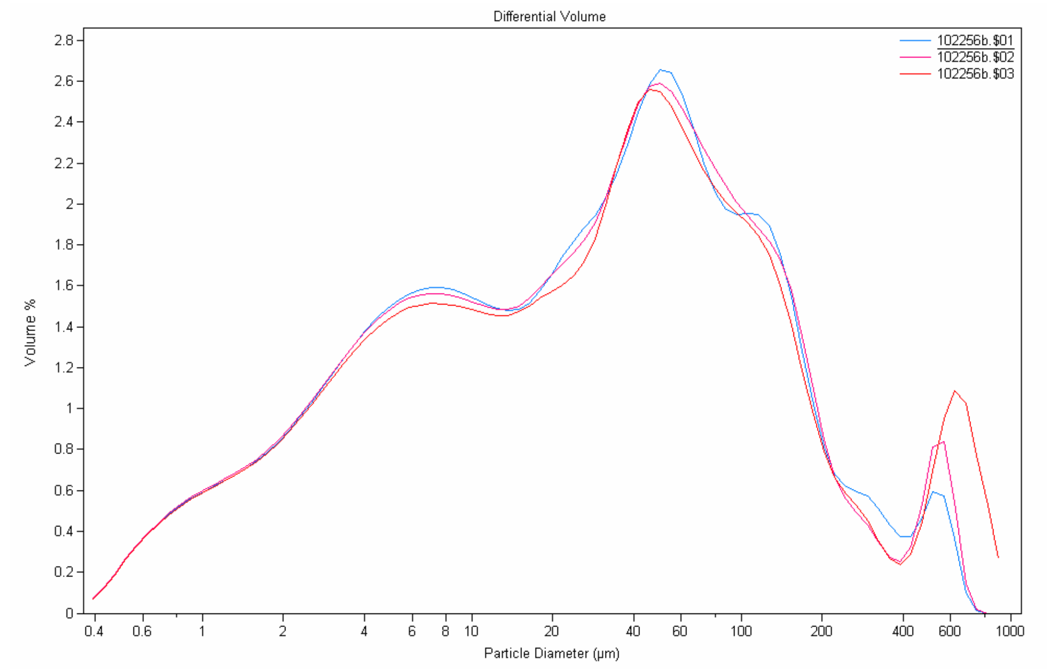

Table A65. Grain size distribution from Coulter Counter for the oxidized layer.

COULTER LS	3/30/2006 14:04		
File name:	fluff.$01 (oxidized layer)		
From	0.375	95% Conf. Limits:	0
To	948.2	95% Conf. Limits:	127.4
Volume	100 mL	S.D.:	45.75
Mean:	37.73	Variance:	2093
Median:	15.12	C.V.:	121.3
D(3,2):	6.3	Skewness:	1.568
Mean/Median Ratio:	2.495	Kurtosis:	1.74
Mode:	9.371	Specific Surf. Area	9525
Volume %	fluff.$01 Particle Diameter µm <	fluff.$02 Particle Diameter µm <	fluff.$03 Particle Diameter µm <
10	2.732	2.639	2.578
25	6.045	5.878	5.766
50	15.12	14.73	14.41
75	57.12	55.74	54.94
90	110.5	107.9	104.6
	fluff.$01	fluff.$02	fluff.$03
Channel Diameter (Lower) µm	Diff. Volume %	Diff. Volume %	Diff. Volume %
0.375	0.056	0.059	0.06
0.412	0.1	0.104	0.106
0.452	0.147	0.153	0.156
0.496	0.208	0.216	0.221
0.545	0.257	0.267	0.273
0.598	0.298	0.31	0.317
0.657	0.335	0.348	0.357
0.721	0.37	0.385	0.394
0.791	0.398	0.415	0.425
0.869	0.421	0.439	0.45
1.149	0.483	0.505	0.52
1.261	0.51	0.534	0.55
1.385	0.543	0.569	0.586
1.52	0.586	0.613	0.633
1.669	0.643	0.672	0.693
1.832	0.714	0.745	0.767
2.01	0.799	0.832	0.856
2.207	0.899	0.935	0.96
2.423	1.02	1.05	1.08
2.66	1.15	1.19	1.21
2.92	1.29	1.33	1.36

3.206	1.44	1.48	1.51
3.519	1.6	1.64	1.67
3.862	1.76	1.8	1.83
4.241	1.92	1.96	1.98
4.656	2.08	2.11	2.13
5.111	2.22	2.25	2.26
5.611	2.35	2.37	2.38
6.158	2.46	2.47	2.49
6.761	2.55	2.56	2.57
7.421	2.62	2.62	2.62
8.147	2.66	2.65	2.65
8.944	2.67	2.65	2.65
9.819	2.65	2.63	2.62
10.78	2.59	2.57	2.57
11.83	2.51	2.48	2.48
12.99	2.4	2.38	2.39
14.26	2.29	2.28	2.28
15.65	2.17	2.17	2.18
17.18	2.05	2.07	2.08
18.86	1.94	1.97	1.97
20.7	1.82	1.84	1.84
22.73	1.7	1.7	1.69
24.95	1.59	1.56	1.53
27.38	1.5	1.44	1.41
30.07	1.46	1.39	1.35
33	1.47	1.41	1.36
36.24	1.52	1.49	1.45
39.77	1.62	1.62	1.58
43.66	1.73	1.75	1.74
47.93	1.85	1.88	1.89
52.63	1.96	1.97	2.01
57.77	2.06	2.05	2.12
63.41	2.14	2.11	2.2
69.62	2.19	2.16	2.25
76.43	2.2	2.18	2.26
83.9	2.16	2.16	2.21
92.09	2.09	2.13	2.12
101.1	2.02	2.09	2.04
111	1.97	2.05	1.96
121.8	1.92	1.98	1.87
133.7	1.82	1.83	1.71
146.8	1.6	1.53	1.41

161.2	1.24	1.1	0.991
176.8	0.807	0.598	0.526
194.2	0.394	0.221	0.186
213.2	0.127	0.041	0.033
234.1	0.021	0.003	0.002
256.8	0.001	0	0

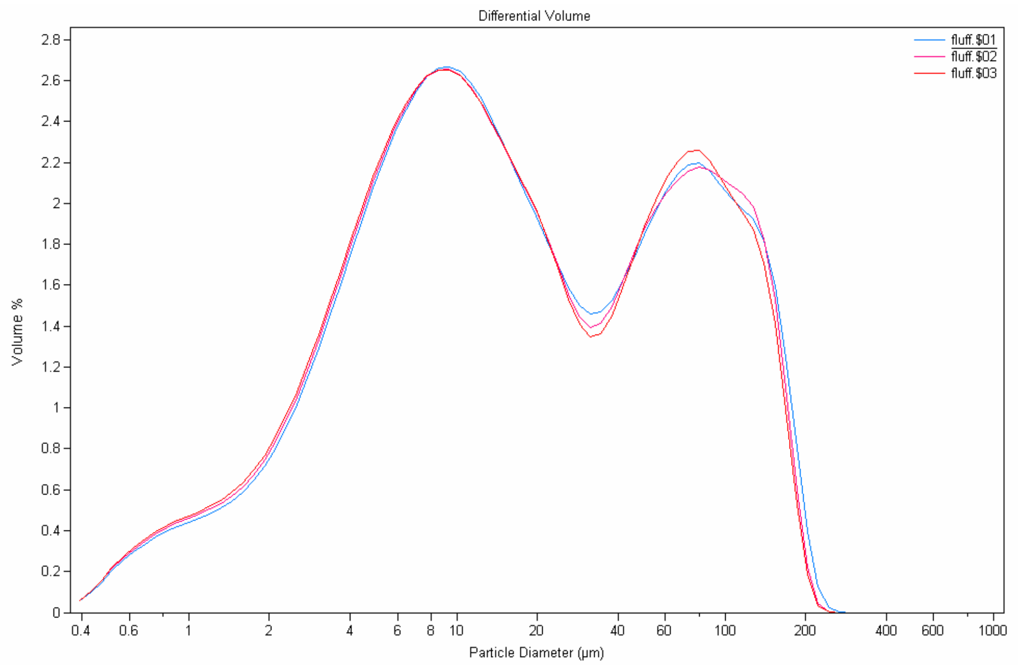

Appendix B: Sediment Transport Details

A detailed analysis of the bed displacement and suspended sediment transport results from the model simulations is presented in this appendix. The intent of this analysis is to describe the means by which the sediment loads travel within the system and how sediment is deposited in certain areas. These results are an elaboration of Chapter 3 which presents the sediment model in general. Chapter 4 discusses the effects of vessels, therefore the vessel effects are not considered here.

This analysis is presented in the following sections for ease of view and reference. Any links among sections are noted as necessary. Each section begins with a reference map so that various points within the area are labeled and distinguished with ease. The points are color-coded and consistent throughout the figures and text for each section. The time labels on the plots are given in hours with midnight of October 1 specified as hour 2208.

Houston Ship Channel

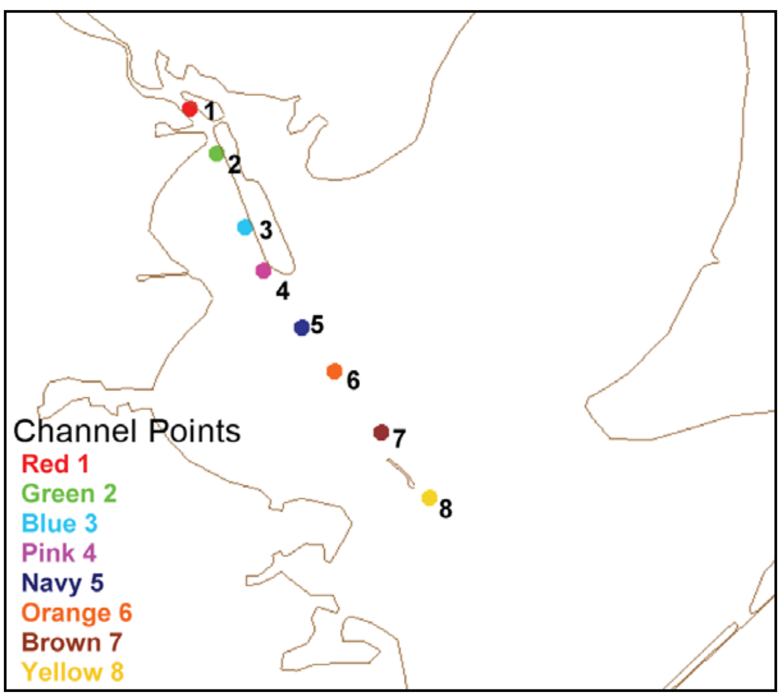

Figure B1. Channel reference map.

Figure B1 is a reference map of the area and several points within the Houston Ship Channel. These points are color coordinated to the following plots and are consistent for any points discussed in the channel.

High Flow Water Year

Figure B2 shows the bed displacement over time at each of these eight points along the channel. It indicates that the points upstream of and along Atkinson Island experienced the most deposition after the year-long simulation, but deposition at these points occurred later than at points further downstream.

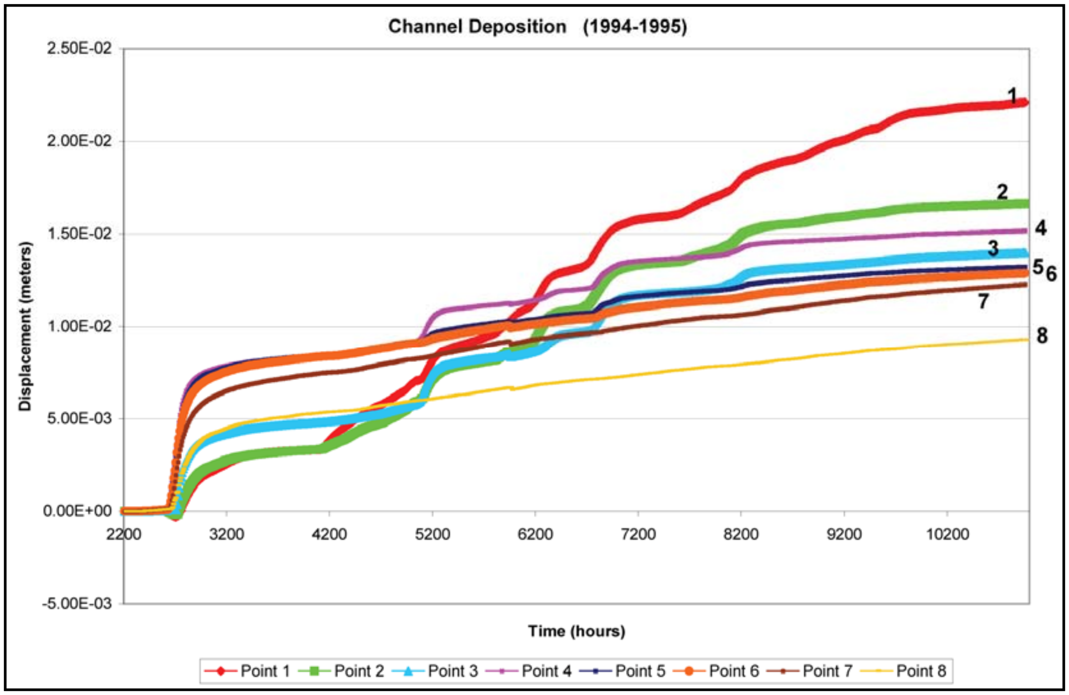

Figure B2. Bed deposition over time for the high flow year at points along the channel.

The initial sediment transport is generated by erosion along the boundaries of the model. In East Galveston Bay, this sediment accounted for 0.75 to 1.5 cm of deposition over the year. As the boundaries, especially those along Smith and Eagle Points, erode, suspended sediment is transported into the channel and drifts upstream such that the deposition in the channel begins in the area around and upstream of Red Fish Reef (see Figures B3 and B4). Points 8, 7, and 6 experience the first deposition when sediment has not yet entered the system in significant quantities from the rivers. The field data indicate that the bed sediment becomes finer upstream along the channel, verifying that there is an upstream drift of suspended sediment such that the coarser grains settle quickly and the finer grains settle much slower and travel further upstream.

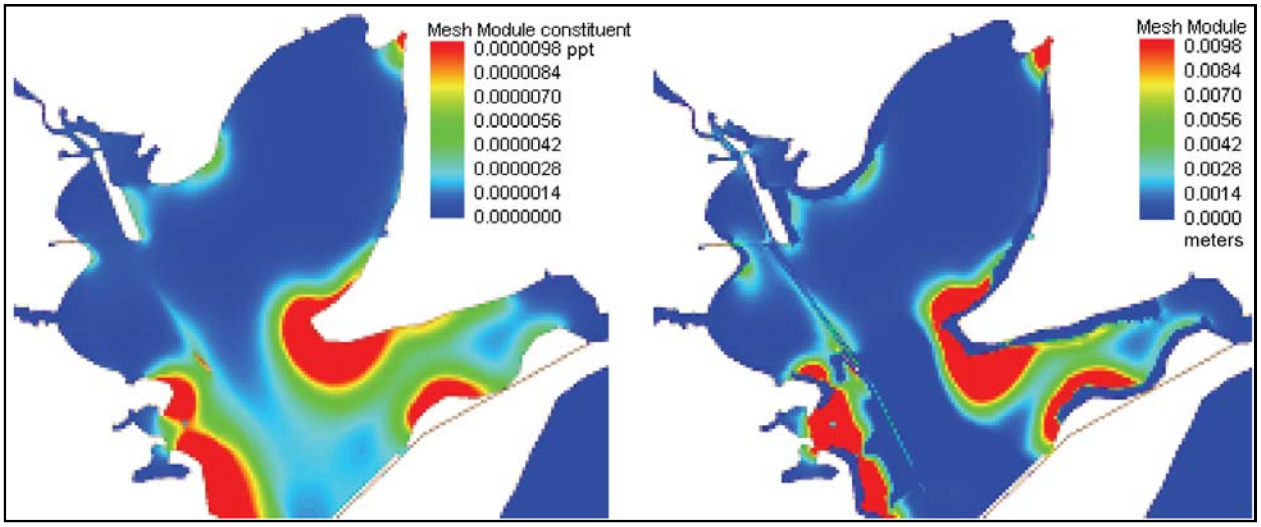

Figure B3. Suspended sediment concentration (left) and bed displacement (right) at hour 2308 (high flow water year).

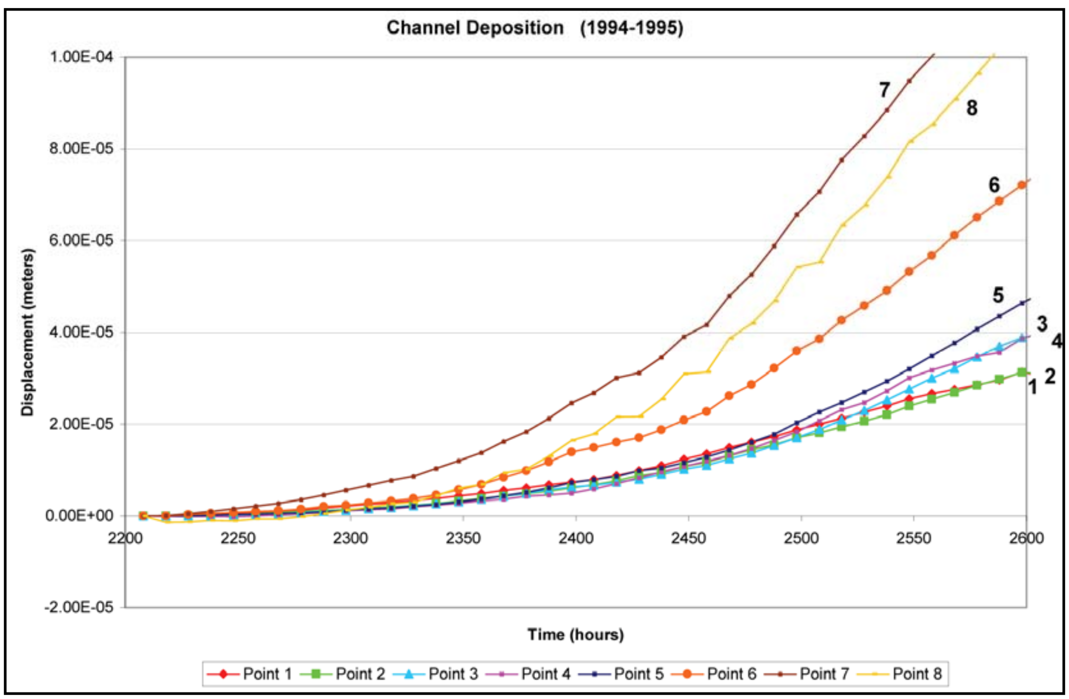

Figure B4. Channel bed displacement for the initial 400 hours.

As time progressed a high flow event was encountered from the San Jacinto and Trinity Rivers, supplying a large amount of sediment into the system. The largest amounts of deposition in the system were attributed to the inflow conditions. This is indicated by the slope changes in the deposition for various points along the channel (Figure B2) in conjunction with the flows from the rivers (Figure 17). As large concentrations flowed downstream from the San Jacinto River, the sediment deposited first at locations further downstream. The early deposition patterns indicate a drift upstream of sediment, so this may still have been occurring as the load was reduced. The settling velocity of the grains was such that they remained suspended for a given time and were able to travel further downstream before reaching the bed. The flow, however, impacted the speed at which the sediment was advected downstream and therefore the distance sediment traveled before settling on the bed. Figures B5 and B6 show the bed displacements during a high flow event that began around hour 2618 and continued until approximately hour 3000. The points just downstream of Atkinson Island experienced the most deposition from this flow event. Figure B6 also illustrates that the response to the event was delayed for the points along Atkinson Island and near Red Fish Reef indicating that the sediment deposition was greatest in the region between these landmarks. It is apparent that the points located most upstream (Points 1 and 2) actually experienced some erosion before deposition began to occur. At the time this deposition occurred due to the high flow entering from the San Jacinto River, Points 3 and 4 experienced the first deposition due to the high flow. However, Point 3 then experienced a small amount of erosion for approximately 80 hours until the shears due to the inflow dropped. At that time, the rate of deposition increased quickly, but leveled off at a much lower value than at the downstream locations. Deposition began at Points 5 and 6, downstream of Atkinson Island, later than at Points 3 and 4. The rate of deposition for these locations was about the same as that for Point 4, probably because these locations did not have high shears from the inflow condition. Points 7 and 8 began to experience deposition later than all other points except Points 1 and 2. It is interesting that the deposition rates at Points 3 and 8 converged to similar levels as did the deposition rates at Points 4, 5, and 6. This indicates that the shoaling caused by this high flow event was concentrated in the area between Atkinson Island and Red Fish Reef. The amount of deposition along Atkinson Island and downstream of Red Fish Reef was much less than that between these locations.

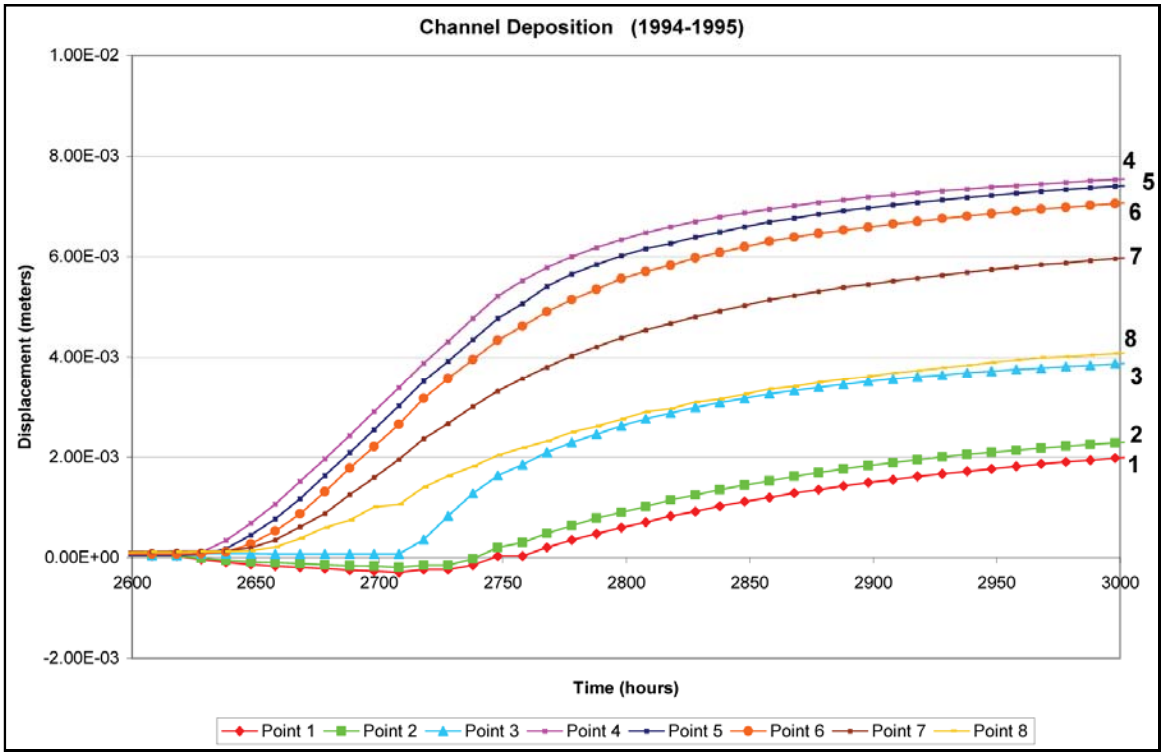

Figure B5. Channel bed displacement during and after an extreme high flow event.

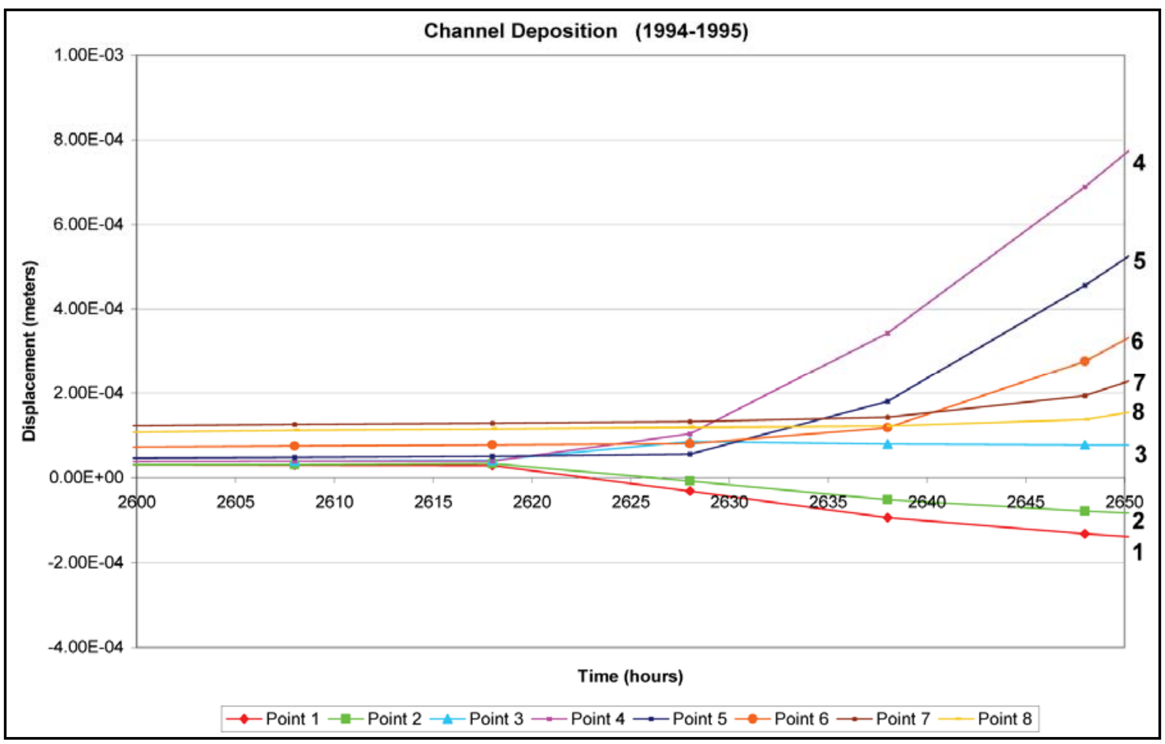

Figure B6. Channel bed displacement for smaller time frame during the initial high flow event.

Another high flow event on the San Jacinto River occurred between hours 5048 and 5208. The suspended sediment during this event only extended as far as the southern tip of Atkinson Island, indicated by Point 4 in Figure B1, and shown by the high concentration sediment plume at its greatest extent downstream in Figure B7. The deposition at this location increased whereas the points further downstream did not have a significant increase in bed displacement. The drastic increase in the rate of deposition at Points 1, 2, 3, and 4, as shown in Figure B8, indicates that these locations received the suspended sediment being supplied by the San Jacinto River. Point 5 had a slight increase in deposition rate, but the points further downstream were not affected by this inflow condition since the flow was not high enough to push the suspended sediment further down into the system.

These two high flow events indicate that the extent to which shoaling occurs at a location is highly dependent on the extent to which the sediment plume reaches. Because this area is primarily a depositional environment, there is little erosion of the bed or re-suspended sediment transport from the shallows into the channel. The characteristics of the sediment, such as settling velocity and critical shears for erosion and deposition, control the location and degree of deposition due to the incoming sediment loads from the major rivers.

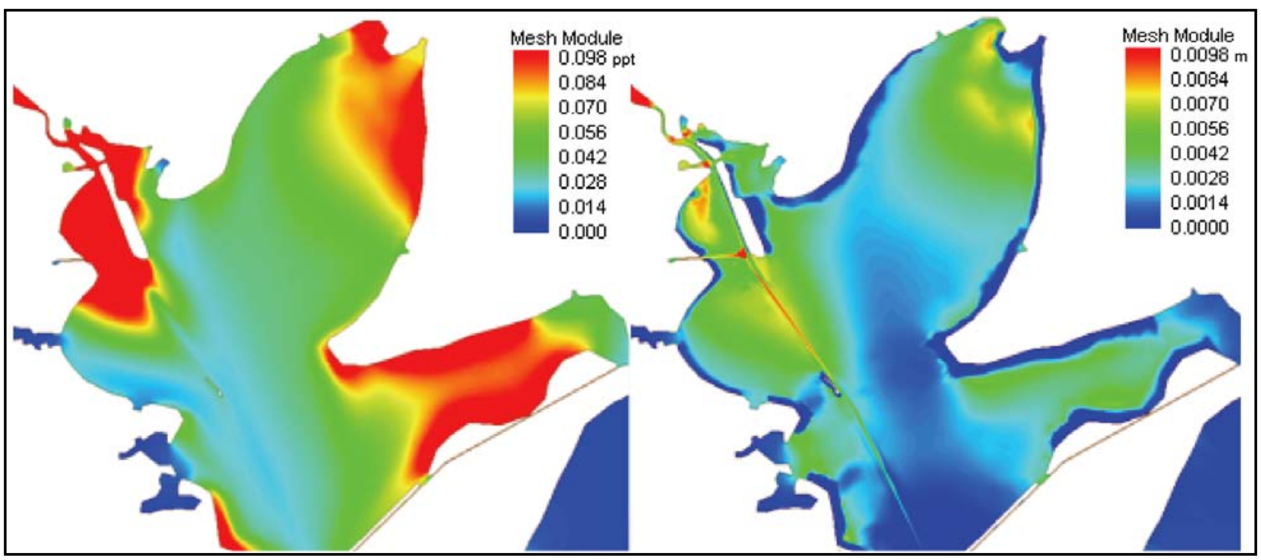

Figure B7. Suspended sediment concentration (left) and bed displacement (right) at hour 5128 (high flow water year).

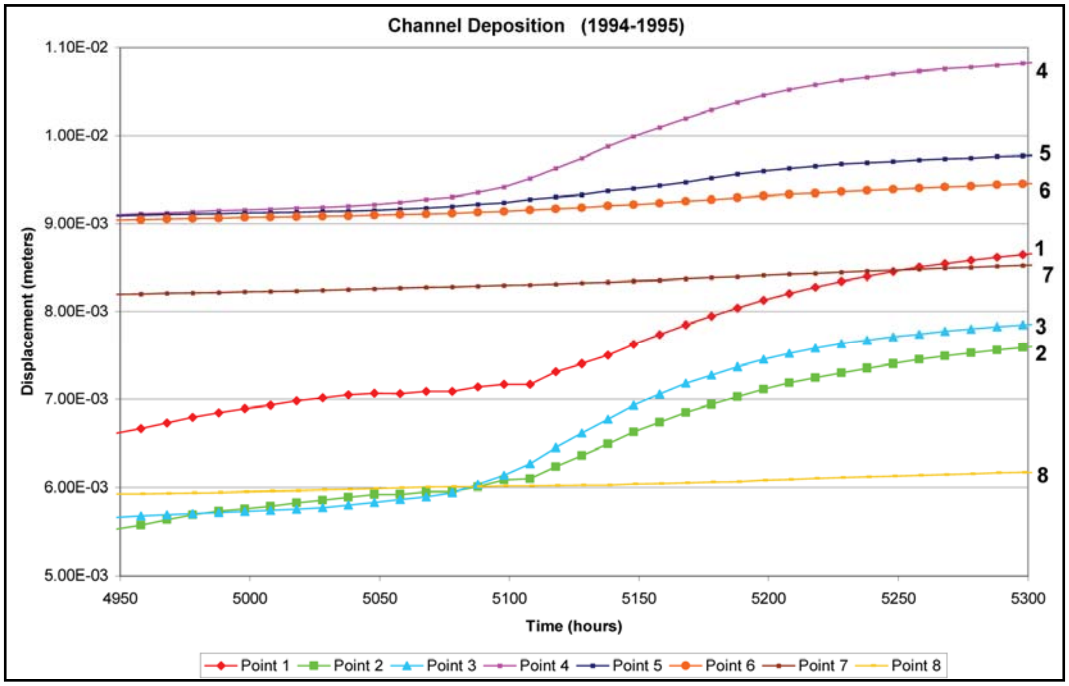

Figure B8. Channel bed displacement during and after a mild high flow event.

The distribution of deposition along the channel from Morgan's Point to Bolivar Roads for the high flow water year at 3, 6, 9, and 12 months can be seen in Figure B9. The maximum deposition began in the area between Bayport and Red Fish Reef, but over time and with larger inflow events, the location of maximum displacement shifted upstream. As discussed previously, the shift in maximum deposition upstream of Bayport is due primarily to the magnitude of the flow events on the San Jacinto River and is possibly enhanced some by the upstream drift of suspended sediment due to the currents in the channel.

Low Flow Water Year

Figure B10 shows the bed displacement over time at each of the reference points along the channel for the low flow water year. It indicates that the points directly upstream and downstream of Red Fish Reef experienced the most deposition after the year-long simulation with the exception of point 1. Point 1 is located upstream of Barbour's Cut, so any small sediment loads will deposit at this location without traveling further downstream. The points along Atkinson Island received less deposition for the lower flows than for the higher flows. As noted previously, when no suspended sediment has been supplied by the rivers, the erosion of the boundary edges causes deposition in Galveston Bay, near Smith and Eagle Points, and in the channel around the area of Red Fish Reef. The boundary erosion near Atkinson Island is not significant enough to generate large amounts of deposition in the channel, at least not when compared to deposition further downstream. Again, the tendency for the suspended sediment to drift upstream is evident and determined by the flows in the system, which have net flows in the flood direction for most of the year. The flow of sediment upstream in the channel is indicated in Figure B11, as are the high deposition areas near Red Fish Reef.

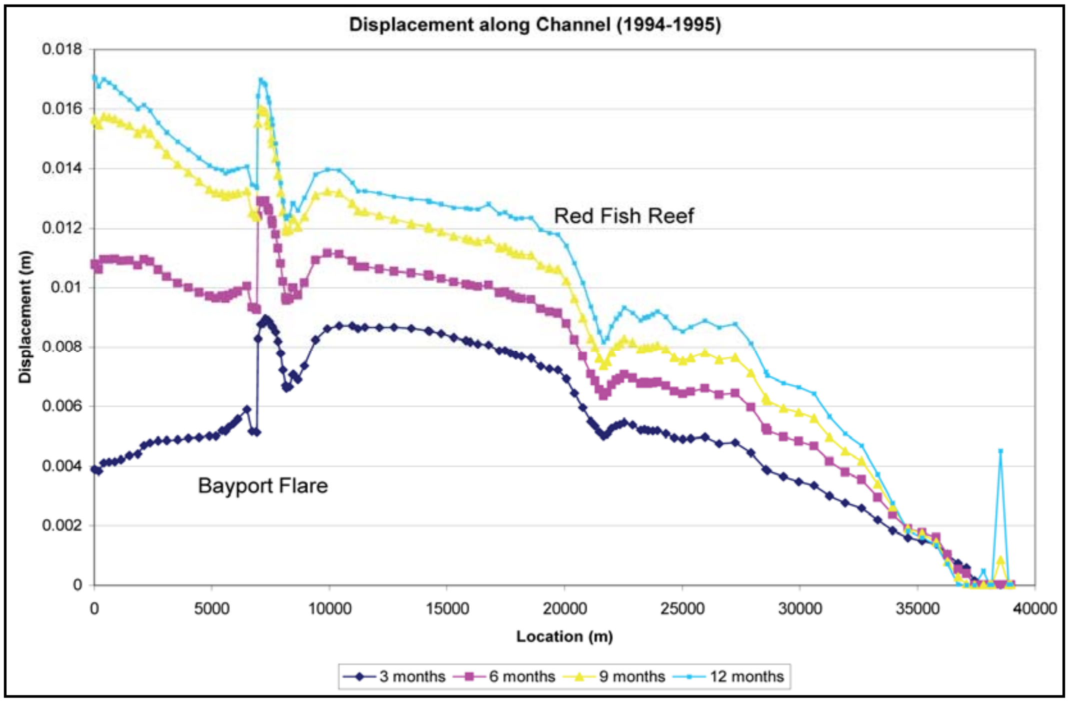

Figure B9. Distribution of bed displacement along the channel at 3, 6, 9, and 12 months.

The distribution of deposition along the channel for the low flow water year simulation is shown in Figure B12. Although much lower in magnitude than from the high flow water year, the maximum deposition occurred in the area just upstream of Red Fish Reef. Over time this maximum deposition became more pronounced with a fairly uniform deposition along Atkinson Island and a sharp decline downstream of Red Fish Reef.

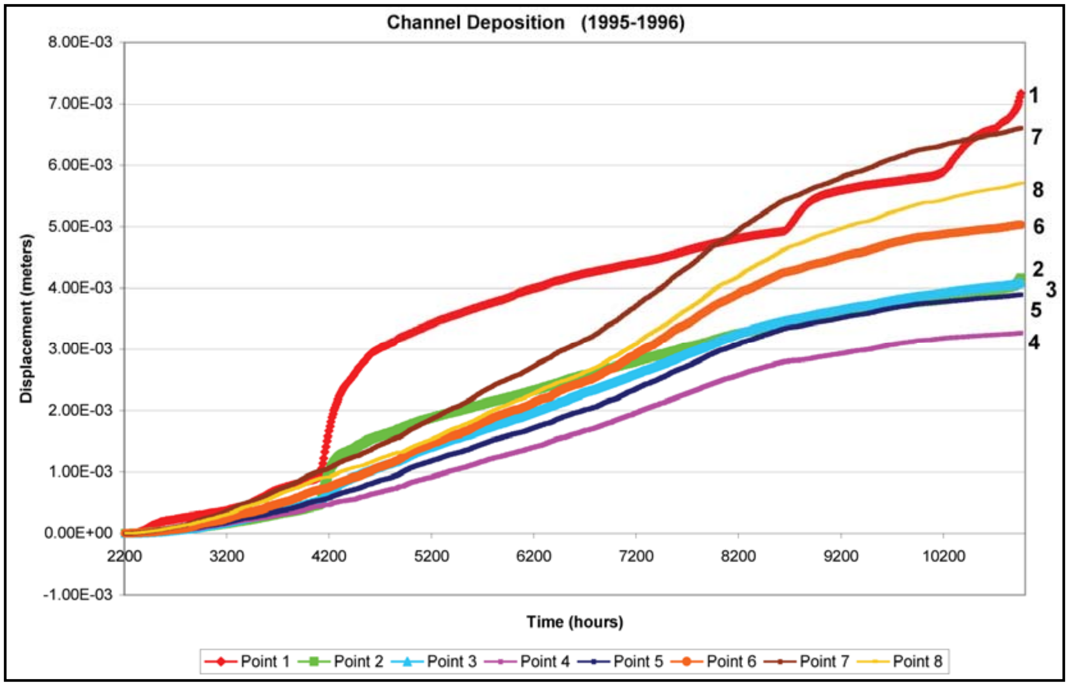

Figure B10. Bed deposition over time for the low flow year at points along the channel.

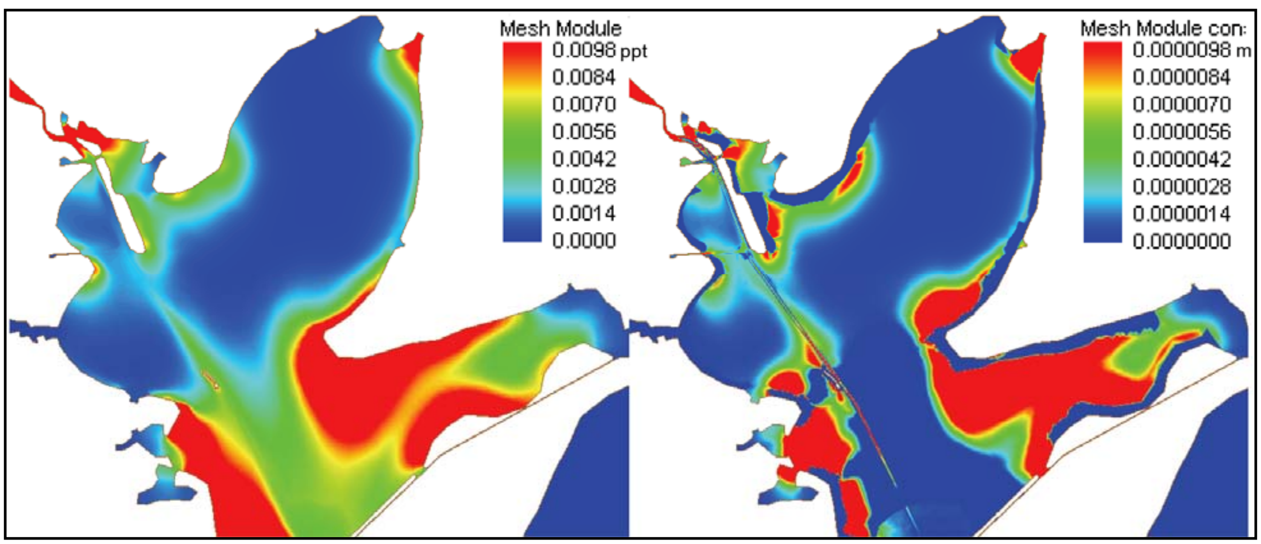

Figure B11. Suspended sediment concentration (left) and bed displacement (right) at hour 2328 of the low flow water year.

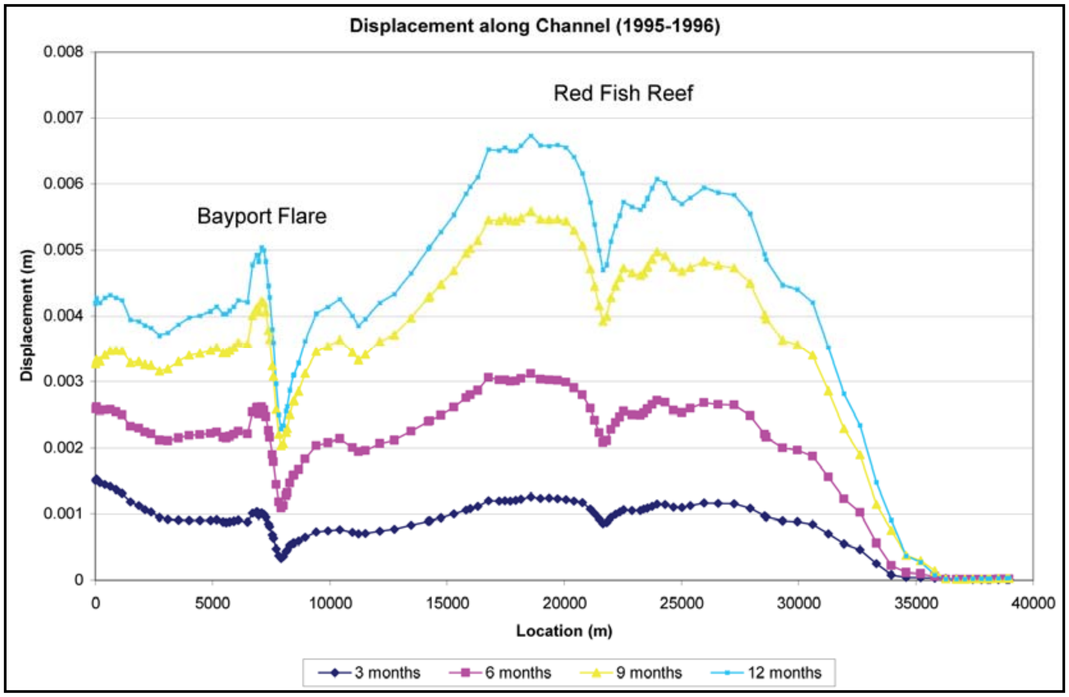

Figure B12. Distribution of bed displacement along the channel at 3, 6, 9, and 12 months.

Combined Results

Figure B13 shows the bed displacements at the completion of both water years, run independently. As expected, the low flow generated much less deposition in the system due to the lower sediment loads coming from the Trinity and San Jacinto Rivers. The pattern of deposition was slightly different for the two years. The deposition in East Galveston Bay is identical for the two years because this area only experiences shears generated by the tidal boundary changes that are large enough to cause erosion of the boundary edges. The deposition near the river entrances was substantially larger for the high flow year because of the increase in sediment loading along with the higher flows. The maximum deposition along the channel shifted downstream for the low flow water year for the reasons previously discussed. This pattern is shown in Figures B9 and B12. The area between the channel and Smith Point receives very little deposition. This behavior is seen in the field. This location is marked by oyster beds that require firm material on which to attach.

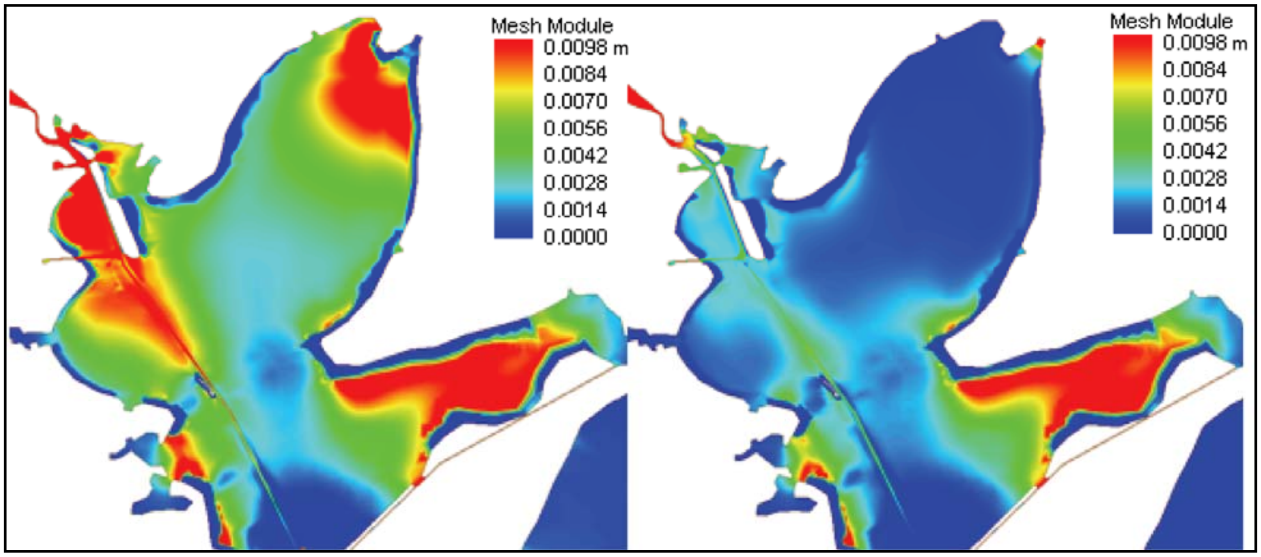

Figure B13. Bed displacement at the completion of the high flow (1995, left) and low flow (1996, right) water years.

Bayport Channel and Flare

High Flow Water Year

The Bayport Channel had quite a bit of shoaling during both flow years. The high flow water year had a large amount of shoaling in the Bayport Flare, where the Bayport Channel joins the Houston Ship Channel. The erosion of the boundary edges provided suspended sediment to the Bayport Channel; the sediment pushed toward the ship channel but erosion also provided sediment to be deposited in the Bayport Channel near its bay boundary. Using Figure B14 as a reference map, Figure B15 shows the history of deposition in the Bayport Channel. The location closest to the Houston Ship Channel, Point 1, received the most deposition. Point 2 initially experienced more deposition than Point 3, but over time Point 3 exceeded Point 2 in the amount of sediment that fell to the bed. At the time of the initial high flow event (hour 2618), sediment was deposited in the Bayport Flare area first. Points 1 and 2 received/experienced deposition about the same time, whereas deposition at Point 3 occurred approximately 10 hours later. This delay could be related to the tidal cycle and the transport of the sediment with the ebb and flood of the system.

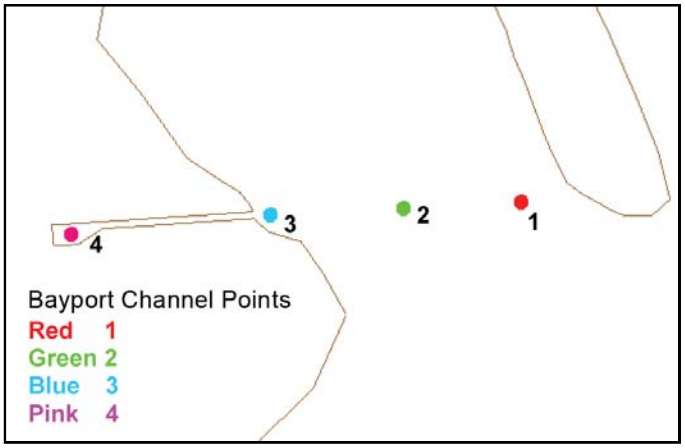

Figure B14. Bayport Channel reference map.

Point 4 (in the port) had less overall deposition, but there was a steady rate of shoaling at this point and under high sediment load events, the shoaling increased greatly – true for all of these locations. All locations appeared to have similar rates of deposition and reacted very much the same to the various flow events.

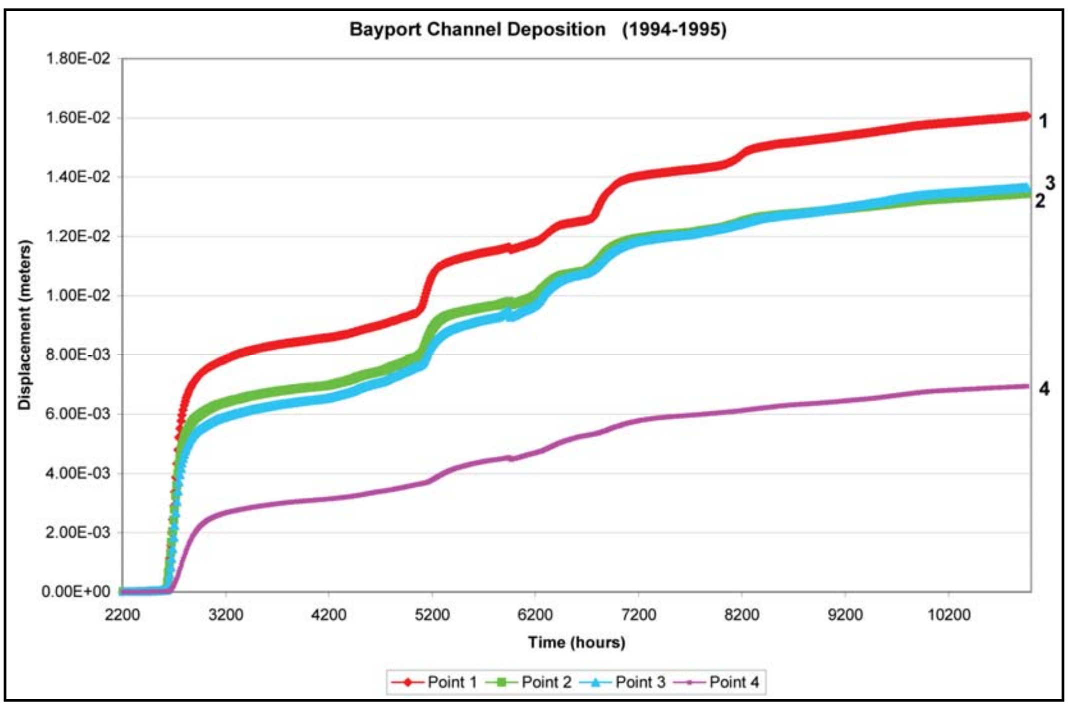

Figure B15. Bed deposition over time for the high flow water year at points along the Bayport Channel.

Low Flow Water Year

The low flow year had very steady rates of deposition at all four locations (see Figure B16). Initially, Points 1 and 3 experienced the most deposition because of their locations near the ship channel and near the boundary edge, respectively. A significant flow event from the San Jacinto River at approximately hour 4148 of the low flow year (1996 water year) was the cause of the sharp increase in deposition, especially at Point 3. Because of the transport of the sediment plume, the increase in deposition was not largest near the channel. The suspended sediment did not travel down the channel but rather out into the western bay due to the currents in the channel as indicated in Figure B17. The bottom currents were strong and directed in the upstream direction. The surface currents were also primarily moving in the upstream direction, although they were not as strong. After this flow event the rates of deposition were fairly constant with the largest rate being closest to the ship channel. Point 3 near the Bayport channel's entrance to the bay had a slightly lower rate of shoaling, followed by shoaling at Point 2 and then at Point 4 as apparent in the changing distances between the lines in Figure B16. The further decrease in rate of deposition around hour 8000 was simply due to a decrease in overall suspended sediment in the system. The inflowing sediment load was low for an extended period such that the majority of sediment in the system was deposited and very little was being eroded from the boundary edges or was entering into the system.

Western Trinity Bay

Upper Bay

High Flow Water Year

The upper lobe of Trinity Bay to the west of the Houston Ship Channel (see Figure B18) experienced deposition as indicated in Figure B19. The initial deposition occurred at Points 3 and 1. When the high flow event began at hour 2618, the deposition rate increased first at Point 2 because of its vicinity to the shoreline where velocities are the lowest (see Figure B20). The low velocities led to low shear stresses on the bed, allowing for the sediment to fall to the bed more easily rather than remaining in suspension. Point 1 reacted slower but with a greater rate of deposition, likely due to its position near the ship channel at Morgan's Point, such that the amount of shoaling quickly became greater for this location. Points 4 and 3 reacted last (approximately 40 hours later than Point 2) and with a lower rate. The suspended sediment that traveled into the area remained in higher concentrations in the area of Points 3 and 4. Once this high flow event passed, the rates of deposition for the points were fairly uniform and leveled off until another large flow event occurred. A flow event around hour 5000 caused more deposition to occur at Point 4 than at Points 3 or 2. This event pushed suspended sediment into the entire upper lobe, but the highest concentrations were located near the channel and towards the upper west side, which is why Points 1 and 4 had a greater rate of deposition although all locations experienced the effects of the sediment load. This sediment pattern was consistent for the many high load events and was the cause for Point 4 having a higher rate of deposition and ultimately more deposition than Points 3 and 2.

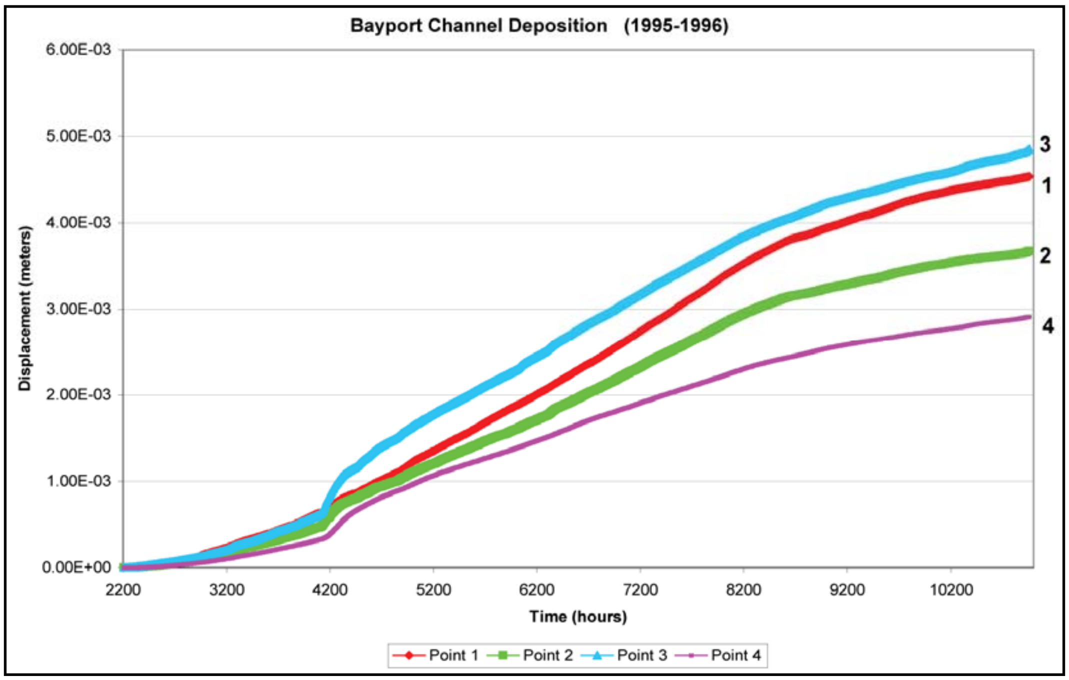

Figure B16. Bed deposition over time for the low flow year at points along the Bayport Channel.

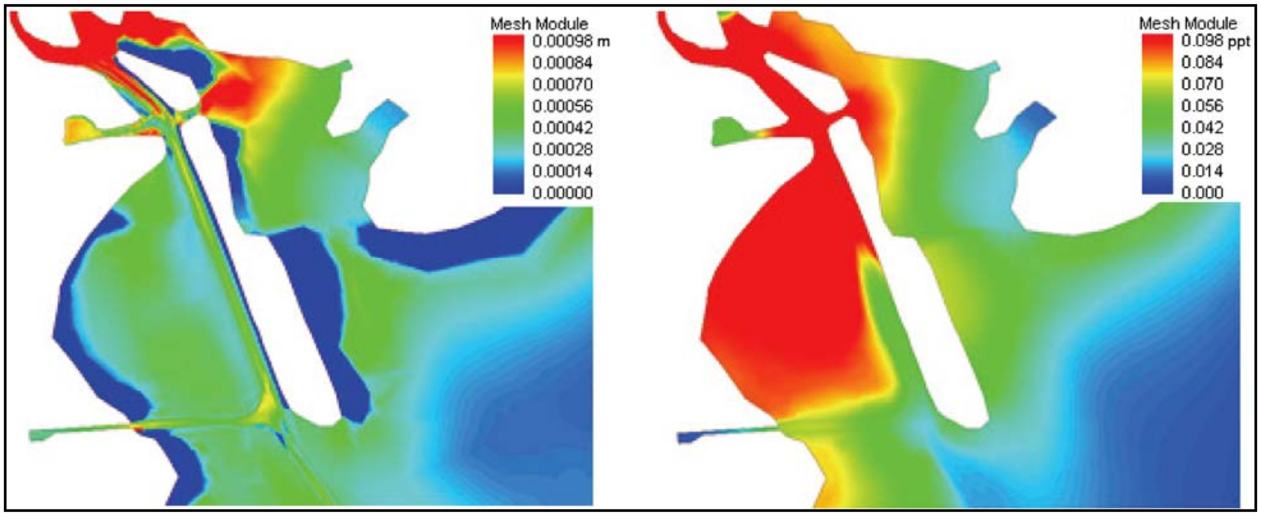

Figure B17. Bed displacement (left) and suspended sediment concentration (right) at hour 4148 of the low flow water year.

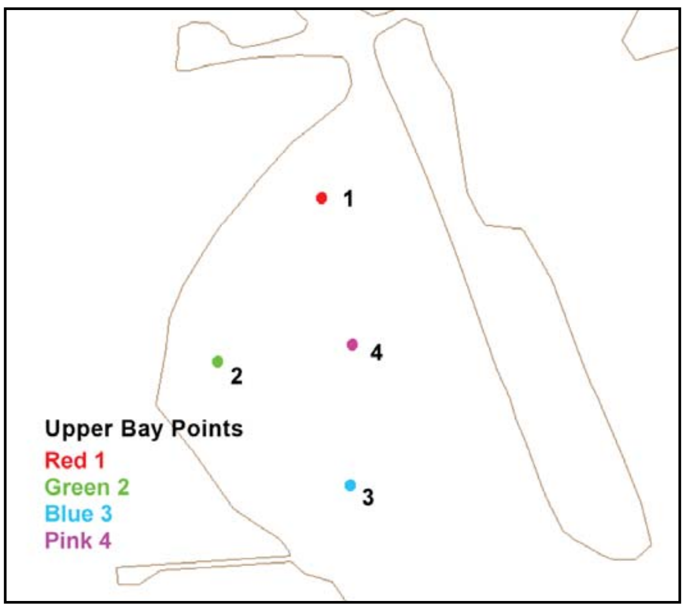

Figure B18. Western Trinity Bay, upper lobe reference map.

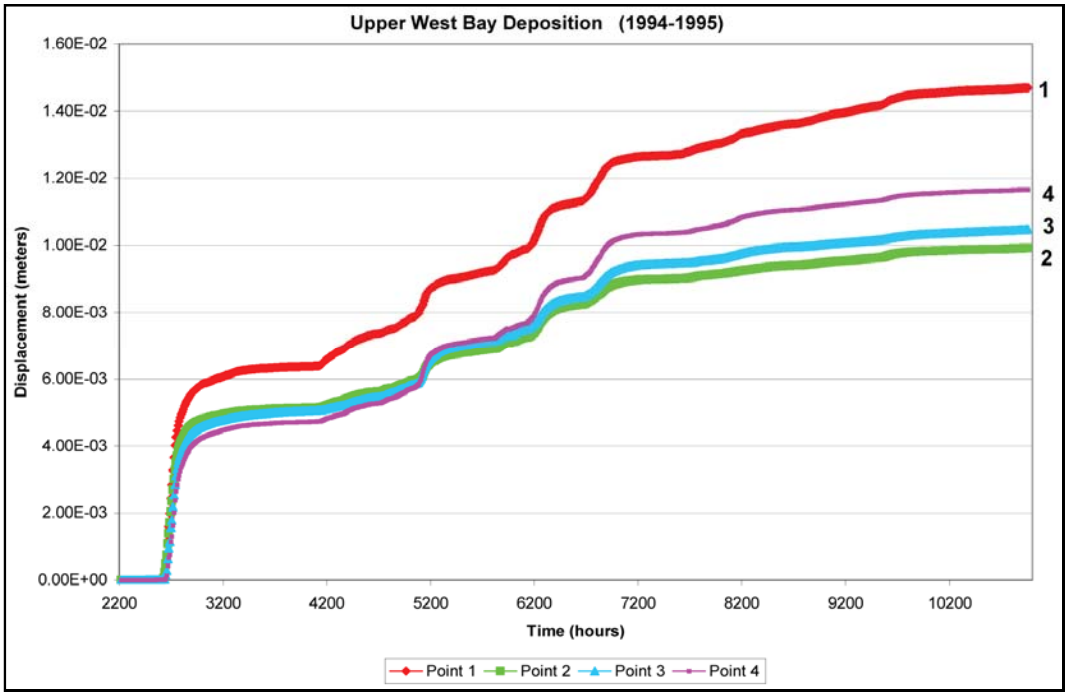

Figure B19. Bed deposition over time for the high flow water year at points in the upper lobe of Western Trinity Bay.

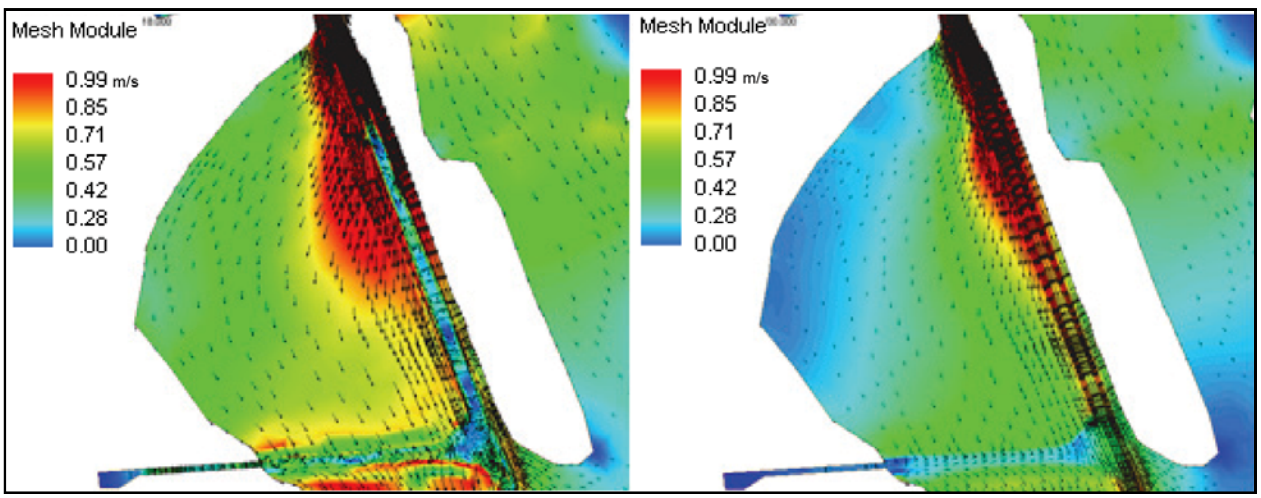

Figure B20. Velocity contours and vectors for hour 2618 (left) at the start of a high flow event and hour 2700 (right) at the end of the same event and typical of the flow pattern.

Low Flow Water Year

The low flow water year (see Figure B21) began with deposition in this area due to erosion of the boundary edges. Point 1, most upstream, had the most deposition. Point 2 had the least because of the lower velocities in this area, shown in Figure B20, causing less erosion of the boundary edges. Point 3 is near the Bayport Channel and closer to the constriction at the south end of the lobe such that velocities are higher creating more erosion that leads to bed deposition. Since this flow year had very few high sediment loads entering the system, the erosion of the boundary edges near Points 1 and 3 had the largest impact on the deposition. The high flow event around hour 4200 provided Point 4 with deposition for the same reasons discussed for the high flow year.

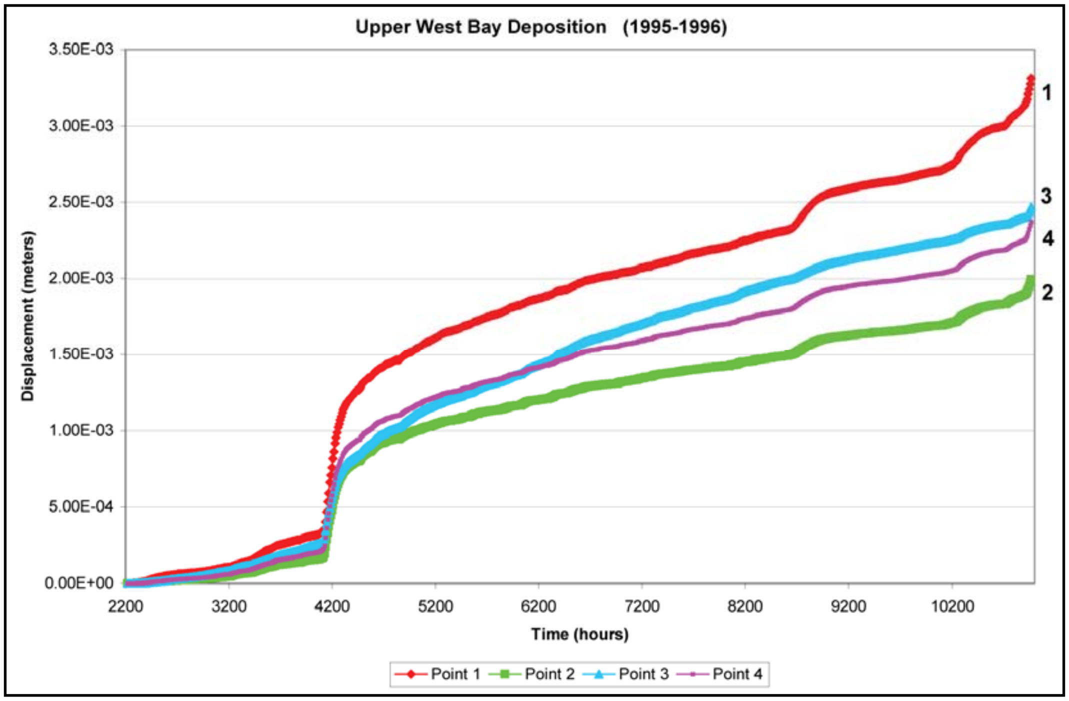

Figure B21. Bed deposition over time for the low flow water year at points in the upper lobe of Western Trinity Bay.

Lower Bay

High Flow Water Year

The lower lobe of the bay on the western side of the Houston Ship Channel had the most deposition throughout the high flow water year at Point 1. Using Figure B22 as a reference map, the bed displacements at all points in this area can be seen on Figure B23. Point 1 is just south of the Bayport Channel so there is the likelihood of boundary edge erosion causing some of this deposition as well as it being the most upstream location to experience sedimentation from the flow events on the San Jacinto River. Point 5, in the center of the lobe, ultimately had slightly less deposition than Point 1; however, during the high flow event at hour 2618, this location experienced deposition first and more than any other point in this area as shown on Figure B24. Point 5 is in the path of the highest suspended sediment concentration flows into the area and as the fresher flows come into the system, the high concentrations get pushed to the center of the lobe and into the channel where they remain in suspension the longest. Point 2 experienced deposition from this event at about the same time as Point 5 because of its upstream location and vicinity to the shoreline. This location near the shoreline has lower velocities such that the bed shears are lower and sediment can fall to the bed more easily. Point 3, followed by Points 1 and 4, did not receive/experience deposition until 10 to 20 hours after deposition at the other locations. Although Point 1 had deposition last, its rate of deposition quickly became greater than the rate at all others in this area except Point 5 until other flow events occurred which did not extend far into this southern lobe allowing Point 1 to experience more deposition overall. Point 3 had the least deposition overall due to its location furthest downstream and near the boundary away from the ship channel. This area had lower velocities such that suspended sediment will be more likely to fall out here, but very high sediment loads and flows will be required for large quantities of suspended sediment to reach this far downstream. Although Point 2 experienced more deposition from the initial high flow event, Point 4 ultimately had about the same deposition by the end of the year-long simulation. As noted previously, the later flow events were not as strong and had the largest impact on locations further upstream as indicated in the slope changes of the various locations presented in Figure B23, with the greatest change at Point 1 and the smallest change at Points 3 and 4. All points, except Point 4, had about the same rate of deposition during the second half of the year when few flow events were occurring. This slope indicates that in this area the driving effect on sedimentation differences in the lobe is the extent to which the high sediment load flow events reach. The increased rate of deposition at Point 4, especially when no flow events were occurring, was caused by the erosion of boundary edges and the location of Point 4 near Eagle Point. Smith and Eagle Points experienced large amounts of erosion and subsequent nearby deposition because of the extent at which they constrict the tidal flows coming in from the Gulf of Mexico.

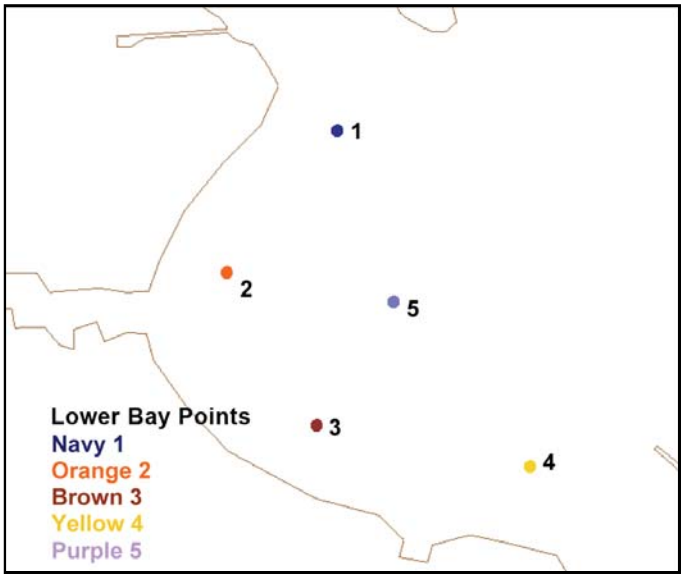

Figure B22. Western Trinity Bay, lower lobe reference map.

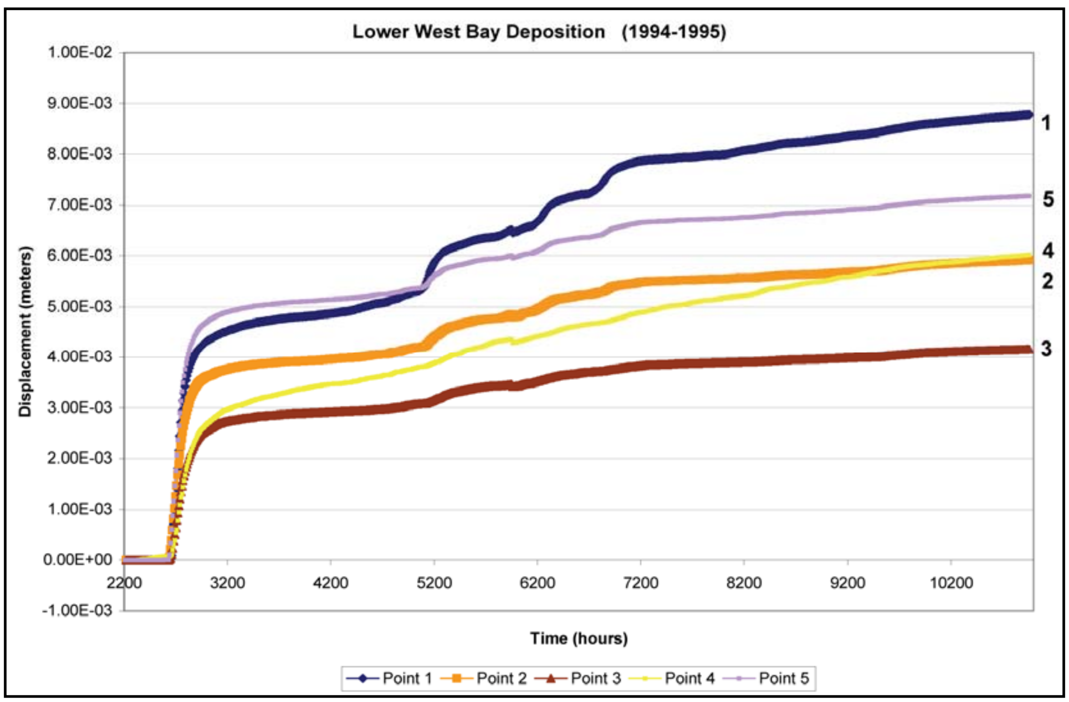

Figure B23. Bed deposition over time for the high flow water year at points in the lower lobe of Western Trinity Bay.

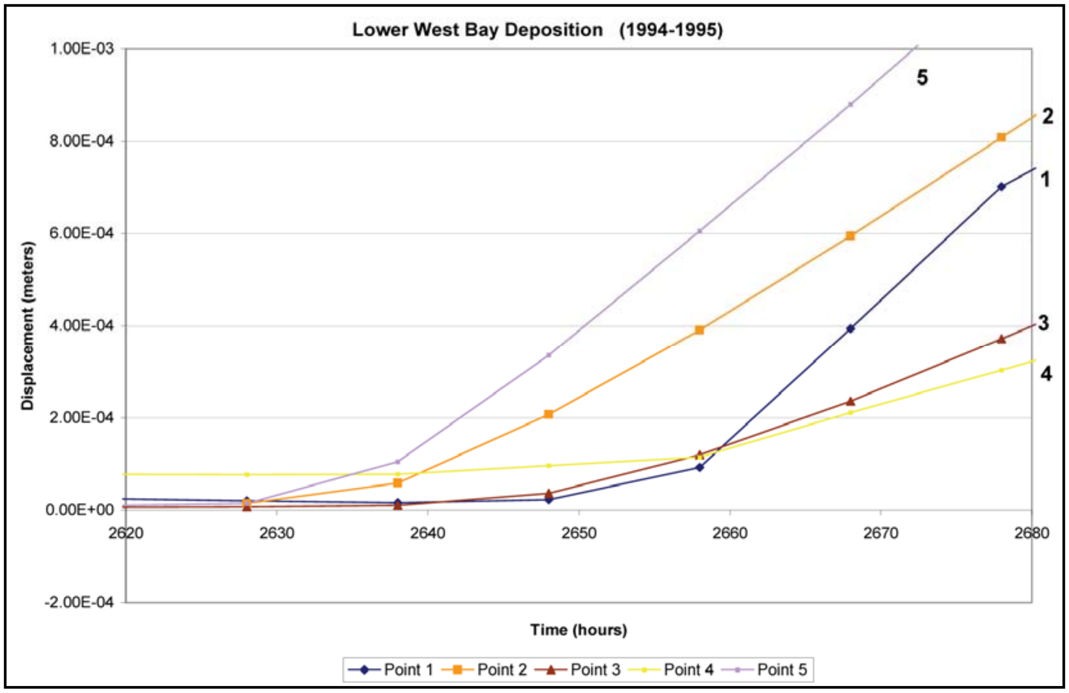

Figure B24. Bed displacements for a smaller time frame during the initial high flow event.

Low Flow Water Year

The low flow water year (water year 1996) follows the same general observations as the high flow water year. The bed depositions at several locations along the channel are shown in Figure B25. Point 4, closest to the erosion occurring at Eagle Point, had the most consistent rate of deposition and was affected the least by any flow events on the San Jacinto River. Point 1, furthest upstream near Bayport, experienced the effects of the flow events more than the other locations because the flow events for this water year were generally not as large as those from the previous year and did not extend far into the lower lobe of the bay. Points 2 and 5 experienced very similar rates of deposition. Because the high suspended sediment concentration areas in the central portion of the lobe were not as prevalent as during the high flow year, Point 5 did not experience the increase in deposition. Point 3, in the downstream section and a large distance away from the channel, had the least amount of deposition but did have a fairly constant rate of deposition throughout the year, as did all of the other locations. Point 4 had a decline in its rate of deposition around hour 8200 when the flows from the major rivers had been low for an extended period of time such that very little suspended sediment was entering the system and the hydrodynamics were keeping the higher concentrations of sediment in the area downstream of Smith and Eagle Points.

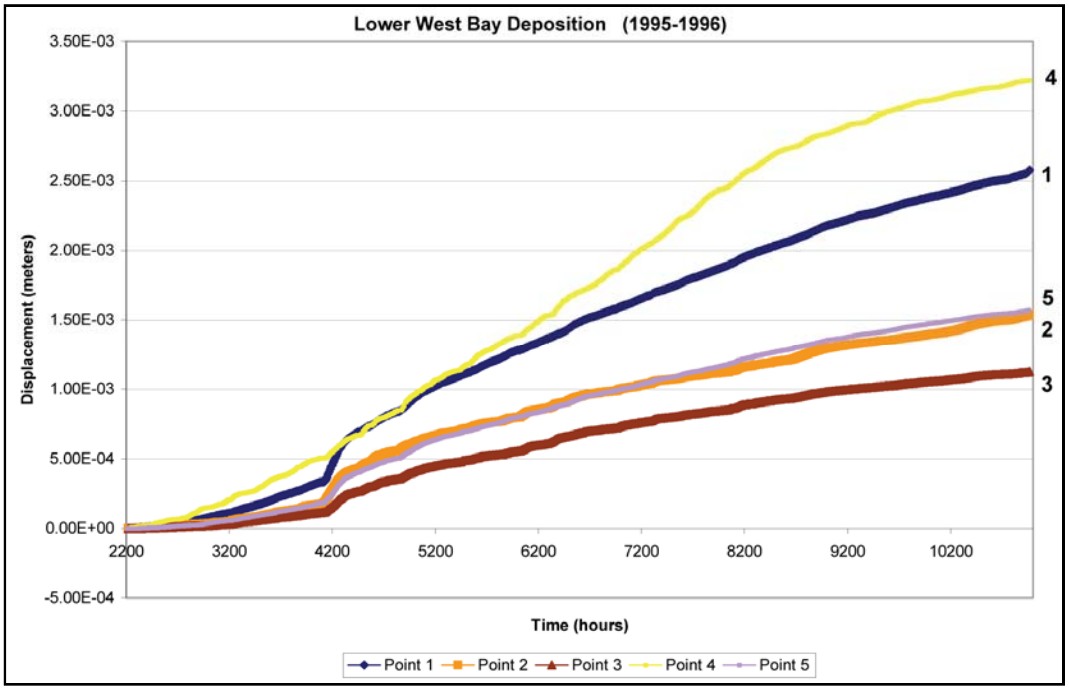

Figure B25. Bed deposition over time for the low flow water year at points in the lower lobe of Western Trinity Bay

Eastern Trinity Bay

High Flow Water Year

The Eastern side of Trinity Bay experienced deposition differently than the areas to the west of the Houston Ship Channel. Figure B26 is a reference map for several locations in this area and Figure B27 shows the high flow year bed displacements over time at these locations. Initially deposition occurred at Points 4, 8, and 1. Points 4 and 8 gained sediment that was being eroded from the boundary edges. Point 1 is immediately downstream of the entrance of the Trinity River, so its deposition will be greatly impacted by the sediment loads from the river. Points 3 and 7 experienced deposition for the same reason as Points 4 and 8, but in smaller magnitudes. Point 5 was affected by the inflow of sediment from the Trinity River and its initial deposition lagged that of Point 1 in time and magnitude.

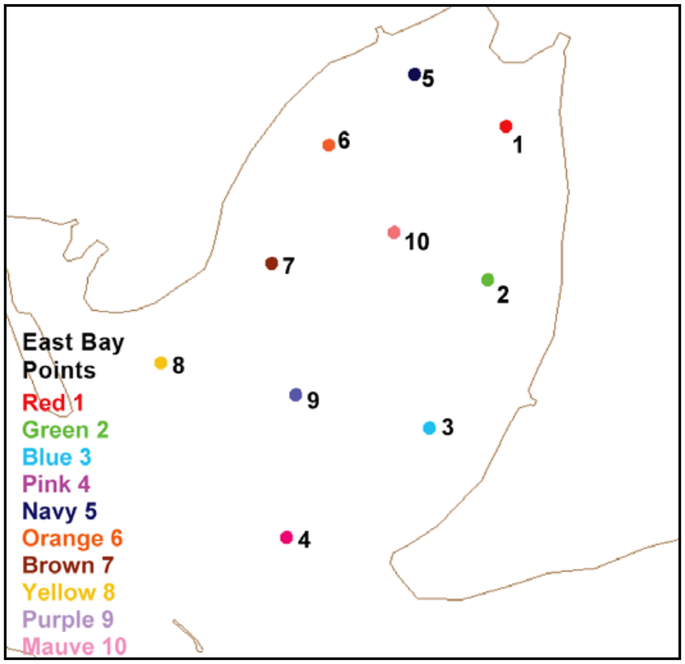

Figure B26. Eastern Trinity Bay reference map.

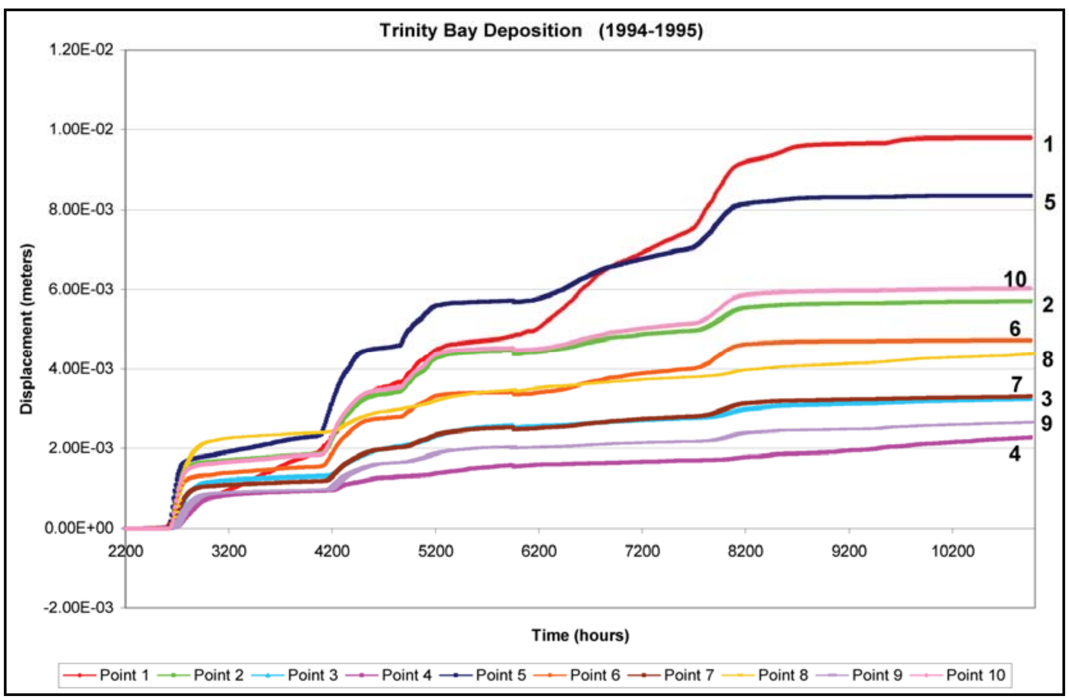

Figure B27. Bed deposition over time for the high flow water year at points in Eastern Trinity Bay.

The high flow event in the system at hour 2618 was the first cause for major deposition in the area. Deposition from this event occurred first at Point 5. This location also had the highest rate of deposition because of its location being protected from the high flows of the river and likely lower velocities. Deposition next occurred at Points 2, 10, and 6, which are approximately equal distances from the Trinity River's entrance to the bay. Point 8 began to experience the effects of this event at about the same time as these three locations, but the sediment being deposited at Point 8 was from the San Jacinto River as opposed to the Trinity River. The San Jacinto flows were of higher concentrations such that the greatest deposition from this event was at Point 8. Points 6, 10, 2, and 8 initially had similar rates of deposition, but Point 8 continued to experience deposition after the others due to the lower amount of sediment entering the system from the Trinity River. Deposition next occurred at Point 7, followed within 10 hours at Point 3. These two points (Points 7 and 3) reacted almost identically throughout the entire year-long run because of their equal distance from the Trinity River entrance and their proximity to the eroding boundary edges. Point 9 experienced deposition several hours after all of the other points located around the boundary or closer to the river's entrance. This location (Point 9) is in the center of the bay towards the ship channel where the two flows converge last such that lower concentrations of sediment occur in this area. Figure B28 illustrates this concept. Point 4 was the last to react to this high flow event. It is located further downstream than any of the other points in this area so the high concentrations of suspended sediment take longer to reach this location and are not as high once they get there because some sediment has deposited along the way. The rate of deposition at this point is also the lowest for these same reasons. The high flows associated with the event prevent Point 1 from experiencing high magnitudes of deposition. However, over time and with high sediment concentration flows of lower speeds, Point 1 will ultimately have the most deposition over the year-long simulation.

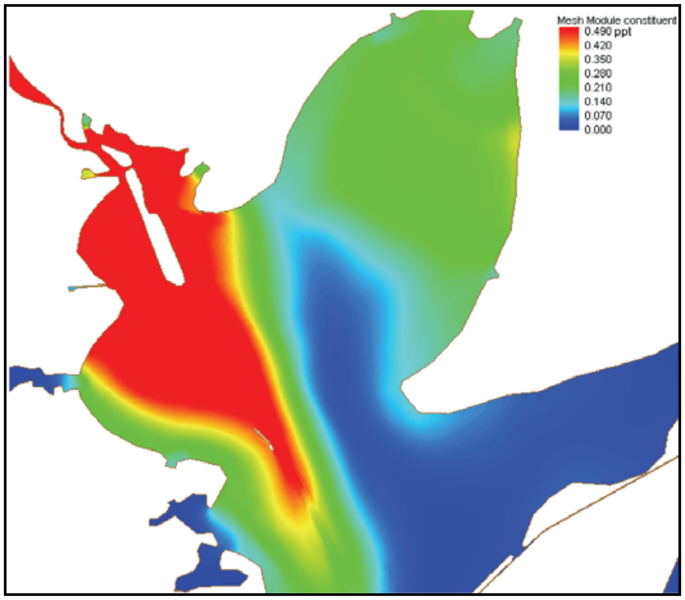

Figure B28. Suspended sediment at hour 2698.

Low Flow Water Year

The deposition occurring during the low flow water year (water year 1996), seen in Figure B29, is much different than that from the high flow water year (water year 1995). Point 4 had the most deposition during the low flow and the least during the high flow. This difference is likely due to the limited amount of suspended sediment entering the system from the rivers such that the boundary edge erosion dominates the transport in the system. Point 8, which had fairly low deposition during the high flow year, had the second highest amount of deposition for the low flow year. This was caused, in part, by the boundary edge erosion, erosion from the back side of Atkinson Island, and its proximity to the San Jacinto River such that sediment from that river reached this location. Points 5 and 6 had the least amount of deposition, likely due to their location near the northern shore of Trinity Bay. At Points 5 and 6 the flows are not pushing sediment into the area and any suspended sediment is primarily transported further south into the bay. The points with the greater amounts of deposition (Points 4, 8, 3, 9, and 7) are all located near the boundary edges and towards the Houston Ship Channel. The points with the least deposition (Points 1, 2, 10, 6, and 5) are all located near the Trinity River inflow and the northern section of the bay. The transported sediment during this flow year was concentrated in the constricted areas, such as between Smith and Eagle Points and along Atkinson Island and the western sections of the bay. The concentration, as well as the overall bed deposition, decreased northward through Eastern Trinity Bay.

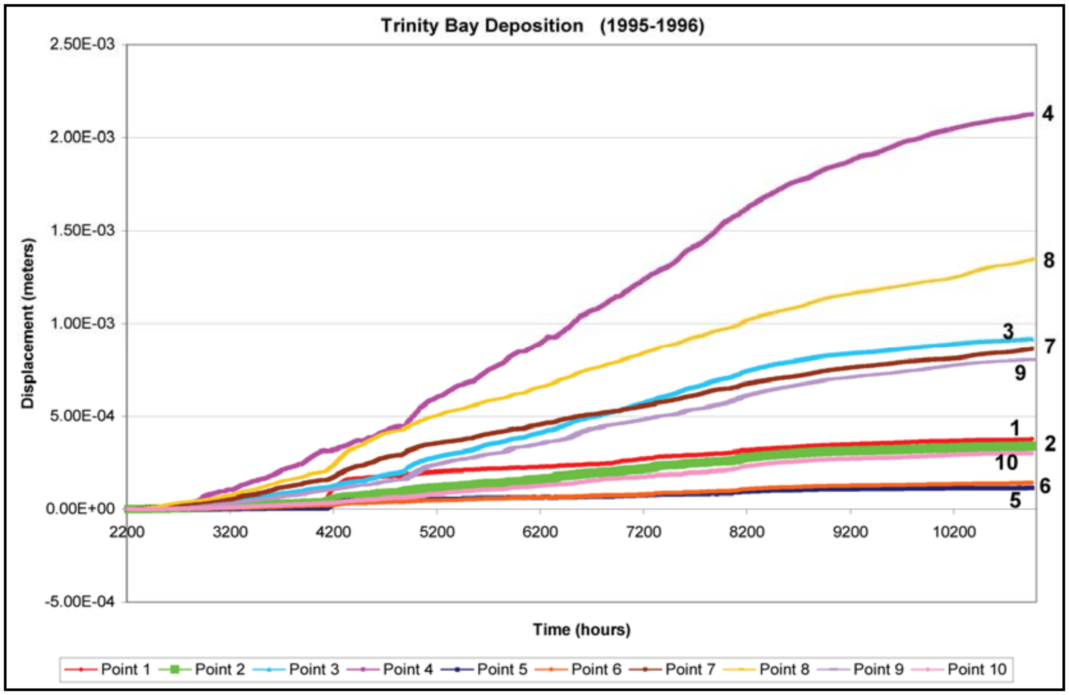

Figure B29. Bed deposition over time for the low flow water year at points in Eastern Trinity Bay.

Summary

The paths of sediment transport within the model domain indicate that the San Jacinto River has the greatest impact on the deposition in the area. When the river inflows are low, the erosion along the model boundaries is the primary source of suspended sediment in the system. The magnitude of the flow events determines the extent to which the sediment travels downstream through the system and, therefore, the locations of sediment deposition. The high flow water year had more defined deposition patterns in the area as expected since sedimentation is an event-driven process, dependent on the shear stresses generated on the bed to define if sediment suspends, deposits, or erodes. Overall, the Trinity River has little influence on the sediment reaching the Houston Ship Channel. There is an upstream drift of suspended sediment in the channel, but the influence of this drift is defined by the size of the flows entering the system from the rivers. This appendix gives a detailed account of how sedimentation in each area of the model domain is affected by the varying flows in the two water years simulated in the absence of ship effects.

REPORT DOCUMENTATION PAGE

Form Approved OMB No. 0704-0188

1. REPORT DATE *(DD-MM-YYYY)*	2. REPORT TYPE	3. DATES COVERED *(From - To)*
July 2008	Final report	

4. TITLE AND SUBTITLE

Houston-Galveston Navigation Channels, Texas Project; Navigation Channel Sedimentation Study, Phase 2

5a. CONTRACT NUMBER

5b. GRANT NUMBER

5c. PROGRAM ELEMENT NUMBER

6. AUTHOR(S)

J. N. Tate, R. C. Berger, and C. G. Ross

5d. PROJECT NUMBER

5e. TASK NUMBER

5f. WORK UNIT NUMBER

7. PERFORMING ORGANIZATION NAME(S) AND ADDRESS(ES)

Coastal and Hydraulics Laboratory
U.S. Army Engineer Research and Development Center
3909 Halls Ferry Road
Vicksburg, MS 39180

8. PERFORMING ORGANIZATION REPORT NUMBER

ERDC/CHL TR-08-8

9. SPONSORING / MONITORING AGENCY NAME(S) AND ADDRESS(ES)

U.S. Army Engineer District, Galveston
P.O. Box 1229, Galveston, TX 77553-1229

10. SPONSOR/MONITOR'S ACRONYM(S)

11. SPONSOR/MONITOR'S REPORT NUMBER(S)

12. DISTRIBUTION / AVAILABILITY STATEMENT

Approved for public release; distribution is unlimited.

13. SUPPLEMENTARY NOTES

14. ABSTRACT

The U.S. Army Engineer District, Galveston, recently enlarged the Houston Ship Channel in depth and width. Preliminary evaluations of the enlarged channel indicate a higher than anticipated rate of deposition in the channel reach near Atkinson Island. A Coastal and Hydraulics Laboratory investigation (Tate and Berger 2006) was charged with determining if this higher deposition rate is a permanent feature or only a temporary issue. A preliminary study focused on the change in currents, as determined by the model, from the pre-enlarged channel to the new configuration and a sediment tracer analysis. The results of this study determined that the dredging should have been only about 20-30 percent higher than for the pre-enlarged channel. This implies that the large increase is due to other considerations, such as dredge disposal escape, channel dimension equilibrating, or vessel impacts on the shoaling. This preliminary study used the sediment model in an unvalidated state for early results to aid planning. In addition to an unvalidated model, other limitations were that the sediment pathways and loadings were not modeled but assumed. A more general validated tool will be able to estimate the causes of the shoaling with the enlarged channel and suggest approaches to reduce the deposition rate. A full sediment model of the area will be useful to direct decisions to try to reduce dredging and dredging costs. Knowing that there are many factors that contribute to sediment transport, the logical next step is to develop and validate the sediment model. With a validated sediment model, testing and decision making can be made while considering many factors simultaneously. This report presents the sediment model validation process and comparison of the model to field data. The end result is a model that is capable of reproducing tides, circulation, salinity, and sediment transport in Galveston Bay.

15. SUBJECT TERMS

Channel deepening	Houston-Galveston Ship Channel	Shoaling
Dredging records	Hydrodynamic model	Vessel effects
	Sediment model	

16. SECURITY CLASSIFICATION OF:			17. LIMITATION OF ABSTRACT	18. NUMBER OF PAGES	19a. NAME OF RESPONSIBLE PERSON
a. REPORT	b. ABSTRACT	c. THIS PAGE			19b. TELEPHONE NUMBER *(include area code)*
UNCLASSIFIED	UNCLASSIFIED	UNCLASSIFIED		192	